GEOCHEMISTRY OF THE ALBUQUERQUE MUNICIPAL AREA

ALBUQUERQUE, NEW MEXICO

by

Linda May Logan

Independent Study

Submitted in Partial Fulfillment of the
Requirement for the Degree of

Master of Science in Hydrology

The New Mexico Institute of Mining and Technology
Socorro, New Mexico

October 1990

TABLE OF CONTENTS

LIST OF FIGURES

LIST OF TABLES

ABSTRACT

Available water quality and environmental isotope data for precipitation, mountain springs, the Rio Grande, and ground water were used to look at changes in chemical composition through the water cycle from initial atmospheric water quality to ground-water quality. Historical and present-day hydrodynamic models, ground-water temperatures, recharge water quality, mineral equilibria, and major ion concentration and distribution were all combined to interpret the water-quality variations throughout the area.

Several new interpretations have resulted from the apparent contradictions in data interpretation. Deep wells previously thought to be protected from surface contamination by their depth and distance from recharge boundaries contain tritium which indicates part of the water produced is, at most, 25 years old. Tijeras Canyon drainage, characterized by cool ground-water temperatures and water-quality shifts, persists several kilometers down gradient showing the far reaching influence of shallow, potentially contaminated, ground water in the deep-basin aquifer. High sodium and chloride ground water, near the mountain front, can be explained by arid-climate pedogenic (soil) processes. Seepage velocity calculations indicate flow rates of about 1200 years from the mountain-recharge area to the river. A high permeability zone, midway between the mountain-front and river-recharge areas, disrupts the geochemical trend by capturing west and eastward flowing ground water and isotopically-light, high elevation recharge. High chloride and sodium "islands", and geochemical and isotopic trend discontinuities across a flow field can be explained by arid-climate pedogenic processes and the hydrodynamic system.

ACKNOWLEDGMENTS

This independent study was done under the direction of Dr. Fred Phillips whom I want to thank for his valuable advice and guidance. I am indebted to the City of Albuquerques Public Works Department for giving me unpublished data essential to the conclusions contained in this study. I especially want to thank W. K. Summers of the City's Public Works Department, Planning Group for his guidance and encouragement through many aspects of this study. A special thanks to a dear friend Shirley (Thieda) Skipworth for her many hours of drafting and encouragement. Financial assistance was generously provided by my best friend and life-long partner Bob Logan, whom I can not thank enough for his tireless support and encouragement.

INTRODUCTION

The Albuquerque municipal area encompasses New Mexico's largest city and adjacent communities where wells provide ground water to over 400,000 people. As the municipal area grows and its population increases, the communities' demand for water also increases.

To meet this growing demand, ground-water specialists must understand the sources and amounts of available ground water, and its geochemical evolution in order to plan future development. Knowledge of the natural variations in both the chemical and physical parameters of local ground water allow us to evaluate the potential for ground-water pollution and detect the effects of heavy pumpage on water quality. We must understand every aspect of our ground-water system to protect this fundamental resource and to continue to provide good quality water.

To date, Albuquerque Basin geochemistry has been studied in general, but local variations in ground-water geochemistry have not been studied in detail.

Objectives and Scope

The first objective of this study is to establish the areal distribution of geochemical, isotopic, and thermal variations in ground water. The second objective is to evaluate the hydrology, geology, geophysics, water quality, and thermodynamics to suggest mechanisms which may cause this distribution of ground water characteristics. The third objective is to update the hydrodynamic model of the study area using current data.

The scope of this study is restricted to available information on the geochemistry, physical parameters, and aquifer characteristics of the deep basin-fill ground water system. To look at the geochemistry of deep basin-fill ground water, water-quality data used in this study are restricted to deep wells, 244 m (800 ft) or greater. Shallow monitoring-well data are used to construct the water table map and for isotope distribution maps. Quantitative analysis is used to provide thermodynamic constraints on mineral dissolution and mass balances. All other techniques are qualitative interpretations.

Method

To construct a conceptual model of the hydrodynamic and geochemical systems I integrated published and unpublished data on the geological, hydrological, and geochemical characteristics of the local aquifer.

First, I compiled data for historical and recent ground-water quality and well construction from the Albuquerque Public Works Department, U. S. Geological Survey (USGS) published reports, and USGS computer data base, WATSTORE. Minor sources of data were extracted from various published and unpublished reports listed in the appendices and references in the back of this study. Second, I tabulated the geochemical data and converted dissolved constituent concentrations reported in milligrams per liter (mg/L) and parts per million (ppm) to milliequivalents (meq/L) using conversion factors published in Hem (1970). Third, I organized the data using a LOTUS-123 spreadsheet from which I generated frequency and regression analyses, and graphically presented the data. Additional graphs were produced using GRAPHER, a graphics software program with more flexibility than LOTUS 123. Fourth, I constructed maps of major ions, pumping temperatures, environmental isotopes, hydraulic conductivity, and mapped the difference between recharge and well geochemistry to examine variations in

ground-water constituents. Mineral solubility indices (using PCWATEQ) and mass balance calculations along regional flow paths helped explain observed geochemical variations and infer the mechanisms causing geochemical shifts. The appendices, in the back of this report, contain the data used in this study.

For this study, I used a qualitative rather than quantitative approach to data interpretation to compensate for the irregular spatial and temporal data distribution, and data quality control (Summers, 1972; Einerson and Pei, 1988). Problems arose from incomplete information about well construction, water sampling techniques, and methods of chemical analyses - some chemical analyses did not ionically balance or were incomplete. For most interpretations I discarded analyses with more than 5 percent ion balance error. I used incomplete chemical analyses when it was the only data available. A similar problem arose with published theoretical data for aquifer characteristics; empirical data were used when available.

Location

The Albuquerque area is centrally located in the State of New Mexico in Bernalillo County along the Rio Grande. Its eastern and western limits roughly coincide with the base of the Sandia Mountains and the West Mesa. The northern and southern limits of the study area are roughly 1.6 km (1 mi) and 6.4 km (4 mi), respectively, from the

Bernalillo County boundaries, an area of nearly 542 km^2 (209 mi^2). Figure 1 is a reduced copy of the City map showing the township and ranges, and some major streets and highways. The extent of urbanization can also be seen on figure 1.

Previous Studies

Geology

Bryan (1909), wrote the first published report on the geology of the Albuquerque area. In later studies, authors included the Albuquerque area in broad regional studies or limited, site specific reports. Kelley (1977) synthesized his work and the work of others into a memoir of the entire Albuquerque Basin in which he includes a description of the pre-Tertiary and Tertiary deposits of the study area. Lambert (1968) described the Quaternary unconsolidated sediments of the Albuquerque area. The most current work is by Lozinsky (1988), in which he described a new model for the Albuquerque Basin depositional history.

Hydrology

The hydrology of the Albuquerque area was not as well studied as the geology until ground-water development accelerated in the 1950's. Theis, in 1936, constructed a water-table map for the Rio Grande flood plain, the City's primary source of water at that time. In 1961, Bjorklund

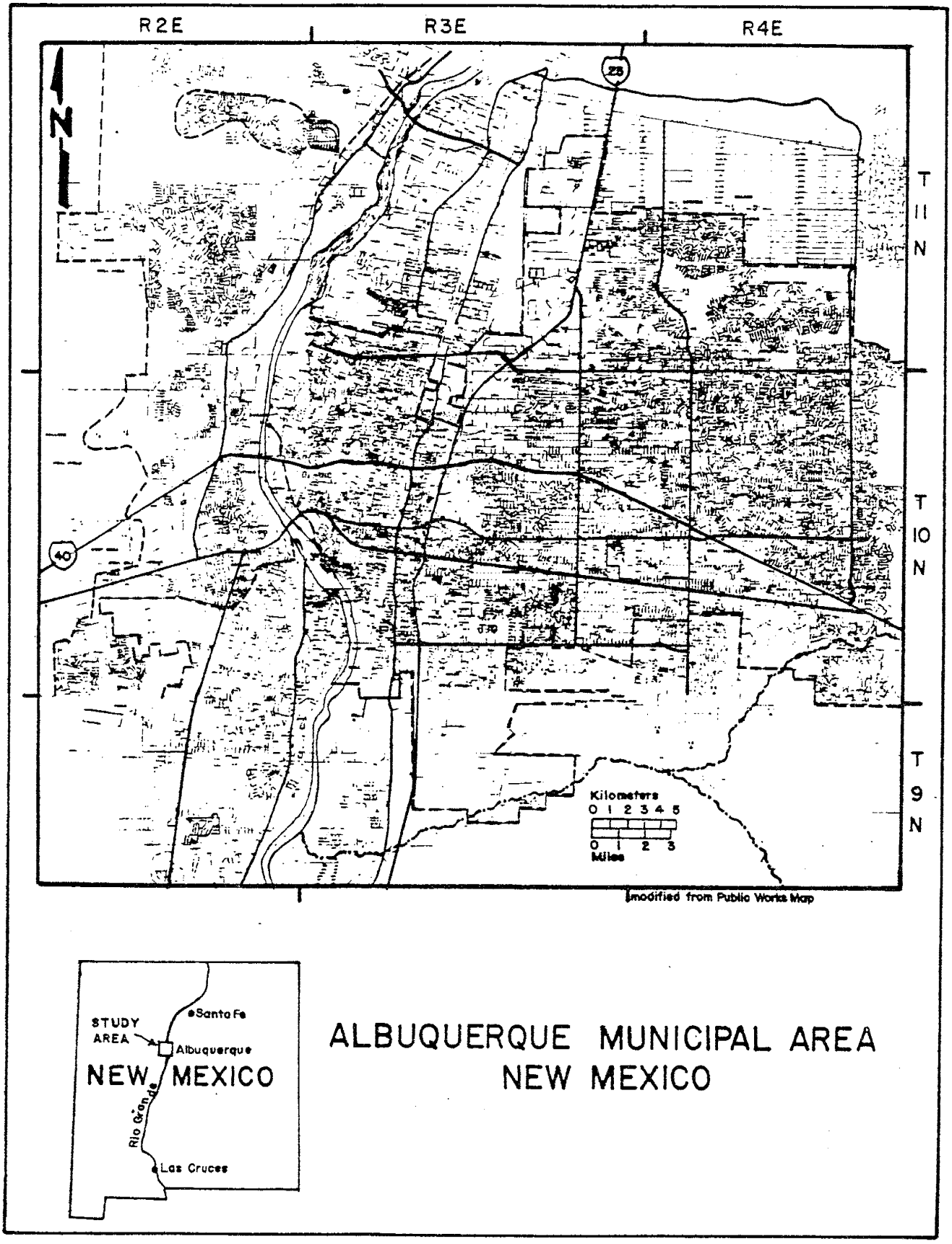

Figure 1: Location of study area showing Albuquerque, New Mexico and surrounding communities.

and Maxwell compiled the first comprehensive qualitative study of the valley-fill (Rio Grande flood plain) and basin-fill (Albuquerque Basin) sediments and their water bearing characteristics. Reeder and others (1967) used the data compiled by Bjorklund and Maxwell (1961) to quantitatively study the river and well-field interactions. Using a digital model approach, Brutsaert and Gebhart (1975) updated the work of Reeder and others (1967). The U. S. Army Corps of Engineers (USACOE, 1978) compiled the most current information on surface and ground-water characteristics in the area. Kernodle and Scott (1986) and Kernodle and others (1987) coded three-dimensional digital programs for simulating steady-state and transient ground-water flow for the Albuquerque-Belen Basin from estimated and measured geohydrologic parameters. Anderholm (1988) wrote a general study of the geochemistry of the Albuquerque-Belen Basin.

ENVIRONMENTAL SETTING

Albuquerque is an urban community located in the arid southwest. Over the last 50 years, the community has changed from an agricultural village of a few thousand people to a city of several hundred thousand people. The arid climate, geology, and the Rio Grande's flood plain all influence the quantity and quality of water available to this growing community. Soils and vegetation, and the community itself through agricultural practices and urban development influence the quantity and quality of water recharging the aquifer.

Demographics and Urbanization

Residential, commercial, and industrial developments cover most of the study area. In 1986, the Bureau of the Census population update estimate for the City of Albuquerque is about 367,000 people while the surrounding

communities have an estimated 34,000 people. Albuquerque has experienced about a 7 percent increase in population and commercial growth since 1969 (Bureau of Census, 1986, and Bureau of Economic Analysis, 1986).

Meteorology

Climate

The Albuquerque area has a typical arid continental climate with low precipitation, cool dry winters, warm summers, low relative humidity and abundant sunshine (N.O.A.A., 1981, Environmental Science Service Adm. 1966). Maximum and minimum temperatures vary over a wide range. For a 70 year period, normals ranged from 8°C (46°F) in January to 33°C (91°F) in July (National Weather Service of Albuquerque, 1981).

Local topography greatly influences the amount of precipitation the area receives. Generally, the higher elevation areas receive greater amounts of precipitation as a result of the cooling effect on a rising air mass. Sandia Crest, at an elevation of 3170 m (10,400 ft), receives about 61 cm (24 in) of moisture per year while the Albuquerque Airport, at 1618 m (5310 ft) receives fewer than 23 cm (9 in) per year. Figure 2 graphically shows the annual variations in precipitation between the Sandia Crest and the airport. The official average annual precipitation for Albuquerque is 20.98 cm (8.26 in). Mean monthly

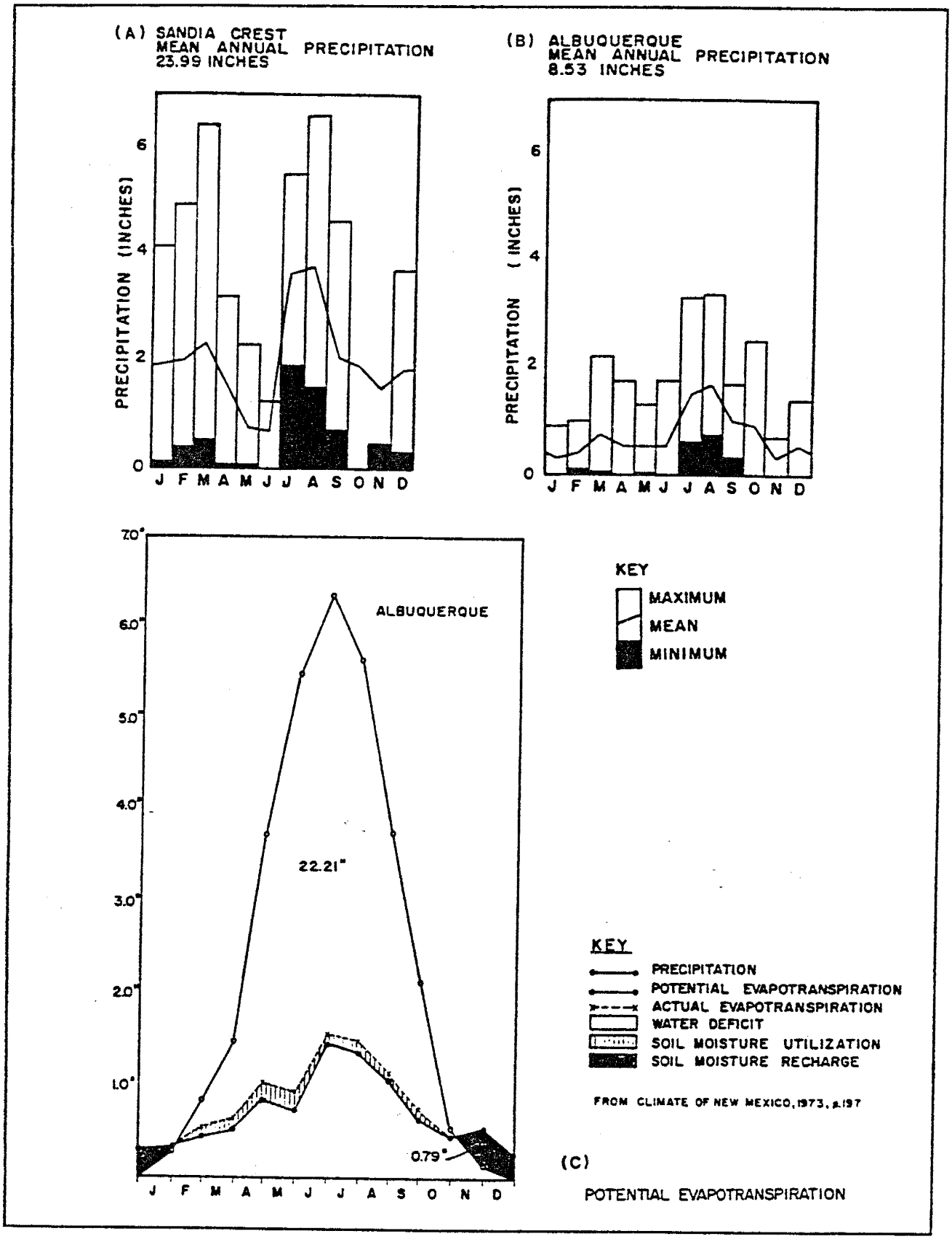

Figure 2: Elevation effect on mean annual precipitation (A,B); Thornthwaithe evapotranspiration graph for Albuquerque (C). (USACOE, 1979, fig. 2.6 and 2.7)

precipitation ranges from 0.91 cm (0.36 in) in January to 3.66 cm (1.44 in) in July (USACOE, 1979).

Summer precipitation comes from the Gulf of Mexico and falls predominantly in July, August and September. Characteristically these are convective storms. Warm moist air masses are orographically or convectively lifted, condensing as they cool. Summer storms do not distribute precipitation uniformly over the Albuquerque area but rather, as locally intense rains of short duration. Figure 3 graphically shows the duration and volume of precipitation for four summer storms and the difference in volume at two locations for one storm (O'Brien & Assoc., 1971). The storm of July 9, 1988 (not shown on figure 3) dropped 2.54 cm (1 in) of rain at the Albuquerque Airport, while fewer than eight miles to the northeast, over 18 cm (7 in) of rain fell near the mouth of Embudo Canyon (Albuquerque Journal, July 10,1988). Summer storms of long duration and low intensity rarely occur in the Albuquerque area (N.O.A.A., 1981).

Winter is the driest time of the year with the dominant source of precipitation from the Pacific Ocean. As winter storms move across the continent they lose most of their moisture before they reach New Mexico. As a result, available moisture is greatly reduced, and what does reach the area usually falls in the form of snow. Winter precipitation accounts for less than 14 percent of the total mean annual precipitation.

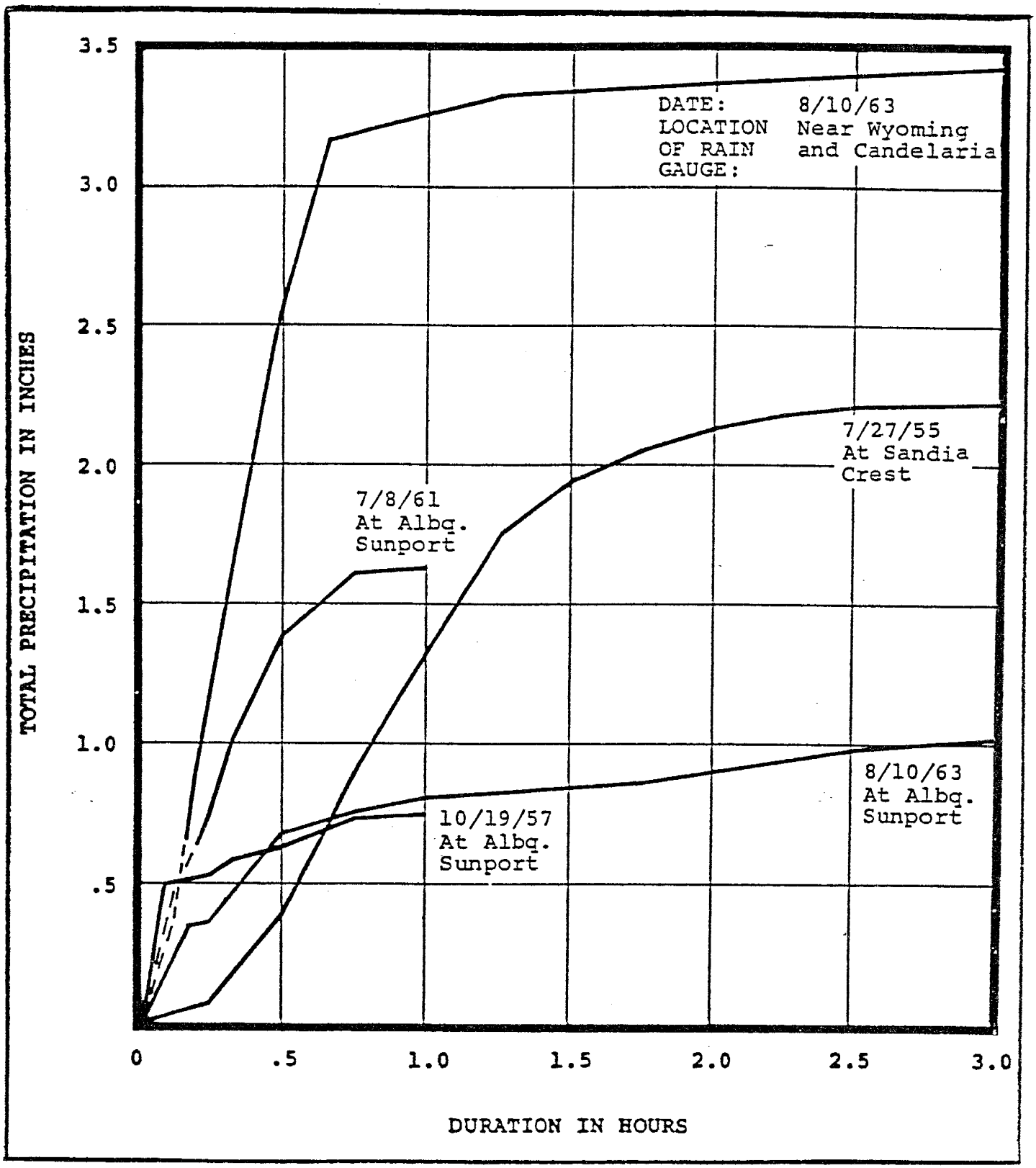

Figure 3: The intensity, duration, and distribution of summer storms are variable within the study area (O'Brein & Associates, 1971).

Evapotranspiration

Estimated evapotranspiration losses are about 95 percent of the precipitation for the Albuquerque area. High daytime temperatures coupled with low relative humidity and a high percentage of available solar radiation create a soil moisture deficit for most of the year. For the Albuquerque area, the computed rate of potential evapotranspiration, using the Thornthwaite method, is 78.5 cm (30.9 in) (USACOE, 1979). Figure 2c shows the potential evapotranspiration (ET) curve, and the actual ET curve imposed on the average precipitation curve for Albuquerque. From these curves you can see the only months of potential recharge would be from November to January. The Thornthwaite method does not account for the vegetative density of a region and may be too high for the spring and early summer and too low for the mid-summer months (Fetter, 1980).

Soils

The following soil characteristics summary for central Bernalillo County is from the United States Department of Agriculture's (1977) soil survey. Soils affect ground-water quality by contributing minerals and gases to the water as it percolates through the soil. Soil texture influences infiltration rates thus helps determine if either moisture flows below the zone of evapotranspiration

to recharge the aquifer or if moisture remains near the surface precipitating dissolved solids as caliche or salts in the soil zone as it evaporates.

Soils in the Albuquerque area fall into four main categories: (1) soils which form on parent rock in the steep uplifted areas; (2) soils on old piedmont and alluvial fans adjacent to the uplifted areas; (3) soils in arroyos and terraces incised deep into the old alluvial fans and in the flood plain of the Rio Grande with its associated terraces; (4) and a soil of minor spatial extent developed on the basalt flows northwest and southwest of the City.

On figure 4, soils type 12 and 13 formed on the steep slopes of the Sandia and Manzano mountains. These soils developed on the residuum from weathered parent rocks of limestones, granites, schists and sandstones at elevations of 1830 to 3200 m (6,000-10,500 ft). Bedrock is usually within 24 to 76 cm (10-30 in) of these soils and the soil is very cobbly, stony, loamy and well drained.

Deep soils on the piedmont and old alluvial fans (types 4,5, and 6 on figure 4) on high mesas east and west of the City are generally well drained with a surface layer of fine sandy loam and underlayers of gradually more coarse, sandy to gravely, calcareous loam.

In the Rio Grande flood plain, Tijeras arroyo and dissected terraces are the deep soils with a surface layer of calcareous loam underlain by layers of fine sandy loam and old alluvial sand and gravel (type 1,2,3 on figure 4).

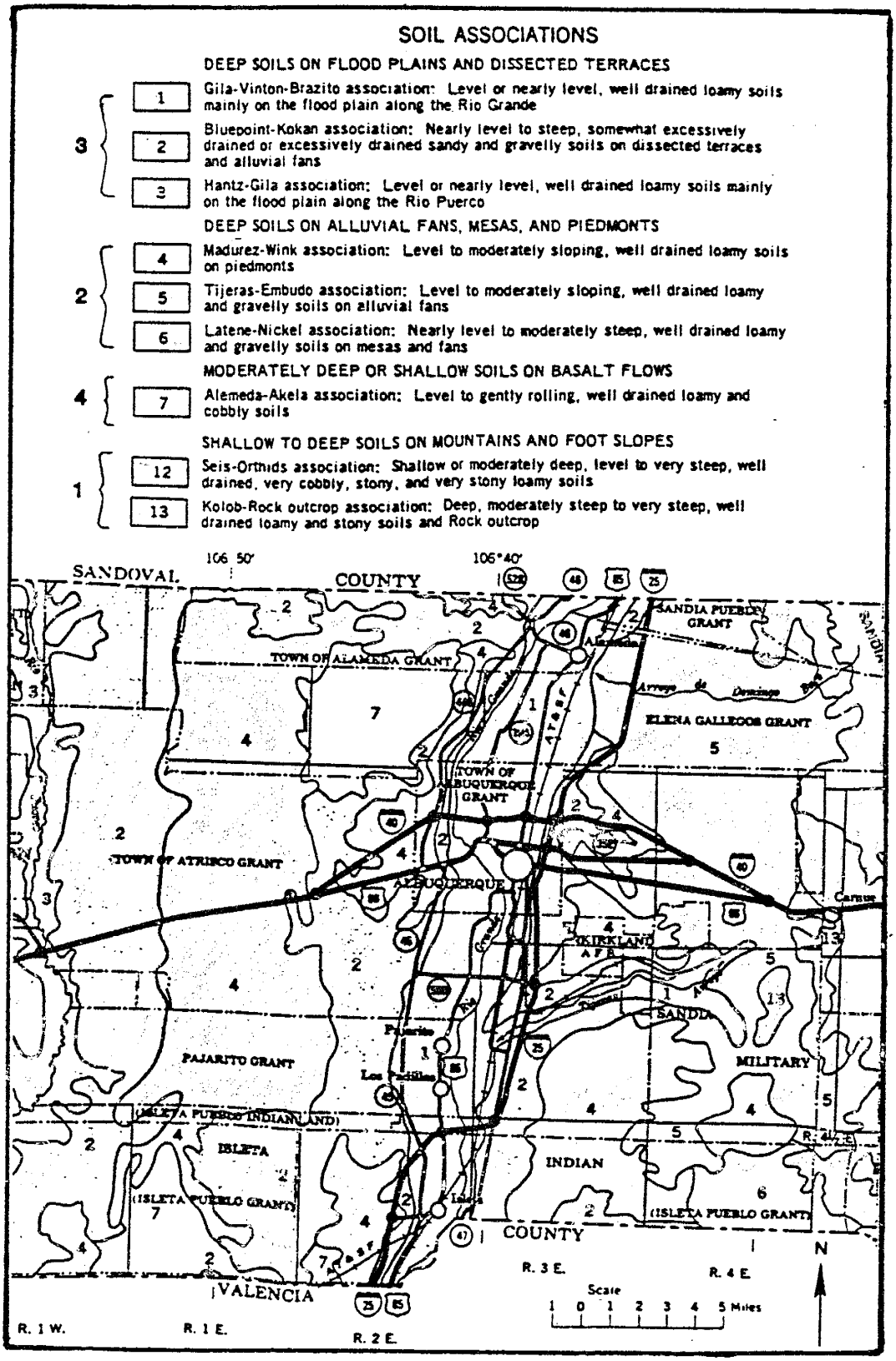

Figure 4: Index map of soil associations for central Bernalillo County (USDA-SCS, 1977).

Two areas on the West mesa are underlain by basaltic flows with 51 to 102 cm (20-40 in) of well drained loamy cobbly soils (type 7 on figure 4).

Vegetation

Native vegetation is dependent on altitude and water availability. Near the top of the Sandia Mountains, at elevations over 2440 m (8000 ft), stands of conifers and aspens dominate the flora with fields of wildflowers and grasses. At elevations between 1830 to 2440 m (6000-8000 ft) oneseed juniper and pinon pine trees are dominant with grasses and some pricklypear and cholla cacti. On high mesas, east and west of the City, at elevations up to 1830 m (6000 ft) sparse vegetation consists primarily of grasses, tumbleweeds, sage and various cacti. Near the mouth of canyons emanating from the Sandia Mountains, phreatophytes grow on the banks of arroyos and in the alluvial fan deposits. O'Brien, et al. (1971) suggested these are indicators of perched water tables or springs. In the tributaries and flood plain of the Rio Grande, at elevations of 1478 to 1829 m (4850-6000 ft), phreatophytes, such as cottonwoods, fourwing saltbush, and grasses abound (USDA,SCS,1977; O'Brien & Assoc., 1971).

Physiography

The Albuquerque area is in the Basin and Range physiographic sub-province called the Mexican Highlands. The Rio Grande flows southward through a long narrow

structural basin bounded on either side by fault blocks, alluvial fans and erosional terraces. Lambert (1968) divided the area into five topographic segments: (1) the inner valley of the Rio Grande; (2) the Llano de Albuquerque; (3) the Sandia piedmont plain; (4) the inner-valley border surfaces, (5) and the Sandia Mountains. In this study a combination of Lambert's (1968), Kelley's (1982) and local nomenclature is used to describe physiographic or geographic areas. Figure 5 is modified from Kelley's (1982) map showing the location and names of physiographic features in the study area.

The Rio Grande's flood plain (inner-valley) slopes southward about 1 m/km (5 ft/mi). It is a shallow, flat-bottomed trench 4.8 to 6.4 km (3-4 mi) wide bordered by dissected scarps rising about 4.6 to 122 m (15-400 ft) above the valley floor. Quaternary alluvium fills the incised inner valley of the Rio Grande.

On the western boundary of the study area, the Llano de Albuquerque forms a north-trending upland plain 8 to 10 km (5-6 mi) wide and sloping to the southeast at 8 to 13 m/km (40-70 ft/mi). The valley border surfaces formed on the flanks of the topographically high Llano de Albuquerque are locally known as the "West Mesa" (II and III on figure 5) These westward bordering mesas are coalesced alluvial deposits dissected by tributary streams which exposed axial stream gravels of the ancestral Rio Grande. A small area is overlain by basalt fissure flows which form a resistant cap

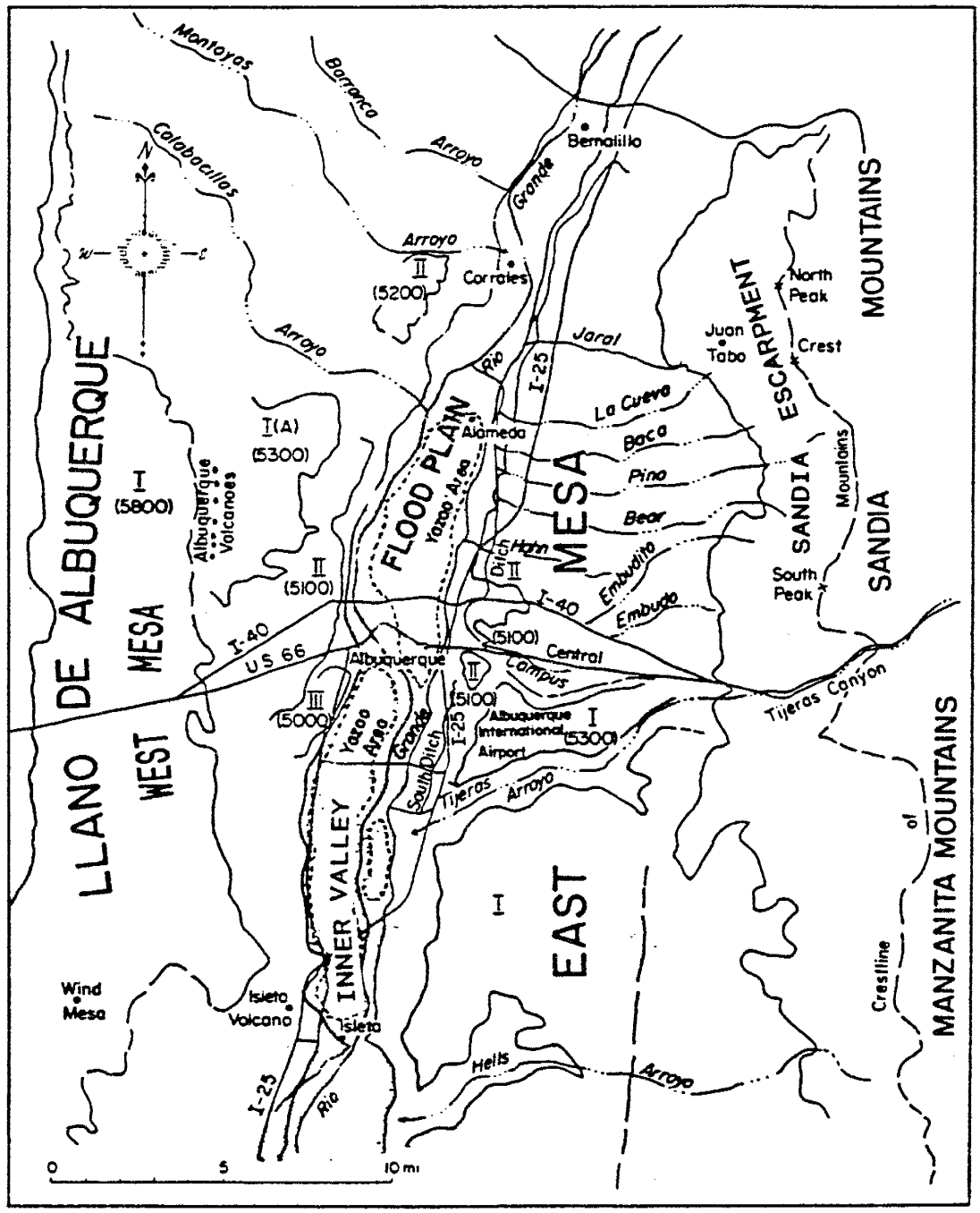

I. High mesas
I(A). Volcanoes submesa
II. West and east terraces
III. Lower terrace along Coors Boulevard

Elevations above sea level are shown in parentheses.

Figure 5: Physiographic features and local nomenclature (modified from Kelley, 1982).

rock (IA on figure 5; Kelley, 1977).

On the eastern side of the flood plain, the bluffs and eroded slopes rise toward the coalescing fans of the alluvial Sandia piedmont plain, locally called the "East Mesa" (I and II on figure 5). This partially dissected piedmont plain slopes westward 38 m/km (200 ft/mi) from its eastern boundary to 3 m/km (15 ft/mi) on its western edge. The piedmont extends westward from the base of the Sandia Mountains for 11 to 13 km (7-8 mi) to the present-day inner valley. Piedmont deposits are coalesced alluvial fans which interfinger with a succession of former inner valleys of the Rio Grande. Altitudes of the piedmont plain vary from about 1,829 m (6000 ft) near the base of the Sandia Mountains to about 1478 m (4850 ft) in the flood plain of the Rio Grande (Lambert, 1968).

Rising above the piedmont plain are the block-faulted Sandia Mountains which slope eastward and are the main source of detrital material forming the piedmont plain at its westward base.

GEOLOGIC SETTING

Regional Geology

Rio Grande Rift Basins

The Albuquerque area lies within the Rio Grande depression, a structural trough formed by a series of linked basins trending north-south through central New Mexico to southern Colorado. These tectonic structures are part of the northward extension of the Basin and Range Province. Figure 6 shows the staggered uplifts and benches of pre-Tertiary rocks along the boundaries of this extensive system of horsts, grabens and tilted fault-block mountains in central New Mexico (Kelley, 1977).

Laramide wrench faulting in the Eocene and two subsequent episodes of crustal extension formed the Rio Grande rift basins. The first extension episode occurred in the Oligocene, producing broad, relatively shallow basins. Volcanism was active at the same time both in and out of the rift basins (Morgan et al., 1986; Lozinsky,

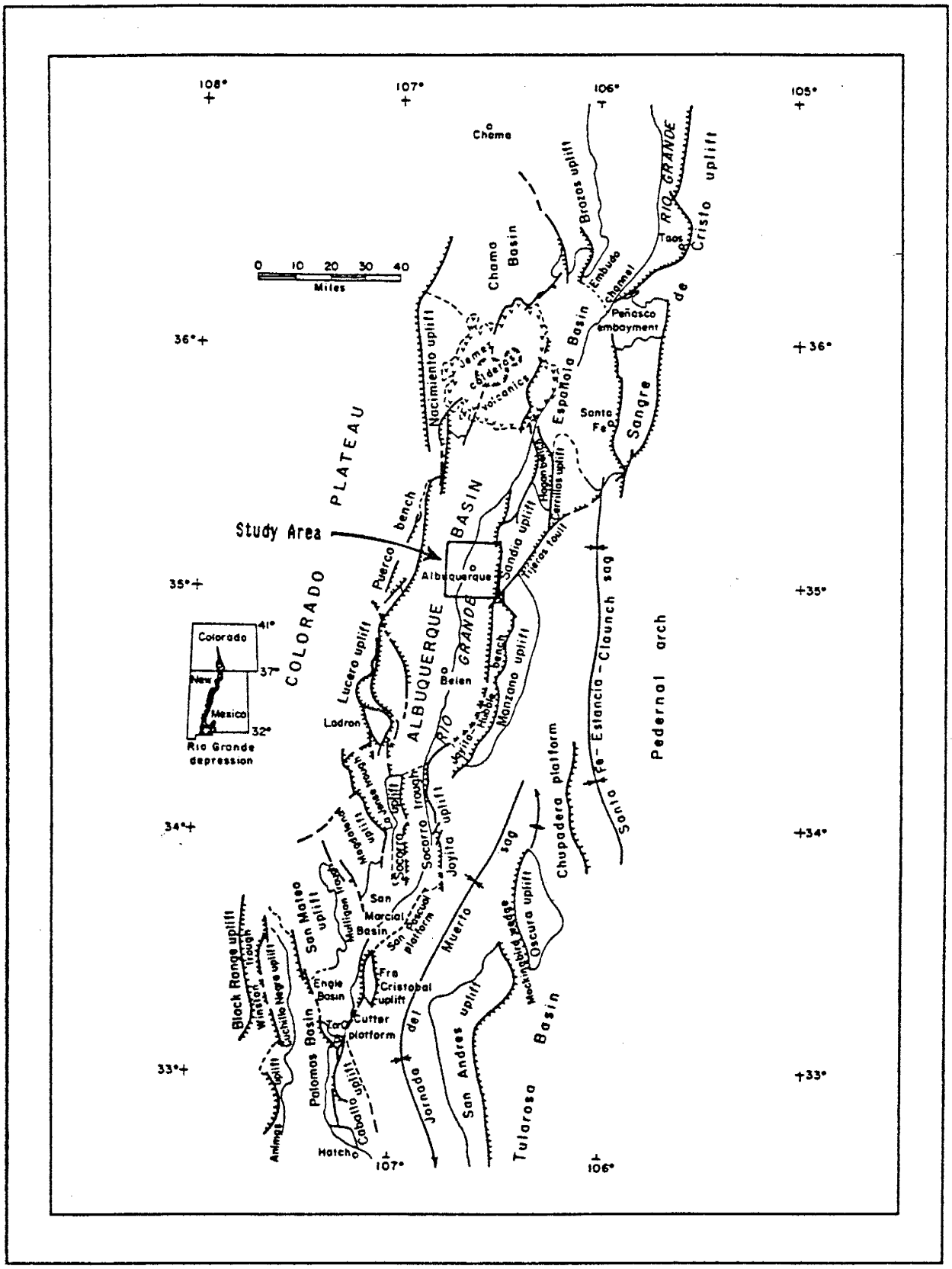

Figure 6: Tectonic map of the Rio Grande Rift system in New Mexico (modified from Kelley, 1977, fig. 13)

1988). Active tectonism continued from late Oligocene to mid-Miocene. During the mid-Miocene, tectonic and volcanic activity were low. A second episode of crustal extension began in the late Miocene with accelerated block faulting and volcanism (Morgan et al., 1986).

As the grabens subsided, the structural valleys filled with alluvial sediments, volcanic rocks and interstitial waters from the depositing streams. Long low-dip alluvial slopes formed in the subsiding basins. These basin-fill deposits are an estimated 5500 m (18,000 ft) thick in some areas (Kelley, 1977).

Albuquerque-Belen Basin

The study area lies in the Rio Grande rifts largest structural basin, the Albuquerque-Belen Basin (outlined on figure 6). Bordering this basin on the west are the Colorado Plateau, a region of high mesas and plateaus, and the southern extension of the Nacimiento uplift. On the northern end of the basin is the Jemez volcanic complex. The eastern basin boundary is formed by the uplifted Sandia-Manzano-Los Pinos eastward tilting fault blocks. Closing the basin to the south is the Socorro constriction (Kelley, 1977).

Lozinsky's (1988) interpretation of the Albuquerque-Belen Basin development history is the basis for the following discussion. From seismic reflection data, Lozinsky suggested the Albuquerque-Belen Basin was

initially two closed basins which formed during the initial rifting episode. Detritus from sedimentary and plutonic rock accumulated in these basins through middle Oligocene time. Lozinsky termed these basin-fill sediments pre-Santa Fe Tertiary deposits to distinguish them from the principal basin-fill sediments of the Santa Fe Group. Both drainage basins were closed at this time.

Earliest Santa Fe Group deposition (30 to 15 Ma) began during the first rifting episode about mid-Oligocene. Sedimentary and volcanic terrains contributed sediment at a rate of about 24 to 74 m/Ma. At about 10 Ma the eastern uplifted areas began to shed Precambrian-granitic detritus into the basins.

Renewed tectonic activity (10 to 5 Ma) during the second extension episode increased the sedimentation rate to 200 to 600 m/Ma causing rapid aggradation to fill and connect the two basins into a single basin. Basin-fill materials came from sedimentary, volcanic and Precambrian-granitic terrains. Mafic volcanism increased its contribution to the sediment accumulating in the closed drainage basin.

Basin drainage shifted from closed to through-flowing at about 5 Ma with the development of the ancestral Rio Grande. Two major tributaries joined the ancestral Rio Grande to deposit a large fluvial plain in the central basin. Sedimentation rates slowed to about 20 to 30 m/Ma. Through-flowing streams mixed and deposited sediments from surrounding highlands and from sources outside the basin.

Local Geology

Locally, a broad plain of low slope had formed at the level of the present-day Volcano Cliffs (IA on figure 5) at 1720 m (5600 ft) and the University of New Mexico at about 1580 m (5160 ft) during the Pleistocene (1 Ma). The ancestral Rio Grande meandered across this broad plain continuing to fill the basin (Kelley, 1977, 1982).

A line of fissure-controlled eruptions spread 5 to 6 sheets and many sills and dikes of basalt onto and into the wide plain which gently sloped toward the Rio Grande. The West Mesa volcanic field was active between 0.5 to 1 Ma and has been extinct for roughly 0.25 Ma (Kelley, 1982).

Santa Fe Group deposition ended by about 0.5 Ma when the drainage system changed from a depositional to an erosional regime. A series of entrenchment cycles began to carve the present-day inner-valley. (Kelley, 1977, 1982; Lozinsky, 1988). About 20,000 years ago the river returned to a depositional mode, filling its eroded valley with 20 to 40 m (75-130 ft) of mud, sand, and gravels which now form the inner-valley aquifer (Lambert, 1968; Kelley, 1982). Subsequent drainage from the mountain flanks and the river have exposed past episodes of basin filling. Figure 7 is Lambert's (1968) cross-section showing the Quaternary and Tertiary deposits and several cut and fill cycles that formed the present-day Rio Grande inner valley.

On the west side of the river rises the high mesa Llano de Albuquerque. This surface is part of the larger

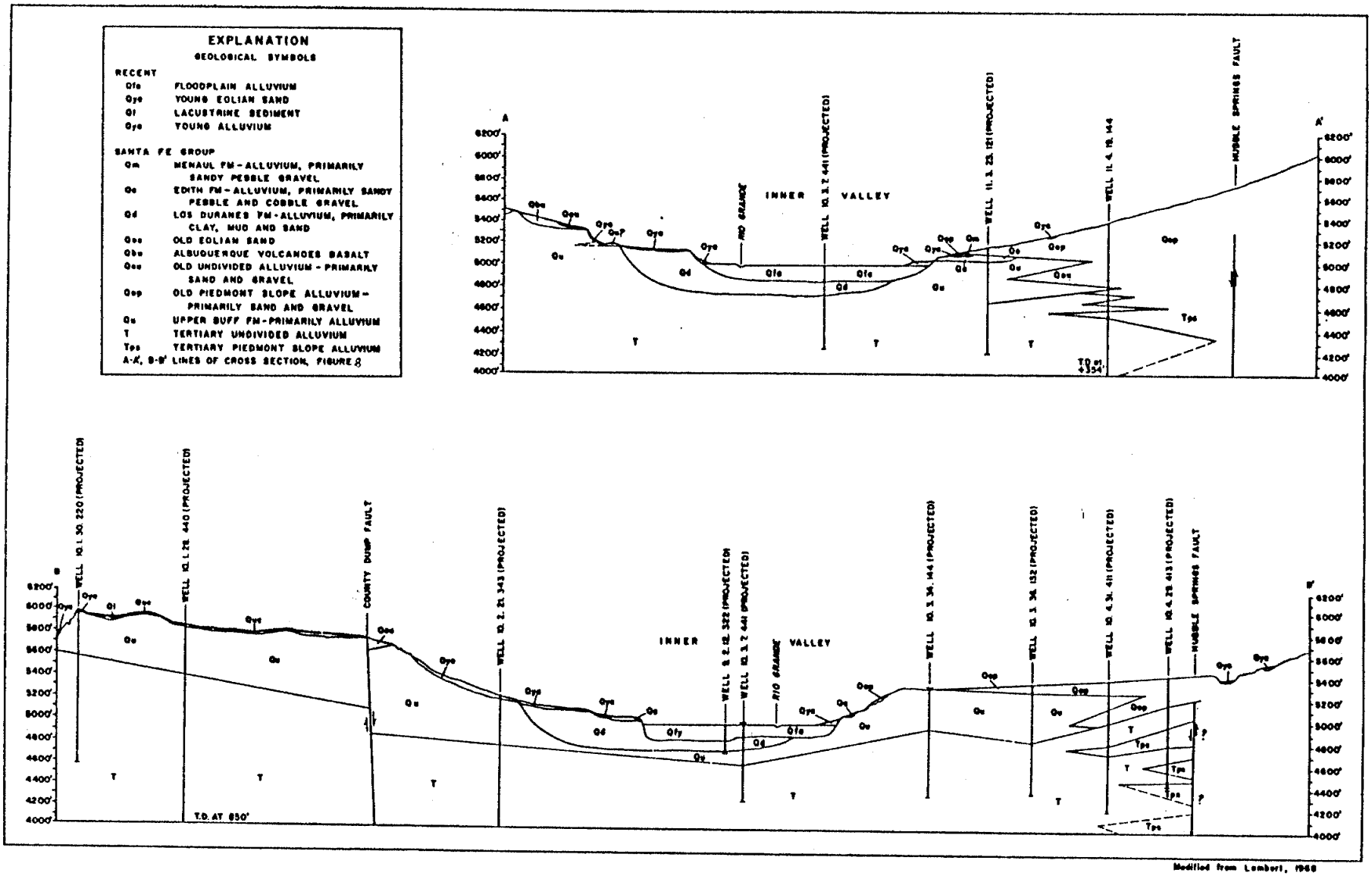

Figure 7: Quaternary and Tertiary facies relationships. Line of sections shown on figure 8, A-A', B-B'(Lambert, 1968).

Ceja Mesa which is 80 km (50 mi) long and 8 km (5 mi) wide. The central portion of Ceja Mesa near Albuquerque was uplifted about 91 m (300 ft) and tilted along two sets of fault zones found on the east and west sides of the mesa. The uplift and tilting of the Ceja Mesa is apparently associated with the southern extension of the Nacimiento uplift to the north (Kelley, 1982). The high mesas formed by the uplifted Ceja Mesa and the incised inner valley were subsequently eroded by the Rio Grandes tributaries.

Bounding the Albuquerque area on the east is the tilted fault block of the Sandia Mountains. As the great trough subsided in the late Miocene, the Sandia block tilted 15 degrees eastward exposing 1200 vertical meters (4000 ft) of Precambrian granitic rock to erosion. Near the top of this steep escarpment is the Great Unconformity, encompassing over 1 billion years, which is capped by several hundred meters (200' ft) of Pennsylvanian age (310 Ma) limestone (Kelley, 1982). Figure 8 is a modified segment of Kelley's (1977) Albuquerque Basin geologic map which shows the spatial relationship and surface exposures of the local geology.

Stratigraphy

Table 1 is a generalized stratigraphic chart of Albuquerque basin geologic units compiled by Bjorklund and Maxwell (1961). These units range in geologic age from

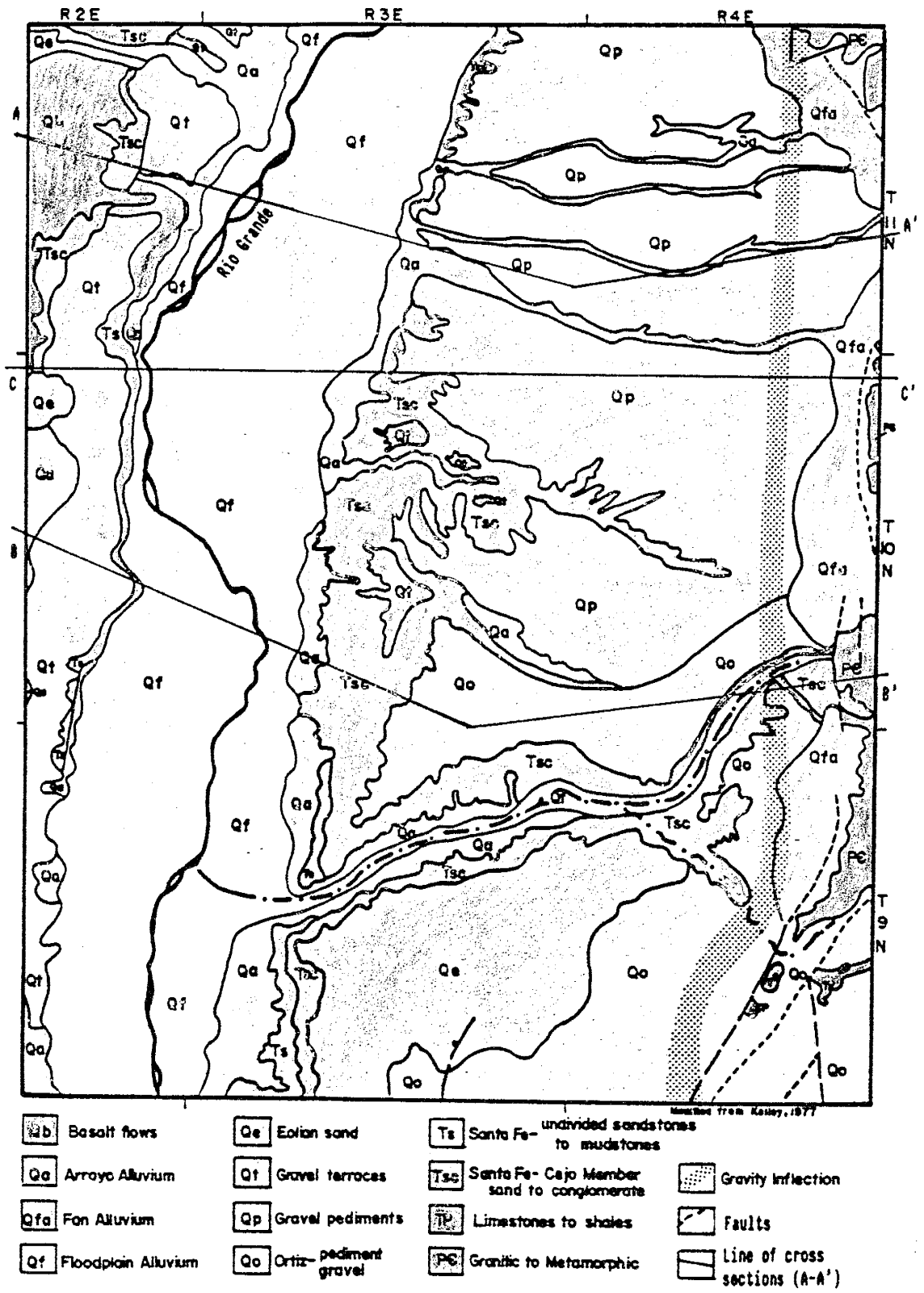

Figure 8: Geologic map of the Albuquerque area with the line of section for figure 7 (A-A',B-B') and figure 9 (C-C').

Table 1: Generalized stratigraphic chart of local geologic formations and their water bearing characteristics (Bjorklund and Maxwell, 1961).

ERA	SYSTEM	SERIES	UNIT	THICKNESS (FEET)	LITHOLOGY	WATER-BEARING CHARACTERISTICS
CENOZOIC	QUATERNARY	RECENT	ALLUVIUM	0 TO 120±	COBBLES, GRAVEL, SAND, SILT, AND CLAY; UNCONSOLIDATED. GENERALLY UNDERLIES VALLEY FLOOR.	YIELDS LARGE QUANTITIES OF WATER OF GOOD TO FAIR QUALITY TO IRRIGATION, INDUSTRIAL, STOCK, AND DOMESTIC WELLS. WATER GENERALLY HAS A HIGH SILICA CONTENT.
			BAJADA DEPOSITS	0 TO 300±	BOULDERS, COBBLES, GRAVEL, SAND, AND SILT, CONSISTING OF FRAGMENTS OF FELDSPAR, QUARTZ, AND IGNEOUS AND METAMORPHIC ROCKS; UNCONSOLIDATED TO LOOSELY CONSOLIDATED.	GENERALLY LIE ABOVE THE WATER TABLE EXCEPT ALONG THE MOUNTAIN FRONT AT THE CONTACT WITH PRE-TERTIARY ROCKS. YIELD SOME WATER TO CONTACT SPRINGS AND MAY YIELD WATER TO A FEW DOMESTIC AND STOCK WELLS.
		PLEISTOCENE (?)				
	TERTIARY	MIOCENE (?)	SANTA FE GROUP	0 TO 6,100	BOULDERS, COBBLES, GRAVEL, SAND SILT, AND CLAY; UNCONSOLIDATED TO CONSOLIDATED BUT GENERALLY WEAKLY CEMENTED. INCLUDES INTERBEDDED VOLCANIC MATERIAL LOCALLY.	YIELDS LARGE QUANTITIES OF WATER OF GOOD QUALITY TO MUNICIPAL, INDUSTRIAL, IRRIGATION, STOCK, AND DOMESTIC WELLS. WATER GENERALLY HAS A HIGH SILICA CONTENT.
		EOCENE	ESPINAZO VOLCANIC ROCKS OF STEARNS (1943)	400 TO 1,400	BRECCIA, CONGLOMERATE, AND TUFF.	DEEPLY BURIED IF PRESENT; NO WELLS ARE KNOWN TO BE COMPLETED IN THIS FORMATION.
		EOCENE AND OLIGOCENE (?)	GALISTEO FORMATION	900 TO 4,000	SANDSTONE, SAND, CLAY, AND SHALE.	DO.
MESOZOIC	CRETACEOUS	UPPER	MESAVERDE GROUP	1,500 TO 2,000	PREDOMINANTLY GRAY TO BLACK SHALE, INCLUDES SEVERAL PROMINENT BEDS OF BUFF-COLORED TO GRAY SANDSTONE AND SOME THIN BEDS OF COAL.	NO WELLS TAP THIS UNIT BECAUSE OF GREAT DEPTH. SANDSTONE BEDS YIELD WATER OF FAIR TO POOR QUALITY TO STOCK AND DOMESTIC WELLS IN ADJOINING AREAS.
			MANCOS SHALE	600 TO 2,500	PREDOMINENTLY GRAY TO BLACK SHALE; INCLUDES SEVERAL BEDS OF BUFF-COLORED TO GRAY SANDSTONE.	DO.
		LOWER	DAKOTA SANDSTONE	75 TO 110	SANDSTONE, BUFF TO TAN; INTERBEDDED SHALE.	DO.
	JURASSIC	UPPER	MORRISON FORMATION	210 TO 660	SHALE, GREEN, PINK, GRAY, AND MAROON, AND WHITE AND BUFF SANDSTONE MEMBERS.	DO.
		ZUNI SANDSTONE	BUFF SANDSTONE	100 TO 140	SANDSTONE, BUFF.	DO.
			SUMMERVILLE FORMATION	60 TO 120	SANDSTONE AND SANDY SHALE, RED TO GRAY.	DO.
			TODILTO LIMESTONE	40 TO 250	TWO BEDS OF LIMESTONE SEPARATED BY A THICK BED OF GYPSUM.	BURIED DEEPLY; YIELDS LITTLE OR NO WATER. WATER HAS A HIGH SULFATE CONTENT.
			ENTRADA SANDSTONE	100 TO 225	SANDSTONE, CROSS-BEDDED, RED TO GRAY.	BURIED DEEPLY; YIELDS WATER TO STOCK AND DOMESTIC WELLS IN ADJOINING AREAS. QUALITY OF WATER GENERALLY POOR BECAUSE OF HIGH SULFATE CONCENTRATION.
	TRIASSIC	UPPER	CHINLE FORMATION	1,100	SHALE, RED, AND CHANNEL DEPOSITS OF SHALY SANDSTONE; CONTAINS BEDS OF RED SANDSTONE AT TOP AND BOTTOM.	BURIED DEEPLY; YIELDS NO WATER TO WELLS. SANDY ZONES YIELD WATER TO DOMESTIC AND STOCK WELLS IN ADJOINING AREAS. QUALITY OF WATER GENERALLY IS POOR.
PALEOZOIC	PERMIAN		SAN ANDRES LIMESTONE	47 TO 470	INTERBEDDED LIMESTONE, GYPSUM, AND SANDSTONE.	BURIED DEEPLY; YIELDS WATER TO STOCK AND DOMESTIC WELLS IN ADJOINING AREAS.
			GLORIETA SANDSTONE	70 TO 220	SANDSTONE, FINE-GRAINED, BUFF TO WHITE, CONTAINS GYPSUM IN SOME AREAS.	DO.
			YESO FORMATION	400 TO 1,100	SANDSTONE AND SILTSTONE, TAN-BROWN TO RED.	BURIED DEEPLY; YIELDS LITTLE OR NO WATER TO WELLS.
			ABO FORMATION	810 TO 950	SANDSTONE, FINE- TO COURSE-GRAINED, AND SILT STONE; RED TO GRAY.	BURIED DEEPLY; YIELDS SMALL QUANTITIES OF WATER TO STOCK WELLS IN ADJOINING AREAS.
	PENNSYLVANIAN		MADERA LIMESTONE	450 TO 2,000	LIMESTONE, GRAY TO RED; UPPER PART INCLUDES MORE CLASTIC MATERIAL THAN LOWER PART.	BURIED DEEPLY; ARKOSIC MEMBER YIELDS SMALL QUANTITIES OF WATER TO STOCK AND DOMESTIC WELLS IN ADJOINING AREAS.
			SANDIA FORMATION	0 TO 415	SANDSTONE, SHALE, AND LIMESTONE, BROWN, GRAY, RED, AND BLACK; UPPER PART GENERALLY CLASTIC MATERIAL, LOWER PART GENERALLY LIMESTONE.	BURIED DEEPLY; YIELDS SMALL QUANTITIES OF WATER TO STOCK AND DOMESTIC WELLS IN ADJOINING AREAS.
PRECAMBRIAN				15,000+	METAMORPHIC AND IGNEOUS ROCKS.	SUPERFICIAL WEATHERED AND FRACTURED ZONES YIELD SMALL QUANTITIES OF WATER OF SPRINGS AND WELLS ALONG MOUNTAIN FRONT FOR STOCK AND DOMESTIC SUPPLIES.

Precambrian plutonic and metamorphic rocks to Quaternary alluvium. Unit names and ages for the Tertiary deposits have been refined by later workers such as Lambert (1968), and Lozinsky (1988) but unit age divisions and names are still controversial. It is beyond the scope of this study to present the arguments for unit divisions. Bjorklund and Maxwell's chart illustrates the sequence of basin geologic units and gives a summary of their water-producing characteristics which are pertinent to this study.

Precambrian Source Rocks

The Sandia Mountain escarpment is predominantly composed of Precambrian Sandia Granite, a light colored porphyritic pluton which outcrops for about 32 km (20 mi) from Township 9 North, section 14 to Township 12 North, section 7. Figure 8 shows some outcrops of the Sandia Granite along the eastern boundary but most exposures lie beyond the map area. The average mineral composition for the granite is 35 percent quartz, 15 percent microcline phenocrysts, 35 percent albite and oligoclase, and 10 percent biotite. Accessory minerals are commonly sphene, magnetite and epidote with some occurrences of hornblende, muscovite, tourmaline or pyrite (Kelley and Northrop, 1975).

Precambrian plutonic rock derived from the steep escarpment is the main source of detrital material for the alluvial fans and basin-fill deposits at the base of the Sandia Mountains. Precambrian metamorphic and Pennsylvanian

limestones on the west-facing escarpment contribute minor amounts of basin-fill material to the study area.

Tertiary and Quaternary Deposits

Tertiary and Quaternary sediments outcrop over most of the study area with minor volcanic occurrences (figure 8). Collectively these deposits are an assemblage of alluvial-slope fans, flood-plain alluvium, pediment covers, playa deposits, thin eolian blankets, and volcanics.

Near the base of the Sandia uplift, unconsolidated, ill sorted, poorly stratified, clastic sediments form coalescing alluvial-slope fans (bajada) to a maximum depth of 3048 m (10,000 ft) (Lambert,1968). These bajada deposits consist of gravels, sands, and micacious silts. Sediment grain sizes decrease down slope from the apex of individual fans. Lambert's cross-section, figure 7, illustrates the abrupt variability of these fan deposits both laterally and vertically, and their regular interfingering with the ancestral Rio Grande fluvial deposits.

Tertiary Rio Grande flood-plain deposits are a mixture of poorly consolidated to unconsolidated sediments with interbedded volcanic rock and debris derived from the northern highlands and local bajadas. Detrital material of quartz and feldspar fragments, clasts of volcanic, metamorphic and sedimentary rock are boulder to clay size. Quaternary deposits of reworked Tertiary sediments cover

the incised flood plain and its tributaries. These deposits are 25 to 35 m (80-120 ft) thick and are more organic rich than the older basin-fill deposits.

Surficial deposits of weathered granitic and metamorphic rocks form pediment covers on canyon floors along the westward facing Sandia Mountain front. Eolian blankets and playa deposits form thin veneers of reworked Quaternary and Tertiary sediments on the older deposits forming the East and West Mesas (Lambert, 1968).

In the subsurface, a few basalt flows and tuff beds are interbedded with the basin-fill material of the West Mesa (Kelley & Kudo, 1978). Detrital tuff and pumice are commonly found in the Santa Fe beds of both the East and West Mesas (Lambert, 1968).

Caliche beds occur in several locations on the East and West Mesas, and the Llano de Albuquerque. Caliche beds interbedded with basin fill were found in deep drill holes (Bjorklund and Maxwell, 1961, O'Brien and Assoc., 1971).

The name Santa Fe Group is commonly used as a synonym for the basin-fill deposits containing the areas principal aquifer; a usage that implies both a depositional history and a geologic time sequence. In this study, the unit which contains the principal water bearing unit will be called the basin-fill sediments, and the thin flood-plain deposits of reworked basin-fill will be called the inner-valley deposits of the Rio Grande. Together the hydraulically connected basin-fill and inner-valley sediments form the aquifer.

Geophysical Investigations

Several geophysical investigations conducted over the Albuquerque Basin and specifically on the West and East Mesas have added to our general knowledge of the basins geometry, boundaries, and nature of the basin fill.

Joesting and others (1961) conducted gravity and aeromagnetic surveys across the central portion of the Albuquerque basin. They found gravity highs in areas of anomalously high water temperatures on the West Mesa and near travertine deposits on the East Mesa. High gravity values are indicative of denser Paleozoic and Precambrian rocks while low gravity values indicate detrital material. Fault zones are generally characterized by steep gravitational field gradients created by rapid density changes over a short horizontal distance. Several closed gravity lows are roughly coincidental to Bjorklund and Maxwell's (1961) tentative ground-water trough under the West Mesa. Joesting and others (1961) suggested these gravity lows are low density, thick sequences of basin fill which are probably related to ancient basin drainage. However, they suggested their anomalous magnetic findings are probably related to horst-like displacement of pre-rift rock and shallow buried volcanic rock under the West Mesa.

In 1980, Birch correlated gravity surveys with density information from deep drill holes to estimate the geometry and volume of upper post-rift deposits in the basin. These

deposits form the principal aquifer throughout the valley. He estimated the average thickness of basin-fill to be about 1.5 km (4900 ft) and the thickness along the eastern margin to exceed 2.5 km (8200 ft). Birch was looking for highs (horsts or igneous intrusions) of low permeability rock which might influence the ground-water flow regime. Figure 9, a projection from Birch's east-west profile, shows a downthrown block of pre-basin Jurassic to Cretaceous rock beneath a field of large capacity wells (Ponderosa well field). On the West Mesa a block of Jurassic to Cretaceous age rock is tilted downward into the basin and could serve as a low permeability barrier to ground-water flow in the more transmissive basin-fill material (Birch, 1980).

Jiracek and others (1982) concentrated their study on the Llano de Atrisco, a segment of the Llano de Albuquerque or West Mesa. They detected apparent resistivity highs and shallow anomalous temperatures where Joesting (1961) measured a gravity high. After comparing their findings with Birch's (1980) gravity data they concluded that the cumulative data were consistent with a shallow horst-like structure. A water well drilled near this site was completed in "rock" hard strata at 418 m (1371 ft) (Bjorklund and Maxwell, 1961). Modeling of the magnetic patterns suggest sill-like bodies, which are probably permeable lava flows and do not act as hydraulic barriers. Their temperature gradient survey is consistent with the U.S. Geological Survey's findings of about 30°C/km (Jiracek

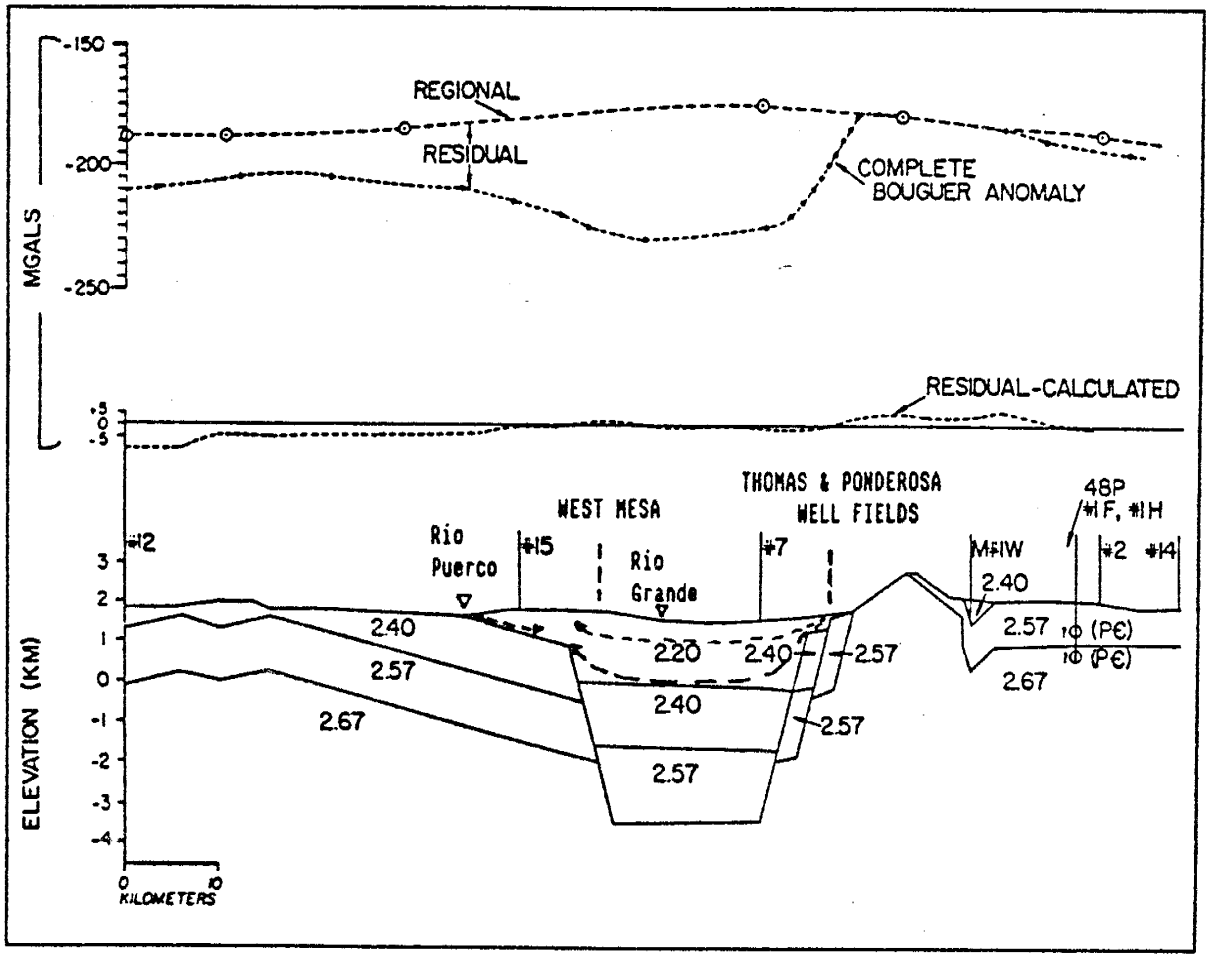

Geologic Age	Thickness (km)	Density (gm/cm³)
Neogene (post-rifting deposits)	1.5 - 2.5	2.20
Jurassic, Cretaceous to Paleogene	1.5	2.40
Paleozoic and Triassic	1.0	2.57
Precambian		2.67

(Modified from Birch, Profile 13, 1980)
profiles not included

Figure 9: Birches interpretation of gravity data along a line located approximately paralell with township 11 north on figure 8 (section line C-C').

and others, 1982).

On the East Mesa, geophysical surveys across the Sandia fault (believed to be the major displacement fault for Sandia Uplift) show abrupt changes in depth to basement rock from 800 m (2600 ft) to more than 1300 m (4300 ft) in about 100 m (325 ft) of horizontal distance (Grant 1982). Aligned with the Hubbell Spring fault are a series of fresh water springs. A high travertine mound is offset 0.8 km (0.5 mi) to the east of the intersection of the Tijeras fault and the Hubbell Spring fault (believed to be an extension of the Sandia fault). The travertine mound covers 97 km^2 (240 ac) and is 38 m (125 ft) high. Travertine is also found along the Coyote Springs arroyo which leads away from the carbon dioxide emitting spring. According to Grant (1982), these travertine hills are evidence of a major fault system through which great volumes of water freely migrated. Subsequently, the migrating fluids plugged the permeable fault zone thereby ending the spring activity (Grant, 1982).

Lozinsky (1988) suggested seismic reflection data from Shell Oil Company showed the basin consisted of two half grabens. In the northern part of the basin, this study area, the faults and eastward tilting half graben are down thrown along listric faults.

These grabens, horsts and faults may serve as conduits or barriers along which deep, geothermally heated, basin waters flow to the near surface. Deep, upward-moving basin waters may be induced into the low pressure cells

created by heavy pumpage of the aquifer.

Two schematic drawings through the central portion of the Albuquerque Basin illustrate geophysical survey interpretation. Figure 10, a block diagram from Black's (1982) article, and figure 9, Birch's cross-section both show the structures which could provide the mechanisms for forced convection of deep basin water upward along low-permeability blocks and the juxtaposition of Cretaceous beds high in salts to high capacity water supply wells. Each mechanism could potentially influence the geochemistry of the water produced near these structures.

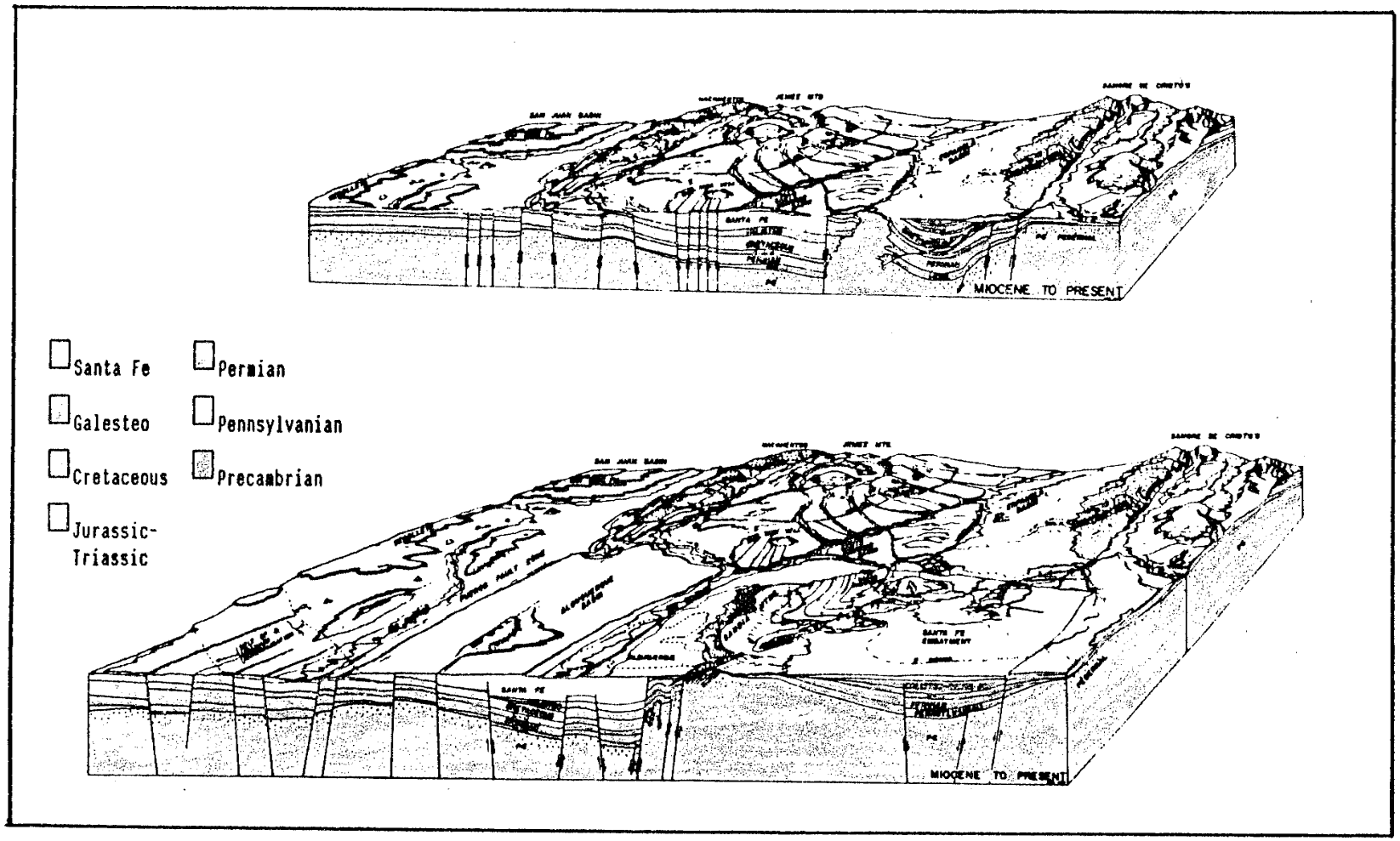

Figure 10: Block diagrams of central New Mexico showing deep basin structures and faults which may serve as barriers and conduits influencing ground-water quality and temperature (Black, 1982).

HYDROLOGIC SETTING

The conceptual model for the regional hydrodynamic system used in this study is based on work done in the 1960's. Current investigators believe the basin ground water system has remained essentially unchanged outside the influence of the City of Albuquerque. In contrast, the local hydrodynamic system has experienced major changes in the last four decades. To reflect these changes I started with the ideas of previous workers and updated their maps to express new information.

Regional Hydrology

The Albuquerque-Belen Basin contains a ground-water system that flows through an area of about 7680 km^2 (2960 mi^2). The largest volume of ground water flows through unconsolidated sediments which are thin on the mountain-front pediments and more that 4400 m (14,450 ft) thick in the central basin. The water table slopes north to south

at about the same gradient as the Rio Grande.

Sources of basin ground water are from the basin margins and flood-plains. Inflow along the basin margins comes from the northeastern and western Espanola and San Juan basins and bordering mountain-fronts. Additional water enters the ground-water system through the flood plain from stream channel seepage, irrigation return flow, septic tank discharge, and infiltration from canals and drains. Precipitation infiltration adds a small amount to the ground water (USACOE, 1979).

Water-bearing alluvial sediments are hydraulically connected and act as a single, large, aquifer. The aquifer may be divided into three water-bearing units, the primary unit and two minor units. Figure 11 shows the spatial and hydraulic relationships between units.

The primary aquifer unit produces from 1 to 11 m^3/min (300-3000 gpm) of water from high-capacity wells. These extensive, thick deposits, called here the basin-fill sediments, underlie the two minor units and provide the public water supply to the City and surrounding communities.

The second unit consists of reworked sediments from the older basin-fill, laid down as thin coverings on terraces and in arroyos. Included in the second unit are young fan and pediment covers deposited along the base of mountain escarpments. These marginal units are usually shallow and are minor sources of water for small domestic and stock wells. Water-table perching may occur on

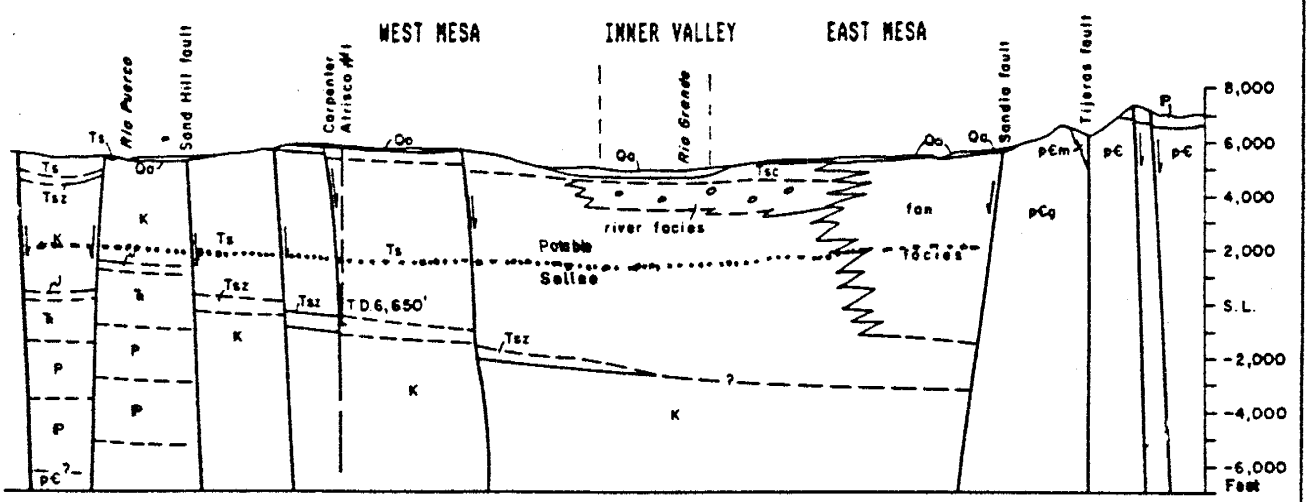

GENERAL TERMINOLOGY

Basin-fill deposits (primary unit Ts, Tsc, river & fan facies)

Pediment and arroyo covers (minor unit Qa)

Flood plain deposits (minor unit Qa)

Fracture flow through Precambrian (pεg)

Low permiability units (K, T, P, P)

Qa Quaternary alluvium
Tsc Tertiary Santa Fe Ceja Member
Ts Tertiary Santa Fe undivided
Tsz Tertiary Santa Fe Zia Member
K Cretaceous
J Jurassic
T Triassic
P Permain
P Pennsylvanian
pεg Precambrian granite

Figure 11: Cross section through the Albuquerque Basin showing the spatial relationship between the water bearing units and Kelly's (1974) estimated depth of potable water (modified from Kelley, 1977).

alluvium-covered pediments near mountain fronts before runoff and spring flow discharge to the adjacent deep basin-fill sediments of the primary unit. These blanketing sediment sheets can produce water at a rate of 1' L/sec (10'gpm) near canyons and in perched water-bearing units adjacent to faults.

The third unit, the inner-valley deposits, consist of reworked older sediments which formed in the Rio Grande's flood plain and main tributaries. These deposits are as much as 55 m (180 ft) thick and can yield water up to 11 m^3/min (3000 gpm) from the Rio Grande flood plain (Bjorklund and Maxwell, 1961). Flood-plain alluvium channels Rio Grande recharge to the primary unit.

Pre-Tertiary strata serve as minor aquifers outside the study area but act as recharge controlling boundaries and sediment sources within the study area.

Figure 12 is the regional water-table map compiled by Titus in 1961 from measured water levels. Figure 13 shows simulated water-levels for 1960 (considered steady state) and 1979 (transient conditions) (Kernodle and others, 1986, 1987). Outside the influence of Albuquerque, the water table should remain effectively stable unless population pressures increase the water demand elsewhere in the basin. With the exception of the Albuquerque area, this large basin aquifer has remained essentially unaffected by man's activities throughout most of it length (USACOE, 1979).

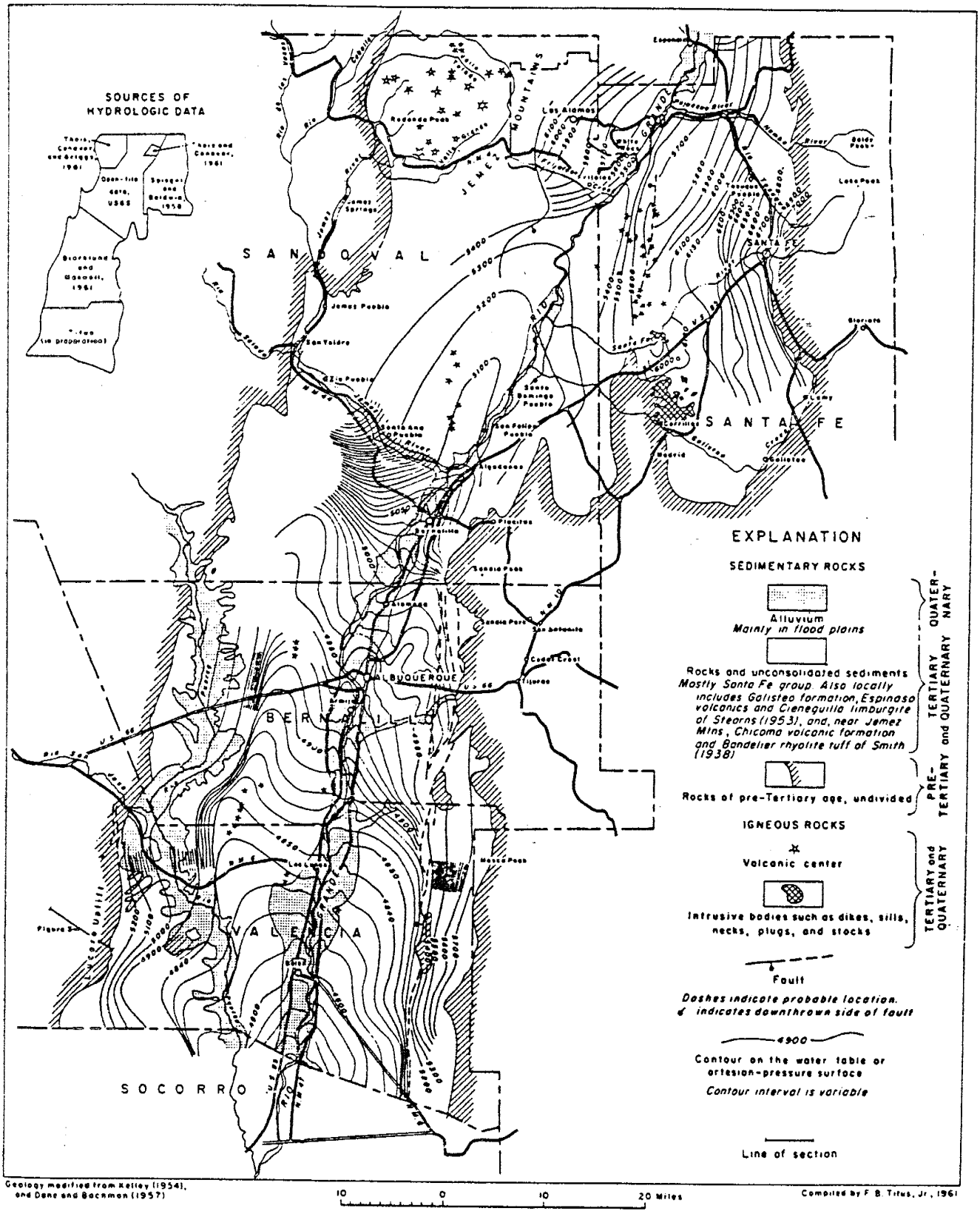

Figure 12: Water-table and artesian-pressure-surface contours for ground water in the Rio Grande trough (Titus, 1961, figure 1).

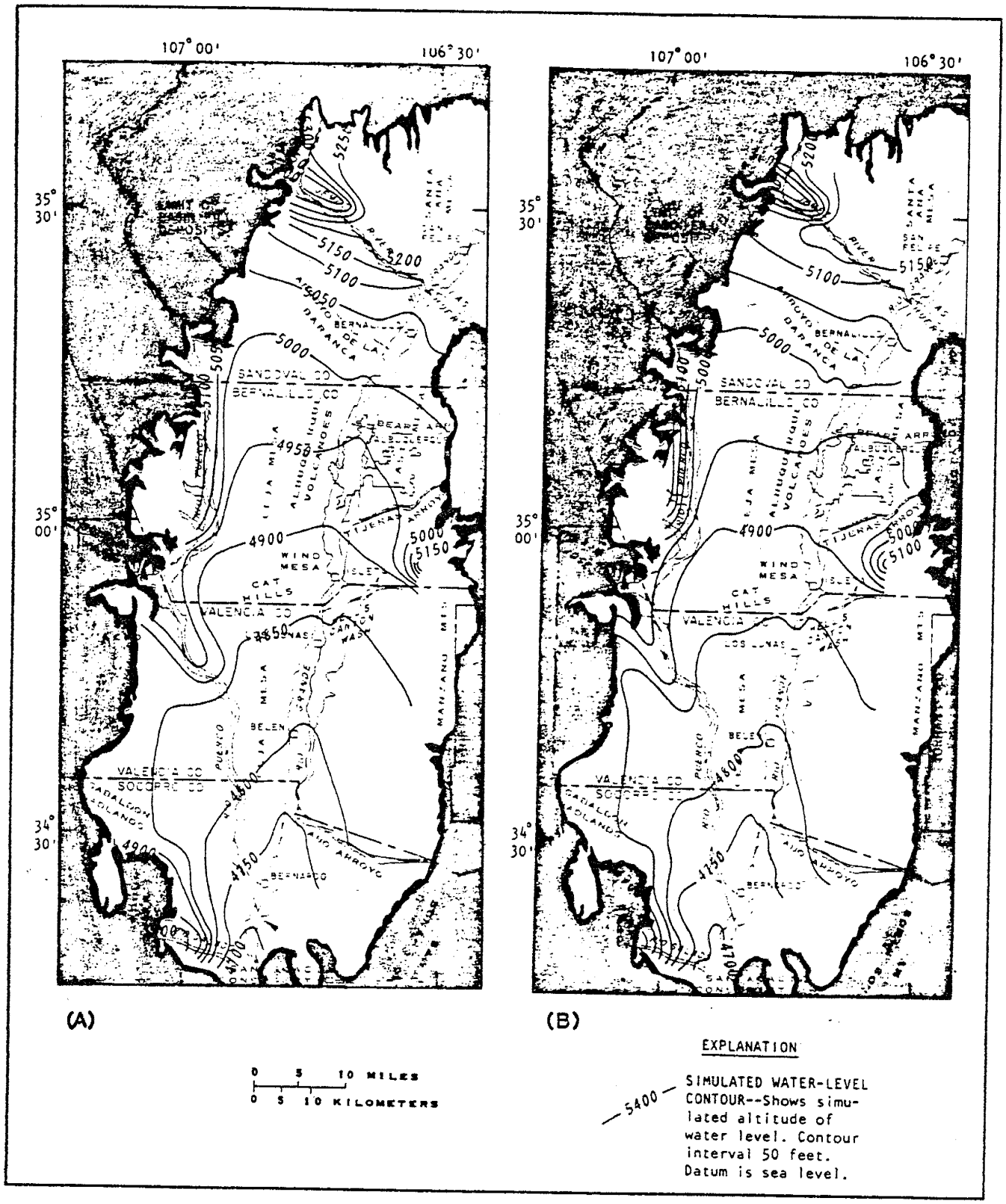

Figure 13: Steady-state simulated water-level contours (A) for the upper 200 feet of saturated thickness for the year 1960 (Kernodle and Scott, 1986). Transient-state simulated water level contours (B) for the year 1979 (Kernodle and others 1987).

Local Hydrology

Surface Drainage

Only one perennial stream traverses the study area, the Rio Grande. Flow is highly variable from year to year and season to season. Spring snowmelt from mountainous areas along the Rio Grandes upper reaches contribute half its annual flow from May to June. The Rio Grandes average flow for the period 1967 to 1977 was 31 m^3/sec (793,000 ac-ft/yr) (USACOE,1979).

Ephemeral streams drain the mountain-front canyons, alluvial fans, and high mesas during high intensity storm events but runoff rarely reaches the river. Storm runoff rapidly infiltrates into the coarse, sandy arroyo floors resulting in wide channels at the arroyo heads which decrease in width toward the river (Bjorklund and Maxwell, 1961).

Figure 14 shows the study areas natural drainage system, the through flowing Rio Grande with its ephemeral tributaries and numerous high mesa arroyos. East and West Mesa drainage is not evenly distributed. East Mesa arroyos drain a larger area therefore are more numerous and better developed than West Mesa arroyos. Surface drainage may influence well geochemistry in some wells so I included well locations with respect to arroyos on figure 14.

Tijeras Arroyo, located in the southeastern portion of the study area, is the largest tributary of the Rio Grande

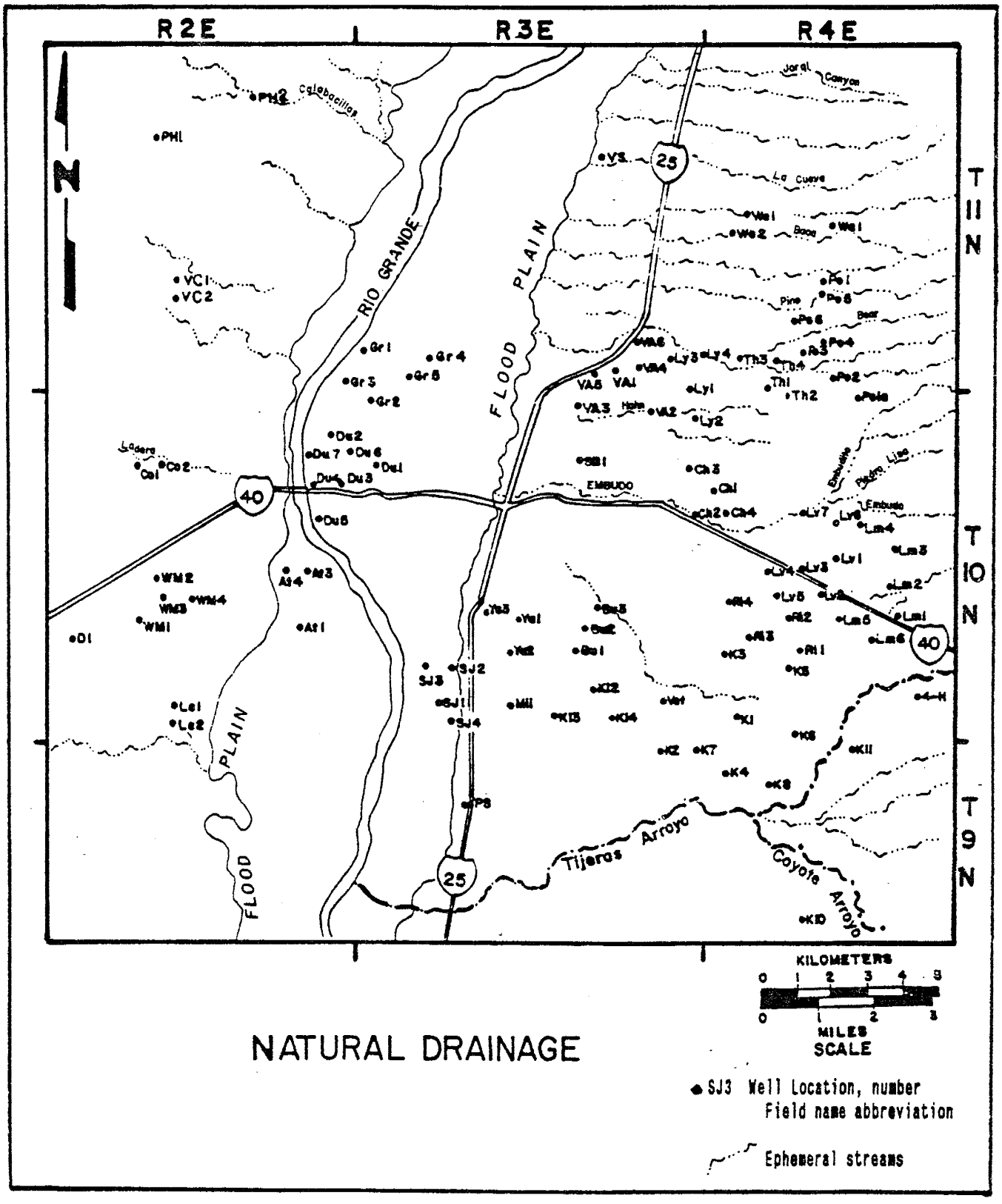

Figure 14: The mountains and high mesas are drained by a series of arroyos which decrease in width toward their distal end.

on the East Mesa. During storms of long duration or flash floods, large volumes of water flow through this wide arroyo but surface water seldom reaches the Rio Grande.

West of the Rio Grande, the West Mesa and Llano de Albuquerque form a divide between the Rio Grande and the Rio Puerco. This high eastward-sloping West Mesa drainage area is smaller than the westward-sloping East Mesa drainage area. Arroyo de las Calabacillas, located in the northwestern portion of the study area, is the largest West Mesa tributary to the Rio Grande (Lambert, 1968).

Artificial Drains

A complex system of artificial drains, channels, irrigation ditches and flood retention impoundments transverse the inner-valley flood plain and mesas.

The Albuquerque area has a long history of destructive flood events from both Rio Grande peak flows and flash flooding on the mesas. In 1925, the Middle Rio Grande Conservancy District (MRGCD) was formed to address the irrigation and flood-control problems along the river. Between 1930 and 1935, a system of levees, drains and irrigation ditches were constructed to control seasonal flooding, drain waterlogged bogs for farming, and distribute irrigation water. In the early 1950's, the U.S. Bureau of Reclamation expanded this system which now includes 939 km (587 mi) of main canals, 638 km (399 mi) of lateral channels, and open and buried tile drains in the

inner-valley (Kelley, 1969; Thompson, 1986). Figure 15 shows the MRGCD inner-valley system of drains, channels and canals. This complex system of mostly unlined canals adds to ground-water recharge and is the primary control on the nearly steady state water-levels in the flood plain.

Figure 16 shows the flash-flood control structures on the East and West Mesas. Several major arroyos draining the high mesas have been concrete lined and have had large diameter subsurface drains and retention ponds constructed along their courses to control flash-flood runoff. As a result, storm runoff is carried to the river in lined channels and very little water infiltrates as mid-fan aquifer recharge.

Aquifer Boundaries

Locally the Rio Grande ground-water basin is bounded on the east by nearly impermeable Precambrian granitic and metamorphic rocks. Beyond the study area, the west side of the aquifer is bound by upfaulted, fine-grained, Cretaceous age rocks. Downfaulted pre-Tertiary rock, as deep as 5500 m (18000 ft) form the nearly impermeable aquifer bottom. The top of the aquifer is defined by the water table which varies from the Rio Grande surface elevation to about 275 m (900 ft) deep on the Llano de Albuquerque. Both north and south ends of the basin aquifer are open. Physical boundaries of small areal extent within the aquifer include fissure volcanics, cemented fault zones and interbedded playa deposits. Thick, discontinuous clay lenses may

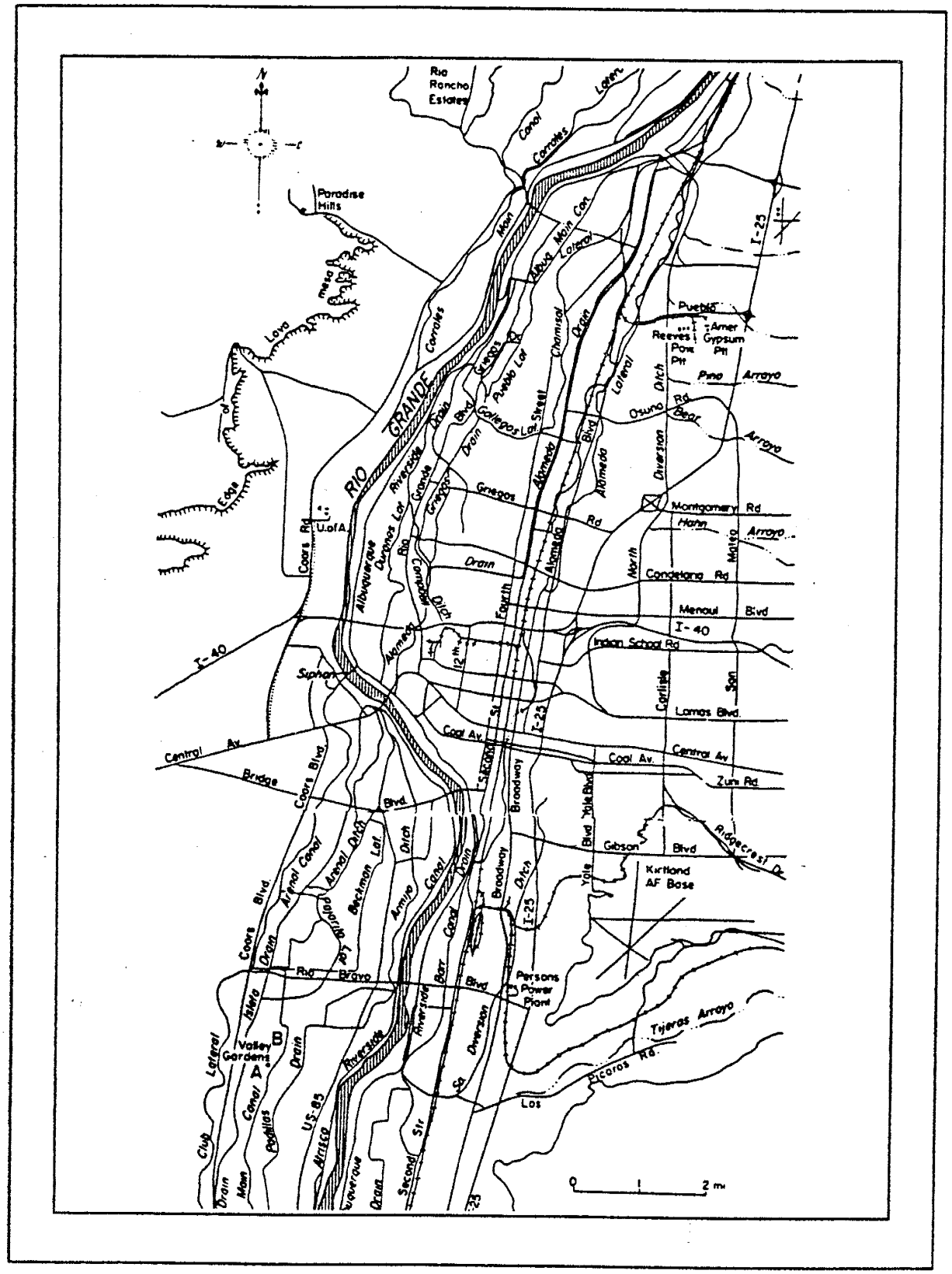

Figure 15: The Middle Rio Grande Conservancy District (MRGCD) flood-plain irrigation and drain system (Kelley, 1982).

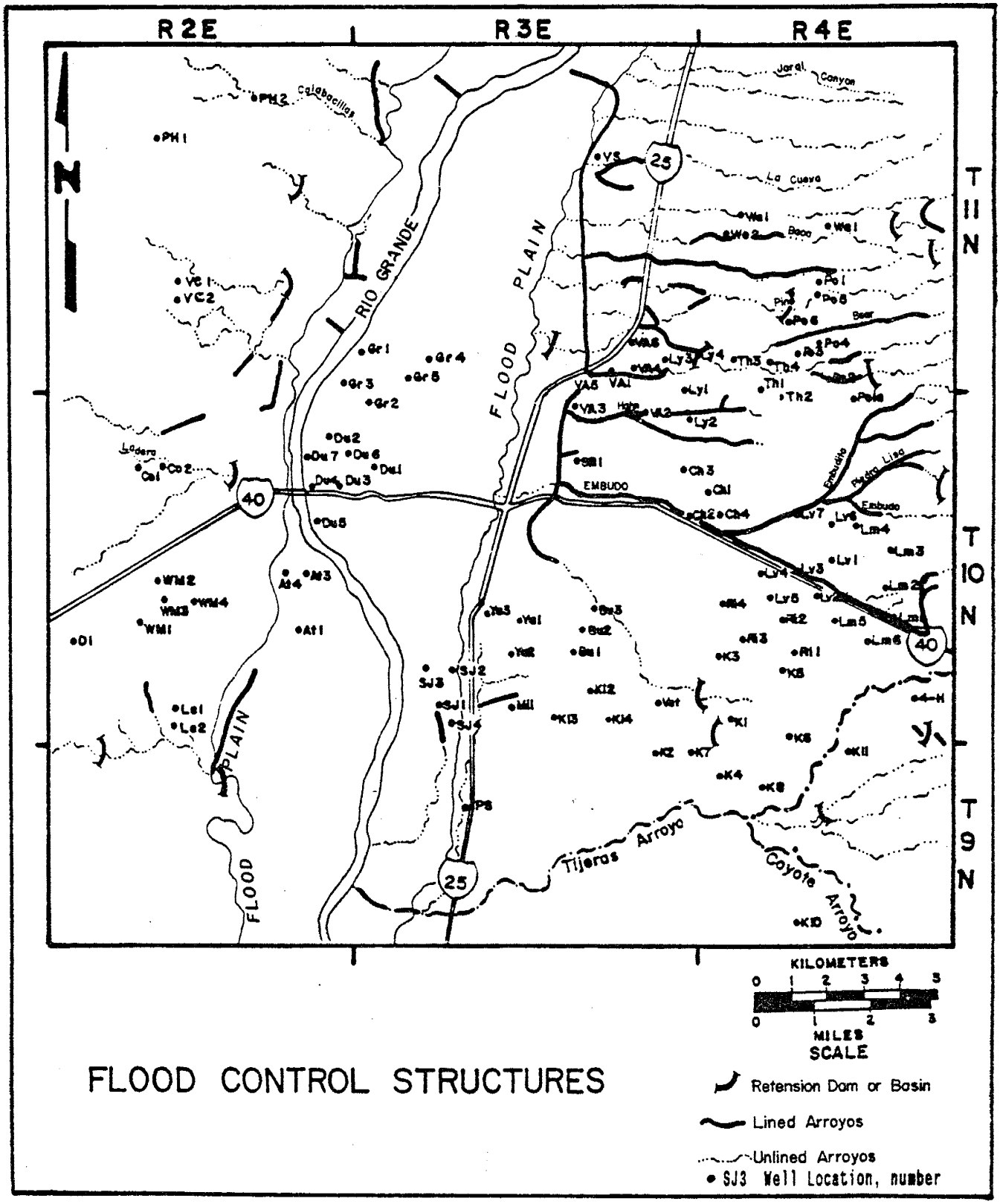

Figure 16: Concrete liners, rip-rap, and water-retention basins are built along arroyos to route flash floods.

create zones of semi-confinement in an otherwise unconfined aquifer (Bjorklund and Maxwell, 1961, and Kelley, 1977).

Recharge

Local recharge comes from mountain-front inflow, precipitation, the river, MRGCD canals, and irrigation return flow.

Titus (1980) stated that recharge from the Sandia watershed occurs in both winter and summer with very little runoff leaving the mountain area, but with ground water flowing out from its entire perimeter as inflow.

Precipitation infiltrates through ephemeral streams, arroyos draining the mesas, and through West Mesa lava flows. The amount of precipitation recharging the ground water supply is controlled by rainfall intensity and duration, as well as the soils, vegetative cover, permeability, temperature, and existing soil moisture content. Using arroyo geometry, Hearne and Dewey (in press) estimated about 0.35 to 0.40 m^3/sec (8-9 million gal/d) of water recharges the aquifer along the eastern basin boundary through the Tijeras and Bear Canyon arroyos (Kernodle and Scott, 1986). Recharge through the West Mesa lava flows was considered insignificant by previous investigations.

Production wells in the Rio Grandes inner-valley lower the water table and high river stages during spring runoff increase the hydraulic gradient between the river and the water table, thereby periodically increasing the recharge

rate from the river to ground water.

Inner-valley canals, drains, irrigation return flow, and septic tanks function as artificial recharge sources. Bjorklund and Maxwell (1961) estimated that one-third of all water flowing through irrigation canals and applied to irrigated fields is returned to the ground-water system. The Corps of Engineers (1979) estimated two-thirds of this water infiltrates to the water table as return flow. Drains designed to lower the water table 40 years ago now serve as recharge channels (USACOE,1979).

Discharge

Ground-water discharge occurs through pumping wells, the river surface, evapotranspiration, drains, springs and seeps. From 1967 to 1977, the Corps of Engineers (1979) estimated 3.75×10^6 m^3 (304,000 ac-ft) of water was removed from storage.

In the Albuquerque area, municipal wells discharge large volumes of water. Wells adjacent to mountain and river recharge boundaries intercept recharge near its source, causing some mid-mesa wells to dewater about 30 m (100 ft) of aquifer over the last 40 years.

As the mid-mesa water table declines, near-river wells draw an increasing amount of water from the river. Mean annual water losses from the Rio Grande from 1958 to 1968 averaged 975,000 m^3/km (1272 ac-ft/mi) of reach. By 1978, channel loss increased to 1.61×10^6 m^3/km (2098 ac-ft/mi)

of reach (USACOE, 1979).

Open water bodies lose about 1.5 m/yr (5 ft/yr) to surface evaporation while evapotranspiration from the inner-valley bosque is about 1 m/yr (3 ft/yr). The Corps of Engineers (1979) estimated about 16 percent of the total discharge was lost through phreatophyte transpiration.

Middle Rio Grande Conservancy District (MRGCD) drains were designed to discharge ground water by intercepting the rising water table during peak river flows. Extensive pumping has lowered the inner-valley water table so now these drains rarely serve as discharge channels.

Springs and seeps are a minor source of discharge near the mountain fronts. Spring-fed streams rapidly infiltrate as they flow onto the porous alluvium.

The Corps of Engineer's (1979) water balance indicated that municipal pumpage and riverside drains accounted for most of the discharge in the Albuquerque Basin.

Hydraulic Characteristics

The Rio Grande ground-water basin aquifer system can be characterized as hydraulically anisotropic, heterogeneous, and unconfined with local semiconfined areas. Table 2 summarizes the aquifer hydraulic properties measured and estimated by various workers.

Using Theis' recovery method, Bjorklund and Maxwell (1961) measured near-well transmissivities for 23 wells in the Albuquerque area which averaged 2760 m^2/d (230,000 gpd/ft). The Corps of Engineers (1979) calculated

TABLE 2: AVERAGE AQUIFER HYDRAULIC PROPERTIES

	INNER-VALLEY ALLUVIUM	BASIN-FILL ALLUVIUM		SOURCE
		EAST of Rio Grande	WEST of Rio Grande	
TRANSMISSIVITY (T)		1441 m/d (116000 gpd/ft)	66 m/d (52800gpd/ft)	(6)
		8421 - 62 m/d (678000-5000 gpd/ft)	1366 -298 m/d (110000-24000 gpd/ft)	(7)*
HYDRAULIC CONDUCTIVITY (K)		13.8 m/d (45 ft/d)		(1)*
	15 m/d (50 ft/d)	12.2 m/d (40 ft/d)	9.1 m/d (30 ft/d)	(4)+
		6.5 m/d (21 ft/d)	2.1 m/d (7 ft/d)	(6)
	4 - 9 m/d (13-28 ft/d)		0.006 - 0.53 m/d (0.02-1.74 ft/d)	(4)*
STORATIVITY (S)		S = 0.001		(3)*
Unconfined (S_y) (S = Syb)	S_y = 0.2			(1)*
		S_y = 0.15		(2)#
		S_y = 0.1		(4)+
Specific storage (S_s)		S_s = 3.3 10^{-6}/m (10^{-6}/ft)		(4)+
POROSITY (n)				
ANISOTROPY		1:500	1:500	(4)+
			1:60 - 1:600	(5)*

* = measured parameter
\# = estimated from lithology
\+ = estimated using digital computer
b = well depth - water level = saturated thickness

Sources:

(1) Bjorklund and Maxwell (1961)
(2) Kelly (1982)
(3) Layne-Western (1985)
(4) Kernodle and others (1987)
(5) Wilkens (1987)
(6) Geometric mean of all available data
(7) Range of all available data

transmissivities from specific capacities, using Meyer's (1963) method, which averaged 53 percent lower than Bjorklund and Maxwell's (1961) measured transmissivities. In 1985 and 1987 the City had 76 of their wells tested. Private engineering firms conducted in-well pump-tests for 70 production wells and used semilog time-drawdown and recovery analysis methods to interpret the data. They used curve-matching techniques to interpret data for 6 additional wells using near-by production wells as observation wells. Both pump-tests conducted in production wells and tests using observation wells with long screens violate several of the principal assumptions inherent in these analytical techniques.

Figure 17 shows spatial variations in hydraulic conductivity and associated depositional environments across the study area (conferred with Summers, City Planning Group). Most map construction data came from the City's 1985-1987 tests with supplemental data from Bjorklund and Maxwell (1961) and the Corps of Engineers (1979). To calculate hydraulic conductivities (K) for gravel-packed wells, I used the following equation:

K = Transmissivity/(well depth-depth to water)

Appendix VI contains a table of transmissivity data categorized by their source and year of measurement.

Kernodle and others (1986, 1987) used hydraulic conductivities of 12 m/d (40 ft/d) on the east side and 9 m/d (30 ft/d) on the west side of the Rio Grande to

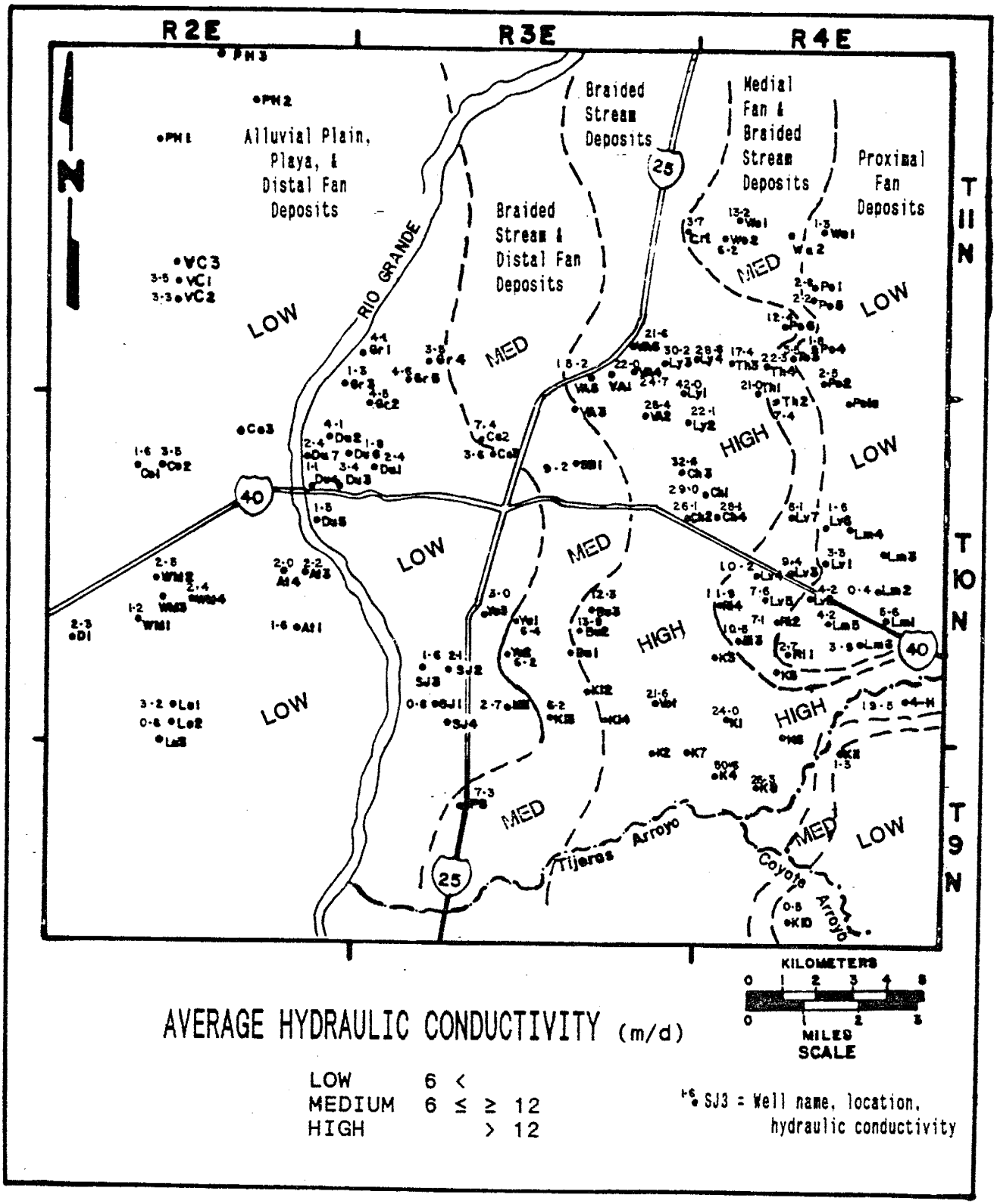

Figure 17: Hydraulic conductivity increases then decreases from east to west indicating the extent of sediment sorting with distance from the source area and the associated depositional environments.

calibrate their basin digital model. Their calibration values are in good agreement with Bjorklund and Maxwell's (1961) basin average of 14 m/d (45 ft/d). Hydraulic conductivities in this range are associated with an average silty sand to clean sand aquifer matrix (Freeze and Cherry, 1979).

Specific storage (S_s) for either the shallow inner-valley alluvium or the the basin-fill alluvium are not known. Kernodle and others (1987) used $S_s = 10^{-6}$ in their three-dimensional ground-water flow model.

Bjorklund and Maxwell (1961) estimated a specific yield (S_y) of 0.2 for the shallow inner-valley alluvium but not for the deeper basin-fill alluvium. Kelly (1982) assumed $S_y = 0.15$ to calculate the volume of mined ground water from the basin-fill alluvium. Kernodle and others (1987) found $S_y = 0.1$ gave the best results in aquifer response simulation tests.

Local Ground-Water Development

History of Ground-water Development

The following discussion is based on well data and historical information compiled by Bjorklund and Maxwell (1961), the Corps of Engineers (1979) and Kelly (1982).

Since the time that Theis (1938) first studied Albuquerque's shallow inner-valley water resources, striking changes in the City's underlying aquifer geometry and flow direction have taken place. Figure 18a shows a modified

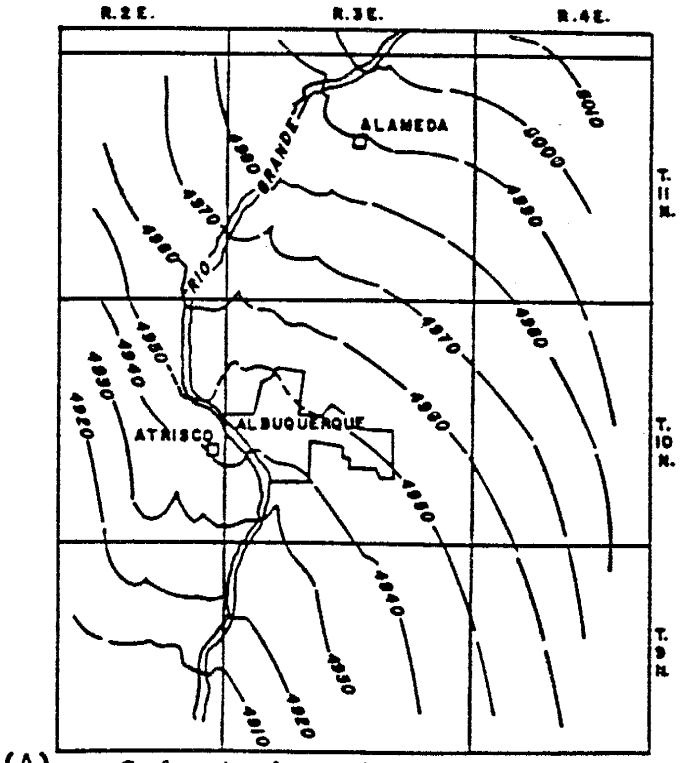

(A) *Configuration of water table in Albuquerque area in October, 1936. Elevation contours in feet.*

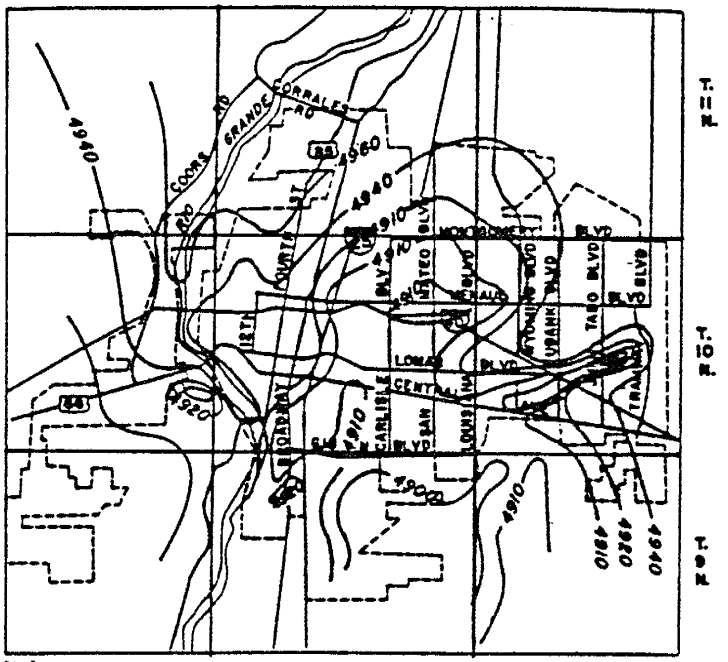

(B) *Configuation of water table in Albuquerque area in 1978. Elevation contours in feet.*

Figure 18: In 1936 (A) the only shifts in the water-table are due to MRGCD drains. After 42 years of pumpage (B) the water table configuration east of the river has been profoundly changed (USACOE, 1979; Kelly, 1982).

version of Theis's 1936 water-table map in contrast with figure 18b, the Corps of Engineers 1978 water-level map showing the effects of 42 years of pumpage (units are in feet above sea level).

At the time of Theis' study, Rio Grande channel losses were greater than Albuquerque's water consumption; therefore man's impact was trivial and the river-aquifer water levels were at steady state. Water-level deviations seen on figure 18a were caused by the MRGCD drains and canals. The City's primary public water supply came from hand-dug and shallow-drilled wells in the inner-valley alluvium. In 1932, the City drilled its first deep well through the inner-valley alluvium into the older basin-fill deposits. Low water demands and the MRGCD drains ability to maintain a constant water level allowed inner-valley steady-state water levels to prevailed from earliest settlement to after 1936.

Nine dug wells and thirty drilled wells produced Albuquerque's water supply from 1922 to 1949. In 1950, the City drilled its first well on the East Mesa and in 1963 the first City well was drilled on the West Mesa. An additional 35 wells were drilled between 1950 and 1959.

Figure 19a and 19b illustrate Kelly's (1982) change-in-water level maps (units are in feet) showing effects of heavy pumpage in the inner-valley and East Mesa well fields. Figure 19a is after 24 years of pumpage from 1936 to 1960, while figure 19b is for the next 18 years of pumpage from 1960 to 1978. By 1978, water levels declined

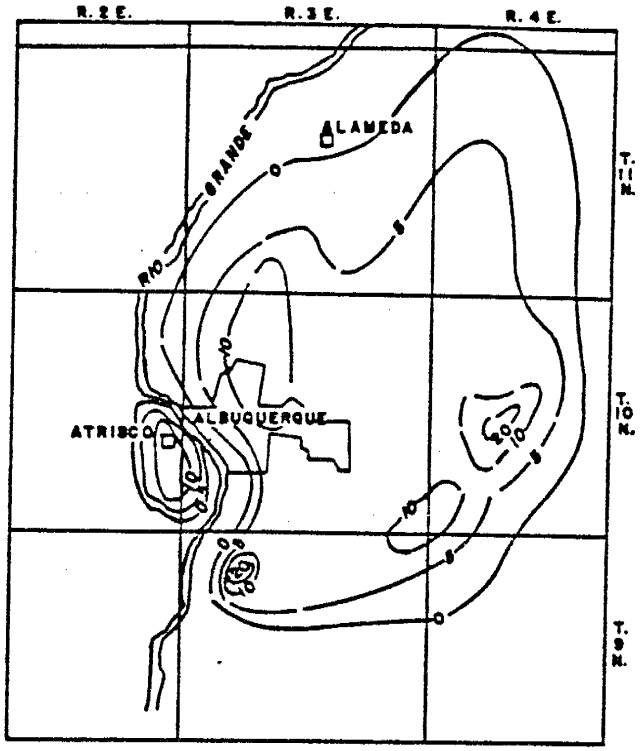

(A) *Water level change in Albuquerque area for period of 1936 to 1960. Contours in feet.*

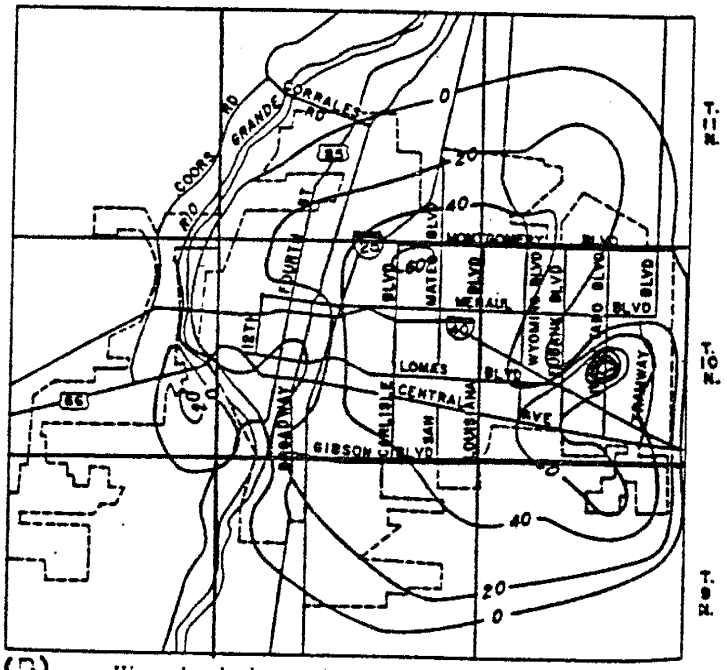

(B) *Water-level change in Albuquerque area, 1960 to 1978. Contours in feet.*

Figure 19: Water level changes between 1936 and 1960, 24 years (A), was approximately trippled in the following 18 years (B) between 1960 and 1978 (USACOE, 1979; Kelly, 1982).

1.5 m (5 ft) over most of the East Mesa with declines of 12 to 18 m (40-60 ft) or more in areas of heavy pumpage.

From 1960 to 1969, the City drilled 31 more wells and from 1970 to 1979 they drilled an additional 30 wells.

Figure 19b, the 1978 water-level-change map, shows almost complete water-level recovery of old inner-valley well fields several years after pumpage ceased.

Figure 20 shows currently operating well fields and well locations to aid in locating fields in the following discussion of figure 19b. Of the two still-operating inner-valley well fields, Atrisco showed little change from its 1960 water levels while the Duranes field was down 6 m (20 ft). The mid-fan Leyendecker and Charles fields are down 15 m (50 ft); and near-mountain front Lomas and Love fields are down more than 40 m (130 ft) from their 1936 water levels.

Water-level changes on figures 19a and 19b, show East Mesa ground-water mining has little effect on the inner-valley water levels. Recharge from the extensive MRGCD system of drains and canals greatly tempers the influence of ground-water mining outside the inner-valley flood plain (Bjorklund and Maxwell, 1961, Kelly, 1982).

Current Ground-water Development

Figure 20 shows the location of well fields and wells in the current municipal water supply system. In the last eight years, 1980 to 1989, 12 wells have been drilled, 2 were replacement wells. Of the 12 wells, 7 are in service

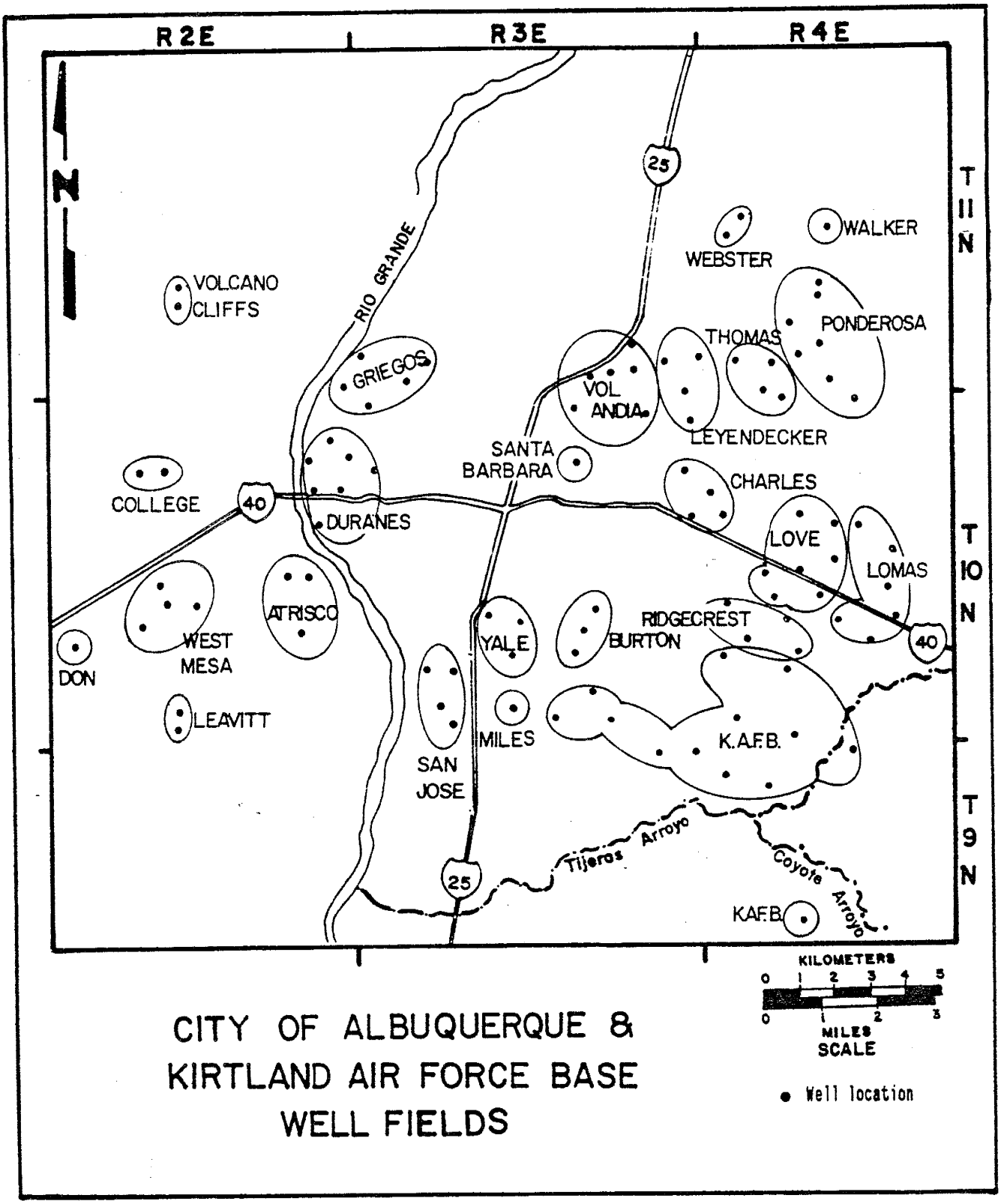

Figure 20: Well fields are aligned with the north-south trending water distribution system designed to efficiently deliver water to the municipal area.

and 5 are not equipped. Eight of the new wells were drilled in the high to medium transmissive zone in the mid-fan area shown in figure 17.

At any one time, there are 85 to 90 municipal wells producing the City's water supply. Water is pumped from a well to a central collecting point where it is filtered, chlorinated and stored ready to be pumped into the City's distribution system. City water well depths range from 90 to 544 m (296-1786 ft) with 85 of the City's 90 wells deeper than 244 m (800 ft). Appendix III is a list of completion data for wells used in this study.

Water Levels

Water-level measurements in municipal wells are taken under less than ideal conditions. Cyclical pumpage, variable aquifer recovery rates, well interference, and variable rates of downward flow prevent us from knowing the water tables height, or slope at any point in time. Water levels measured in areas with steep downward gradients appear to be from 3 to 12 m (10-40' ft) or more below the actual water table. Deep well water levels are low during the peak use summer months and partially recover through the low production winter months.

Figure 21 is a water-table map for the winter of 1988 to 1989 (conferred with Summers, City Planning Group). Most control points are monitoring wells screened over short intervals at or near the water table. Deep wells high on the mesas were used to roughly estimate the water

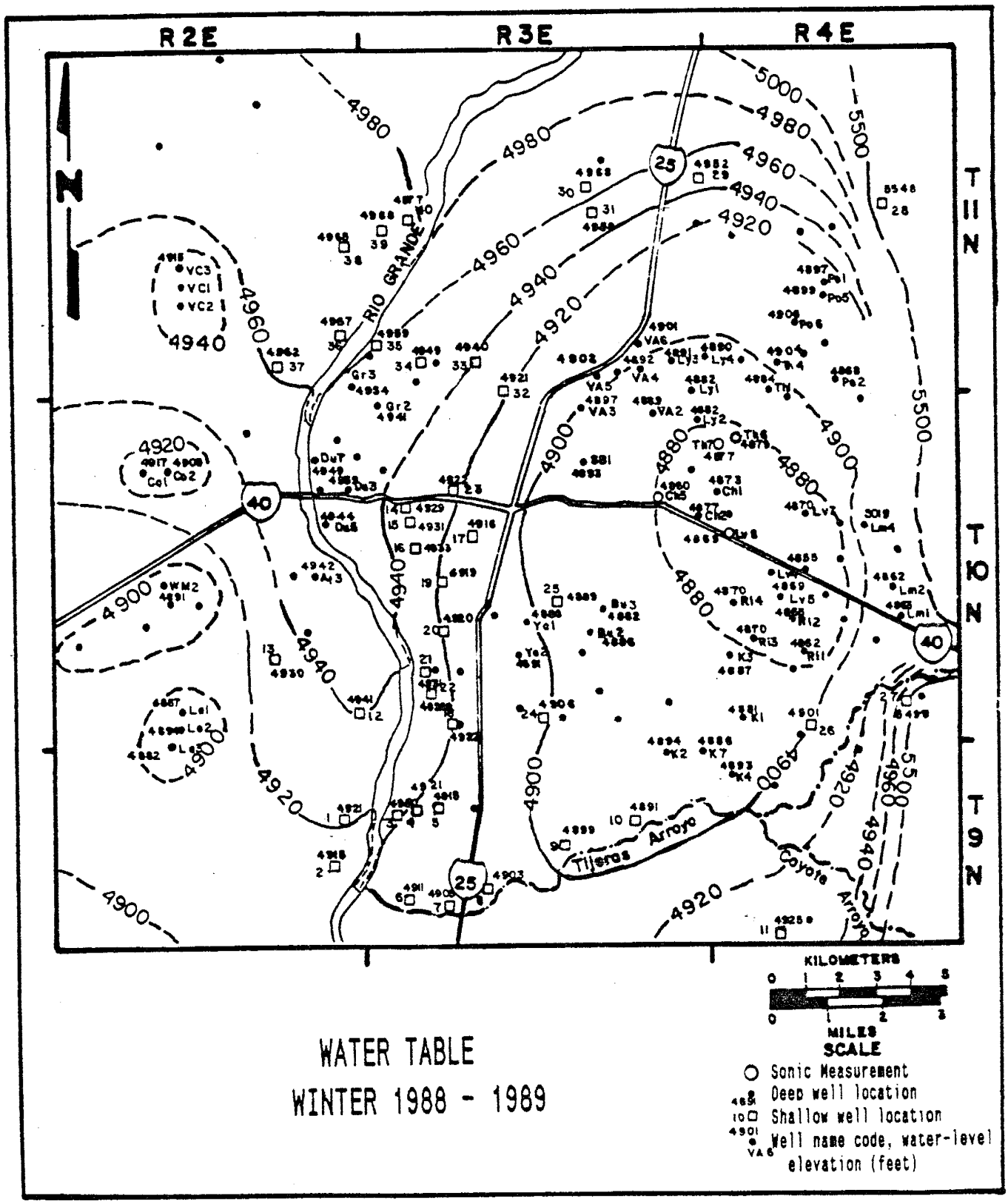

Figure 21: Water levels in shallow monitoring wells indicate the water table position while downward vertical flow in deep wells cause the water levels to lie several inches to tens of feet below the water table.

table, assuming it lies some where above the measured water level. Table 3 lists the map codes and data used in constructing the water-table map.

Figure 22 shows the change in water-level depth since 1936. To compare figures 18 and 19 with present maps, I used english units (feet) to construct the water-level change and water-table maps. I superimposed Kelly's (1980) modified version of Theis's 1936 water-table map (figure 18a) on the current, winter 1988-1989, water-table map (figure 21) and connected points of equal elevation. This map is designed to show water-level changes from steady-state conditions to the present. Ground-water declines in West Mesa well fields are uncertain without shallow-well control data. The water-table position is estimated from wells with a downward vertical flow component.

An elliptical bulls-eye has formed under the East Mesa. North-south elongation may be due to the high transmissive zone that roughly extends across the mid-fan facies. Comparing the hydraulic conductivity map (figure 17) with the water-level change map (figure 22); the 30 m (100 ft) contour lies mainly in the low hydraulic conductivity zone with some elongation toward the northwest into the high hydraulic conductivity zone. The 30 m (100 ft) contour may reflect decreased water-levels due to boundary effects of pumping centers intercepting the nearly-impermeable, granitic, basin boundary and/or pumpage in a low transmissive zone.

TABLE 3: Construction data for Winter 1988 - 1989 Water Level Map

MAP INDEX	DEPTH TO WATER(ft)	WATER ELEV(ft)	DATE MEASURED	MAP INDEX	DEPTH TO WATER(ft)	WATER ELEV(ft)	DATE MEASURED	MAP INDEX	DEPTH TO WATER(ft)	WATER ELEV(ft)	DATE MEASURED
At3	11	4942	1/23/89	Ri2	551	4865	1/27/89	22	16	4926	
Bu2	398	4886	12/29/88	Ri3	518	4870	1/19/89	23	15	4922	7/22/88
Bu3	336	4882	12/27/88	Ri4	478	4870	12/12/88	24	401	4906	11/01/88
Ch1	445	4873	3/30/89	SB1	247	4893	2/09/89	25	280	4889	
Ch2	391	4877	8/24/88	SJ2	100	4892	2/26/88	26		4901	
Ch5	360	4860	SONIC-88	Th1	560	4884	3/15/89	27	51	5498	12/06/88
Co1	423	4917	2/09/89	Th3	528	4886	11/03/88	28	317	5548	9/ /88
Co2	321	4908	2/10/89	Th4	580	4904	3/23/89	29	342	4952	9/ /88
Du3	24	4939	6/06/89	Th6	530	4879	SONIC-88	30	95	4968	9/26/88
Du5	18	4944	6/02/88	Th7	465	4877	SONIC-88	31	128	4958	9/20/88
Du7	15	4949	4/19/89	VA2	321	4889	4/12/89	32	75	4921	10/17/88
Gr2	27	4941	12/13/88	VA3	215	4897	2/22/89	33	34	4940	9/ /88
Gr3	19	4954	12/13/88	VA4	311	4892	11/10/88	34	23	4949	9/ /88
K1	502	4881	1989	VA5	211	4902	1/25/89	35	10	4959	9/ /88
K2	424	4894	1989	VA6	278	4901	1/05/89	36	8	4967	9/ /88
K3	467	4887	1989	VC3	431	4915	1/23/89	37	148	4962	9/ /88
K4	469	4893	1989	WM2	278	4891	7/20/88	38	57	4977	6/16/89
K5	567	4867	1989	Ya1	273	4888	1/06/89	39	27	4968	9/ /88
K7	463	4886	1989	Ya2	237	4891	5/09/89	40	100	4965	9/ /88
K8	483	4895	1989	1	9	4921	9/ /88	*	60	4910	10/31/88
Le1	197	4887	1/24/89	2	11	4915	2/01/89	*	98	4907	10/31/88
Le2	177	4894	1/23/89	3	8	4920	9/ /88	*	56	4909	10/31/88
Le3	203	4882	12/19/88	4	7	4921	9/ /88	*	76	4907	11/01/88
Lm1	736	4863	5/18/88	5	17	4915	9/ /88	*	50	4909	
Lm2	718	4862	8/18/88	6	38	4911	11/03/88	*		4930	
Lm4	558	5019	6/07/89	7	114	4906	10/31/88	*	34	4926	9/ /88
Lv1	596	4868	1/20/89	8	143	4903	11/02/88	*	46	4934	9/ /88
Lv3	540	4864	4/06/88	9	203	4899	11/02/88	*	38	4936	
Lv4	511	4855	1/03/89	10	277	4891	11/02/88	+	25	4950	9/ /88
Lv5	530	4869	3/31/88	11	456	4925	1/09/89	+	458	4927	9/ /88
Lv7	574	4870	1/04/89	12		4941	1989	+	288	4901	8/15/89
Lv8	445	4869	SONIC-88	13	76	4930	10/17/88	+	409	4902	6/19/88
Ly1	404	4882	12/12/88	14	31	4929	9/ /88	+	249	4901	8/15/89
Ly2	418	4882	1/03/89	15		4931		+	430	4900	6/19/88
Ly3	377	4891	11/03/88	16		4933		+	478	4957	10/10/88
Ly4	439	4890	4/26/88	17	44	4916	9/ /88	+	482	4937	10/10/88
Po1	752	4897	12/20/88	18		4922		+	884	4911	9/ /88
Po2	737	4868	8/12/88	19	38	4919	10/19/88	+	917	4949	
Po5	731	4899	2/02/88	20	29	4920	5/18/88	+	768	4962	9/ /88
Po6	652	4906	2/09/89	21		4921		+	396	4989	9/ /88
Ri1	583	4862	3/07/89								

MAP INDEX = well codes on figure 21
* = DATA NOT SHOWN ON MAP BUT USED IN INTERPRETATION
+ = LOCATION POINT OUT OF MAP BOUNDARY BUT USED IN INTERPRETATION
CITY WELL WATER ELEVATIONS ARE ADJUSTED FOR 2 FOOT MEASURING POINT

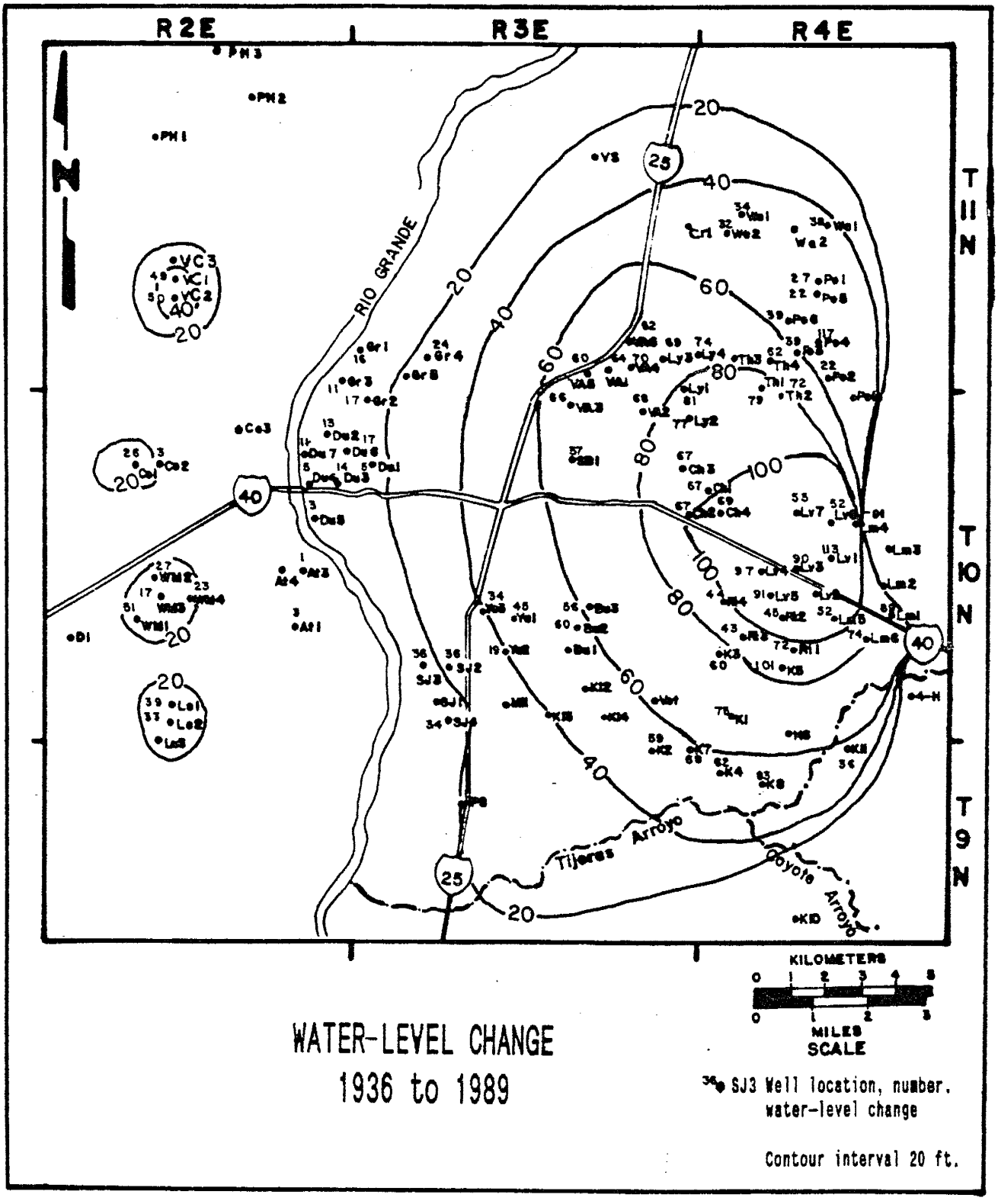

Figure 22: Water-level change contours are based on the difference between the 1936 water table and the 1989 water-table contour intercepts. Well water-level changes are based on the initial minus the 1989 water level.

Ground-water Mining

Long term water-level declines are related to drought conditions and to over-pumping relative to recharge rates, particularly away from the influence of the Rio Grande (Bjorklund and Maxwell, 1961).

The Corps of Engineers calculated 3 billion m^3 ($4x10^9$ yd^3) of aquifer had been dewatered between 1960 and 1978. Based on the water-level change map (figure 22), my calculations for dewatered aquifer since 1936 yields a volume of 5.5 billion m^3 ($7x10^9 yd^3$). This is an extremely crude estimation, but without shallow-control wells on the far east and west perimeters of the study area, the water table position in areas of heavy pumpage is uncertain and therefore are not included in the calculations. Areas are assumed tabular; I did not adjust for edge slope. It is beyond the scope of this report to refine the estimation of ground-water mining. The main point is the increased rate Albuquerque is dewatering its aquifer. The City Water Departments rule of thumb for average annual water-level decline is about 1 m/yr (3 ft/yr).

Kernodle and others (1987) simulated basin water balance showed 25% of the total annual volume of water discharged by wells, outside the flood plain, was derived from storage depletion.

Hydrodynamics

Heavy pumpage has changed ground-water flow directions throughout most of the study area. Figure 23 is a cross-section along a flow path on Kelly's modified 1936 water-level map (figure 18a). I adjusted the equipotential line locations to reflect the East Mesa mid-fan high permeability zone. The Rio Grande was a gaining stream at this time (Theis, 1938). Recharge from the Bear-Pino-Baca Canyons flowed through shallow pediment covers before cascading downward into the older, deeper water-saturated sediments. Seepage velocity calculations suggest the flow rate through the pediment cover from position (A) to about Birch's (1980) magnetic inflection (A'), takes about 25 years. From (A') to the Rio Grande (A") the hydraulic gradient flattens out and water takes about 1200 years to reach the river above the Rio Bravo Bridge. Seepage velocity calculations are in Appendix VIII.

Figure 24, the same section line as figure 23, shows the equipotential field suggested by water-level data for the winter of 1988-1989, assuming non-pumping conditions. The Rio Grande has become a losing stream. River and mountain-front recharge is intercepted by low pressure zones created by heavy pumpage. Ground-water now flows radially toward the center of the East Mesa rather than toward the river. Water-level decline near the mountain front indicates ground water is being removed from storage at a faster rate than recharge enters the aquifer.

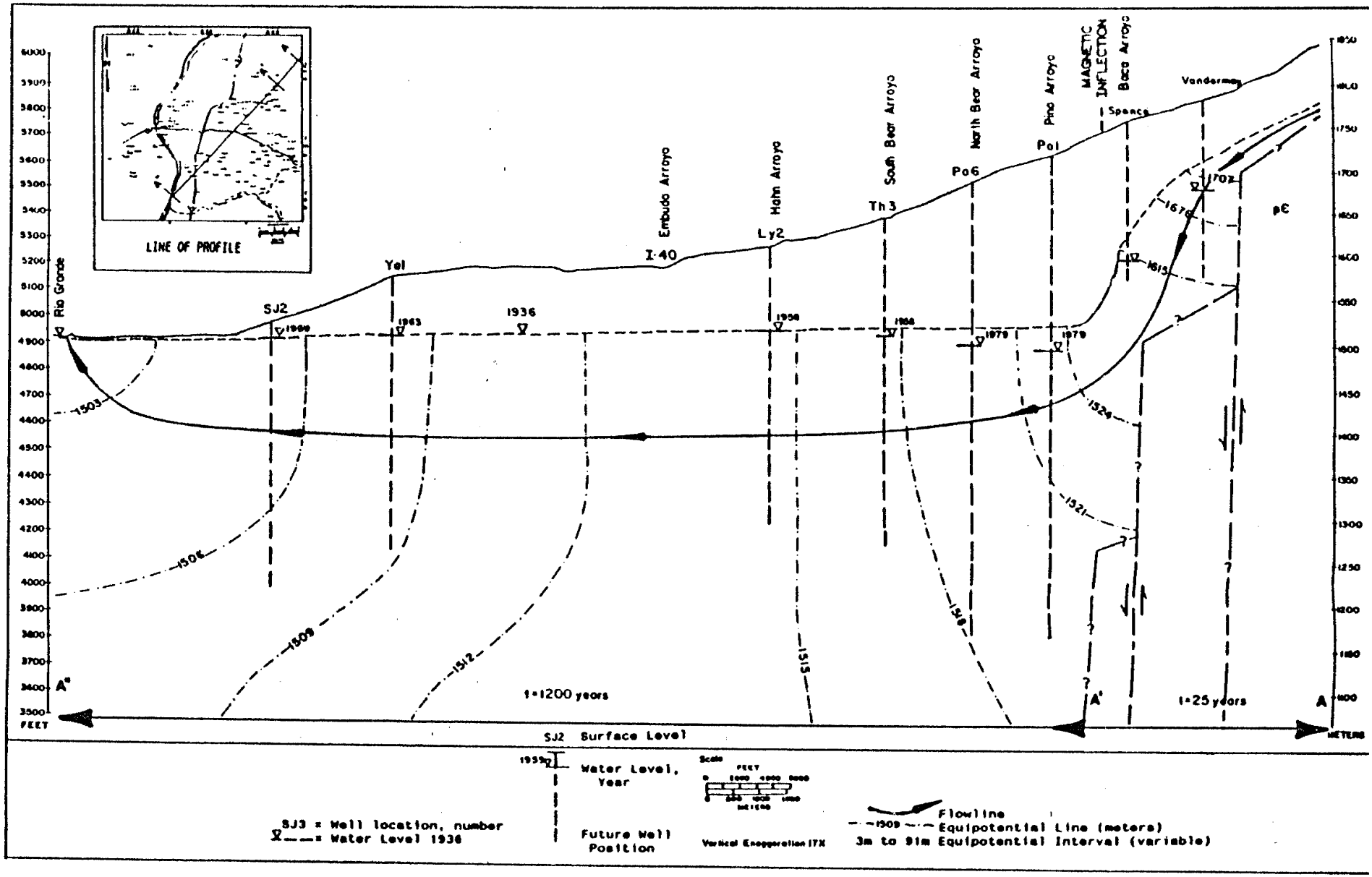

Figure 23: Estimated equipotential field along a 1936 steady-state flow path suggests the Rio Grande was a gaining stream prior to construction of the MRGCD canals. Seepage velocities off the pediment (A - A') are fast while velocities through the basin-fill sediments (A' - A") are considerably slower.

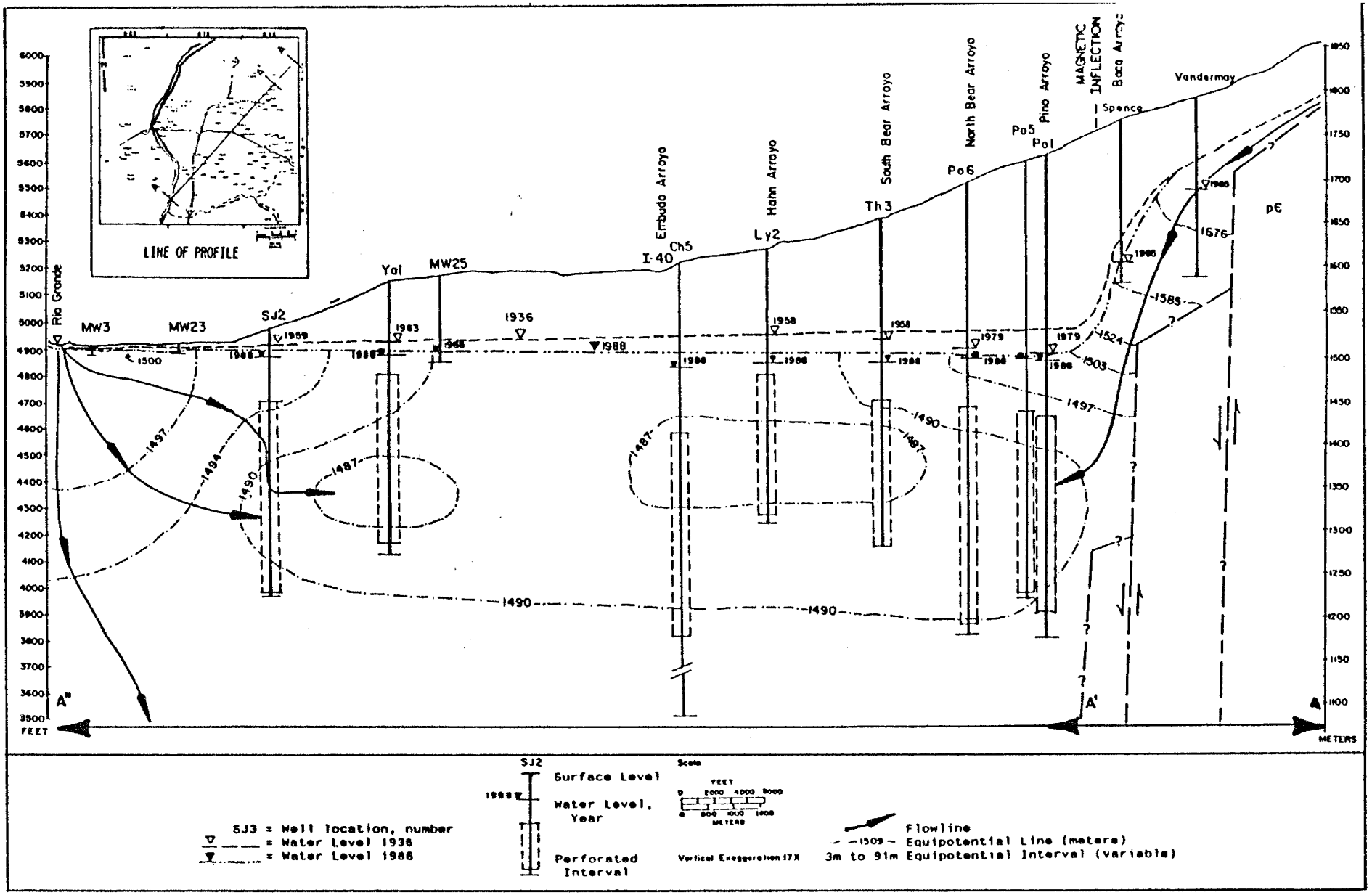

Figure 24: Estimated equipotential field through active well fields for the winter of 1988. Recharge is captured from both the Rio Grande and mountain front areas. Pumpage induced low pressure cells disturb flowlines beneath the wells thereby capturing older deeper basin flow.

Pumped Ground-Water Temperatures

The purpose of this section is look at the areal distribution and frequency of water temperatures, and explain the technique I used for determining anomalous water temperatures. Pumped-water temperature may provide additional evidence for determining the processes that may be influencing the chemical composition and flowpath of the water. Specific wells with unusual temperatures will be discussed in the appropriate section.

Distribution and Frequency:

Figure 25 shows the areal distribution of average pumped ground-water temperatures without regard for differences in well depth or length of screened interval. Cooler ground-water temperatures, below 20°C (68°F), are associated with wells near the river and Tijeras Canyon recharge areas, and some mid-fan wells. Wells producing ground-water temperatures above 28°C (82°F) are deep wells.

Figure 26 is a frequency diagram showing the bimodal distribution of pumped ground-water temperatures for wells over 244 m (800 ft) deep. The first peak is for ground water at 18°C (64°F) and the second peak is for ground water at 24°C (75°F). Very cool ground-water temperatures, below 16°C (60°F), and very warm ground-water temperatures, above 28°C (82°F), are less frequent than ground-water temperatures ranging between 17 and 27°C (62 and 80°F).

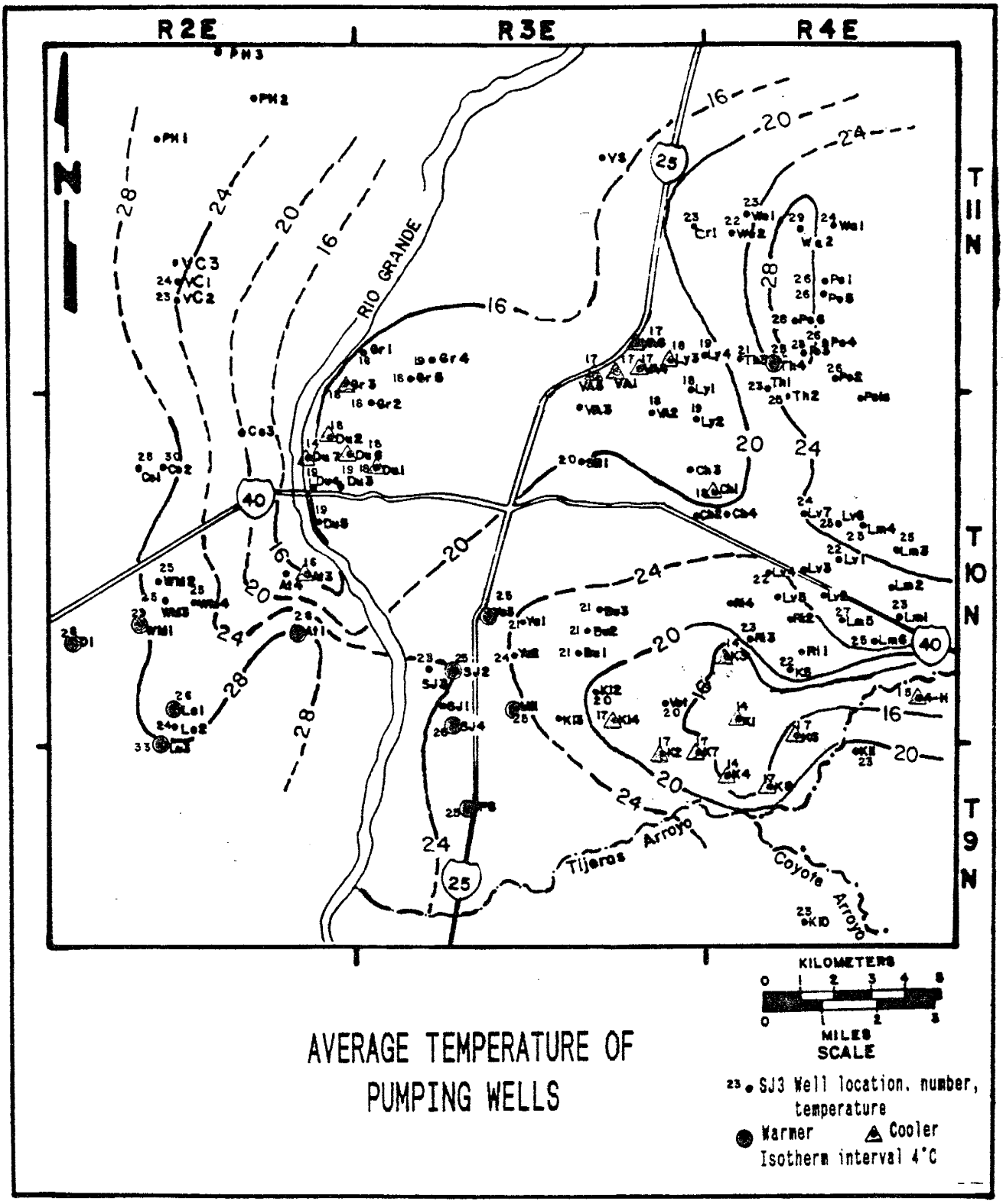

Figure 25: Water temperatures are influenced by the depth of the producing formation, local geothermal gradient and ground waters residence time. Warmer or cooler ground water deviates from the expected temperature.

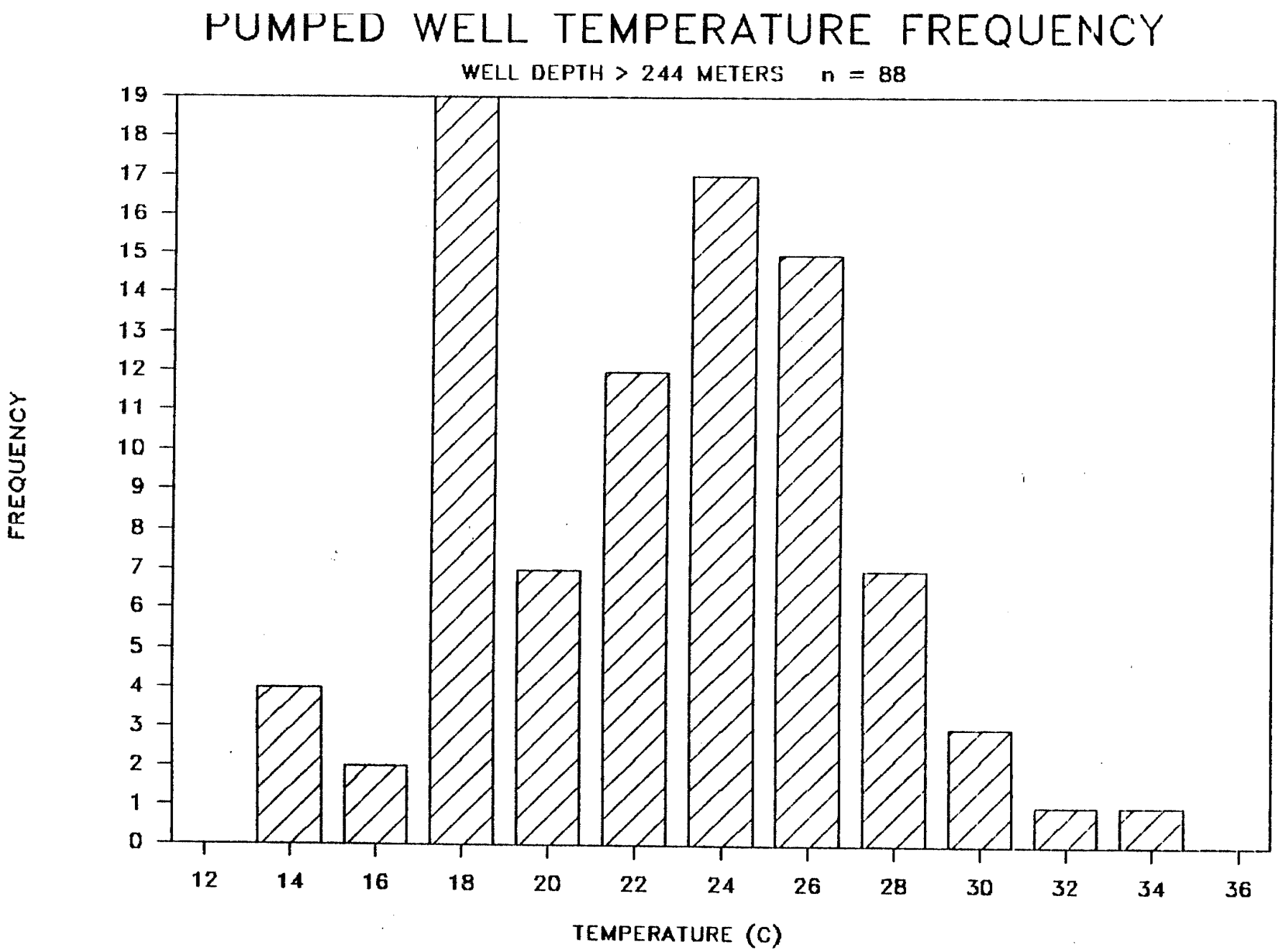

Figure 26: Ground-water temperature frequency for pumping wells is bimodally distributed at 18°C and 24°C with most ground-water temperatures between 22°C and 26°C.

Technique:

Under steady-state conditions, ground-water temperature measured in a deep static well should reflect the local geothermal gradient. For ease of interpretation I used the following simplifying assumptions:

1. the geothermal gradient is linear and uniform throughout the region,
2. ambient flow is horizontal and ground water at a given depth is in equilibrium with the regional geothermal gradient.
3. the pumped ground-water temperature represents the geothermal temperature averaged over the length and depth of the screened interval,
4. all ground water is either;
    (a) produced only from the top of the screen and represents the minimum pumping temperature for the well,
    (b) produced uniformly over the screened interval and represents the average pumped ground-water temperature or
    (c) produced only from the bottom of the screened interval and represents the maximum pumped ground-water temperature.

To estimate the pumped ground-water temperature range for wells in the Albuquerque area I needed to know the local geothermal gradient. I estimated down-hole temperatures using geothermal gradients of 3.4, 14.1, and

24.7°C/km (1, 1.5, and 2°F/100 ft) plus the mean annual air temperature 15.5°C (60°F) (Hilchie, 1982) and compared them with pumped ground-water temperatures.

$$T(z) = Z \cdot G + MAT$$

T = down-hole temperature
Z = depth (meters)
G = Geothermal Gradient (°C/m)
MAT = mean annual air temperature (°C)

Down-hole temperatures plus the ambient air temperature used in this study are 20, 30, and 40°C/km.

Jiracek and others (1982) found the thermal gradient (T(z)) on the West Mesa in good agreement with the thermal gradient determined by the U.S. Geological Survey of about 30°C/km. Grant (1982) listed thermal gradients for Albuquerque Basin deep wells between 29 and 48°C/km (1.5 to 2.5°F/100'+ 60°F).

Discussion:

Assuming wells do not produce water uniformly over their screened intervals the minimum, average and maximum pumping temperatures were calculated for each well using a down-hole thermal gradient of 30°C/km. Figure 27 shows the envelope of "expected" pumping temperatures for wells at a given depth, assuming the well produced all of its water from either the top (minimum), over the total length (average), or bottom (maximum) of the screen.

Wells producing water with temperatures lower than their expected minimum are probably receiving water from a near by recharge source along a short flow path. Low water

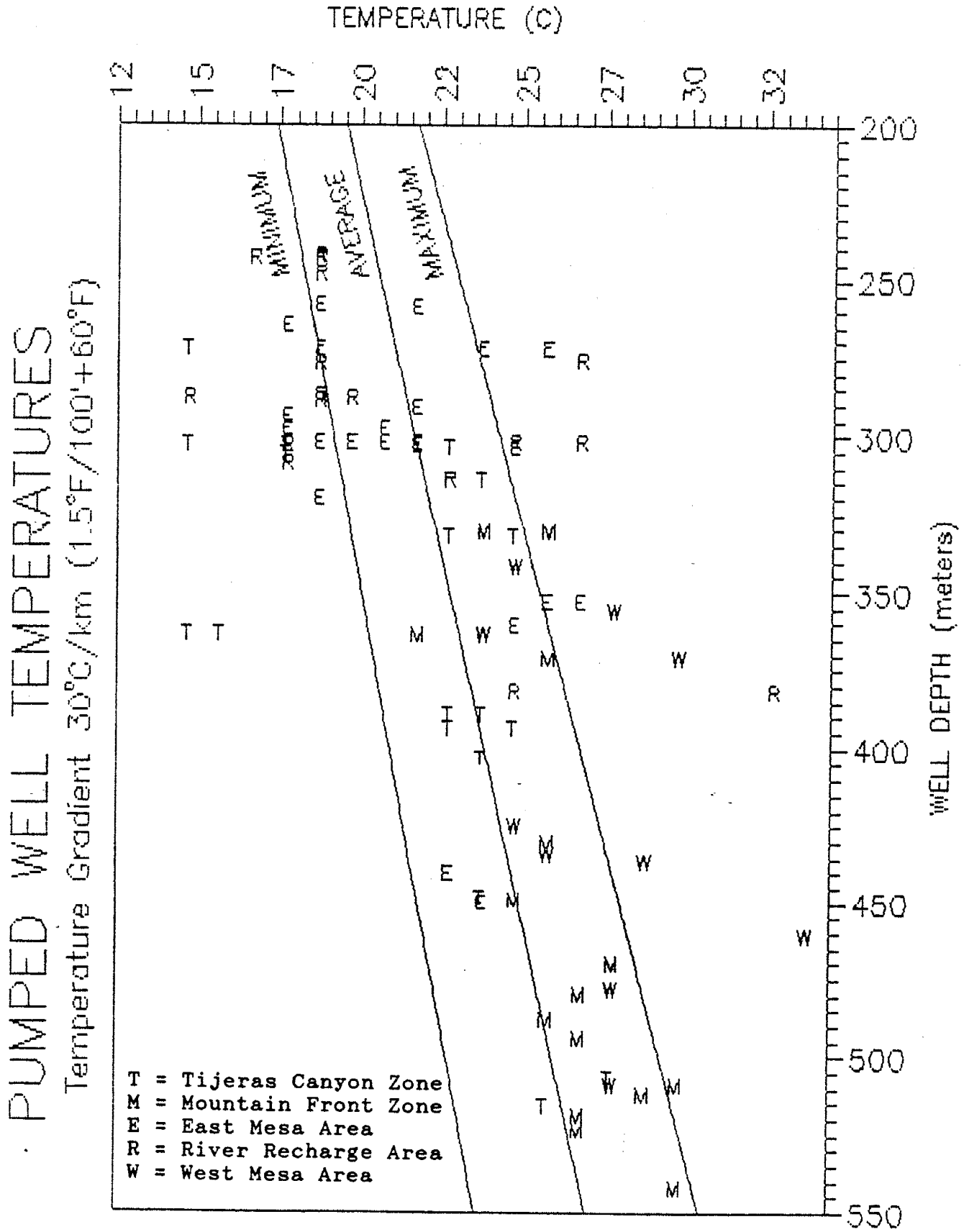

Figure 27: Minimum, average, and maximum temperature envelopes were calculated at the assumed geothermal gradient if all the ground water were produced from the top of the screen, averaged over the entire screen, or from the bottom of the screen.

temperatures may also represent a mixture of warmer, deeper water with cooler, shallower water, such as: mountain-front recharge, storm infiltration through arroyos, or recharge from the Rio Grande and its associated inner-valley irrigation and drainage system.

Wells with pumping temperatures above the maximum expected temperature line probably have a secondary heat source. Wells with warmer than average temperatures may be tapping deeper, older ground water forced upward by upthrown blocks of lower permeability sedimentary beds or geothermal flow moving upward along deep-seated faults, or water associated with buried igneous bodies. The assumed geothermal gradient may by higher in areas associated with buried igneous bodies or basin faulting.

Circled wells on figure 25 are warmer than expected while well locations with triangles are cooler than expected with respect to the down-hole temperature gradient of 30°C/km shown on figure 27. These wells produce ground water with apparently anomalous temperatures which are useful for interpreting the genesis of ground water in that area.

Some well temperatures fluctuate between the expected and anomalous temperature range. From the limited data it appears as if these wells produce cooler water after an idle period with gradually increasing temperatures after extended pumpage. Pumped ground-water temperatures may vary as much as 10C° (18F°) in a well. Atrisco well 1 (At1), West Mesa wells 1 and 4 (WM1, WM4), Leavitte well 1 (Le1), and College well 2 (Co2) all exhibit this behavior.

HYDROGEOCHEMICAL SETTING

In the following sections I will introduce study-area divisions, describe sources of dissolved ions and interpretation techniques , recharge geochemistry, and spatial variations of major geochemical constituents within the study area. After the spatial picture is drawn I will discuss each area division and interpret possible geochemical processes which may explain the observed ground-water geochemistry.

Figure 28 is a hydrogeochemical facies map based on a simple water-type naming system. Water-type names represent the cation-anion pairs with the highest percentage reacting ratio in milliequivalence. It was this map that started me asking the some of the questions I am trying to answer in this study. If I assumed an approximate east to west flow system, what geochemical process would change the dominant cation ratio of ground water? How could a sodium-bicarbonate (Na-HCO3) water be surrounded by calcium-bicarbonate (Ca-HCO3) waters? What could cause calcium-chloride (Ca-Cl) waters in a calcium-

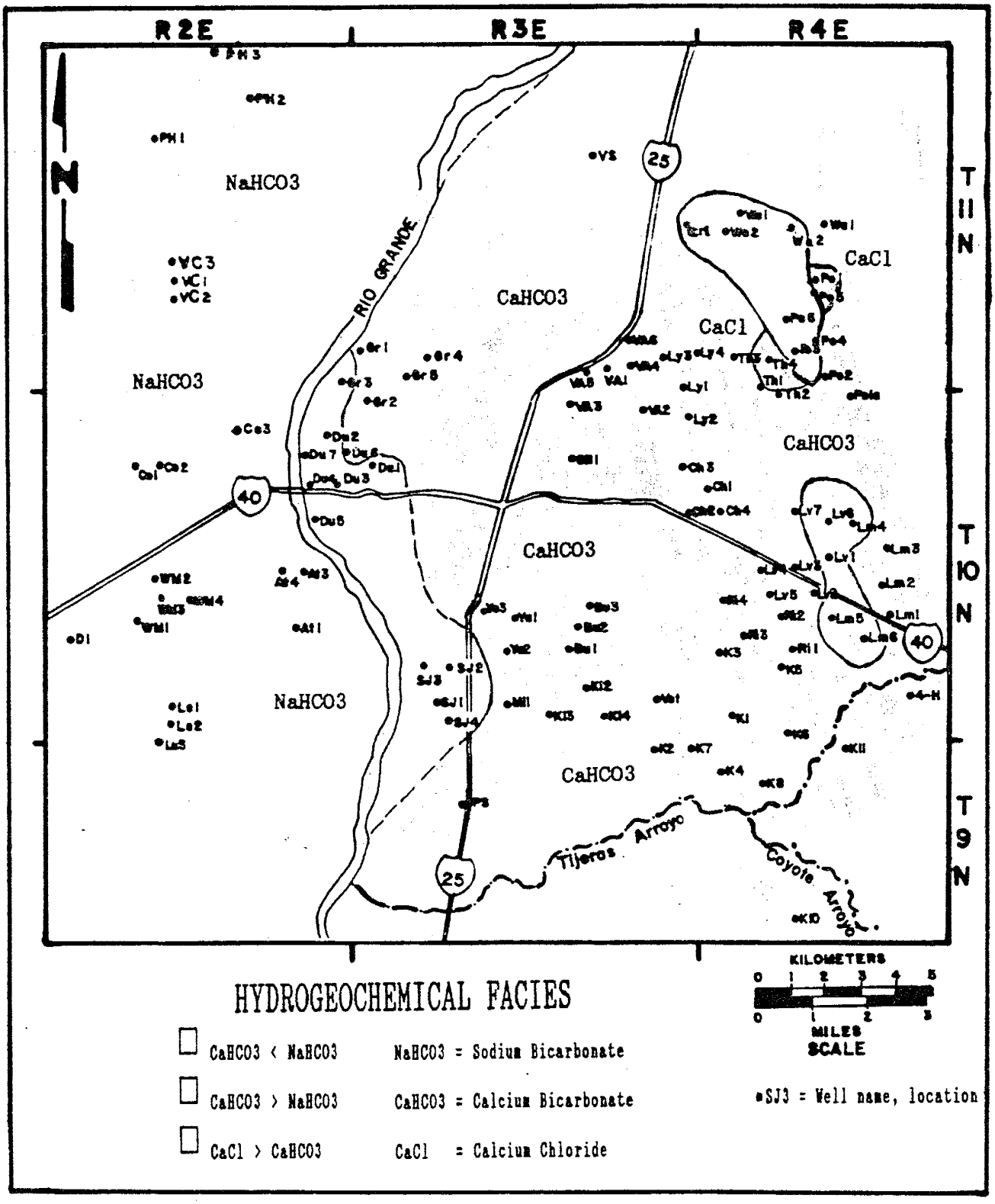

Figure 28: Water-type names are based on dominant cation and anion reacting percentage pairs used for trilinear plotting of major ions. The river and 2/3 of the wells produce Ca-HCO3 water.

bicarbonate dominant system and explain their distribution? If Ca-HCO3 water of the Rio Grande recharges the aquifer, why does recharge and ground water near the river shift to Na-HCO3 dominant waters? Answering these questions uncovered several other perplexing ground water characteristics I will try to answer in this study.

Water-type boundaries are metastable. Near the boundaries, cation and anion pairs are nearly equal and ion dominance may fluctuate between sodium, calcium or chloride from one analysis to another.

Study Area Divisions

Study area divisions are loosely based on the probable ground-water source to an area, geochemical and isotopic trends, and flow directions suggested by the 1989 water-table configuration. Ground-water geochemical trends are gradational, therefore area boundaries are not based strictly on chemistry.

Figure 29 shows the five area boundaries used in this discussion. The mountain recharge area is divided into two zones, the mountain-front zone (MFZ) and Tijeras Canyon Zone (TCZ) based on different recharge processes. The East Mesa or mid-fan area (EMA) lies between the river recharge and mountain recharge areas. The River Recharge area (RRA) includes all wells within the flood plain. The West Mesa area (WMA) includes all wells west of the Rio Grande flood plain physiographic boundary. For ease of discussion, area boundaries will be drawn on all subsequent maps.

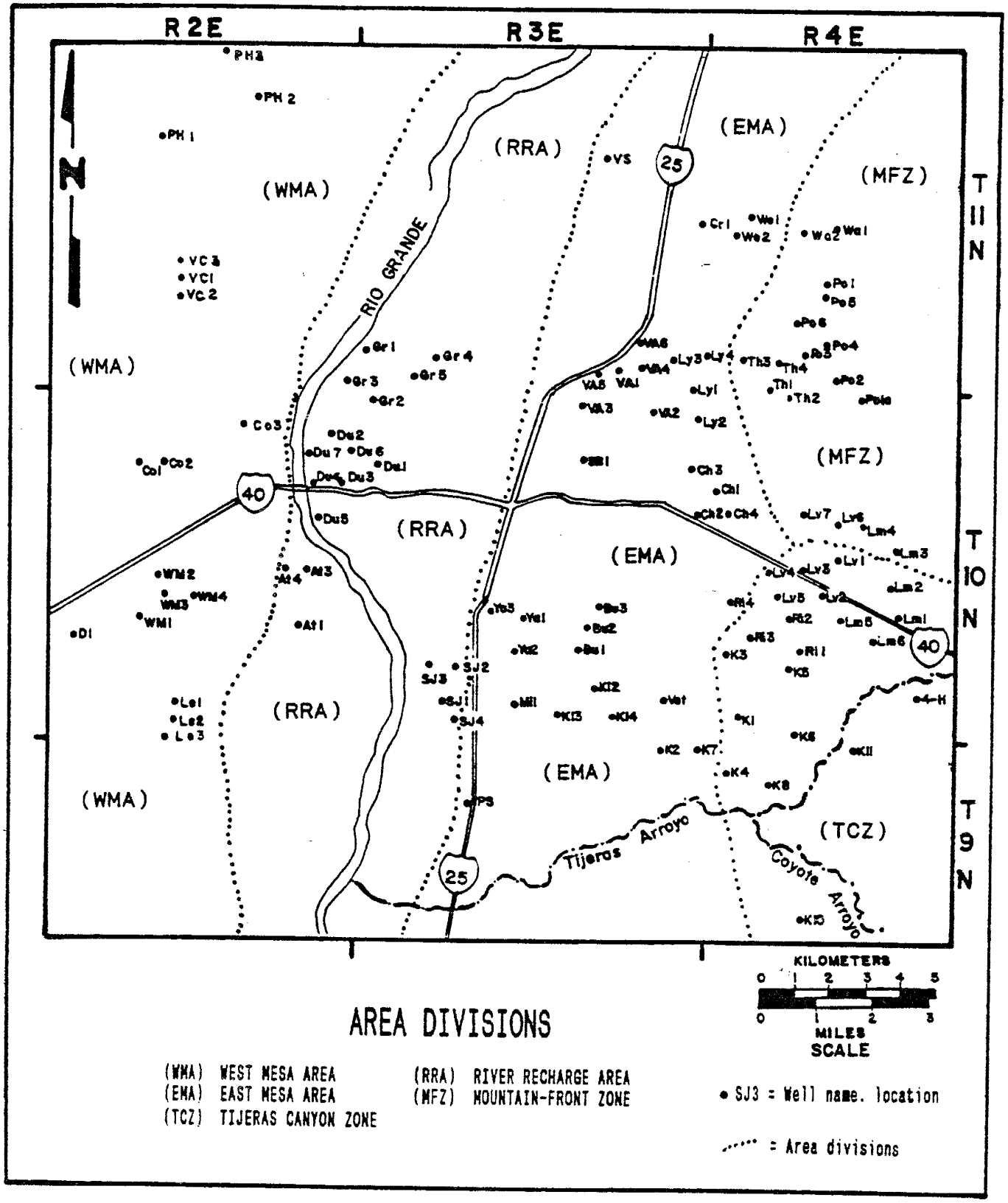

Figure 29: Area divisions are based on proximity to recharge sources, permeability, and geochemistry.

Sources of Dissolved Ions in Ground Water

There are at least four processes contributing to ion species and concentrations in ground water in this area: (1) atmospheric input, (2) soil zone reactions, (3) rock mineral-water interactions, and (4) ion exchange.

The first source of ions in water comes from atmospheric input, ions dissolved in rainwater and snow. Atmospheric input represents the minimum expected ion concentration for springs, streams, and ground water. As storms move across the continent they gain ions from airborne particlulate matter and aersols, and lose ions through precipitation. Atmospheric input is measured from wet or bulk samples. Wet samples contain only rainwater or snow. Bulk samples contain the wet sample and dry-fallout. Dry-fallout comes from airborne particulates that collect on the sample container between storm events (Steele and Wagner 1985, Popp and others 1984).

Popp and others (1984) studied the chemical composition of Albuquerques precipitation. Various aspects of their study covered from one to four years of data collection. Table 4 lists average major ion concentrations and ion ratios in precipitation collected by either wet-only samples or bulk samples.

To compare precipitation chemistry with spring, ground, and surface water chemistry, I drew evaporation lines with ion/chloride ratio slopes. This line represents the ion content of rainwater if the only process occurring

TABLE 4: Precipitation Data for Albuquerque
(Popp and others 1984)

Species (ppm)	Precip. (ppm)	Bulk (ppm)	Wet (ppm)
Ca	2.9	2.1	0.44
Mg	0.18		
Na	0.84	0.3	0.13
K	0.3		
SO4	4.0	2.2	1.0
Cl	1.4	2.7	0.2
pH (1)	5.5		
pH (2)	4.0		
Ca/Cl	2.07	0.78	2.20
Na/Cl	0.60	0.11	0.65
SO4/Cl	2.86	0.81	5.00

(1) Event based average n = 26
(2) Volume weighted average n = 26

is evaporation (Wagner and Steele, 1985). Mineral precipitation due to ion concentration is ignored.

Bulk-rain sample ion content should be more representative of local recharge water than wet-rain sample ion content (Wagner and Steele 1985). What I observe are bulk-rain evaporation line slopes are much lower than wet-rain evaporation line slopes. Bulk-rain slopes do not fit the spring or ground-water data as well as wet-sample slopes. Three possible explanations for this discrepancy are: (1) the volume of dry depositional material trapped in a sample collector may be greater than dry depositional material dissolved in rain because, in an arid climate, dry material freely circulates (recycles) between the ground and atmosphere. (2) the bulk-rain sample set size is smaller than the wet-sample set size therefore may not represent the average bulk chemistry. (3) dry-fall ion contribution may be insignificant in a large-volume storm event of very dilute water. Water from these large volume events infiltrate below the zone of evaporation to become recharge.

Uncertainty in the average precipitation chemistry adds uncertainty to this method of comparative analysis. However, the ground water and spring discharge data fit the wet-sample evaporation line well enough that I believe this technique is useful for suggesting soil zone (pedogenic) enrichment or depletion of certain major ions.

The second process affecting ion concentrations in ground water takes place in the soil zone where the most

profound changes occur. Drever (1982) explains the importance of soil processes to ground water chemical composition in arid regions - he calls this process soil wetting and drying cycles. In this process light rains and snowmelt infiltrate a few centimeters (inches) into the soil during wet periods then completely evaporate during dry periods - depositing dissolved solids as salts within the zone of evaporation. The zone of evaporation is about one meter (39 inches) in New Mexico. Subsequent infiltrating moisture re-dissolves the highly soluble salts and partially re-dissolves the less soluble salts, thereby enriching the water percolating below the zone of evaporation.

As soil water evaporates, minerals precipitate from the bulk solution in the order of the Hardie-Eugster model of chemical divides (described in Drever, 1982). In essence, the abundance of one ion over another will control which mineral will precipitate after calcite. The Hardie-Eugster model for evaporating dilute water until it reaches the concentration of a brine suggest salts precipitate in this order: calcite > gypsum or magnesium rich smectite > chlorides of sodium and potassium (Drever 1982).

During the re-solution process sodium and chloride salts dissolve rapidly while minerals such as gypsum, calcite, and particularly silica dissolve slowly. The order and amount of salt and mineral re-solution is controlled by the kinetics of dissolution of the

precipitated phase and not strictly by solubilities (Drever 1982).

The resultant water affected by wetting/drying cycles may be strongly undersaturated with respect to gypsum, amorphous silica and sepiolite even though the water is depleted (apparent precipitation) in sulfate, calcium, silica and magnesium relative to atmospheric input (Drever 1982).

Shallow ground-water bodies experience the same process in the capillary zone above the water table. If the water table is near the surface, capillarity draws water upward where it completely evaporates depositing its dissolved minerals as salts (Drever 1982). Seasonal fluctuations in the water level will re-dissolve some of these salts and minerals. The resultant water will be undersaturated with respect to some salts but be depleted with respect to the initial concentrations of these ions.

Either water infiltrating through soil subjected to wetting/drying cycles or shallow ground water will show the same results of apparent undersaturation with respect to a salt yet be depleted in that salt with respect to the initial ion concentration.

The third process contributing ions to springs and ground water is the rapid weathering of geologic material in the soil zone. Initially dilute, acidic, oxidizing snowmelt or rainwater infiltrates into the soil where it chemically attacks the fragmented minerals comprising the rock matrix. Hydrogen is consumed as this chemically

aggressive water (≈pH 4) attacks the alumino-silicate minerals. As the minerals dissolved the water (≈pH 8) rapidly becomes less aggressive (Busenberg and Clemency 1976).

The resultant water, higher in total dissolved solids and bicarbonate than the initial atmospheric input, moves from the soil zone into the fractured bed rock. Weathering rates are much lower here. Mineral surfaces are clad with very stable clays, the products of mineral weathering. Below the soil zone weathering occurs primarily by diffusion through this stable clay layer but at a very slow rate (Drever 1982, Stumm and Morgan 1981).

The thermodynamic weathering sequence for common minerals in this area is: gypsum, calcite, Ca-feldspar, K-feldspar, Na-feldspar, Ca and Na smectites, quartz, K-mica, gibbsite, and kaolinite minerals (Stumm and Morgan 1981).

The most abundant minerals in the Sandia Mountains are oligoclase (plagioclase $\approx An_{11}$), microcline (K-feldspar), quartz, and biotite. Smaller amounts of albite and andesine (plagioclases), orthoclase (K-feldspar), and calcite also occur. Accessory minerals are apatite, epidote, hornblende, and magnetite (Kelley and Northrop 1975). Samples from outcrops of alluvial basin deposits contained quartz, calcite, plagioclase and orthoclase as the most common detrital minerals with Ca-smectite, mixed layer illite-smectite, and kaolinite as the most common clay minerals (Anderholm, 1985).

Subsurface sediment samples collected from a borehole over 300 meters (1000 ft) deep near the mountain front (MFZ) contained detrital quartz and feldspars with some iron staining, and 5 percent weathered biotite. Sediments from a flood plain well (RRA), about 244 meters (800 ft) deep, contained less than 1 percent weathered biotite. Clay samples from two deep City test boreholes were analyzed by New Mexico Bureau of Mines. One test well is located in the East Mesa (EMA) high permeability zone while the other test well is out of the study area in the far West Mesa (WMA) fine grained sediments. Sample depths ran from 315 to 718 meters (1036-2365 feet). Clay samples were dominantly Ca-smectite except in one sample where kaolinite was the major clay. Kaolinite and mixed illite-smectite were the second most common clay and illite the least dominant clay (City unpublished data). Both the surface samples of Anderholm and the deep borehole samples of the City's are in agreement with respect to clay mineralogy. Table 5 summarizes the mineralogical information.

George Austin, Senior Minerals Geologist with the New Mexico Bureau of Mines, states these clays are typical of the detrital suite in New Mexico with little or no diagenesis for the samples near the mountain front. The samples from the far West Mesa (WMA) deep well are altered bentonitic ash or a mixture of altered ash and river sediments typical of sediments found in the Rio Grande valley (unpublished letter to the City, 1989).

According to Drever (1982), kaolinites convert to

TABLE 5: Common primary and secondary minerals in the recharge area and aquifer.

LOCATION	SURFACE CLAY MINERALS (parts in 10)		MATRIX MINERALS	Rank Abundance	DATA SOURCE
T12N.R4E.18 NE1/4	Eastern boundary of flood plain				2 (Sample 1)
Santa Fe Edith	Interlayer illite-smectite	3	Quartz	1	
	Ca-smectite	1	Plagioclase	2	
	Kaolinite	4	Orthoclase	3	
	Illite	2	Calcite	4	
			Gypsum	5	
T10N.R1E.18 SE1/4	Eastern boundary Rio Puerco				
Santa Fe Upper Buff	Interlayer illite-smectite	2	Quartz	1	2 (Sample 3)
	Ca-smectite	6	Plagioclase	2	
	Kaolinite	1	Orthoclase	3	
	Illite	1	Calcite	4	
			Dolomite	5	
			Hornblende (?)		
T12N.R4E.7	Eastern boundary of flood plain				
Santa Fe Mid. Red	Interlayer illite-smectite	4	Quartz	1	2 (Sample 9)
	Ca-smectite	3	Calcite	2	
	Kaolinite	2	Plagioclase	3	
	Illite	1	Orthoclase	4	
			Gypsum	5	
			Zeolite	8	
T13N.R4E.32	Eastern boundary of flood plain				2 (Sample 10)
Santa Fe Mid. Red	Interlayer illite-smectite	4	Calcite	1	
	Ca-smectite	3	Quartz	2	
	Kaolinite	2	Feldspar	3	
	Illite	1	Zeolite	5	

LOCATION	SUBSURFACE CLAY MINERALS (parts in 10)		MATRIX MINERALS	Rank Abundance	DATA SOURCE
T11N.R1E.27.431	Far West Mesa well (Soil Amend. Fac.)				3
316 m (1036 ft)	Interlayer illite-smectite	1	Quartz		3
	Ca-smectite	2			3
	Kaolinite	6			3
	Illite	tr			3
371 m (1218 ft)	Ca-smectite	5	Quartz		3
	Kaolinite	4			3
	Illite	1			3
454 m (1490 ft)	Ca-smectite	10	Quartz		3
	Kaolinite	tr	Feldspar		3
721 m (2365 ft)	Ca-smectite	8	Quartz		3
	Kaolinite	2	Feldspar		3
	Illite	tr	Calcite(?)		3

TABLE 5: Common primary and secondary minerals in the recharge area and aquifer.

LOCATION	SUBSURFACE CLAY MINERALS (parts in 10)		MATRIX MINERALS	Rank Abundance	DATA SOURCE
T10N.R4E.6.341	East Mesa well Thomas # 7				3
361 m (1185 ft)	Interlayer illite-smectite	1	Quartz		3
	Ca-smectite	5	Dolomite		3
	Kaolinite	2			3
	Illite	2			3
364 m (1195 ft)	Interlayer illite-smectite	2	Quartz		3
	Ca-smectite	4	Calcite(?)		3
	Kaolinite	2			3
	Illite	2			3

LOCATION	SURFACE AND DETRITAL SUBSURFACE ROCK FORMING MINERALS	MATRIX MINERALS	Rank Abundance	DATA SOURCE
Sandia Mountains	Modal Composition for Tijeras Canyon			4
	K-feldspar (K44)			4
	Plagioclase (An16.5)			4
	Andesine (An44)			4
Sandia Granite				
	Sanidine			4
	Orthoclase (Or96.4, Ab3.6))		0.21	4
	Microcline (same composition)			4
	Albite		0.28	4
	Plagioclase (An27- An28)		0.27	4
	Quartz		0.26	4
Sandia Granite	Microcline		common	1
	Quartz		common	1
	Oligoclase		common	1
	Biotite		common	1
	sphene		accessory	1
	magnetite		accessory	1
	apatite		accessory	1
	hornblend		rare	1
	muscovite		rare	1
	tourmaline		rare	1
	pyrite		rare	1

Data Sources:

1. Kelley and Northrop (1975)
2. Anderholm (1985)
3. City of Albuquerque unpublished letter
4. Affholter (1979)

smectites and mixed layer illite-smectite clays in arid climates. This statement is substantiated by local clay mineralogy.

To use this information I used PCWATEQ (Shadoware, 1987), a computer program written for personal computers, functionally the same as the U.S.G.S. WATEQF (Plummer, et al, 1984) water equilibrium program written for mainframe computers. PCWATEQ calculates aqueous and mineral phases for a given water composition using chemical equilibria data and mass balance to predict mineral phase stabilities.

PCWATEQ calculates equilibrium indices for complete reactions. Intermediate reactions, such as albite to kaolinite can be calculated from the given phase information in PCWATEQ to construct stability diagrams for known mineral phases not included in the program. Assumptions inherent in all stability diagrams is constant temperature, pressure and activity of pure water.

Mineral phase stabilities can be graphically illustrated using stability diagrams. These diagrams can be used to suggest ground water evolution along a flow path by a waters stability relationship to the aquifer matrix minerals and the secondary alteration products (clay minerals) equilibrium boundaries. In natural waters the evolutionary trend is for water in contact with granitic minerals a short time to plot near the gibbsite-kaolinite boundary and to move toward the kaolinite-smectite boundary as residence time increases (Drever 1982).

Drever (1982), Stumm and Morgan (1981), and Garrels and

MacKenzie (1972) did not agree on mineral stability boundary locations or equilibria values. Boundary location calculations are controlled by ion concentrations, and Gibbs Free energy, and the reaction path chosen to represent the weathering sequence. To construct the stability diagrams I calculated intermediate equilibrium constants (K_{eq}) from the log ratio of the solid reactant to the solid product K_{eq}'s. Even with uncertainty in phase boundary locations, the stability diagrams are useful for showing ground-water evolution trends. Mineral equilibria equations are listed in appendix IX.

The fourth process that may alter ground-water ion composition is ion exchange. The measure of a substances ability to exchange cations is called the cation exchange capacity (CEC). The CEC of aquifer media may significantly influence the composition of ground water flowing through it. Chemical reactions and ion exchange occur between dissolved ions in the ground water (bulk solution) and ions on mineral and clay surfaces. A given volume of clay has more than ten times the available surface area of a comparable volume of sand. With greater surface area there are more chemical reaction sites available giving clays a disproportionate importance in controlling ground water geochemistry. In this study I will only discuss clays with respect to ion exchange even though other mineral surfaces may take part in the exchange process.

Drever (1982) states that the exchangeable ions on

clays are dominated by calcium even in arid regions because the regions were much wetter during the late Pleistocene when waters were generally more dilute and calcium was the exchanger. This seems to be the case in the Albuquerque area where Ca-smectites are the dominant clays in both surface and subsurface deposits.

Smectites have a large surface area and CEC. About 80 percent of its surface area is internal surface area. The interlayer cations will freely and reversibly exchange with the dominant ion in the bulk solution. Mixed layered clays of illite and Ca-smectite have about an eighth the surface area of a smectite but have a relatively high CEC. Potassium forms a strong bond to the illite layer in mixed layer illite-smectite clays. Kaolinite has a low CEC and is important in ground water exchange chemistry (Drever 1982).

Exchange sites favor ions with larger ionic charges such as calcium > potassium > sodium. The selective adsorption of potassium over sodium is controlled by the size of the ions hydration sphere. The hydration sphere of sodium is larger than that of potassiums.

To test for ion exchange across the study area I added the concentration of calcium, sodium, and potassium in milliequivalents. If ion exchange were the only process occurring I would expect to see a constant cation sum from east to west along a flow path. The exchangeable ion is not easy to predict but the sum would remain constant.

Figure 30 shows the distribution of cation sums.

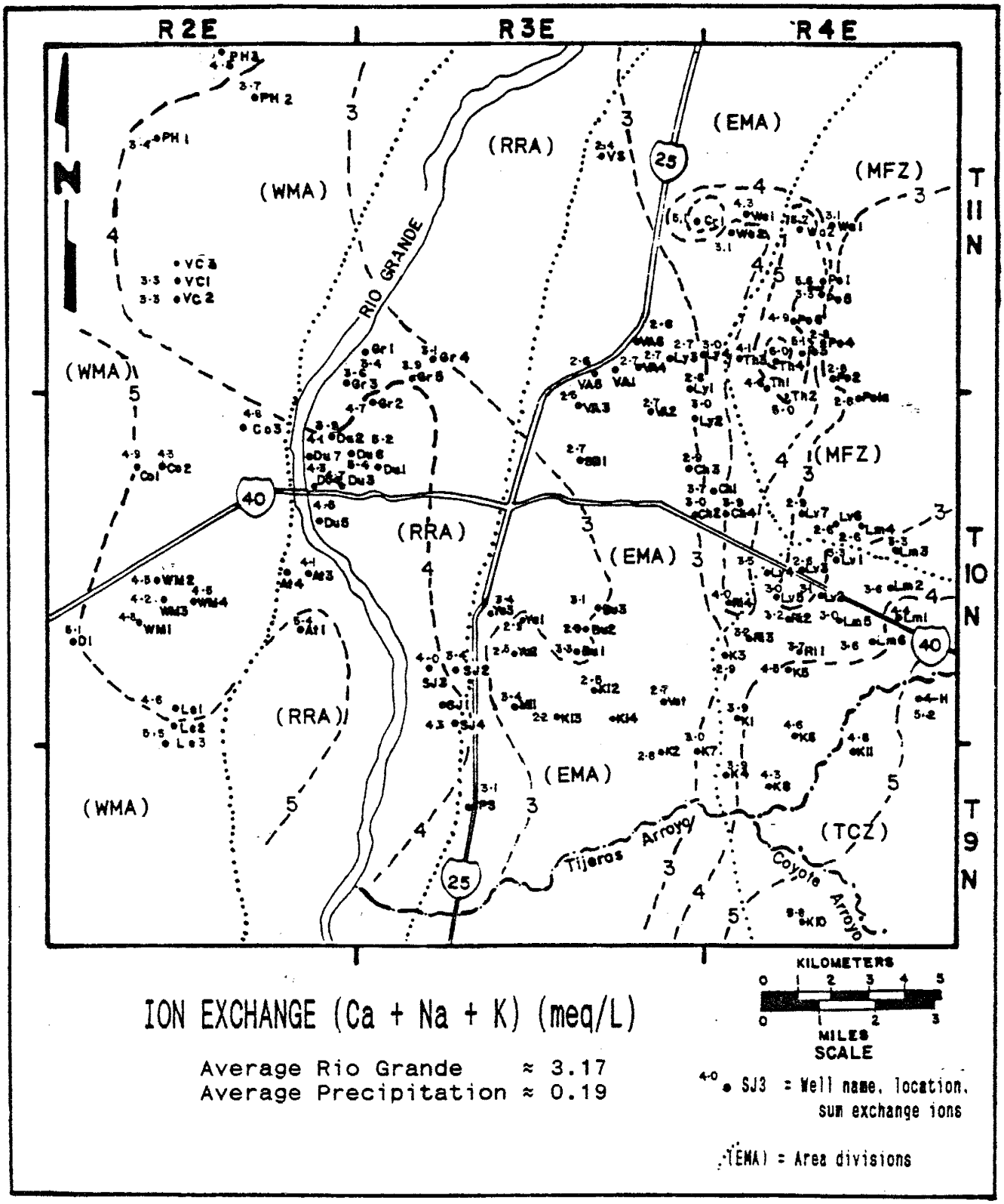

Figure 30: Exchangeable cation sums indicate that changes in ion concentrations along a flow path cannot be explained with a simple ion exchange model.

Total cation concentrations increase and decrease along the 1936 flow path (A to A") shown in figure 23. When comparing figure 30 to the 1988 water-table map, distortions in equal concentration lines appear to be strongly influenced by the current slope of the water table and areas of heavy pumpage.

Ion exchange is occurring, but its importance with respect to other sources or sinks of sodium, potassium and calcium is not clear at this time.

Each of these four ground water altering processes, atmospheric input, soil wetting/drying cycle enrichment and depletion, rock mineral dissolution, and ion exchange will be examined with respect to area divisions later in this study.

Geochemistry of Recharge Areas

The following discussion characterizes the chemistry of water recharging the deep-basin aquifer. Along the mountain front, recharge enters the aquifer through below-surface fracture flow (inflow), springs and ephemeral streams flowing onto shallow pediment deposits above the deep-basin water table, and as run-off infiltrating through arroyo beds crossing the high mesas. In the flood plain, recharge enters the aquifer through the stream bed of the Rio Grande, and nearby drains and irrigation ditches. How deep-well ground-water chemistry differs from recharge water chemistry is the basis for the remaining discussion.

Mountain-Front Recharge

Estimated mountain-front-recharge water chemistry can be determined from Sandia and Manzano mountain springs and the stream draining Tijeras Canyon.

Figure 31 shows the location of springs, Tijeras stream, the drainage divide, edge of the granitic high with respect to the basin-fill deposits, and westward trending arroyos traversing the alluvial fan deposits.

Springs may have encountered granitic or metamorphic rocks, limestone with interbedded marine shales, and/or fluvial shales before surfacing along fault plains. Tijeras stream flows in and through valley-fill alluvium composed of these five rock types. Each host rock type may alter the chemical composition of ground water it contacts.

Processes affecting the chemical composition of mountain-front recharge are deduced from ion ratios of spring water to the ion ratios of precipitation (evaporation line), disequilibrium indices (Log Q/K [PCWATEQ]), and the rock forming minerals spring waters contact.

To test for geochemical alteration of spring waters I made four assumption: (1) that atmospheric input is the source of all initial dissolved major ions; (2) if the ion to chloride ratio increased relative to atmospheric input then ion exchange or mineral dissolution altered the spring discharge; (3) if the ion to chloride ratio decreased relative to atmospheric input then ion exchange or mineral

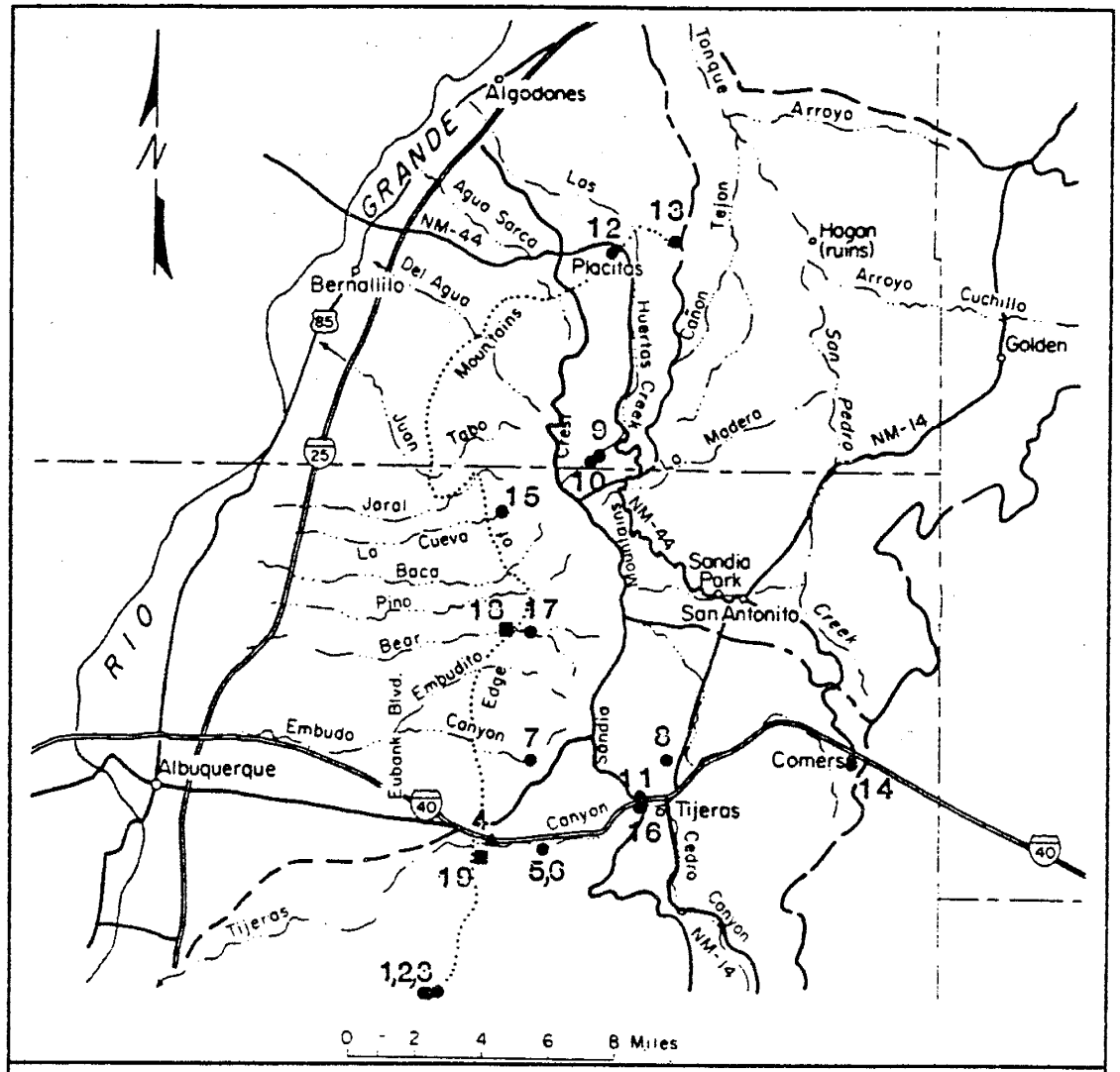

SAMPLE LOCATIONS

● 1 Coyote Spring -1	●10 Head Spring
● 2 Coyote Spring -2	●11 7-Spring -1
● 3 Coyote Spring -3	●12 Placitas Spring -1
▲ 4 Tijeras Stream	●13 Placitas Spring -2
● 5 McDaniel Spring	●14 Brickner Spring
● 6 McDaniel Pond	●15 La Cueva Spring
● 7 Embudo Spring	●16 7-Spring -2
● 8 Hobbie Spring	●17 Bear Canyon Spring
● 9 House Spring	■18 Bear Canyon Well
	■19 Tijeras Canyon Well

Figure 31: Location of springs, shallow pediment wells and Sandia Mountain drainage basins (modified from Kelley & Northrop 1975, fig. 4)

precipitation altered the spring discharge; (4) if the ion to chloride ratio remains essentially constant then increased ion concentrations in spring water is due to evaporation.

Table 6 lists the relative differences in the spring water analyses with respect to the precipitation evaporation line and the disequilibrium index for calcite and gypsum. Also listed are the geologic material the springs discharge from and suggestions for several different processes which may be altering the geochemical composition of the spring waters.

Figure 32 shows the evaporation line for average major ion content in Albuquerques precipitation plotted with the ion content of springs and Tijeras stream. All spring and Tijeras stream data are single analyses and may not represent the average ion concentration in spring discharge. The numbers by each symbol are map codes for identifying and locating springs on figure 31 and table 6.

Figure 32a is the sulfate (SO4) versus chloride (Cl) plot of spring data with respect to the SO4/Cl ratio in precipitation, the rain-evaporation line. More than half the spring-water analyses follow the evaporation line indicating good agreement between atmospheric input and the spring's SO4/Cl ion content. Several springs are depleted in sulfate with respect to atmospheric input which indicates sulfate removal by precipitation or sulfate reduction. Redox potential data is not available therefore sulfate reduction will not be considered in this study.

TABLE 6: Spring analysis summary

SPRING NAME	RAIN DIFF Ca (meq)	RAIN DIFF Mg (meq)	RAIN DIFF Na+K (meq)	RAIN DIFF SO4 (meq)	LOG(Q/K) CALCITE	LOG(Q/K) GYPSUM	GEOLOGIC MATERIAL	ALTERAT PROCESS	MAP-CODE
RAIN									
COYOTE-1 (211)	-36.68	0.17	1.94	-26.39	1.669	-1.268	gr:Qal	1:4	1
COYOTE-2 (112)	-18.12	0.80	-0.17	-14.24	1.377	-1.500	gr:Qal	1:2:4	2
COYOTE-3 (113)	-25.19	0.50	1.58	-18.71	1.507	-1.390	gr:Qal	1:2:4	3
TIJERAS ARROYO	-3.82	1.27	-0.75	-2.85	0.899	-1.377	Qal	1:2:4	4
MCDANIEL SPR	-1.53	1.34	-0.53	-1.00				4	5
MCDANIEL POND	-1.11	1.32	-0.51	-0.93			Qal	4	6
EMBUDO	5.57	2.36	0.69	1.45	0.808	-1.294	gr:Qal	1:2	7
HOBBIE	3.51	0.57	0.27	0.18	0.379	-2.223	ls	2	8
HOUSE	3.03	0.44	-0.26	-0.40			ls:trv	2	9
HEAD	4.63	0.18	-0.01	0.12			ls:trv	2	10
7-SPRING-1	3.53	1.05	0.42	1.36			gr:Qal	2	11
PLACITAS-1	3.22	0.34	0.11	0.20	0.152	-2.291	ls	2	12
PLACITAS-2	2.77	0.70	1.76	0.26	0.271	-1.974	ss:sh:trv	2	13
BRICKNER	2.82	1.50	0.31	1.11			ls	2	14
LA CUEVA	1.51	0.55	0.34	-0.01	-0.383	-2.482	gr	2	15
7-SPRING-2	4.69	0.74	0.32	0.92	0.344	-1.679	ls:trv	2	16

LOG(Q/K) = Disequilibrium Index (PCWATEQ) [+/- 0.5 considered metastable equilibrium]
RAIN DIFF = Ion (meq) - Rain evaporation line (meq)

Alteration Processes:
- 1 = Calcite precipitaion
- 2 = Mineral dissolution
- 3 = Ion exchange
- 4 = Effects of salt accumulation in capillary zone

Geologic material springs discharge through:
- gr = granitic
- ls = limestone
- Qal = alluvium
- ss = sandstone
- sh = shale
- trv = travertine deposits near spring

MAP CODE on figure 31

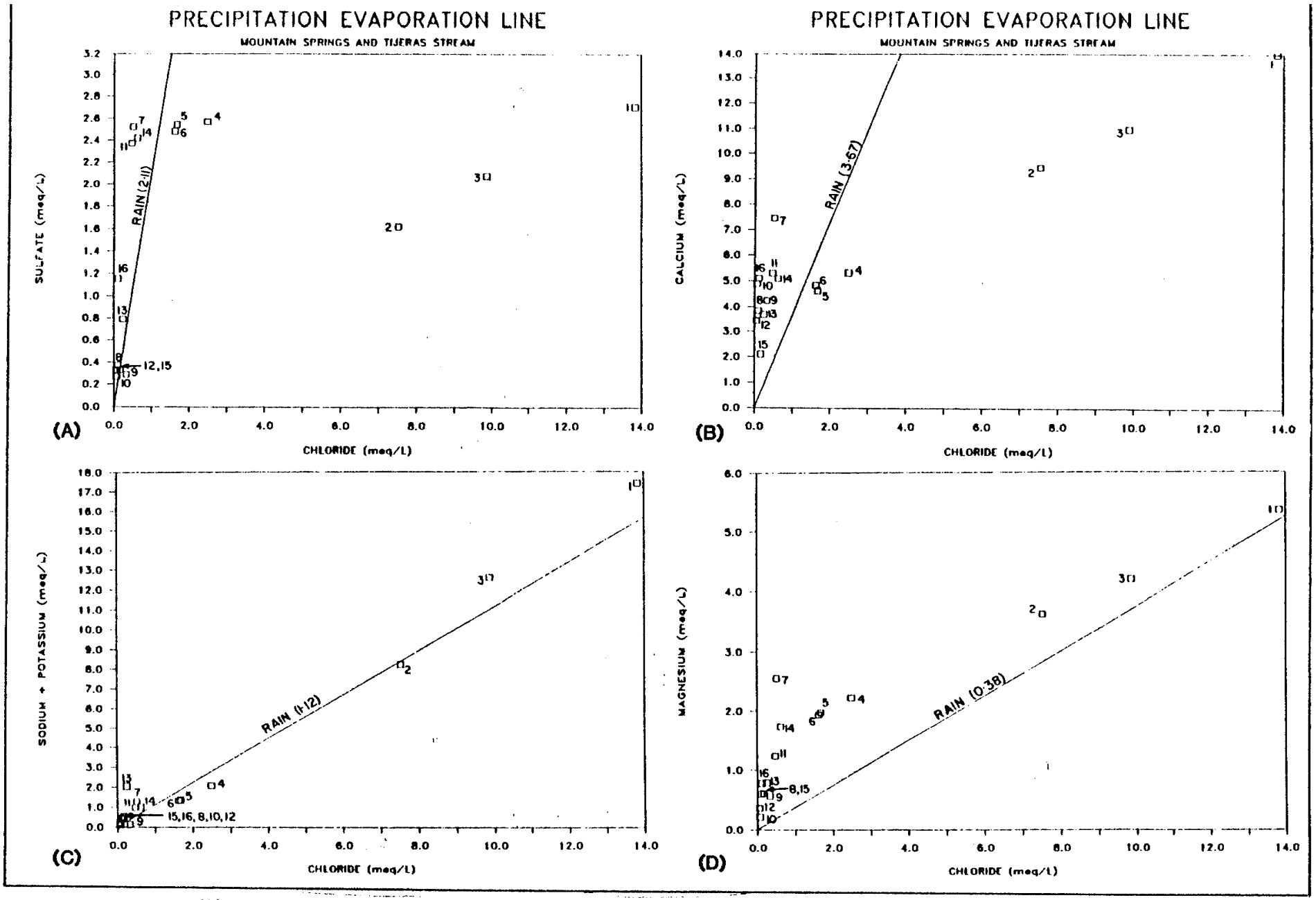

Figure 32: Major ion concentrations in springs with respect to increasing ion concentrations in precipitation with evaporation.

Embudo (7), 7-Springs-1 (11), and Brickner (14) springs have increased sulfate (figure 32a) from 1.1 to 1.45 meq/L (52-70 mg/L SO4) with respect to atmospheric input. Three explanations are: (1) these single analyses for sulfate are not representative of the average spring content; (2) trace amounts of pyrite are present in the granite; (3) re-solution of pedogenic gypsum occurred in the soil zone prior to recharge.

Figure 32b shows that calcium, like sulfate (figure 32a), has considerable scatter about the rain-evaporation line. Calcium is enriched in some springs and depleted in others. Calcium enrichment may occur in the soil zone by rainwater dissolving pedogenic calcite and gypsum or added by dissolution of plagioclase. Calcium is depleted in springs by wetting/drying cycles in the soil zone or in the capillary zone above shallow ground-water bodies.

Springs enriched in calcium are Embudo (7), Hobbie (8), Head (9), House (10), 7-springs (11), and Placitas-1 (12) with more than 3 meq (60 mg Ca) increase in calcium with respect to atmospheric input. Springs depleted in calcium are primarily the Coyote springs and Tijeras stream. These calcium depleted springs are also depleted in sulfate.

Figure 32c shows that sodium in the springs follows the rain-evaporation line very well. Sodium is added by plagioclase dissolution. There are no documented sinks for sodium in this area. Placitas-2 (13) and Coyote 1 & 2 (1,2) have more than 1 meq (23 mg Na) increase in sodium above atmospheric input.

Figure 32d shows all springs and Tijeras stream have a relative increase in magnesium above atmospheric input which I attribute to biotite dissolution. Biotite is ubiquitous in the mountain-front recharge area and is relatively easily weathered. Magnesium increases from 0.17 to 2.35 meq/L (2-68 mg/L) in the springs.

Calcite disequilibrium indices indicate Hobbie (8), La Cueva (15), Placitas 1 & 2 (12,13) springs, and Tijeras (4) stream are metastable (near equilibrium) while all other spring waters are supersaturated and probably precipitate calcite (table 6).

Gypsum disequilibrium indices indicate all spring waters and Tijeras stream water are undersaturated with respect to gypsum. But evaporation line analysis of sulfate and calcium concentrations (figures 32a & 32b) suggest gypsum has precipitated from Coyote's 1,2,&3 springs and the Tijeras stream. A simple explanation is to invoke Drever's (1982) wetting/dying cycles in the soil zone and capillary zone of shallow ground water. Spring and stream water enrichment by re-solution of highly soluble salts produces water undersaturated with respect to gypsum but depleted in calcium and sulfate with respect to atmospheric input.

Figure 33 is a trilinear plot of the springs, rain, and Tijeras stream data. Trilinear plots are useful for demonstrating similarities among different water samples, solution or precipitation of a single salt, and mixtures of

TRILINEAR DIAGRAM

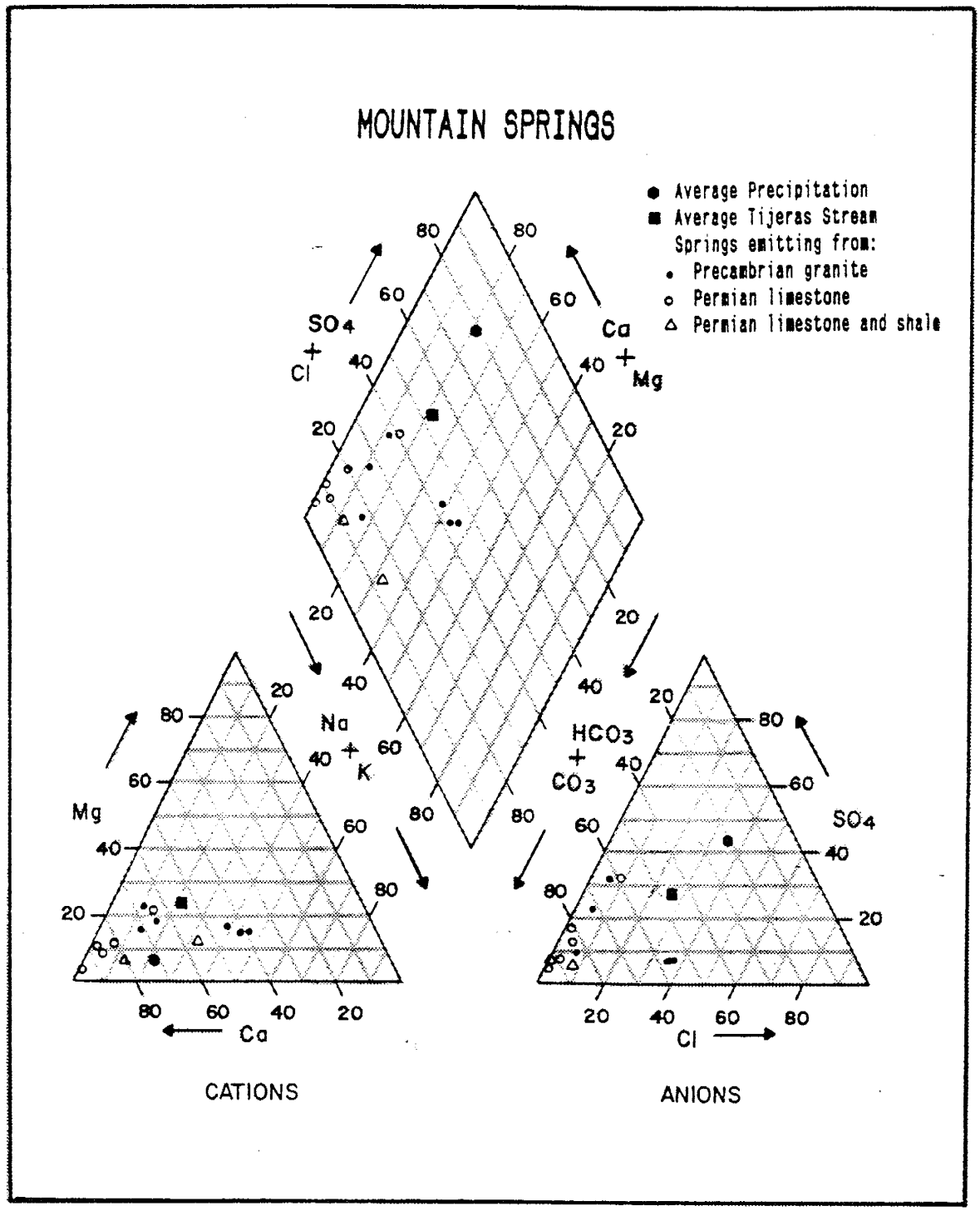

Figure 33: A trilinear plot of spring water analyses show the springs major ion content is influenced by the rock-types waters contact.

waters (Hem, 1970).

In the cation field spring water data scatter about both the rain and Tijeras stream reacting percentages. Spring waters plotting above the 80 percent calcium field emanate from limestone. These springs are low in percent reacting magnesium and sodium. Spring waters emanating from granitic rocks are generally lower in sodium and higher in calcium and magnesium reacting percentages than precipitation. The three Coyote springs cluster below precipitation showing both a depletion in calcium and an increase in sodium and magnesium relative to the precipitation percentage.

In the anion field alkalinity is increasing in all springs above precipitation and Tijeras stream percentages. Reacting percentage of chloride and sulfate are low relative to the total anions in all but five spring waters. The three Coyote springs are about 40 percent higher in chloride and the two Tijeras Canyon springs are about 10 percent higher in sulfate than other mountain spring waters. Two springs emanate from the Yeso formation but from two different depositional environments, Hobbie Spring flows out of limestone while Placitas-2 is from a gypsiferous-red sandstone and shale unit. In a general sense, spring waters from limestones cluster and springs from granitic terrain scatter on the trilinear plot.

Stability diagrams utilizing the log cation activity and pH versus the log activity of dissolved silica show that kaolinite is stable with respect to magnesium,

potassium, calcium, and sodium in spring waters. Diagrams for magnesium and potassium are not included.

Secondary minerals of magnesium or sodium have not been reported in the literature for this area. Rain-evaporation line analysis show an increase in dissolved magnesium for all springs, therefore magnesium is probably added rather than removed from spring waters.

Stability diagrams for the activity of potassium in spring waters show kaolinite is very stable with respect to potassium. Figure 34a shows potassium is depleted with respect to the atmospheric input for most springs. Potassium removal could be from either exchanging with calcium in calcium-smectites to form mixed layer illite-smectite clays or potassium from mineral dissolution is not added to ground water at the rate suggested by the K/Cl ratio of precipitation.

Figure 34b is the reaction quotient versus bicarbonate diagram used to illustrate stability with respect to two clays. Garrels and Mackenzie (1967) suggest the evolutionary pathway from kaolinite to smectite stability for a natural water is controlled by equilibrium with respect to both phases. This theory is supported by the samples apparent asymptotic relationship to the kaolinite-smectite boundary. Smectites in nature vary greatly in composition and may not fit the theoretical boundary (Log $K' = -11.63$) due to differences in equilibrium constants for various smectite compositions. However, the data do

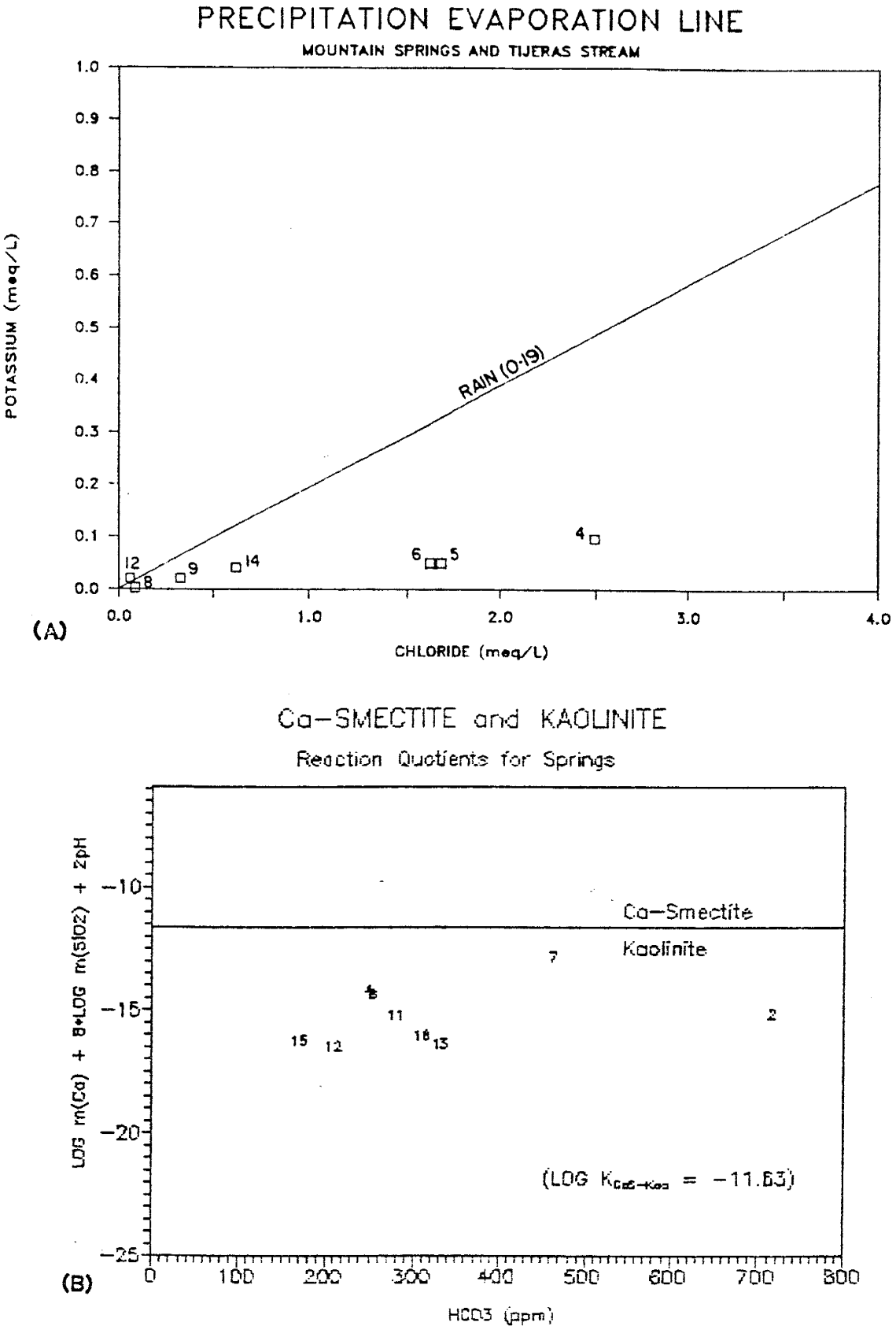

Figure 34: Potassium apparently does not concentrate with evaporation of spring water but is probably removed by illite (secondary clay mineral) formation (A). Spring-waters reaction quotients are approaching equilibrium between calcium smectite and kaolinite (B).

seem to indicate that the chemical composition of the spring waters may be controlled by kaolinite-smectite equilibrium (Drever 1982).

Drever (1982) states it is uncommon for both kaolinite and smectites clays to form at the same time but if they do kaolinite will form in the upper zone and smectites in the lower zones. This trend can be seen in clay samples from the far West Mesa deep test well. Local surface and subsurface clay minerals are listed in table 5.

Figure 35a is an activity ratio diagram for calcium showing the spring water stability with respect to secondary clay minerals of kaolinite, and Ca-smectite. The Na-smectite stability diagram (figure 35b) also shows that spring waters are in equilibrium with kaolinite. Although spring waters appear to be in equilibrium with kaolinite they are evolving toward equilibrium with respect to the Ca-smectite-kaolinite boundary (figure 34b).

Mass-Balance Calculations:

Mass balance calculations similar to Garrels and Mackenzie (1967) assume dissolved solids in the springs come from atmospheric input and dissolution of primary rock minerals the water contacts. To calculate a mass balance I selected a spring similar to the Sierra Spring waters of Garrels and Mackenzie (1967). La Cueva spring emanates from granitic terrain composed of quartz, feldspars and biotite as the primary minerals.

To test the suitability for mass balance calculations

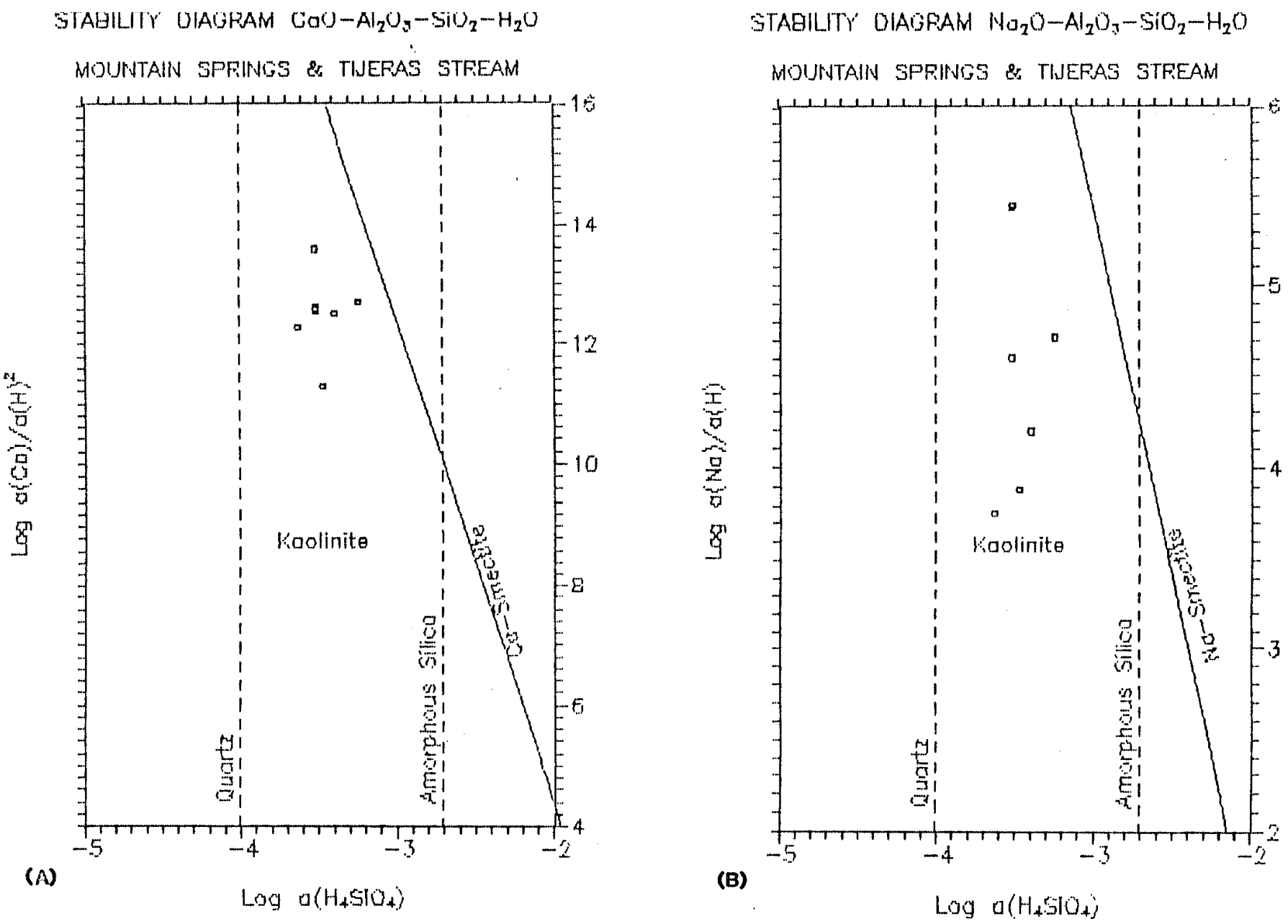

Figure 35: Stability diagrams for secondary clay mineral formation of calcium smectite (A) and sodium smectite (B) with kaolinite.

I checked the validity of several assumptions inherent in mass balance calculations. Table 7 lists various ion ratios for precipitation and La Cueva spring water, and between the spring and precipitation.

TABLE 7: Ion ratios for La Cueva Spring and Precipitaiton (mmoles)

	SO4/Cl	Cl/Cl	SO4/SO4	Ca/Na	Na/Na	Ca/Ca	Mg/Mg	HCO3/HCO3
Rain:	1.054			1.980				
Spring:	1.077			2.008				
Spring/Rain:		3.925	4.011		14.286	14.484	41.064	66.815

If I assume the only source of chloride and sulfate is atmospheric input I would expect the ratio of SO4/Cl for both precipitation and the spring to be the same. The ratios are nearly equal with about a 2% difference which could be either analytical error or sulfate contributed by trace amounts of pyrite in the granitic host rock. Apparently, sulfate has not been depleted by soil zone wetting/drying cycles.

If I assume SO4 and Cl are conservative then the spring/rain ratios of SO4/SO4 and Cl/Cl should indicate the amount of evaporation concentration the spring water experienced. The ratios indicate La Cueva spring water was concentrated by a factor of 4. To achieve a mass balance I need to subtract 4 times the ions in precipitation from ions in the spring to find the amount of dissolved solids

contributed only by rock minerals.

To find the relative amount each ion increased in the spring water I calculated the spring/rain ratios for each ion. Ca and Na increased about 14 times. If the evaporation factor of 4 is subtracted then Ca and Na increase about 10 times, Mg about 37 times and HCO3 about 63 times.

An essential assumption for Garrels and Mackenzie's (1967) mass balance calculations is that all Na and Ca remaining after atmospheric input is subtracted comes from the dissolution of plagioclase. Comparing the Ca/Na ratios for La Cueva spring and precipitation, Ca increases about 1% in the spring water. A 1% increase could be attributed to analytical error. Apparently the spring water gained Ca and Na in the same 2:1 ratio as precipitation.

Calculations using the 2:1 ratio of Ca to Na for dissolving plagioclase indicate an An_{51} content (Labradorite) which is not found locally. If I calculate a mass balance using plagioclase An_{31} (Oligoclase), the common plagioclase in this area, there is insufficient dissolved silica in the spring water.

Garrels and Mackenzie (1967) proposed that dissolved silica to sodium ratio for plagioclase to kaolinite in the ephemeral Sierra spring water is about 2:1 and about 1:1 for the deep circulating perennial spring. La Cueva has a silica to Na ratio of 0.6:1. They suggested some other solid is forming other than kaolinite as the secondary

mineral. Busenberg and Clemency (1976) suggested the silica and alumina (Si:Al) ions remained as coatings on the plagioclase surfaces in a 1:1 ratio and the other ions were removed by diffusion. Kaolinite has a Si:Al ratio of 1:1 but Ca-smectite has a 1.6:1 ratio thereby removing more silica from solution than the formation of kaolinite. Apparently for each Ca (mmol) removed in the formation of Ca-smectite, 7.33 Si (mmol) are removed from solution assuming an ideal Ca-smectite composition.

River Recharge

Analysis techniques for river recharge water quality are similar to techniques used to analyze the mountain-front recharge water quality. Surface water analyses are from the Rio Grande and the MRGCD system of drains, canals, laterals, and irrigation ditches which flow across the flood plain.

Data for the average river water chemistry are hard to find. Numerous chemical analyses have been reported but are usually partial analyses or the mean concentration of a larger data set. Table 8 lists the available river water quality data, sample location, and data sources. The mean and standard deviation (s) are also listed for this composite data. Single analyses averaged with single average values of larger sample sets disproportionately weigh the composite statistics. Additional data is listed in appendix V.

TABLE 8: COMPOSITE DATA FOR ESTIMATING THE AVERAGE RIO GRANDE GEOCHEMISTRY

SAMPLE SITE	DATE	Ca (mg/L)	n = (#)	Mg (mg/L)	n = (#)	Na (mg/L)	n = (#)	K (mg/L)	n = (#)	Na+K-Na (mg/L)	n = (#)	HCO3 (mg/L)	n = (#)	SO4 (mg/L)	n = (#)	Cl (mg/L)	n = (#)	SOURCE
Isleta	1936-1937	54.5	(10)	9.2	(10)	41.6	(10)	4.69	(10)			160.5	(10)	101.8	(10)	21.6	(10)	1
Albuquerque	10/ /37	62	(9)	11	(9)	49	(9)			49	(9)	168	(9)	127	(9)	26	(9)	2
Albuquerque	6/ /38	24	(10)	6.6	(10)									34	(10)	35	(10)	2
Albuquerque	1966-1976	65.9	(2)	9.1	(2)	47.9	(2)	5.9	(1)					150.0	(1)	37.0	(1)	3
Albuquerque	1976-1986	40.9	(24)	6.9	(24)	24.3	(24)	3.15	(24)					65.9	(24)	10.3	(24)	3
Isleta	1969-1982	47.9	(96)	7.7	(96)	33.5	(96)			29.2	(11)	148	(87)	80	(96)	17.2	(96)	4
ABQ-Baralas	11/03/83	51.7	(1)	7.7	(1)	32.2	(1)	3.51	(1)			173	(1)	78	(1)	17	(1)	5
ABQ-Rio Bravo	11/03/83	50.3	(1)	9.4	(1)	29.9	(1)	3.9	(1)			172	(1)	73	(1)	14	(1)	5
Isleta Dam	11/03/83	49.5	(1)	10.6	(1)	39.1	(1)	5.07	(1)			169	(1)	74	(1)	25	(1)	5
ABQ-Rio Bravo	12/ /83													63.4	(16)	12.6	(16)	6
ABQ-I25	12/ /83													65.7	(16)	17.6	(16)	6
ABQ-Barales	12/ /83													63.0	(16)	11.4	(16)	6
Isleta Dam	12/ /83													67.1	(16)	20.6	(16)	6
ABQ-Rio Bravo	1/ /84													56.7	(16)	11.6	(16)	6
ABQ-I25	1/ /84													58.2	(16)	15.8	(16)	6
ABQ-Barales	1/ /84													55.9	(16)	11.8	(16)	6
Isleta Dam	1/ /84													60.5	(16)	17.4	(16)	6
ABQ-Rio Bravo	2/ /84													54.9	(16)	11.5	(16)	6
ABQ-I25	2/ /84													57.6	(16)	13.2	(16)	6
ABQ-Barales	2/ /84													55.7	(16)	8.2	(16)	6
Isleta Dam	2/ /84													59.3	(16)	16.4	(16)	6
ABQ-Rio Bravo	3/ /84													50.8	(16)	10.7	(16)	6
ABQ-I25	3/ /84													52.8	(16)	12.9	(16)	6
ABQ-Barales	3/ /84													49.5	(16)	11.8	(16)	6
Isleta Dam	3/ /84													52.3	(16)	16	(16)	6
ABQ-Rio Bravo	8/27/84	81.6	(1)	7.8	(1)	62.1	(1)	5.46	(1)			159	(1)	193	(1)	35	(1)	7
ABQ-I25	8/27/84	75.2	(1)	10.7	(1)	51.5	(1)	5.46	(1)			162	(1)	182	(1)	32	(1)	7
Isleta Dam	8/27/84	80	(1)	7.3	(1)	50.6	(1)	5.46	(1)			173	(1)	161	(1)	31	(1)	7

	Ca	Mg	Na	K	Na+K	HCO3	SO4	Cl
n (#) =	(157)	(157)	(147)	(41)	(20)	(112)	(412)	(412)
Mean (mg)=	56.96	8.67	41.97	4.73	39.10	164.94	80.11	18.59
Mean(meq)=	2.84	0.72	1.83	0.12	1.70	2.70	1.67	0.52
s (mg) =	16.17	1.48	10.82	0.93	9.90	7.86	41.44	8.34
s (meq) =	0.81	0.12	0.47	0.02	0.43	0.13	0.86	0.24

CODE = DATA SOURCE
1 = Scofield 1938
2 = Bjorklund & Maxwell 1961
3 = USGS-WATSTORE
4 = Anderholm 1988 (WATSTORE)
5 = BID-Potter-11/30/84
6 = City in BID-Potter-11/84
7 = BID-Potter-12/31/84

RIVER EVAPORATION LINE RATIO: Ion(meq)/Cl(meq)

	Ca/Cl	Mg/Cl	Na/Cl	K/Cl	(Na+K)/Cl	HCO3/Cl	SO4/Cl
Composite Data:	5.46	1.38	3.52	0.23	3.27	5.19	3.21
Anderholm Data:	4.88	1.29	2.98		2.59	4.96	3.41

The river-evaporation line based on this composite data do not fit the surface water data as well as the evaporation line based on averages from the U.S.G.S. WATSTORE data base (Anderholm 1988). The WATSTORE data is based on a large sample set of single analyses. Average river water quality data and standard deviations used in this study are from WATSTORE with the exception of potassium, silica and temperature which were not included in Anderholm's report. These three parameters are from the composite data set listed in table 8.

Rio Grande water quality varies from season to season. In the spring, the river stage is high and the water cold and dilute (low in TDS), originating from snowmelt draining the high mountains along its reach. In the late summer the river stage is low and water flowing just below the surface is concentrated by evapotranspiration (high in TDS). MRGCD canals and drains may be full or dry depending on the season and river stage or the function of a particular channel.

Surface water in the channels and river flow over or through sediments derived from granitic highs north of the study area. The suite of primary minerals and clays are essentially the same minerals encountered by mountain-front recharge.

Figure 36 shows the MRGCD's system of irrigation canals and drains in the Rio Grande flood plain, their spatial relationship to the river, and water sample locations and map codes. Water flowing in the MRGCD

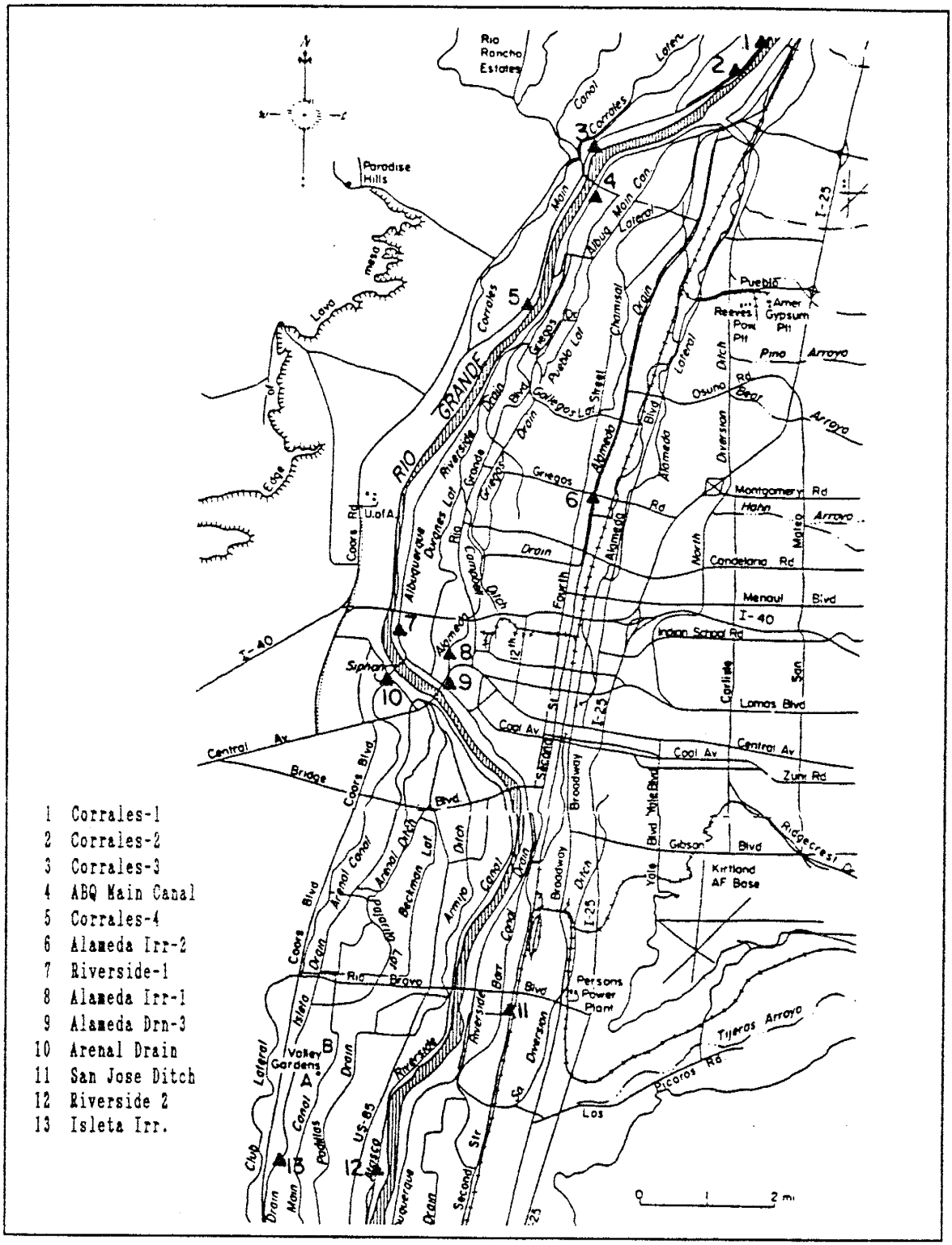

Figure 36: Surface water sample locations from MRGCD drains, canals and ditches (modified from Kelley, 1982).

system either directly or indirectly is feed by the Rio Grande. Surface water is diverted from the river into the canals for irrigation or drains intercept shallow ground water recharged through the stream bed.

Figure 37 shows the Rio Grandes evaporation line plotted with data from the MRGCD channels and the envelop formed by ± one standard deviation. The data represent single analyses for channels at different locations and in two cases different years for the same channel location. These single analyses may not represent the average channel water chemistry.

Shallow channel flow is susceptible to surface contamination, free-surface evaporation, transpiration, and shallow-water-body capillary-zone wetting/drying cycles. About two-thirds of the water flowing through these channels becomes recharge (USACOE, 1979).

Figure 37a shows sulfate is concentrating with evaporation along the line representing one standard deviation above the river-evaporation line. If the river-evaporation line slope were a little steeper all sulfate concentrations would fall within one standard deviation (s ± 0.80 meq). The evaporation line slope may be low for sulfate. If the slope is correct then industrial or agricultural contamination may be increasing sulfate.

Figure 37b shows most of the channel water samples fall within one standard deviation (s ± 0.86 meq) of the river-evaporation line for calcium. Analyses above one standard deviation are either gaining calcium from

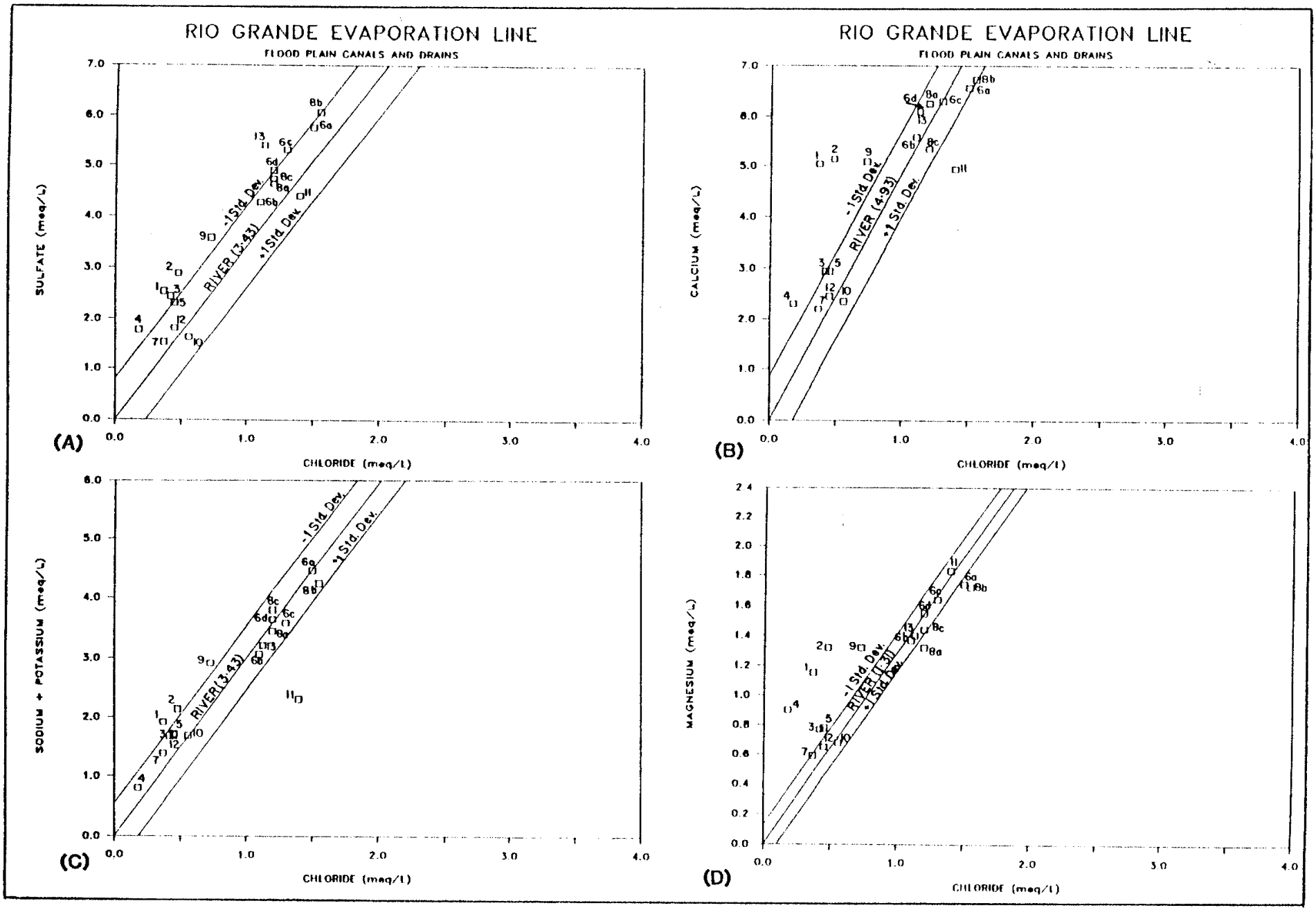

Figure 37: Major ion concentrations in surface waters with respect to increasing ion concentrations in river evaporation.

plagioclase dissolution, surface contamination, or a sample may not represent the average channel chemistry. San Jose (11) ditch falls below the river-evaporation line. Water flows through this ditch part of the year and may be influenced by either surface contamination or calcite may be precipitated due to concentration by evapotranspiration.

Figure 37c shows sodium data scatter about the river-evaporation line within one standard deviation (s ± 0.54 meq) with the exception of San Jose ditch (11). San Jose ditch flows through stockyards and industrial areas and may be reflecting chloride contamination.

Figure 37d shows dissolved magnesium either follows the river-evaporation line within one standard deviation (s ± 0.13) or water samples are enriched. Enriched water samples probably represent dissolution of magnesium rich minerals such as biotite. Small depletions in magnesium may be due to analytical error or a non-representative sample. Magnesium is not removed by forming secondary clay minerals but may be removed by substituting for calcium sites in ion exchange.

Table 9 lists the difference between water sample ion concentrations and the river-evaporation line. Also listed are the calcite and gypsum disequilibrium indices (Log Q/K), possible alteration processes, and map codes. Calcite disequilibrium values indicate the surface waters are either oversaturated (precipitate calcite) or in metastable equilibrium (± 0.5) with calcite.

Gypsum disequilibrium indices indicate all surface

TABLE 9: Near-river surface water analysis summary

CANALS/DRAINS NAME	RIVER-DIFF Ca (meq)	RIVER-DIFF Mg (meq)	RIVER-DIFF Na+K (meq)	RIVER-DIFF SO4 (meq)	LOG(Q/K) CALCITE	LOG(Q/K) GYPSUM	ALTERATION PROCESS	MAP CODE
RIO GRANDE (s)	0.86	0.13	0.54	0.80	0.354	-1.763		
CORRALES-1	3.24	0.67	0.81	1.28	0.342	-1.388	2	1
CORRALES-2	2.80	0.70	0.70	1.25	0.801	-1.352	1:2	2
CORRALES-3	0.89	0.23	0.43	1.01	0.318	-1.559	2	3
ABQ MAIN CANAL	1.42	0.67	0.26	1.16			2	4
CORRALES-4	0.75	0.20	0.38	0.78	0.344	-1.581	2	5
ALAMEDA IRR-2a	-0.76	-0.19	-0.02	0.66			2:3	6a
ALAMEDA IRR-2b	0.21	-0.04	-0.22	0.53			2:3	6b
ALAMEDA IRR-2c	-0.04	-0.03	-0.29	0.89			2:3	6c
ALAMEDA IRR-2d	0.41	0.01	0.06	0.82			2:3	6d
RIVERSIDE-1	0.40	0.11	0.28	0.26	0.213	-1.837	2	7
ALAMEDA IRR-1a	0.40	-0.22	-0.13	0.56			2	8a
ALAMEDA IRR-1b	-0.84	-0.27	-0.38	0.79			2	8b
ALAMEDA IRR-1c	-0.51	-0.10	0.22	0.65			2	8c
ALAMEDA DRN-3	1.53	0.38	0.73	1.09			2	9
ARENAL DRAIN	-0.38	-0.04	0.02	-0.29			2	10
SAN JOSE DITCH	-1.89	0.03	-1.87	0.37			2:4	11
RIVERSIDE-2	0.26	0.07	0.35	0.28	0.279	-1.737	2	12
ISLETA IRR.	0.58	-0.05	-0.16	1.56	0.773	-1.051	1:2:3	13

All surface water flows through flood plain alluvium (Qal) comprised of reworked deposits of granitic material with organic debris.

Rio Grande (s) = standard deviation for average river chemistry (Anderholm 1988)

RIVER DIFF = Ion (meq) - River evaporation line (meq)

LOG(Q/K) = Disequilibrium Index (PCWATEQ) (Consider +/- 0.5 metastable equilibrium)

Alteration Processes:
1 = Calcite precipitation
2 = Mineral Dissolution
3 = Ion Exchange
4 = Effects of salt accumulation in capillary zone

Map Codes on Figure 36

water samples are undersaturated with respect to gypsum.

Figure 38, a trilinear plot of the major ion reacting percentages, shows the surface water diverted from the river geochemically changes as it flows through the shallow channels.

In the cation field magnesium and calcium increase while sodium decreases. This could indicate magnesium and calcium are exchanging with sodium on clay or mineral surfaces.

The general trend in the anion field is increasing percentages of sulfate and decreasing bicarbonate. Some water samples show chloride percentages are decreasing while other samples are increasing in chloride. Increasing sulfate and chloride reacting percentages probably are the result of evapotranspiration concentration. Decreasing chloride probably represents a sample taken while the river stage was high and the water more dilute. In other words, the sample may not represent the average channel water chemistry.

The diamond field on the trilinear plot clearly shows the change in river water chemical composition. Sulfate, chloride, and magnesium are all increasing while bicarbonate is decreasing.

Stability diagrams for the log activity of calcium and sodium suggest surface waters are stable with respect to kaolinite. Diagram codes numbers represent the same samples listed in table 9.

Figure 39a shows the potassium concentration of

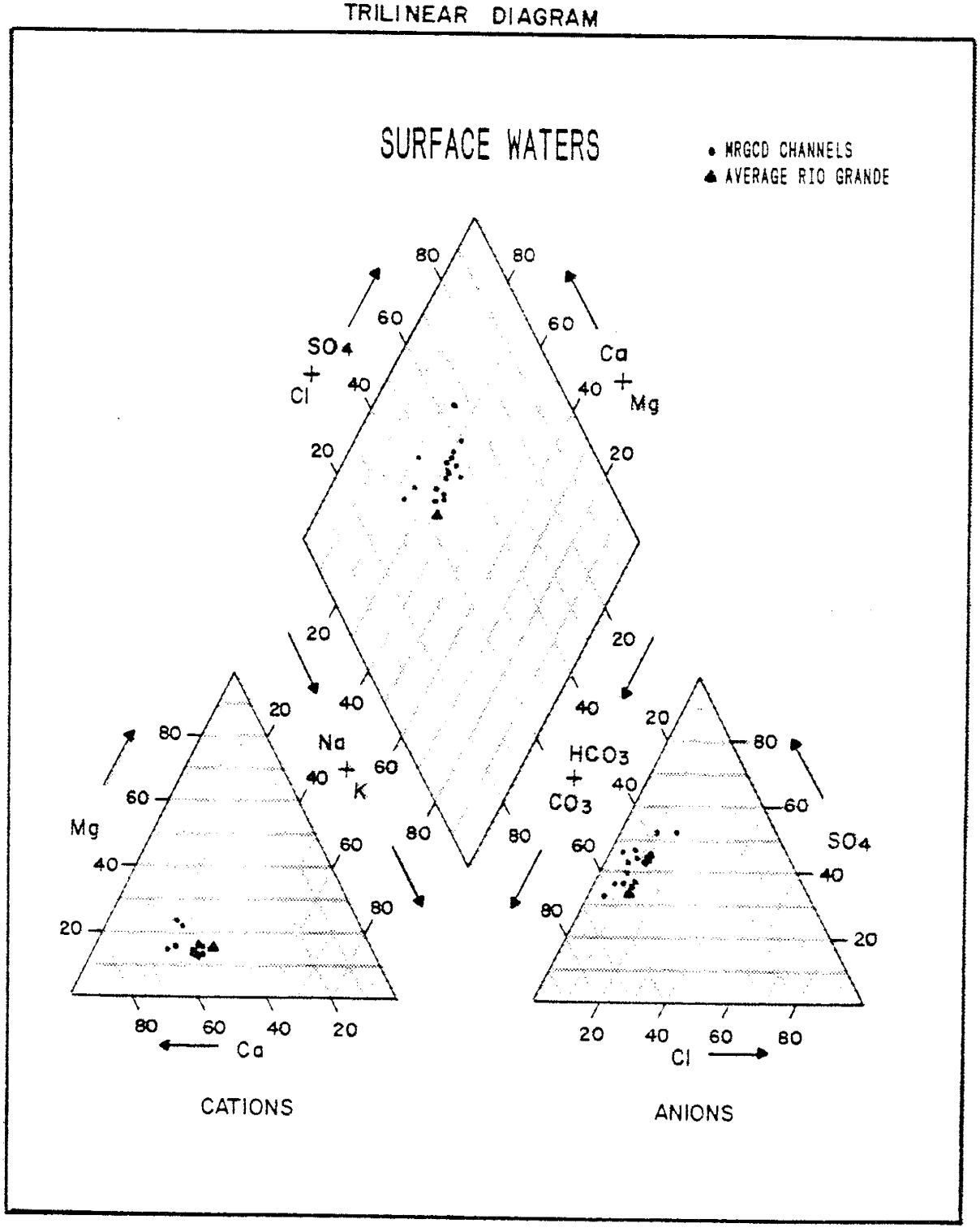

Figure 38: Surface water in the flood plain is diverted from the Rio Grande. Bicarbonate decreases and sulfate increases as diverted water flows away from the river.

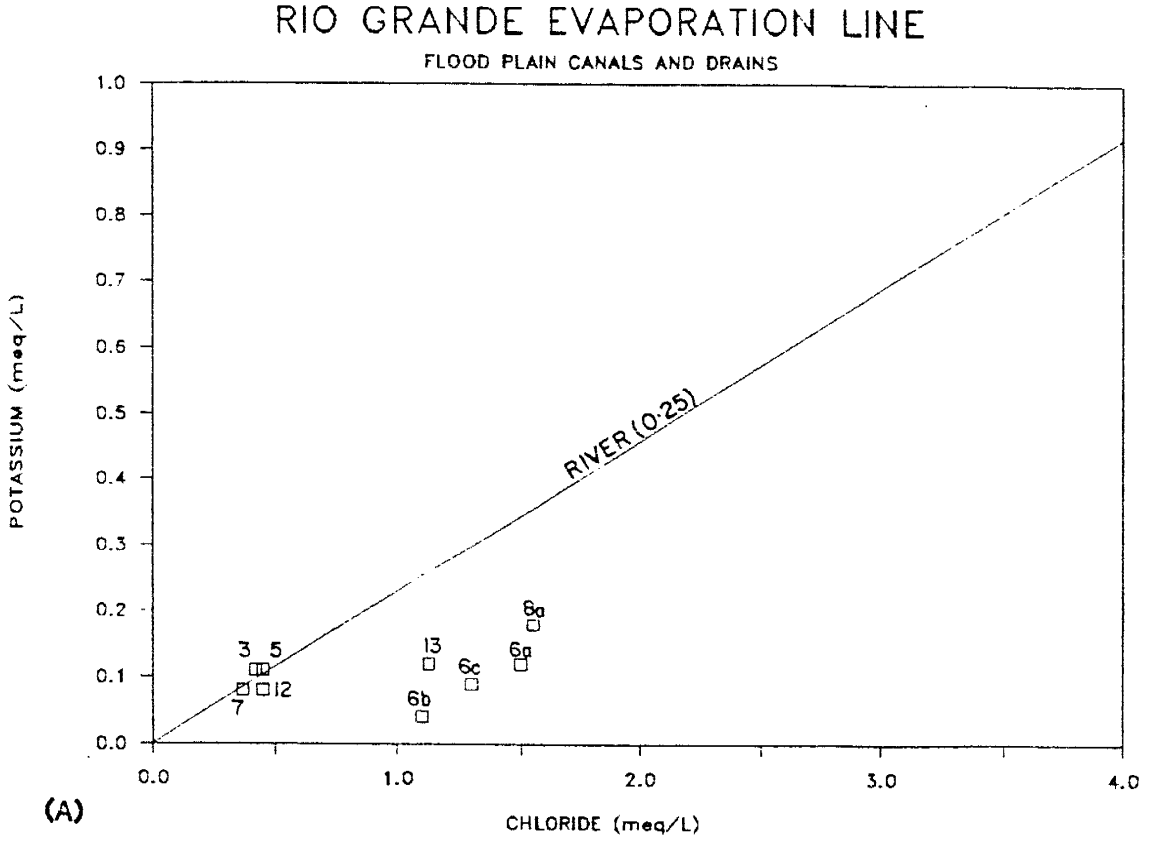

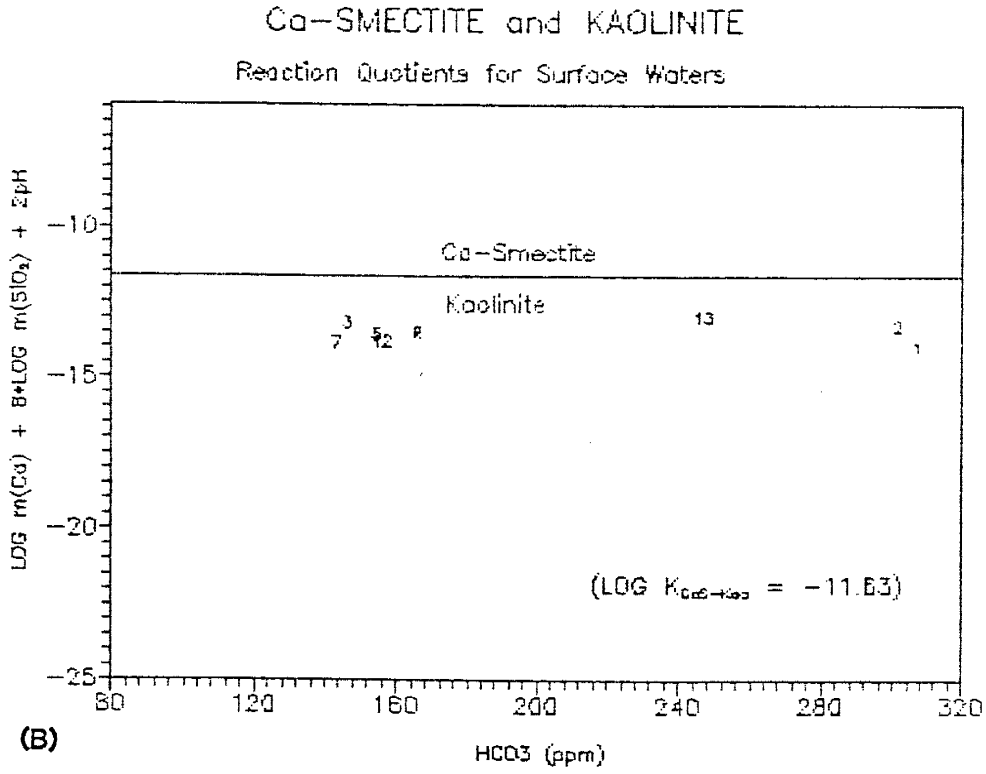

Figure 39: Potassium apparently does not concentrate with evaporation of surface water but is probably removed by illite (secondary clay mineral) formation (A). Surface-waters reaction quotients are approaching equilibrium between calcium smectite and kaolinite (B).

channels relative to the river-evaporation line. Drains adjacent to the river (intercept infiltrating river water) maintain the river K/Cl ratios while canals flowing beyond its influence become depleted with respect to potassium. Depletion is probably due to the strong affinity of potassium for ion exchange. Potassium may be removed from the surface water by exchanging with calcium on Ca-smectites to form mixed layer illite-smectite clays commonly found in this area.

Figure 39b is the reaction quotient versus bicarbonate diagram used to indicate the surface waters stability between two clays. The samples are apparently asymptotic to the kaolinite-smectite equilibrium boundary which suggests the waters composition is controlled by the two clays thermodynamic relationships (Drever, 1982). Surface waters are in equilibrium with kaolinite but are evolving toward the Ca-smectite stability field as the water flows from north to south.

Figures 40a indicates the various surface waters stability relative to Ca-smectite, kaolinite and calcite. The average calculated partial pressure of carbon dioxide for these waters is P_{CO2} = 2.7 (PCWATEQ) which indicates all surface waters are oversaturated with respect to calcite except Corrales 1 (1). Individual equilibrium calculations (PCWATEQ) show that Corrales 1 is near equilibrium with calcite. As water flows from north to south (Corrales 1 [1] to Isleta [13]) it moves toward the Ca-smectite stability fields. Dissolved silica is nearly

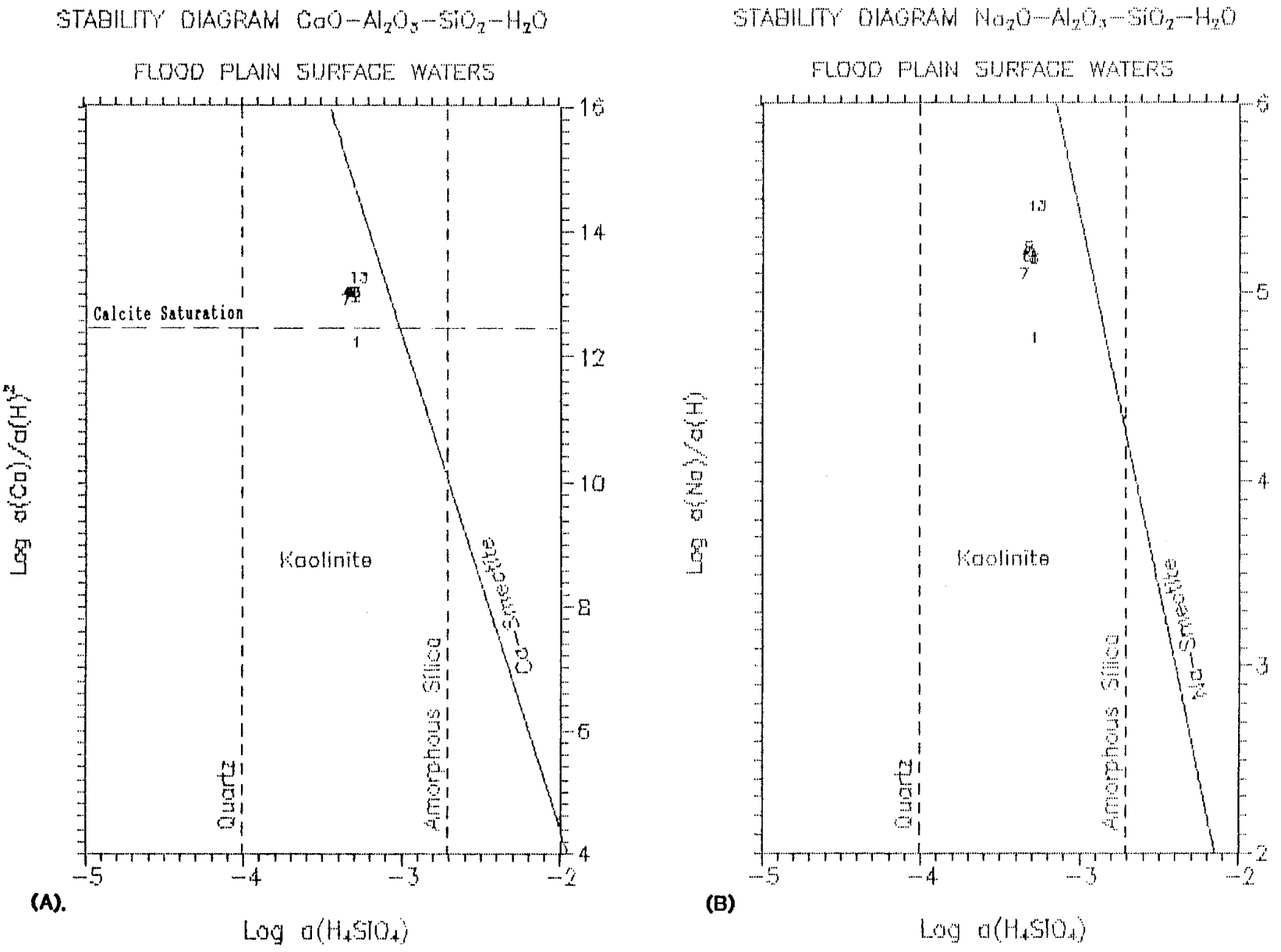

Figure 40: Stability diagrams for secondary clay mineral formation of calcium-smectite and calcite (A) and sodium smectite (B) with kaolinite.

constant.

Figure 40b is the stability diagram for Na-smectite and kaolinite. Local occurrences of Na-smectite per se have not been reported in the literature. Evaporation line analyses of surface waters and the stability diagram both indicate that sodium remains in solution.

Major Ion Distribution

Major ion concentration distribution in units of (mg/L) is not generally useful for determining ground water genesis. These maps are useful for showing the areal distribution of water quality parameters and illustrate areas that deviate from expected values if we assume a simple flow model as suggested by Kelly's 1936 extrapolated water table map (figure 18a). The major ion distribution in the local ground-water system is not monotonic, ground water apparently does not evolve systematically along a flow path but is highly perturbated. Appendix II contains water-quality data used for constructing the following maps.

Figure 41 shows the areal distribution of the average chloride content in ground water. Chloride is considered conservative - the only source is atmospheric input through either mountain-front or river recharge and no sinks. Six areas have chloride concentrations greater than 20 mg/L with the maximum concentration reaching 105 mg/l. Four areas have chloride concentrations below 10 mg/L with the minimum of 5 mg/L. The area highest in chloride

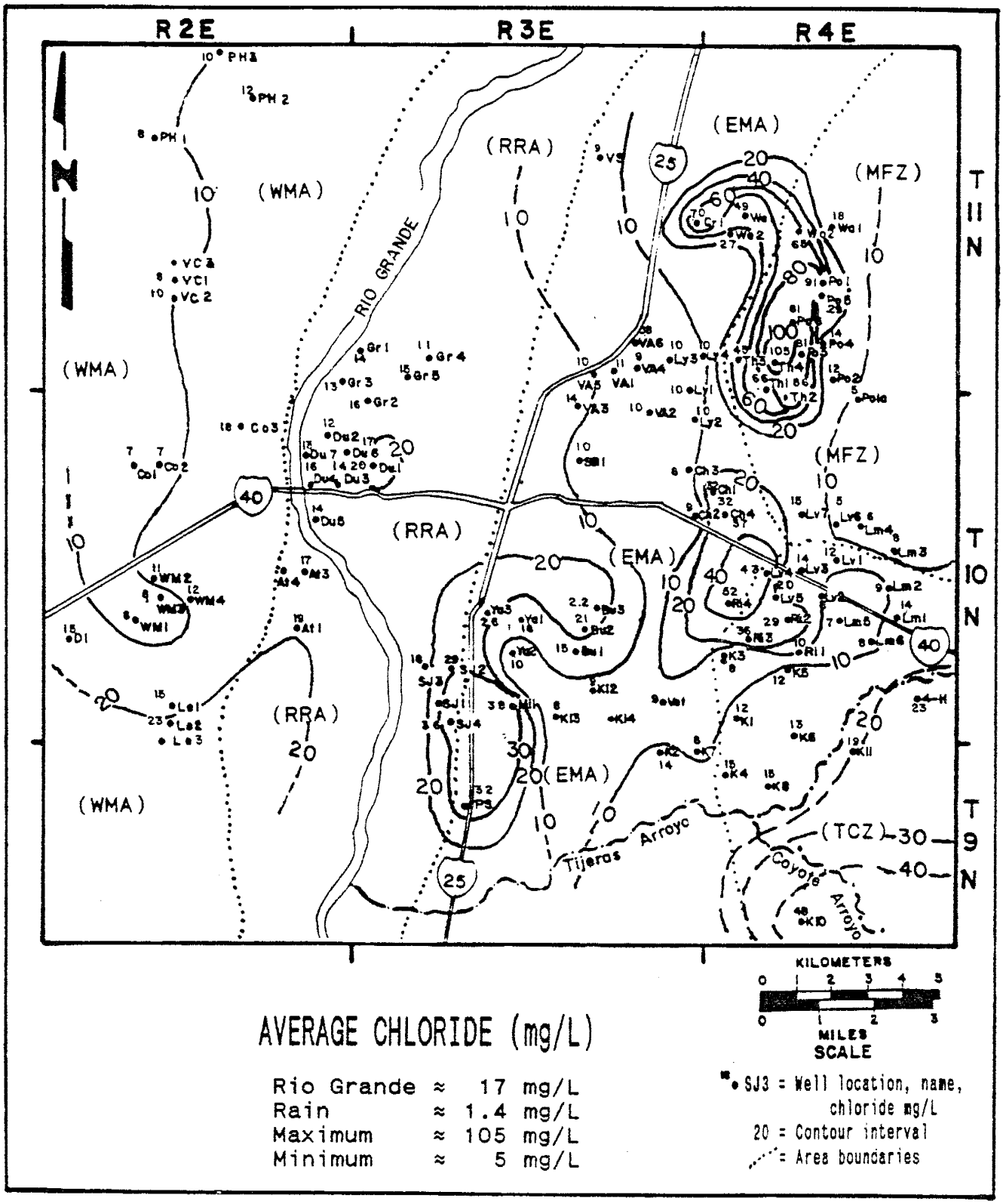

Figure 41: Ground water chloride concentrations are considered conservative in this environment therefore processes other than mineral weathering must account for the elevated chloride areas.

concentration is associated with the two Ca-Cl water types shown on the hydrogeochemical facies map (figure 28). Average recharge chloride concentrations are 17 mg/L for the river and 1.4 mg/L for atmospheric input. There is no apparent chloride trend from mountain-front recharge toward the ground-water axis to the southwest, located out of the study area.

Figure 42 is for the average sulfate content in ground water. Sulfate is also considered a conservative ion - in this environment the only major source is atmospheric input and there appear to be no sinks. A highly variable regional trend appears to increase east to west from about 20 to 80 mg/l. In contrast to the apparent east-west increasing sulfate trend, ground water flowing out of Tijeras Canyon shows a decreasing sulfate trend.

Five areas of relatively high sulfate and four areas of relative low sulfate interrupt the apparent regional trend. Areas of both high and low sulfate concentrations, relative to surrounding ground water, occur over the study area. Average recharge sulfate concentrations are between 4 mg/L and 75 mg/L for atmospheric input and the river. However, the data indicate sulfate concentrations range between 14 mg/L to 130 mg/L.

Figure 43 shows the areal distribution of the non-conservative ions of sodium and potassium. In the study area, sources of sodium are from atmospheric input, ion exchange, and plagioclase dissolution. Sodium sinks are ion exchange and may form minor amounts of the secondary

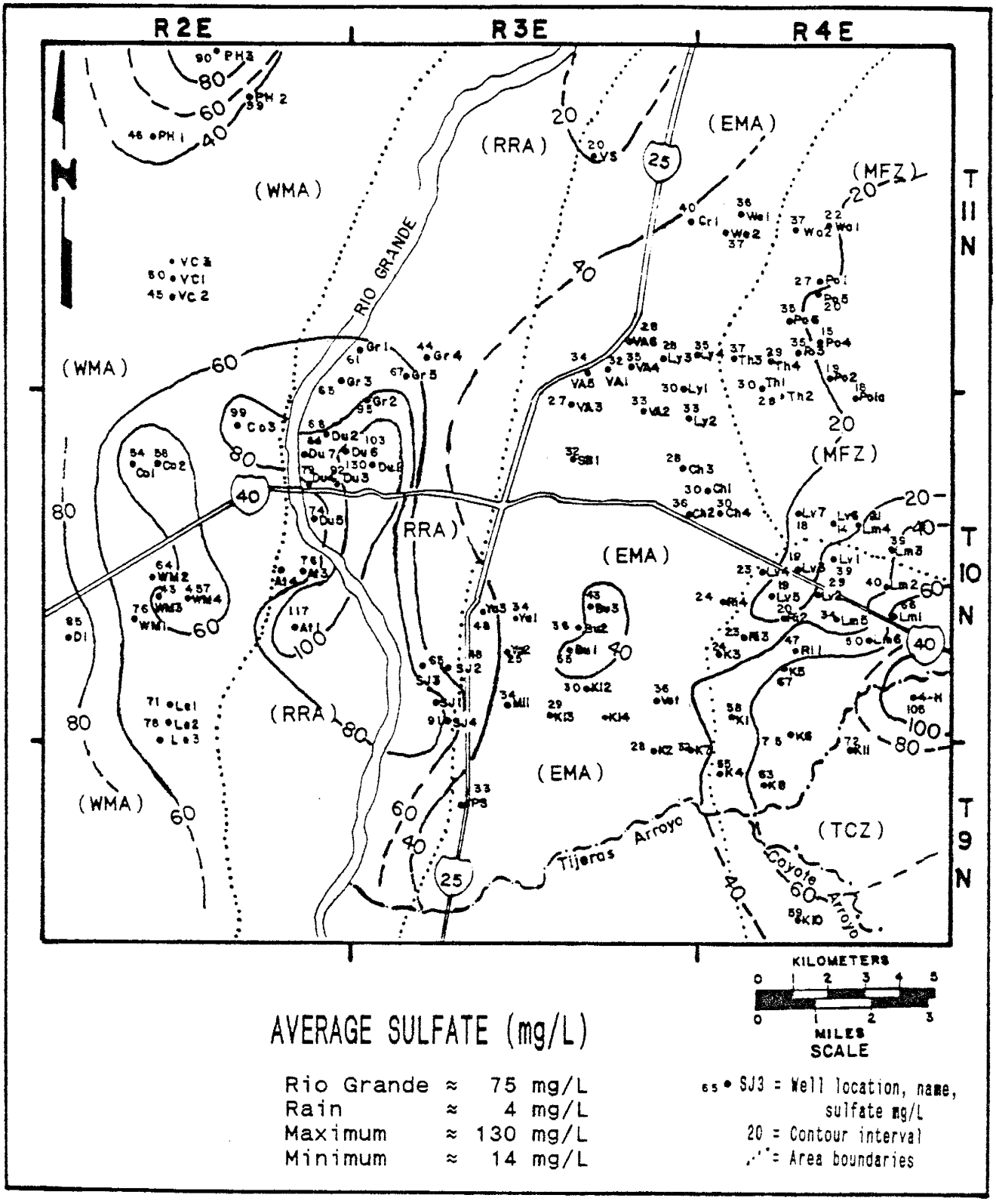

Figure 42: Sulfate concentrations increase near recharge areas indicating the influence shallow ground water has on water produced from deep wells.

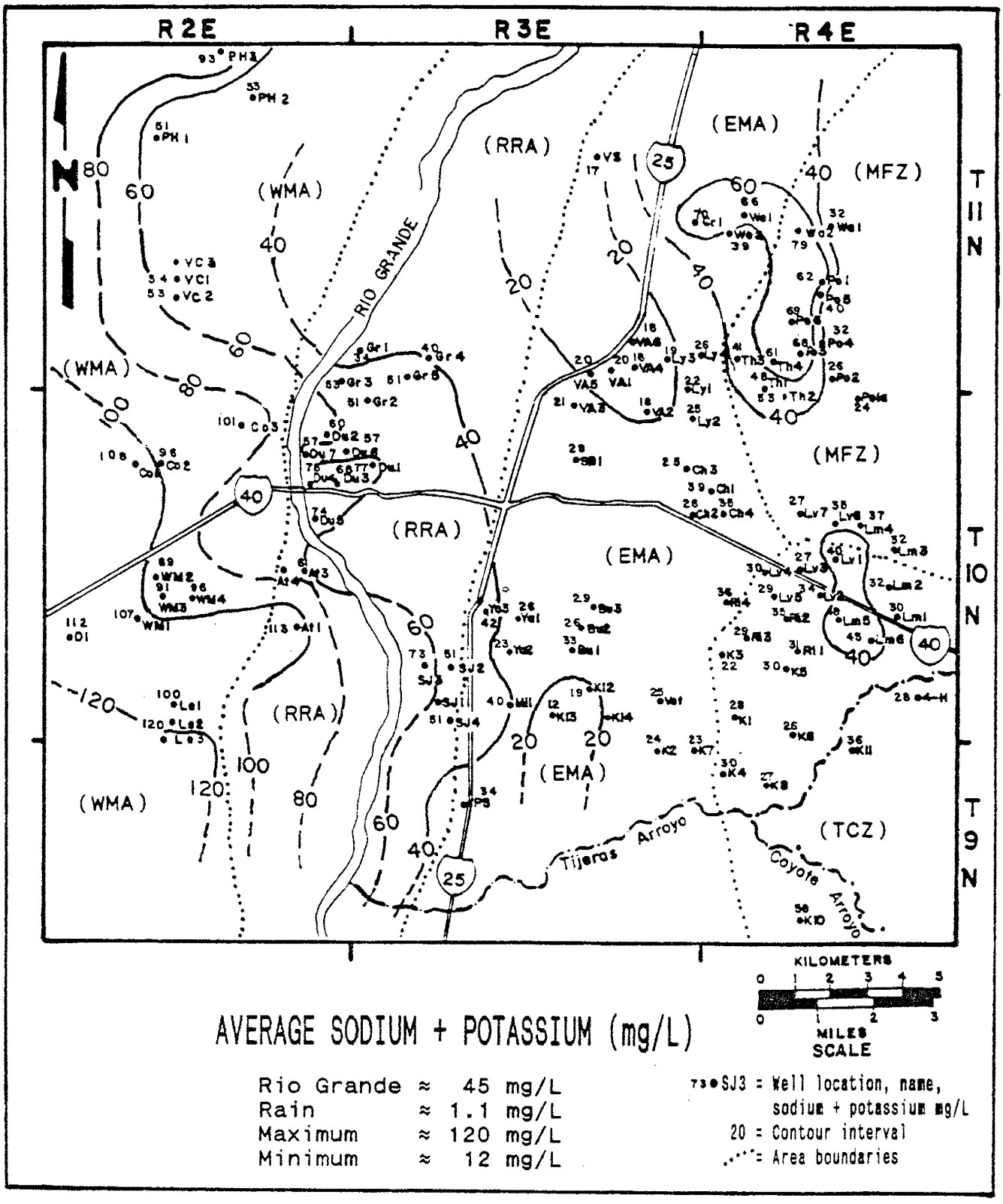

Figure 43: Sodium + potassium concentrations fluctuate between increasing and decreasing from east to west which suggests ground water may not follow a simple flowpath from the mountain recharge area to the basin axis.

clay mineral Na-smectite which has not been reported in this area. Potassium comes from atmospheric input and biotite dissolution with some possibly from orthoclase. Sinks are through ion exchange and secondary clay mineral formation (illite).

Sodium and potassium are treated as sums in most analyses in this study because older data are generally reported as sodium plus potassium in sodium units. For ease of discussion I will use the notation sodium* to distinguish the sum (Na+K=Na*) from the individual sodium ion.

A general east to west sodium* trend does not develop until ground-water flow reaches the flood plain. From about the flood plain westward an increasing sodium* trend ranging from 40 mg/L to 100 mg/L develops. The start of the sodium* trend is near the boundary between calcium and sodium dominant ground water on the hydrogeochemical facies map (figure 28). Two sodium* highs, on figure 43, are associated with the two sodium "anomalies" along the mountain-front on the hydrogeochemical facies map (figure 28). With the exception of the two sodium* highs (MFA) and two relatively low sodium* areas (EMA) the concentrations are fairly uniform east of the flood plain.

Average recharge sodium* concentrations range from 1.1 mg/L in rainwater to 45 mg/L in the Rio Grande. Minimum sodium* found in local ground water ranges from 12 mg/L to a maximum sodium* concentration of 120 mg/L.

Figure 44 shows the areal distribution of calcium in

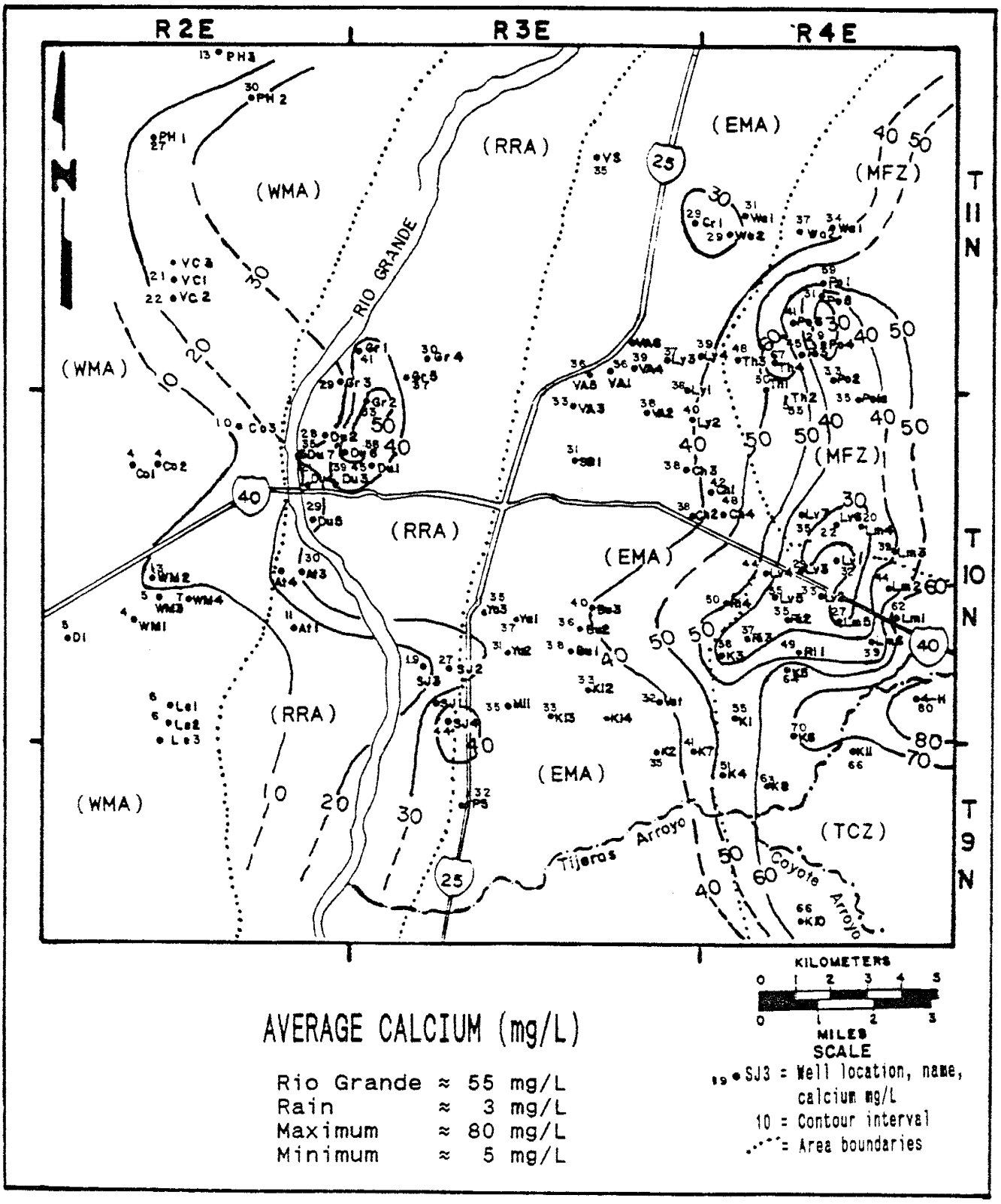

Figure 44: Calcium concentrations in ground water decrease from east to west with several wells producing water lower in calcium then the surrounding wells.

ground water. Calcium is not a conservative ion. Sources of calcium are atmospheric input, ion exchange, and dissolution of calcite, gypsum and plagioclase. Sinks are ion exchange, secondary clay mineral formation (Ca-smectites), and calcite and gypsum precipitation. Calcium forms the clearest monotonic change in ground water content across the study area of all the other major ions. Calcium decreases from about 80 mg/L in the east to less than 10 mg/L west of the Rio Grande. Interrupting the decreasing trend in the east is a large area of relatively low calcium concentrations (MFA). This area is associated with the two sodium highs seen on the hydrogeochemical facies map (figure 28). In the flood plain (RRA), one area of relatively high calcium disrupts the monotonic change from east to west.

Average recharge calcium concentrations range from 55 mg/L in the Rio Grande to 3 mg/L in rainwater. Ground water calcium concentrations range from a minimum of 5 mg/L west of the river to 80 mg/L near Tijeras Canyon.

Figure 45 shows the bicarbonate plus carbonate (bicarbonate*) concentrations in ground water across the area. Two trends are apparent. Near the mountain front (MFA), bicarbonate* decreases from east to west. On the eastern edge of the flood plain (RRA), bicarbonate* trends reverse and begin to increase from east to west. Between the two trends, in the East Mesa area (EMA), bicarbonate* concentrations are the lowest in the study area. In the flood plain area (RRA), some wells producing ground water

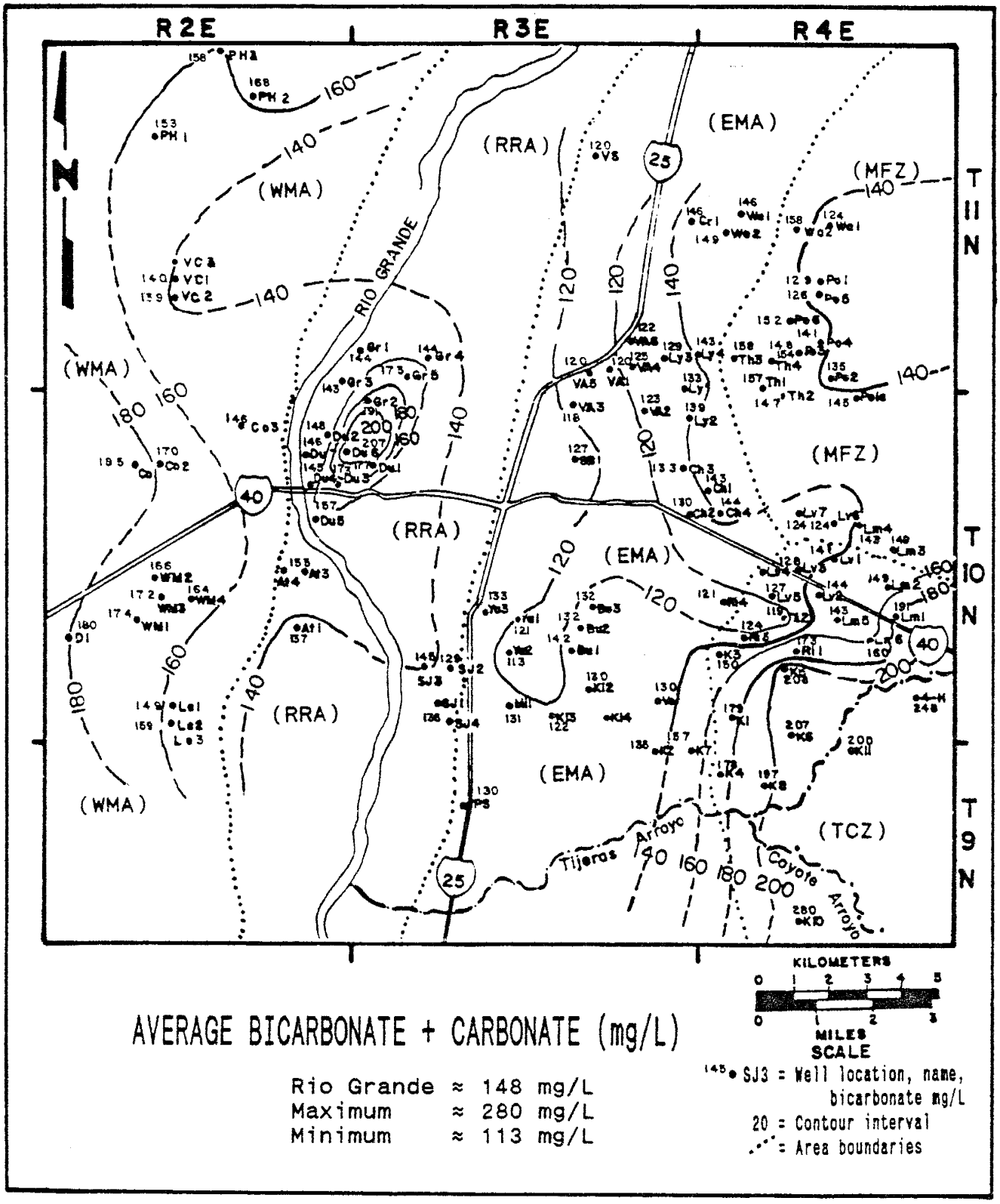

Figure 45: The average bicarbonate content of ground water decreases from the mountain front area (MFZ & TCZ)) toward the river where the bicarbonate content begins to increase.

high in bicarbonate* are surrounded by wells producing ground water relatively lower in bicarbonate*.

Figure 46 shows the areal distribution of silica in parts per million (ppm) through out the study area. Two apparent silica trends are opposite to the bicarbonate* trends. From the mountain front area (MFA) toward the river silica increases from 14 to 73 ppm. From the flood plain (RRA) to the West Mesa (WMA) silica decreases from 73 to 15 ppm.

East of the Rio Grande (EMA), in the increasing trend, the Volandia and Leyendecker well fields produce ground water lower in silica than surrounding wells. In the flood plain (RRA) several wells produce water lower in silica than nearby wells. The San Jose wells appear to be part of the increasing westward trend but form a closed area with the highest silica content in the study area.

Figure 47 shows the areal distribution of total dissolved solids (TDS) across the study area. Four areas of relatively high TDS occur at the mouth of Tijeras Canyon, near the northern mountain front area, and near the river. Three areas of relatively low TDS occur along the mountain front and in the mid-fan area. Ground water west of the river shows less variability in TDS than ground water east of the river.

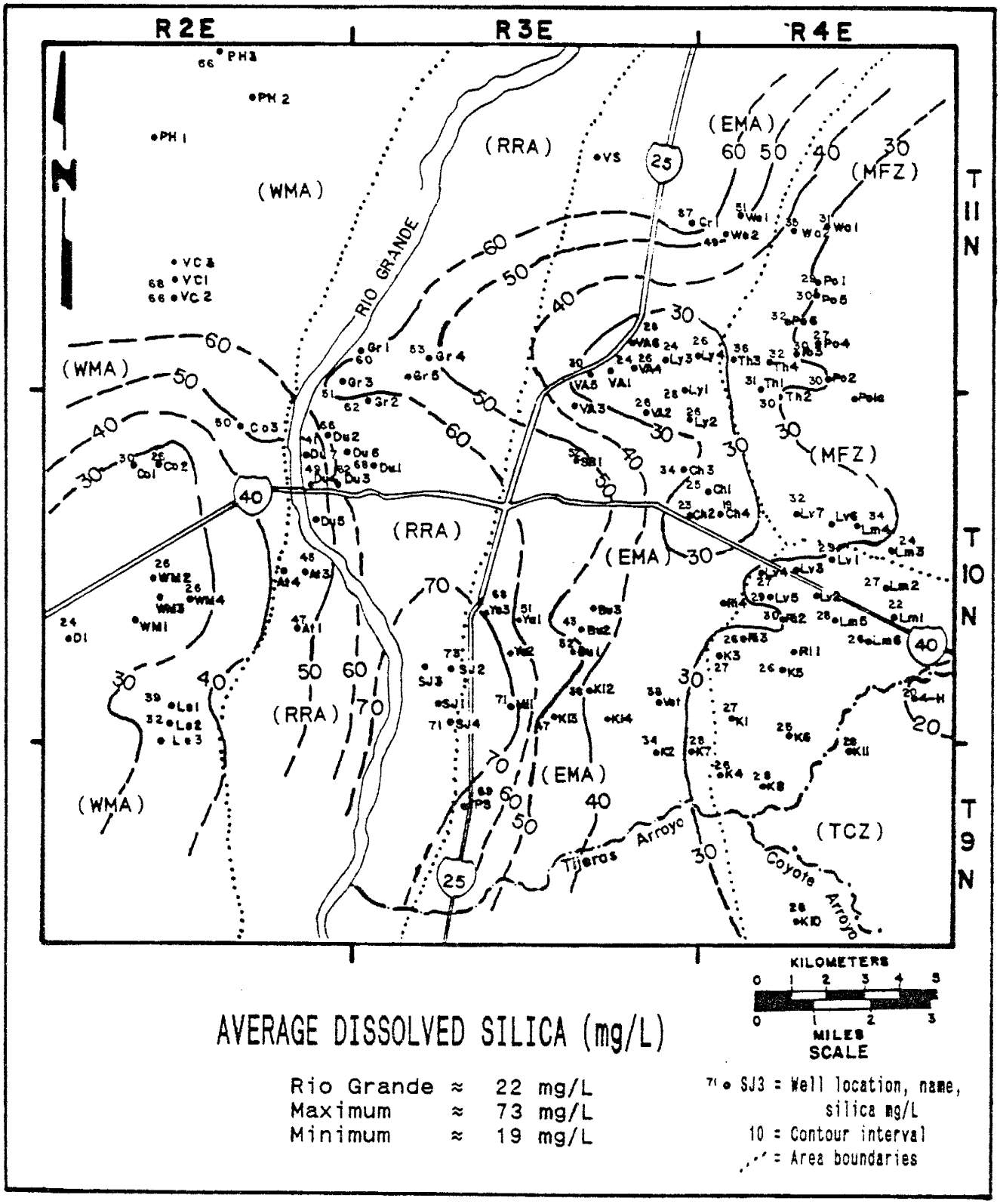

Figure 46: The average silica content of ground water increases from the mountain front area to the river where the trend reverses and silica decreases.

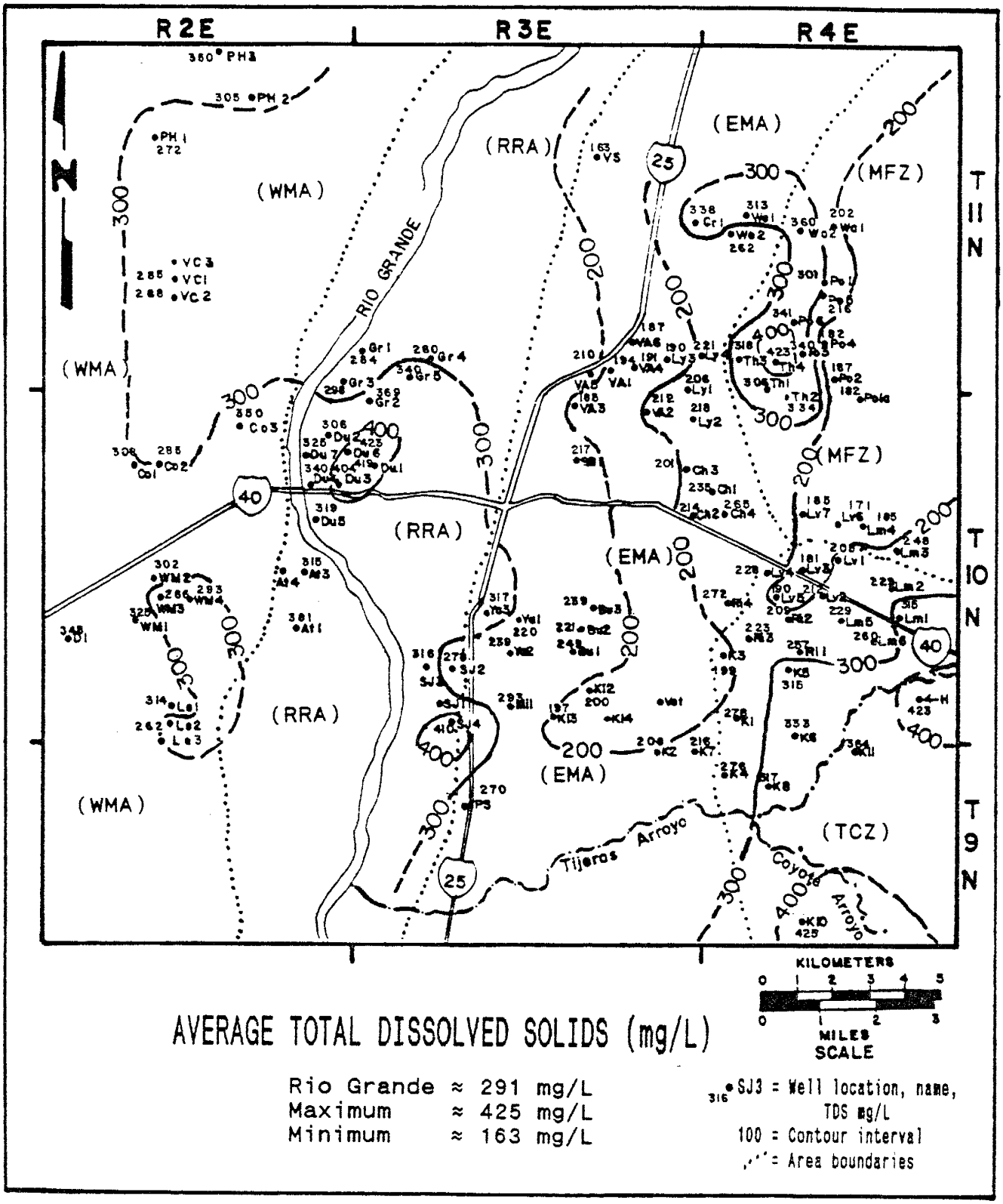

Figure 47: The average total dissolved solids (TDS) in ground water generally increase from east to west with intermittent areas of either higher or lower TDS.

Environmental Isotopes

Isotope data for the study area comes from two sources; Crayton Yapp (1985) and the City of Albuquerque (unpublished data 1987-1989). Yapp limited his study to temporal and spatial deuterium content in recharge sources and ground water while the City focused their study on ground water from municipal and monitoring wells.

The City's water samples were analyzed by the University of Waterloo for deuterium, oxygen-18, and tritium. Major ions and metals from the sample split were analyzed by Wilson Laboratory and/or the City's water quality laboratory. Deuterium and oxygen-18 isotope content of a water sample is referenced to the standard mean ocean water (SMOW) and given in units of permil. Isotope data and its source are listed in Appendix VII.

Crayton Yapp's (1985) 1980 to 1982 monitoring program established the local deuterium baseline for precipitation, the Rio Grande, and five City water wells. Table 10 list the deuterium content of recharge sources from Yapp's two year study.

TABLE 10: Average deuterium in recharge sources:

Sandia Mountain Recharge	δD(‰SMOW)
Bear Canyon Well	-83
Bear Canyon Stream	-80
Embudo Canyon Spring	-80
Tijeras Canyon Well	-70
Rio Grande	-92 (-103 to -79)
(2 year average, non-weighted)	
Average Annual local precipitation	-60
(2 year average, weighted)	

Figure 48a shows the seasonal variability and the volume weighted average of deuterium in local precipitation at 1580 meters (5184 ft) (Yapp, 1985). Most precipitation in this area occurs in the summer months and is isotopically heavier than precipitation from colder winter storms. The shaded areas on figure 48a represent recharge "windows" based on the time of the lowest local evapotranspiration (ET) rates (figure 2a).

Two shallow wells near the Sandia Mountain front are isotopically different. Bear Canyon well (map code 17, figure 31) and stream (18) are isotopically lighter than the Tijeras Canyon well (19). Bear Canyon well penetrates shallow pediment deposits near the granitic boundary where the well intercepts water draining from the topographically high (2900 m [9500 ft]) Bear Canyon drainage basin. Tijeras Canyon well penetrates shallow valley-fill alluvium near the mouth of Tijeras Canyon where it intercepts water draining the narrow canyon elevations of about 2300 m (7500 ft). Each wells water represents the average isotopic content of precipitation draining their respective drainage basins.

Two processes may explain the -13‰ δD difference in deuterium content between the two shallow mountain-front wells (Bear and Tijeras Canyons) and the -20‰ δD difference between mountain-front springs and the average local precipitation.

The first process affecting the isotopic content of precipitation is storm temperature and moisture content. Based on favorable ET rates, most mountain-front recharge

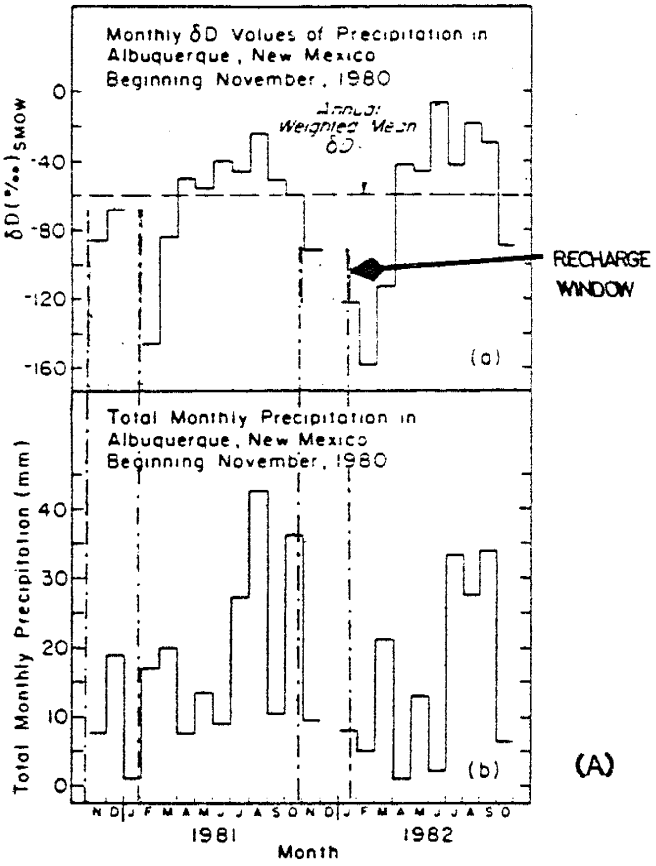

Monthly δD and precipitation amount data for Albuquerque, New Mexico. Monthly precipitation totals were obtained from the local office of the U.S. National Weather Service. Gaps in δD data represent months when the sample was lost or insufficient precipitation was collected for analysis.

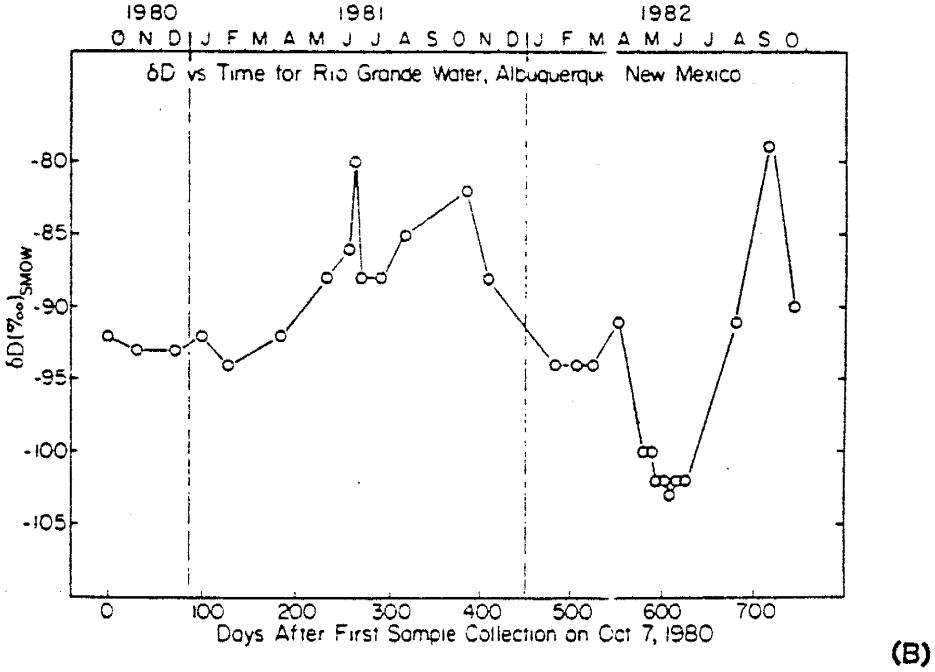

Temporal variations in the δD-values of Rio Grande water at Albuquerque, New Mexico. The δD-values appear to fluctuate around a "baseline" value of ~ — 92‰.

Figure 48: Monthly deuterium content in precipitation (A), and the Rio Grande (B) for a two year period (modified from Yapp, 1985).

should occur during the late fall (figure 48a). Assuming fall and early winter storms are generally cold, near mountain-front springs and ground water would be expected to be isotopically lighter than the average annual precipitation. This process has been termed the "seasonal effect". The average isotopic content of precipitation includes warm summer storms which fall during times of the greatest soil moisture deficit and probably seldom become recharge.

The second process which may also explain the isotopically lighter spring and shallow well water is the elevation effect on isotope content. As storm clouds are orographically lifted they lose their moisture through precipitation. Isotopically heavier molecules prefer the liquid state (fractionation). As a storm loses its moisture through precipitation the isotopic content of the remaining water vapor becomes isotopically lighter and subsequent precipitation becomes isotopically lighter as the storm moves upward. This process is called the "elevation effect".

A simple calculation using a proportionality constant (C) for New Mexico (C is based on a small sample set)

$$C = -35‰/1000m$$

$$(\delta_{Pa} - \delta_{Pb})/(\text{elev } \{b\} - \text{elev } \{a\}) = C$$

δ_{Pa} = deuterium at elevation a

δ_{Pb} = deuterium at elevation b

shows that Bear Canyon stream discharge originates at about 2150 m (7060 ft), and water supplying the Tijeras Canyon well originates at about 1870 m (6130 ft). These elevations are reasonable if the isotopic content of the two wells represent the average isotopic content of precipitation falling in the drainage basins.

Based on the available information, each of these two processes could be occurring. If I assume the first process, seasonal effect, is the controlling process then deuterium seems somewhat high and recharge occurs during the period of lowest precipitation (figure 48a). If I assume the elevation effect on the isotopic content of precipitation is more important than the seasonal effect, then recharge may occur over a wider time period than suggested by the ET window shown in figure 48a. Therefore large volume, isotopically heavier summer storm may be more important to recharge than previously thought. The ET window may not be valid for mountain-front areas because of the steep topography, greater vegetation cover, and greater volume of rainfall relative to the lower elevations. Figures 2a and 2b show the difference in precipitation for the airport (1620 m [5310 ft]) and Sandia Crest (3170 m [10,400 ft]). Isotope data support Titus' (1980) suggestion that, based on the amount of precipitation and surface run-off, mountain recharge occurs throughout most of the year in the Sandia Mountains.

Figure 48b shows the fluctuations in deuterium in the

Rio Grande over a two year period. River recharge is isotopically heavier in the summer from summer storm run-off and lighter during the high-stage spring snowmelt run-off. Yapp's two-year average river deuterium is not discharge-volume weighted.

Generally, the isotopic content of ground water is very near the average annual isotopic content of its recharge source. For the Rio Grande the expected ground-water deuterium in nearby wells should be near -92‰ δD. Wells with lighter or heavier than average deuterium may be reflecting the disproportionate volume of recharge associated with seasonal fluctuations in the river stages or be mixing with deeper older ground water.

Figure 49 shows the average deuterium and oxygen-18 content of ground water with respect to Craig's (1961) meteoric water line (MWL). Stable isotopes in ground water fluctuate between ± 7‰ δD of the MWL showing they are in good agreement with the theoretical isotopic content. Local ground-water isotopic content tends to fall below the MWL more often than above the line which may indicate arid climate effects on the deuterium. The general pattern may also be the result of a small sample set. Average isotope values are based on one to four measurements. As the number of samples used to calculate the average isotopic content increases, the scatter about the MWL may decrease or show more pronounced arid climate effects.

Letters on figure 49 indicate the area divisions found on preceding maps. Wells receiving ground water from

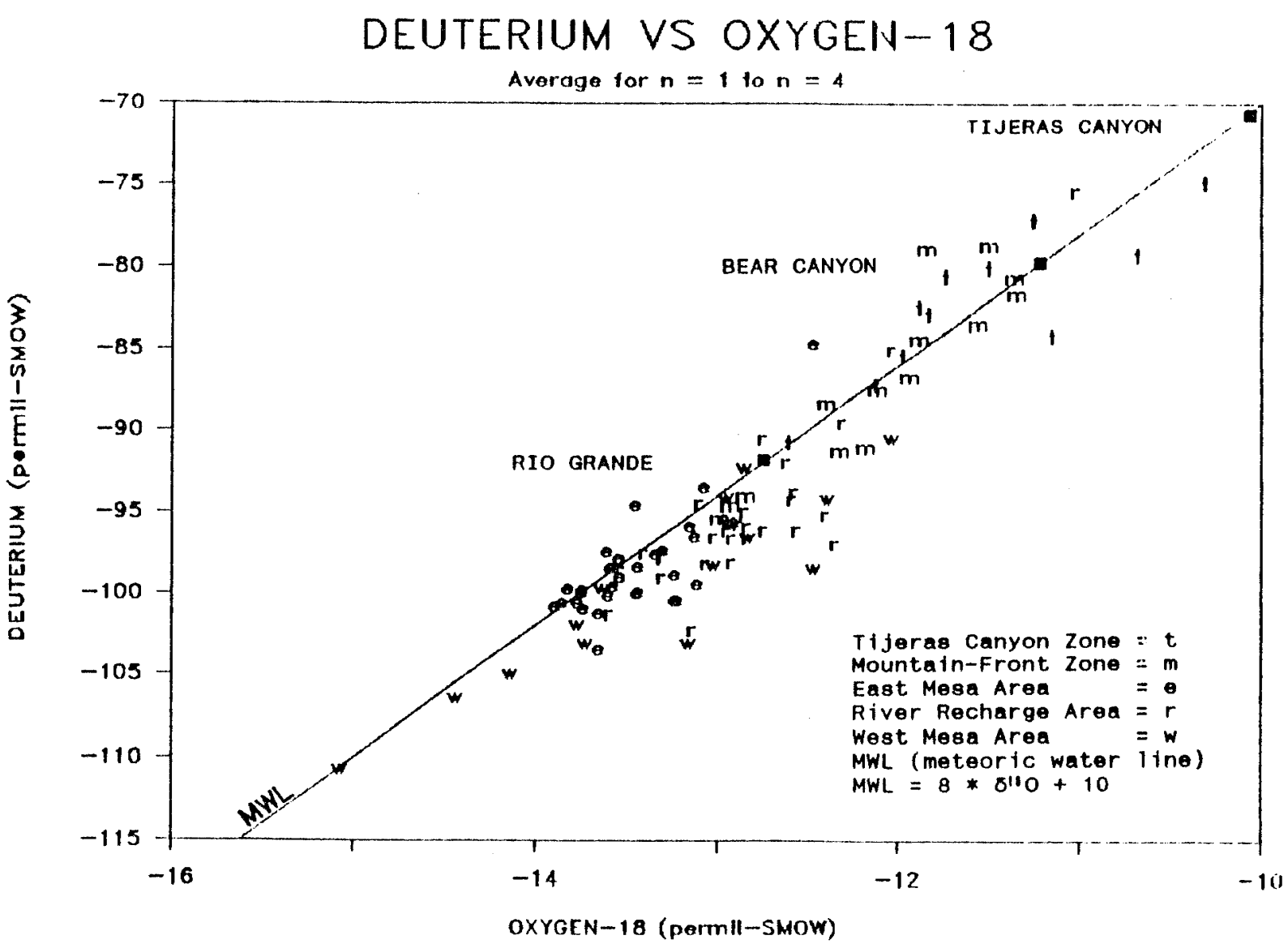

Figure 49: Generally, isotopically heavier ground water scatter above the MWL near the mountain recharge areas and isotopically lighter ground water below the MWL. Rio Grande, Tijeras and Bear Canyon deuterium data is projected onto the MWL.

Tijeras Canyon (t) and mountain-front recharge (m) lie on the isotopically heavy end of the MWL. River recharge (r) wells and East Mesa (e) wells are dominantly in the middle range. West Mesa (w) wells are isotopically the lightest. The general trend is for decreasing isotopic content from east to west.

Both deep and shallow wells (< 240 m [800 ft]) are included in this data which tends to scatter the data from adjacent wells both up and down the MWL. Water samples from shallow wells tend to be isotopically heavier than nearby deep wells. Shallow wells are screened over a short interval near the surface and presumably intercept younger isotopically heavier water. Deep wells are gravel packed to the surface and screened near the water table to over 150 m (500 ft) deep thus intercept both the shallow younger water and the deeper isotopically lighter older water.

Figures 50 and 51 show the areal distribution of the average deuterium and oxygen-18 content in ground-water. Isopleths for both isotopes are similar. Distortions in the isopleths are probably due to pumpage in a vertically, isotopically stratified aquifer. Ground-water isotopic content decreases from east to west to about the eastern boundary of the flood plain (RRA) where the trend reverses. Ground-water isotopic content is heavier in the flood plain (RRA) westward for 1.6 to 8 km (1-5 mi) into the West Mesa area (WMA) where the trend reverses again. Ground water becomes isotopically the lightest west of the flood plain (WMA).

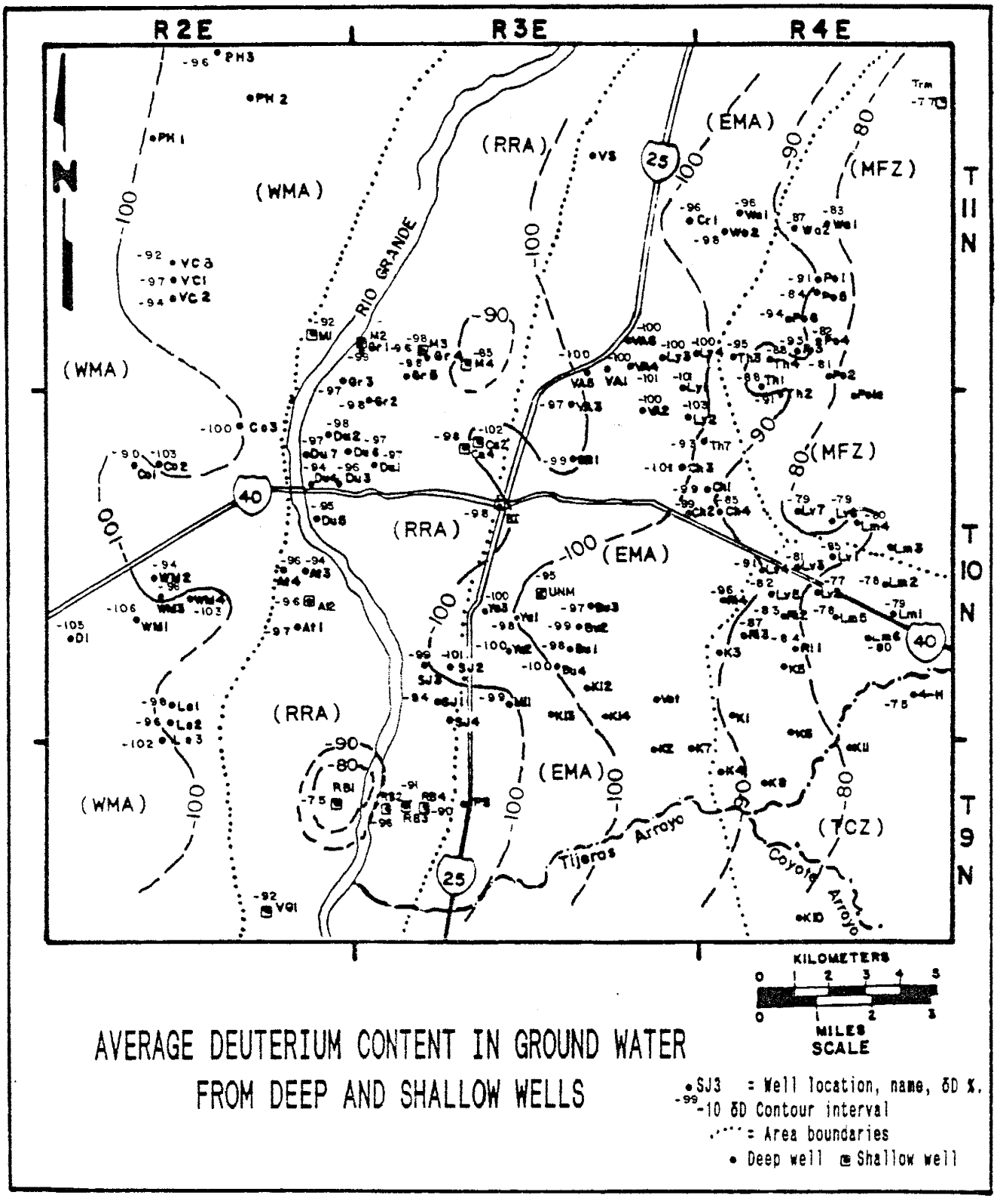

Figure 50: Ground waters deuterium content becomes lighter from the mountain recharge area toward the river. Within the rivers influence, ground water deuterium increases then decreases westward.

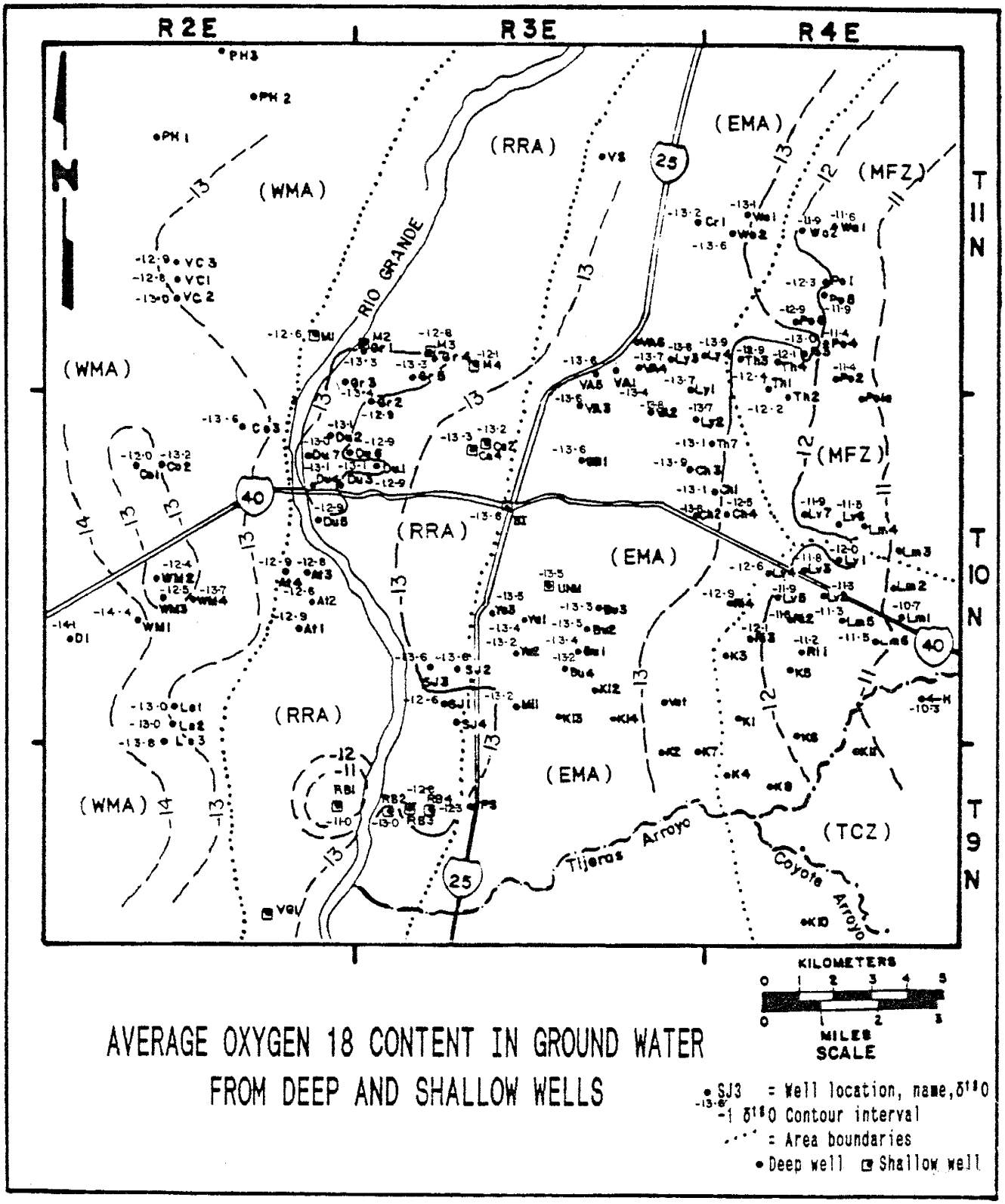

Figure 51: Ground water decreases in oxygen-18 westward. Westward flowing ground water mixes in the wellbore with isotopically heavier river recharge. Further westward, oxygen-18 decreases again.

A correlation between high chloride and light deuterium may indicate a component of deep brine is mixing with shallow ground water in the well. Figure 52 shows high chloride occurs near the mountain-front area (m) but is not associated with the lightest deuterium. Mountain-front wells are near deep basin faults which could provide the mechanism for deep-basin brine flow but chloride versus deuterium evidence does not support this theory.

A decrease in the isotopic content of ground water may indicate a decrease in the mean annual temperature (MAT) of storms contributing water to recharge. East to west decreasing isopleths indicate the MAT has been increasing or the Gulf of Mexico storms (isotopically heavier) are contributing more water to recharge than the Pacific storms (isotopically lighter). This pattern could also mean lighter, relatively shallow ground water is mixing with heavier, relatively deeper water during pumpage.

Isotopically light ground water may have important implications to local ground water ages and flow rates. If light deuterium in ground water (< -100 ‰ δD) indicates a large component of older water (late Pleistocene?) this may mean ground water velocities are an order of magnitude slower than seepage velocity (1200 years) calculations imply. In other words it would take ground water about 24,000 years to move from the mountain-front recharge areas to the river, a distance of about 24 to 32 km (15-20 mi).

Light deuterium could also indicate a well is

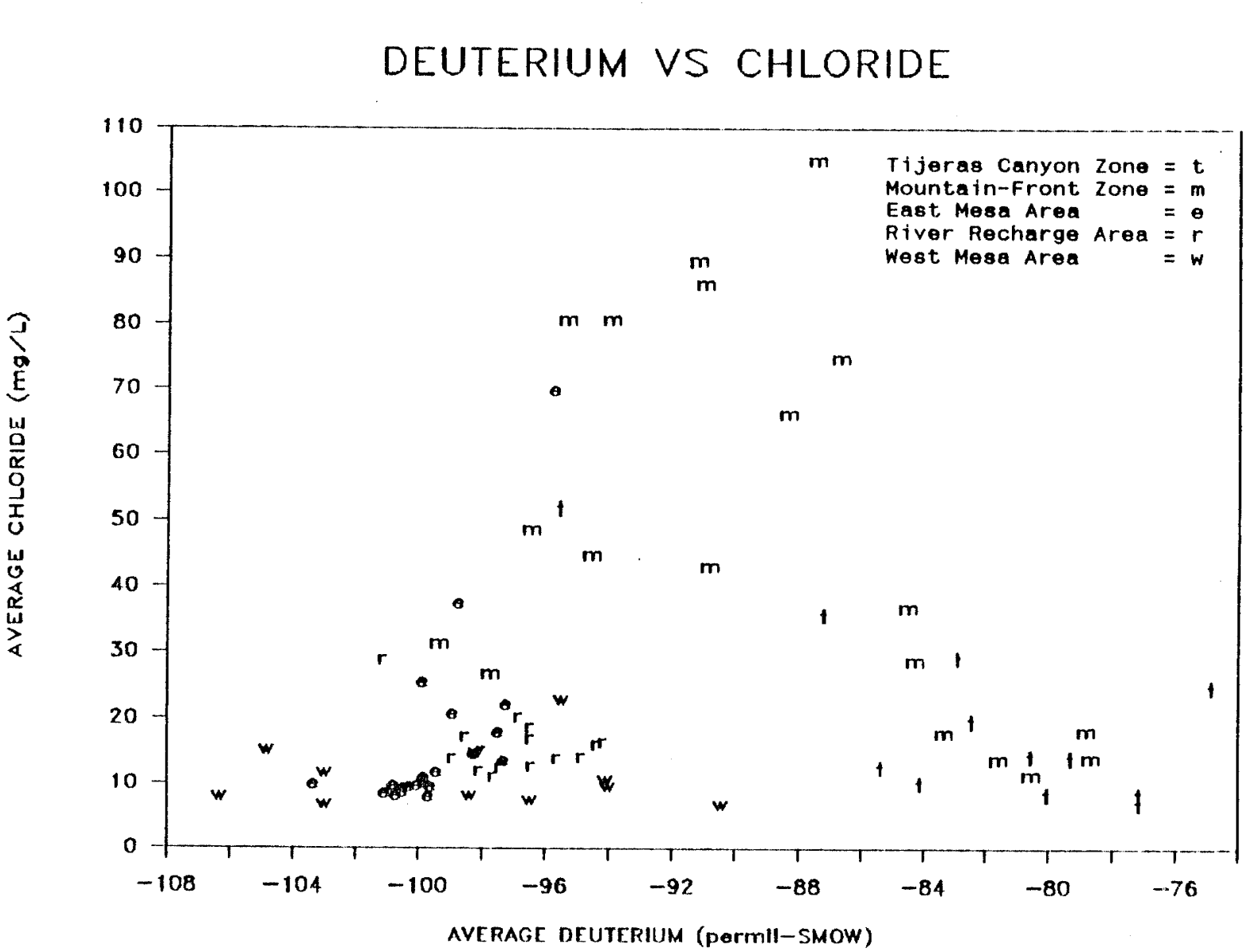

Figure 52: High chloride ground water does not correlate with light deuterium which indicates the chloride is probably not from deep brines.

intercepting deeper older basin flow (Pleistocene) moving down from the north. Pleistocene water would presumably be colder, denser, and lower in TDS than Holocene water and would probably follow a longer, deeper flow path toward the southern end of the Albuquerque-Belen Basin. This deeper flow field would be overlain by younger recharge coming off the mountains and the Rio Grande.

Figure 53 shows the areal distribution of the highest measured tritium counts in deep and shallow wells. Tritium counts in deep wells are not always repeatable and do not correlate with deuterium or oxygen-18. Background tritium is usually below 2 TU for most ground water older than 35 years. Water samples with tritium counts below the average counting error (± 6TU) may have tritium between 2 and 6 TU (a component of younger water) but is below the sensitivity of the analyses.

Figure 54 shows the maximum tritium for wells with respect to distance from the river. The river is at zero meters and the wells may be either east or west of the river. The two dashed horizontal bars indicate the average counting error of ± 6 TU. This graph demonstrates the occurrence of tritium in deep wells located several kilometers from the river or mountain-front recharge areas. This probably means these wells are periodically receiving ground water less than 35 years old in large enough volumes to contribute measurable tritium.

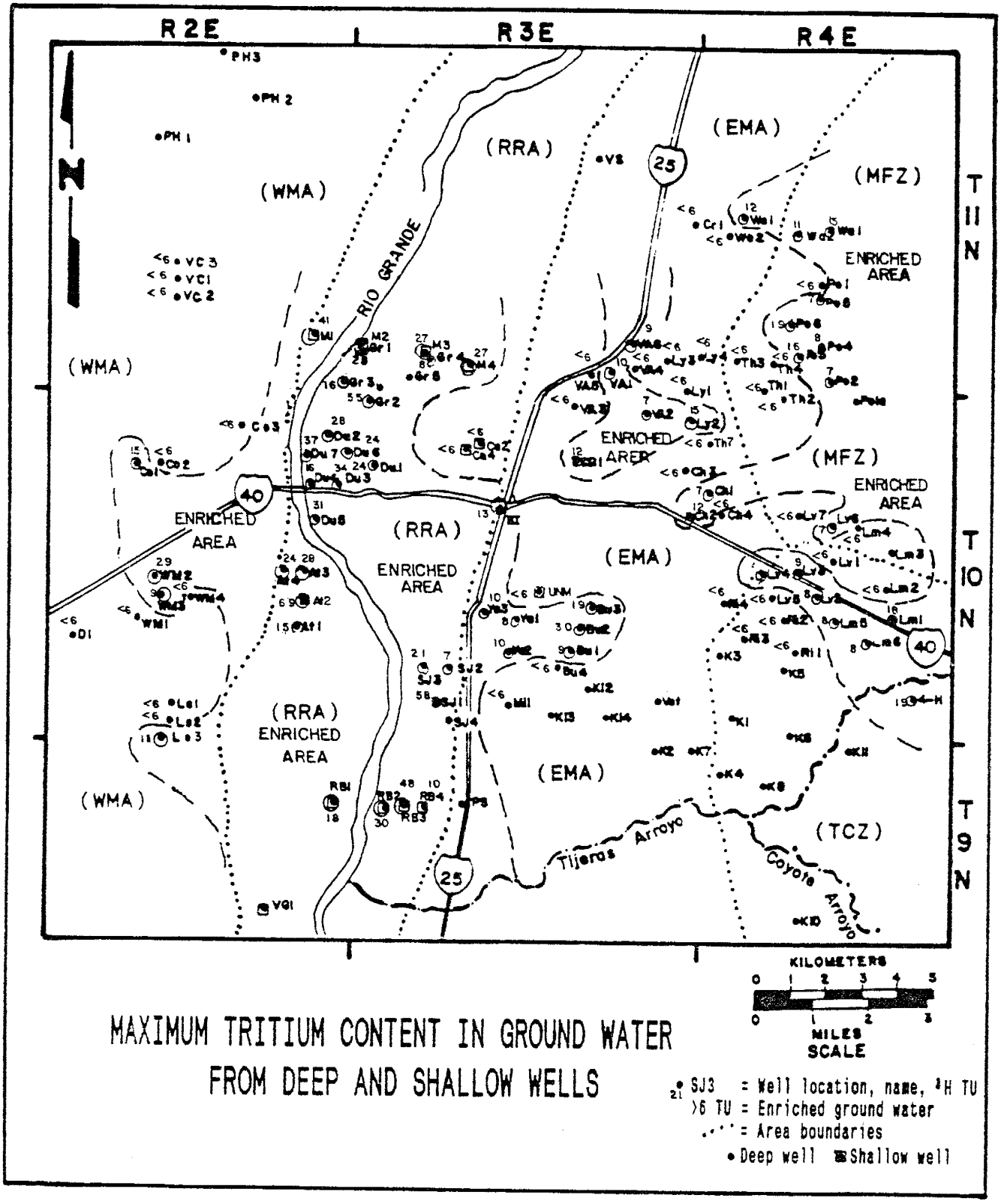

Figure 53: Ground water enriched in tritium (above 6 TU) suggests these wells receive some component of water less than 25 years old.

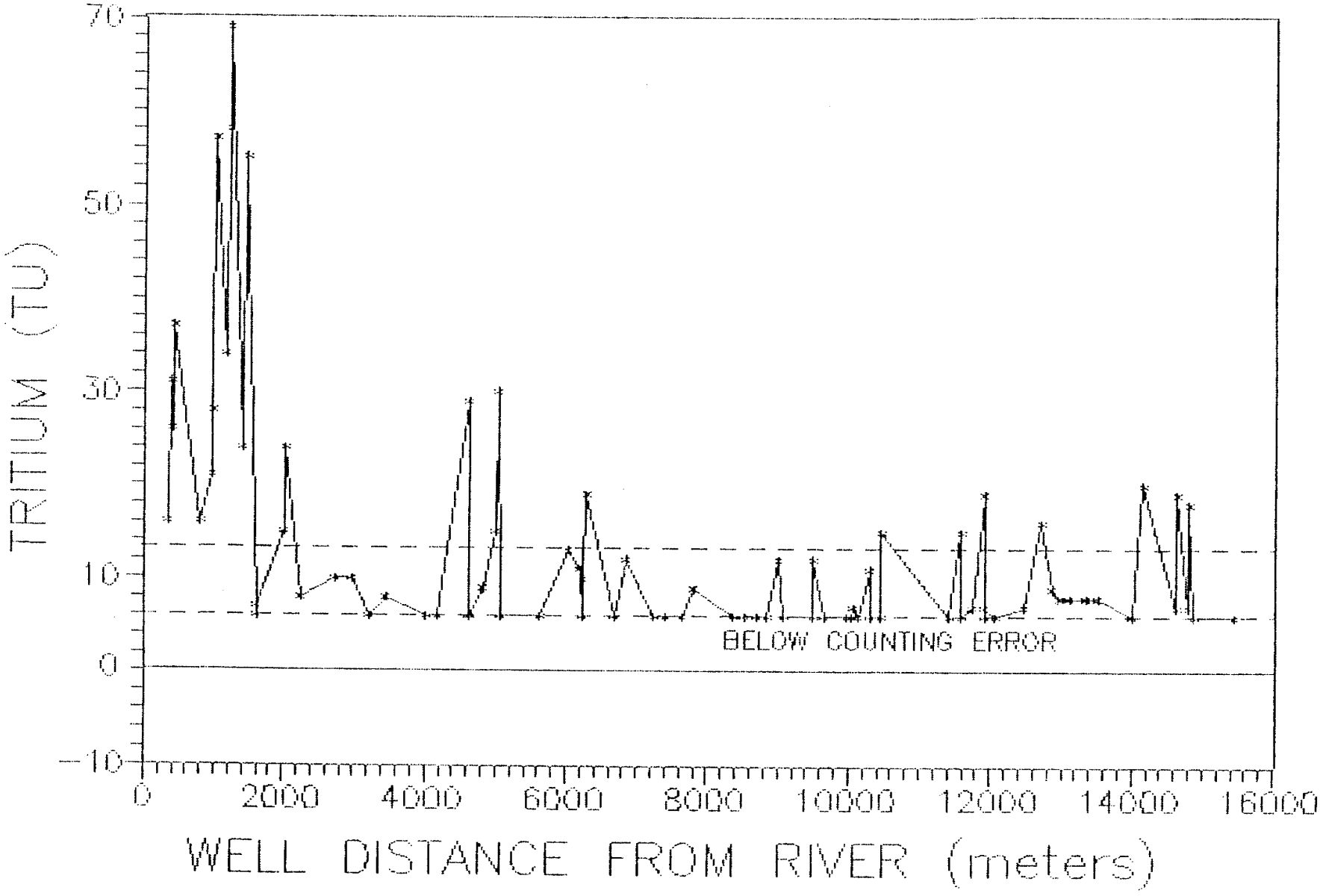

Figure 54: Wells plotted by their distance from the river shows the number of wells with tritium several kilometers from the river recharge boundary.

Data Discussion by Area Division

The mountain front area (MFA) is divided into two zones, the southern Tijeras Canyon Zone (TCZ) and the northern Mountain Front Zone (MFZ). These two zones both receive mountain-front recharge but the Tijeras Canyon zone also receives inflow from Tijeras stream which influences the ground-water quality in the area. East Mesa Area (EMA) water quality is intermediate between mountain and river recharge. Ground-water quality in the River Recharge Area (RRA) and West Mesa Area (WMA) is influenced by river recharge.

Mountain Front Area

Tijeras Canyon Zone

Water draining the Tijeras Canyon drainage basin flows through the shallow canyon-floor alluvium and into the deep basin-fill aquifer. This water is assumed to be the principal source of recharge to wells in the TCZ. Prior to large scale municipal pumpage, Tijeras Canyon drainage flowed toward the southwest (figure 18). Currently, canyon drainage flows toward the northwest where it is captured by an extensive pumping-induced water-table depression (figure 21).

From the mouth of Tijeras Canyon westward, there appears to be a corridor of relatively high hydraulic conductivity (>19 m/d [> 470 gpd/ft^2], figure 17) cutting

through the less permeable near-mountain-front sediments. North and south of this highly permeable corridor hydraulic conductivities are low to medium ranging, from 1.3 to 5.6 m/d (31-137 gpd/ft^2).

In high permeability areas, wells intercepting Tijeras Canyon inflow have lower than expected pumping temperatures (14 to 17°C [57-62°F]) for their screened depth (figures 25 & 27). This "cold" water plume flows several kilometers (miles$^+$) before ground-water-pumping temperatures approach the geothermal gradient. Wells located in lower permeability areas produce water between the minimum and average expected temperature for their screened depth. Apparently, slower water movement through these areas allows enough time for ground water to equilibrate with the geothermal gradient.

To interpret changes in ground-water quality with respect to mountain-recharge water quality I used the rain-evaporation line technique and a "difference" map. The difference map is an areal representation of the difference between the ion/Cl ratio for precipitation evaporation and the average ion/Cl ratio in ground-water. Figure 55 graphically represents the rain-evaporation line analyses for four major ions in ground water from TCZ wells. Standard deviation data is not available for rain therefore I arbitrarily choose ± ½ meq difference between the rain-line and the ground water sample as representing concentration by evaporation. Data index codes are the same as map codes

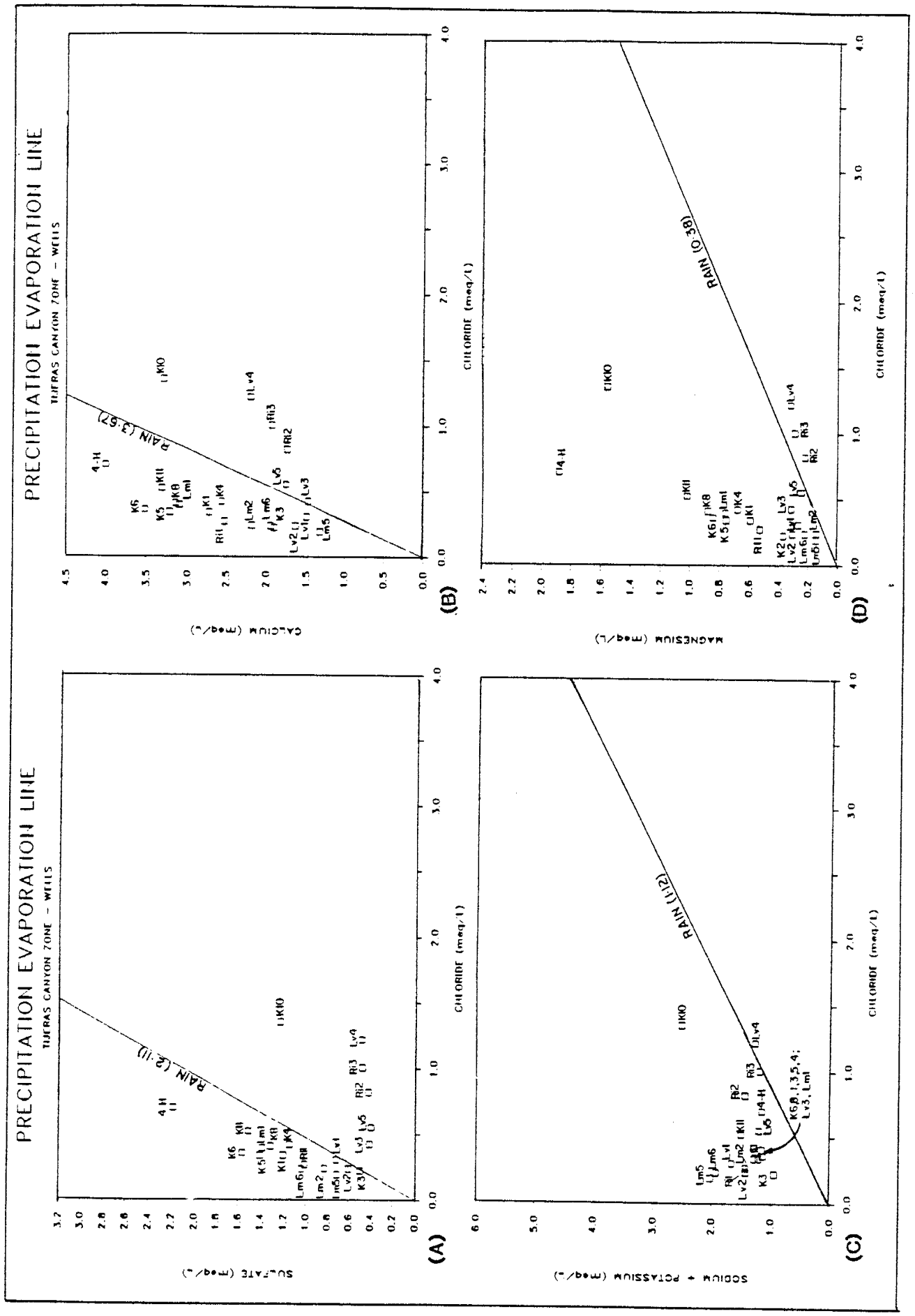

Figure 55: Major ion/chloride ratios in ground water are compared with the same ratio in precipitation, assuming all ions come from atmospheric input.

which are defined in appendices I and III.

Assuming chloride and sulfate are both conservative (rain input is the only ion source and no sinks) I would expect sulfate ratios to plot near the evaporation line. In the TCZ (figure 55a) six wells produce ground water with sulfate below the expected level (less SO4 than rain input), three wells within ± ½ meq (all SO4 from rain input), and the remaining eleven wells produce ground water above the expected sulfate concentrations (more SO4 than rain input). In other words, wells in the TCZ produce ground water either depleted, about equal too, or enriched in sulfate with respect to rain input.

Figure 56 is the sulfate difference map showing the areal relationship of wells plotted on figure 55a. Wells on the northwestern TCZ boundary are depleted in sulfate with respect to the rain-evaporation line. These wells are in the medium permeability area and are associated with the area of deepest pumping-induced water-table depression (figure 21). Ground water produced from these wells may come from both the TCZ and the mountain-front zone (MFZ). Well K10, the farthest well south, also depleted in sulfate, is probably receiving part of its ground water from Coyote Springs drainage. Coyote Springs drains across the northern extension of Hubble bench, a down-thrown fault block covered with a thin alluvial vernier which provides the mechanism for shallow water-table evaporation.

Wells located between the depleted and enriched areas plot near the evaporation line and may either be an average

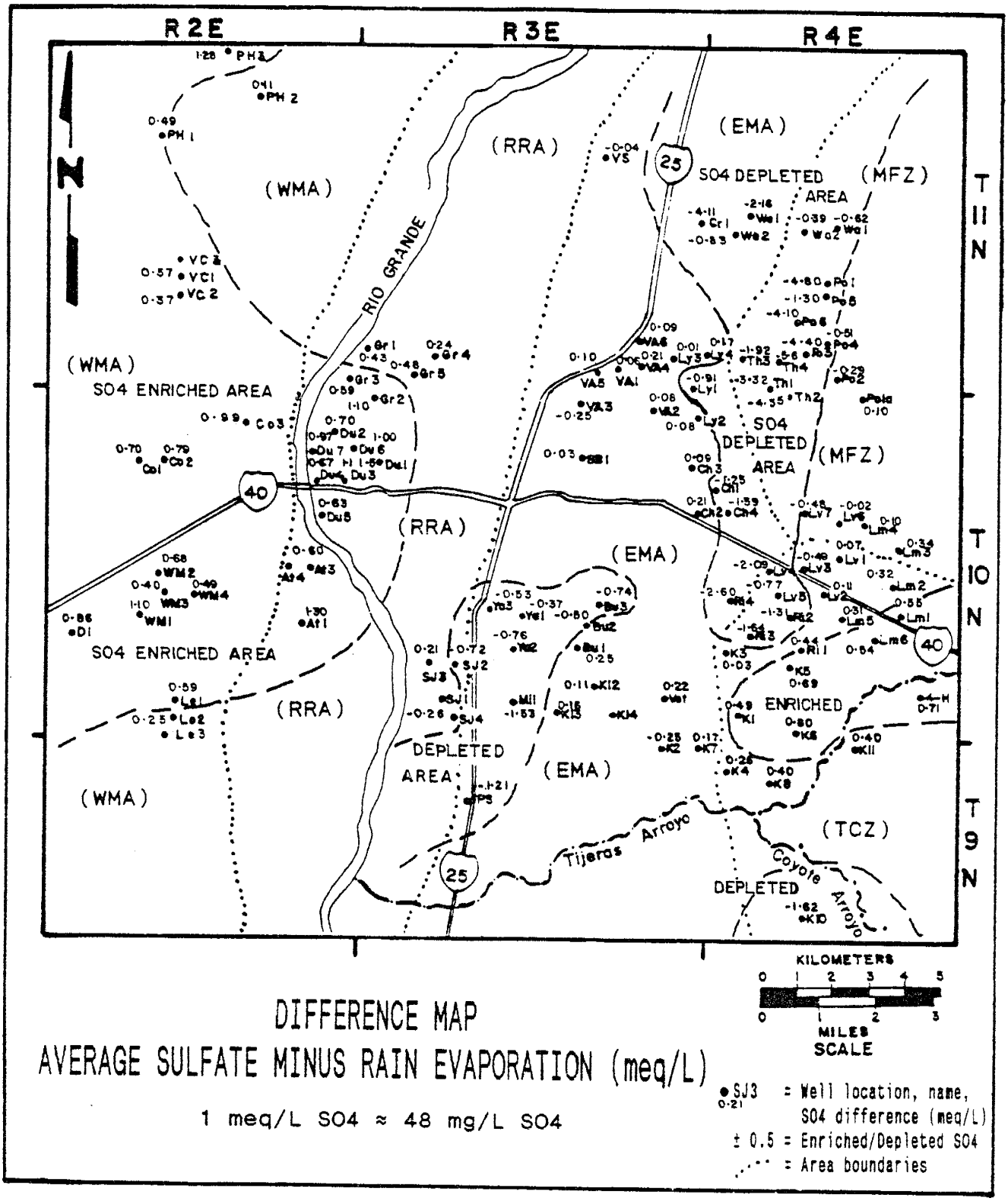

Figure 56: Ground water depleted or enriched in sulfate with respect to atmospheric input is geochemically altered by a processes other than evaporation. This map areally represents graph A in figures 55, 62, and 65.

of both the sulfate enriched and depleted ground water or may represent sulfate concentrated by evaporation only.

Sulfate enriched ground water flowing through the TCZ high permeability corridor decreases in sulfate basinward. Sulfate concentrations in milligrams (figure 41) also reflects this decreasing trend from 105 mg/L at the mouth of Tijeras Canyon to 14 mg/L in the pumping induced water-table depression. Borehole mixing of Tijeras Canyon inflow (evaporation concentrated sulfate) with an increasing percentage of deeper low-TDS ground water could account for the decreasing east-to-west sulfate trend.

Sulfate depleted ground water (below atmospheric input) may be due to pedogenic wetting/drying cycles precipitating sulfate from the soil solution prior to reaching recharge. Increased sulfate in ground water may be explained by either a low SO4/Cl precipitation ratio based on less than average rain sulfate or chloride content, or weathering of trace amounts of pyrite from the granitic material. If sulfate were being added by pyrite dissolution I would expect to see sulfate increase with depth and distance from the recharge boundary but sulfate appears to be decreasing with distance.

Figure 55b, the calcium rain-evaporation line and figure 57, the calcium-difference map, both show depleted calcium in three of the sulfate depleted wells (Ri2, Ri3, Lv5). Two wells between the calcium depleted and enriched areas produce ground water within ± ½ meq of the evaporation line, approximately equivalent to rain input.

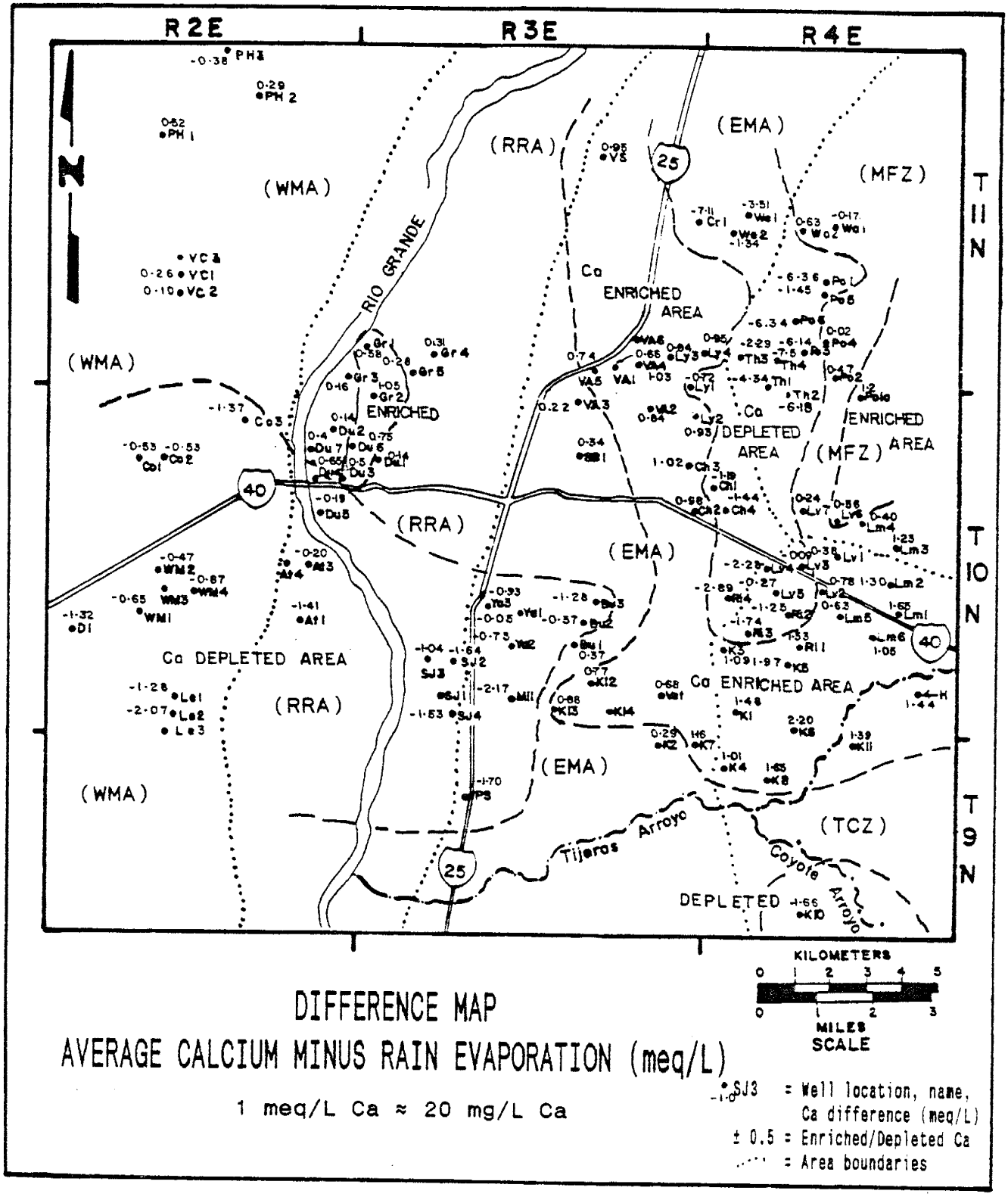

Figure 57: Ground water depleted or enriched in calcium with respect to atmospheric input is geochemically altered by a processes other than evaporation. This map areally represents graph B in figures 55, 62, and 65.

Most TCZ wells show calcium enrichment. Calcium decreases basinward from 80 mg/L at the mouth of Tijeras Canyon to 20 mg/L (figure 44) in the water-table depression. TCZ low calcium areas are coincident with the Na-HCO3 water-type of figure 28 and offset westward of the high chloride area (figure 41).

Figure 55c shows the average sodium* content in TCZ ground water is either within ± ½ meq or enriched with respect to atmospheric input. The sodium* difference map (figure 58) shows a steady increase in excess sodium* as ground water flows away from Tijeras Canyon toward the water-table depression. TCZ's highest sodium* concentrations occur in the low permeability area coincident with the Na-HCO3 water-type on figure 28. Sodium* content varies within about ± 5 mg/L through the high permeability corridor (figure 43) but increases from 28 mg/L at the mouth of the canyon to about 48 mg/L in the low permeability areas in the water-table depression. Ion exchange (figure 30) does not account for the increased sodium*. Areas depleted in sulfate and calcium, and apparently enriched in chloride have sodium*/chloride ratios equivalent to rain input (figure 56,57,41,58).

Figure 55d show ground-water magnesium concentrations either follow the rain-evaporation line within ± ½ meq or are enriched with respect to rain input. Apparently magnesium is being added to the ground water system.

Total dissolved solids (TDS) decrease from 423 mg/L at the mouth of Tijeras Canyon to 190 mg/L in the water-table

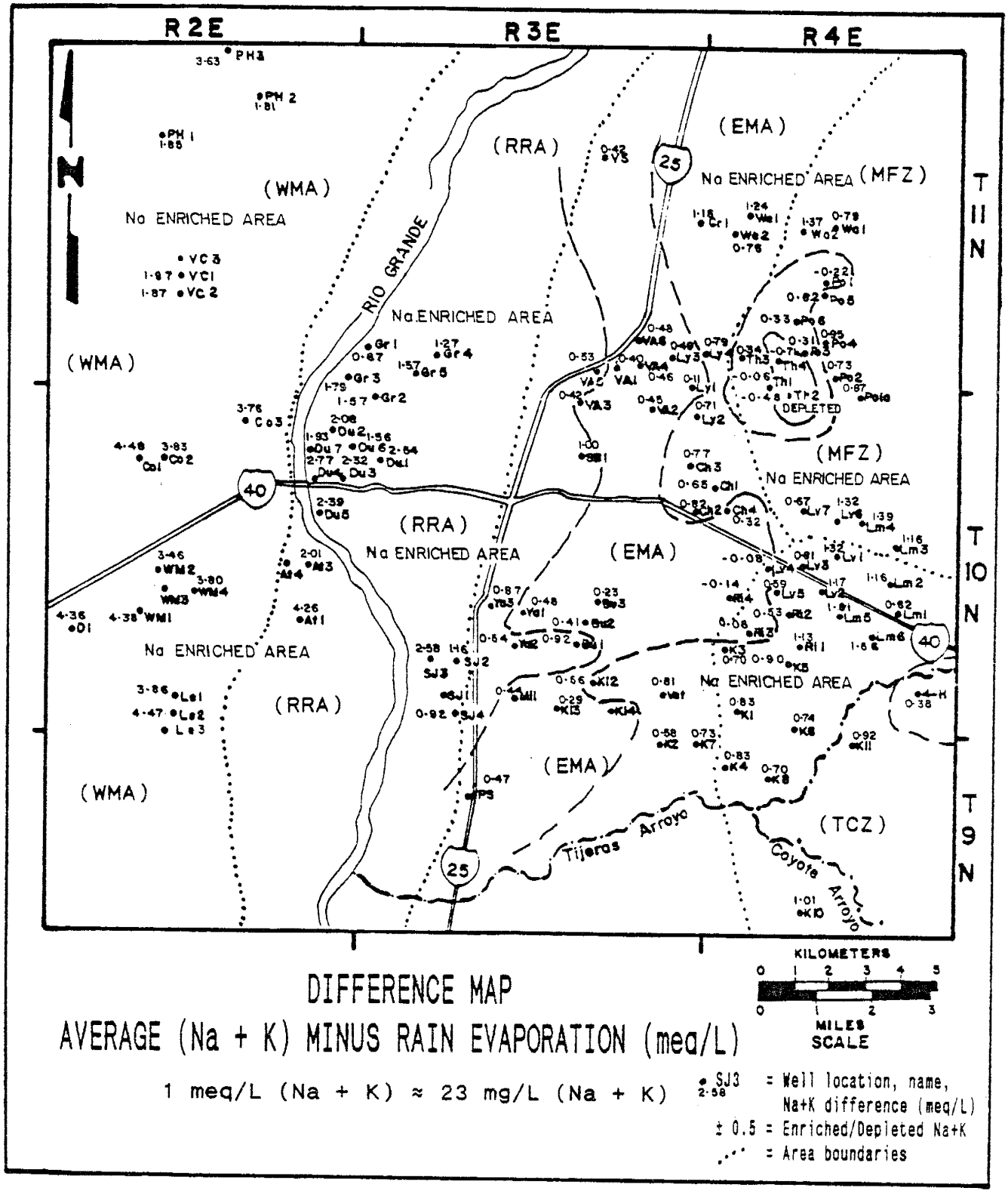

Figure 58: Ground water depleted or enriched in sodium* with respect to atmospheric input is geochemically altered by a processes other than evaporation. This map areally represents graph C in figures 55, 62, and 65.

depression (figure 47) which supports the theory of borehole mixing of high and low TDS ground waters.

Chloride decreases from 25 mg/L to 12 mg/L westward (figure 41) through the high permeability corridor (east to west). From the mouth of Tijeras Canyon toward the water-table depression (east to northwest) chloride decreases from 25 mg/L to 12 mg/L then increases to 52 mg/L. In the TCZ high chloride area, calcium and sulfate are depleted while sodium* and magnesium are nearly equivalent to rain-input which supports the wetting/drying cycle source theory.

Figure 59 is a trilinear plot showing the average anion and cation reacting percentages for TCZ well production. Recharge sources, precipitation (P) and Tijeras stream (T), reacting percentages are plotted to show ground-water quality shifts away from recharge input. The overall ground-water quality trend (diamond field) is to loss sulfate and calcium while increasing chloride and sodium relative to Tijeras Canyon recharge.

In the cation field, the 4-Hills (H) well plots very near the Tijeras stream (T). As ground water flows away from Tijeras Canyon the reacting percentage of calcium and magnesium decrease with increasing sodium*.

In the anion field, bicarbonate reacting percentages increase as ground water flows westward. Figure 45, bicarbonate concentrations in mg/L, shows the opposite trend in that absolute concentrations of bicarbonate decrease westward. This suggests chloride and sulfate are increasing but they are suppose to be conservative.

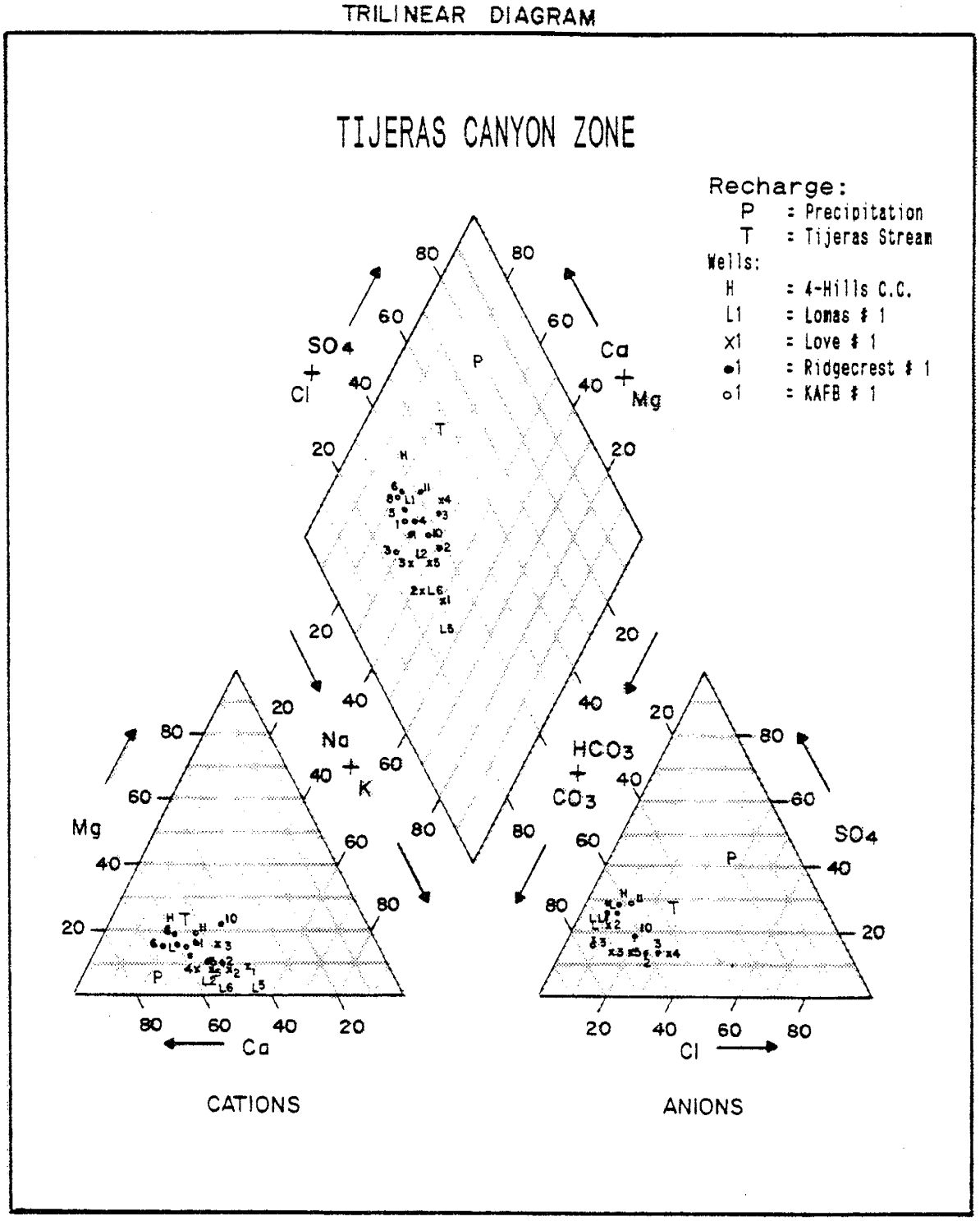

Figure 59: Ground water geochemistry influenced by Tijeras Canyon inflow shows increasing sodium and chloride with decreasing calcium and sulfate with respect to Tijeras Canyon stream.

In the diamond field, ground-water plots in two areas the sodium enriched lower area and the calcium enriched upper area. Generally, ground water produced by wells in the low permeability zone plot in the sodium enriched lower area while wells in the medium permeability zone plot in the middle range. Wells in the high permeability corridor plot in the upper calcium enriched area.

Trilinear plot analyses shows calcium is being removed and sodium added suggesting ion exchange activity. The ion exchange map (figure 30) shows a steady decrease in total cations from the canyon westward through the high permeability corridor, through the low permeability areas, and from the canyon into the ground-water depression. Absolute amounts of calcium and sodium both decrease westward with the exception of the northwestern high sodium area. Ion exchange is probably occurring but is not the controlling process on ground-water ion composition.

Figure 60a shows the rain-evaporation line for potassium. Potassium follows the line with the exception of those wells with high chloride content. Apparently, chloride has increased and potassium remained constant. Secondary clay mineral formation (illite) may control the dissolved potassium content of ground water.

Figure 60b shows TCZ ground-water isotopes scatters within $\delta D \pm 5‰$ about the meteoric water line. Tritium counts above 6 TU occur in deep wells where tritium may vary from less than 6 TU to 19 TU (± 6 TU counting error). In the TCZ, tritium enriched ground water occurs along a

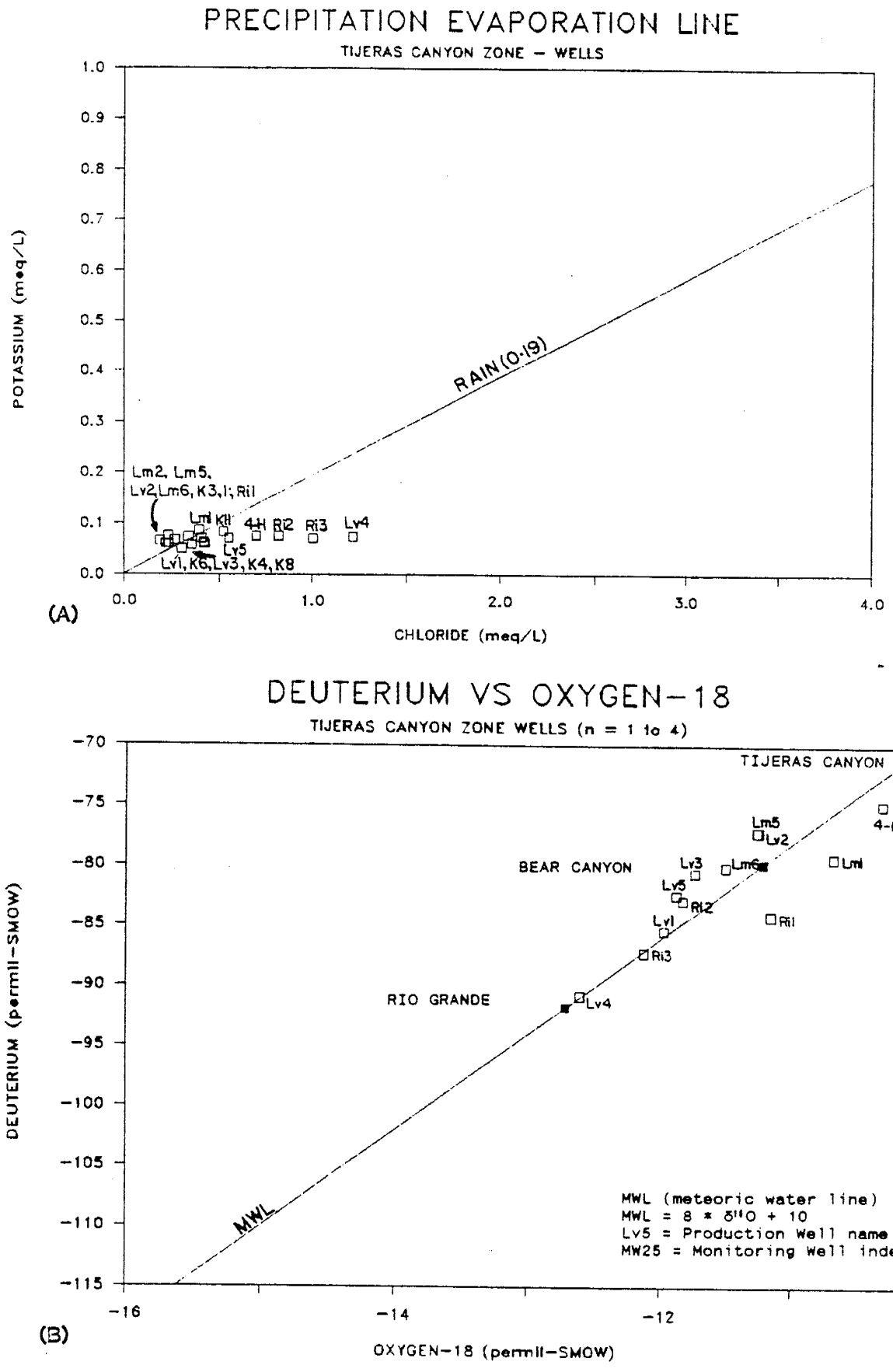

Figure 60: Potassium is nearly constant, concentrations may be contolled by illite formation (A); ground water isotopes scatter near the Tijeras and Bear Canyon recharge sources (B).

present-day flow path from the mouth of Tijeras Canyon into the water-table depression (figure 53). Along this same flow path, ground water becomes isotopically lighter (figures 50,51). This trend suggests ground water is getting progressively older as it flows away from the source area. Inferred seepage velocities are an order of magnitude slower than velocities calculated from Darcy's Law. Borehole mixing of deeper, isotopically-lighter ground water with shallower, isotopically-heavier ground water invalidates velocity estimations based on isotopes.

Figure 61a shows clay mineral stability for calcium smectite and kaolinite along four present-day flow paths shown on figure 61b. Water chemistry from three TCZ wells (T) indicate ground water near the recharge area is in equilibrium with kaolinite but is evolving toward the calcium-smectite equilibrium boundary as water flows toward the water-table depression.

In summary, TCZ ground water appears to be a composite of three sources: (1) Tijeras stream and shallow canyon alluvial inflow; (2) underlain by inflow from the mountain-core fractured bedrock; (3) and deep-basin inflow from the north. Younger mountain-front recharge (stream, alluvium, fracture flow) waters flow from the east (figure 21) while deep-basin ground water flows nearly due south (Kernodle and others, 1987, figure 39).

Tijeras stream and shallow canyon-alluvial flow are characterized by high TDS, sulfate and calcium depletion with respect to atmospheric input, and heavy isotopic

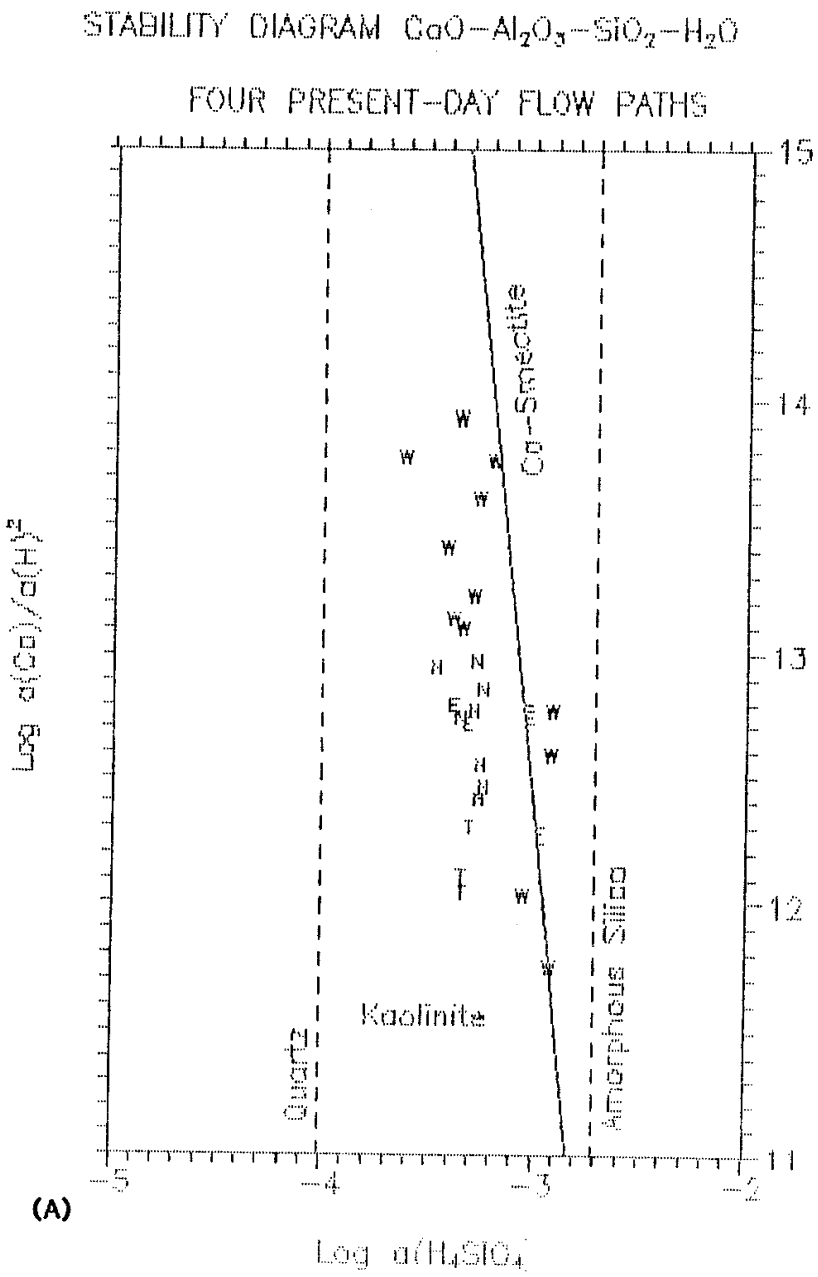

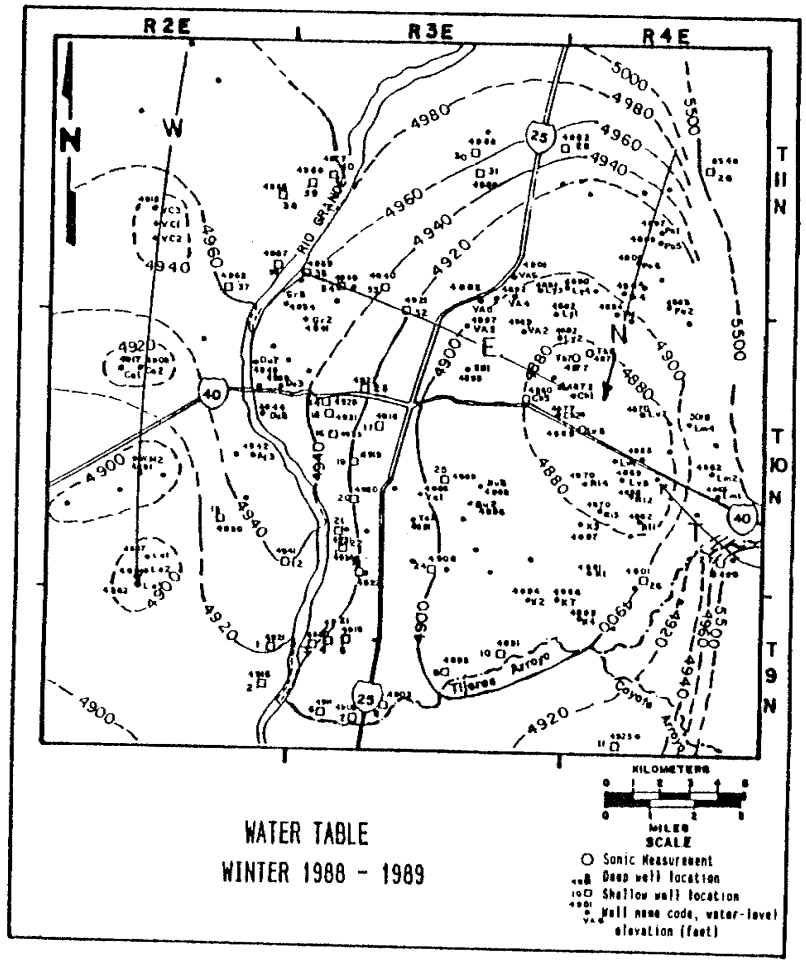

T = Tijeras Canyon
N = Mountain Front
E = River to East Mesa
W = West Mesa

Figure 61: Stability diagram for secondary clay mineral formation of Ca-smectite along 4 different flow paths (A); flow path locations (B).

content with tritium above the counting error of ± 6 TU. Mountain-front fracture inflow is probably geochemically similar to spring discharge characterized by low TDS, calcium and sodium enriched by mineral dissolution, isotopic content is a little lighter than Tijeras stream inflow and tritium is below the counting error of ± 6 TU. Deep-basin flow, characterized by lower TDS than either fracture or alluvial inflow sources, is probably isotopically-light late pleistocene ground water with background tritium (<2 TU).

Shallow wells near the mountain front tap ground water composed primarily of Tijeras stream and shallow alluvial inflow. Deeper, near mountain-front wells receive water from stream and alluvial inflow, as well as mountain-front fracture flow. Wells further west of the recharge area tap all three sources. Some ground-water mixing occurs near the flow boundaries as water moves down gradient but most mixing probably occurs in the borehole during pumpage.

In the water-table depression, wells apparently receive shallow ground water from the northern mountain front recharge area (MFZ) which seems to be strongly affected by soil wetting/drying cycles. All water-quality and ground-water temperature maps show the influence of Tijeras Canyon inflow through the high permeability corridor.

Mountain-Front Zone

Water draining into the northern mountain-front zone (MFZ) flows from high mountainous canyons byway of intermittent streams, springs, fractures and shallow pediment covers before discharging to the deep-basin aquifer. Near mountain-front gradients have steepened and flow directions shifted from the southwest (figure 18a) to nearly due south into the present-day water-table depression (figure 21).

In the MFZ, hydraulic conductivities increase from low near the mountain-front to high in the mid-alluvial fan area (figure 17). Near mountain-front proximal fan deposits are permeably low with hydraulic conductivities ranging from 1.3 to 2.7 m/d (32-66 gpd/ft^2). Medial fan and braided stream deposits have are of medium permeability with hydraulic conductivities between 6.1 and 12.4 m/d (151-303 gpd/ft^2). The high permeability area is composed of braided stream deposits with hydraulic conductivities greater than 20 m/d (< 480 gpd/ft^2).

Wells in the MFZ produce ground-water temperatures within the expected range for their screened depth with the exception of Thomas Well # 4 (Th4) (figure 25). Th4 well produces ground water about 1C° higher than the expected temperature (figure 27). Which may be significant since ground water from this well has the most anomalous geochemistry.

Precipitation-evaporation line analyses (figure 62) of

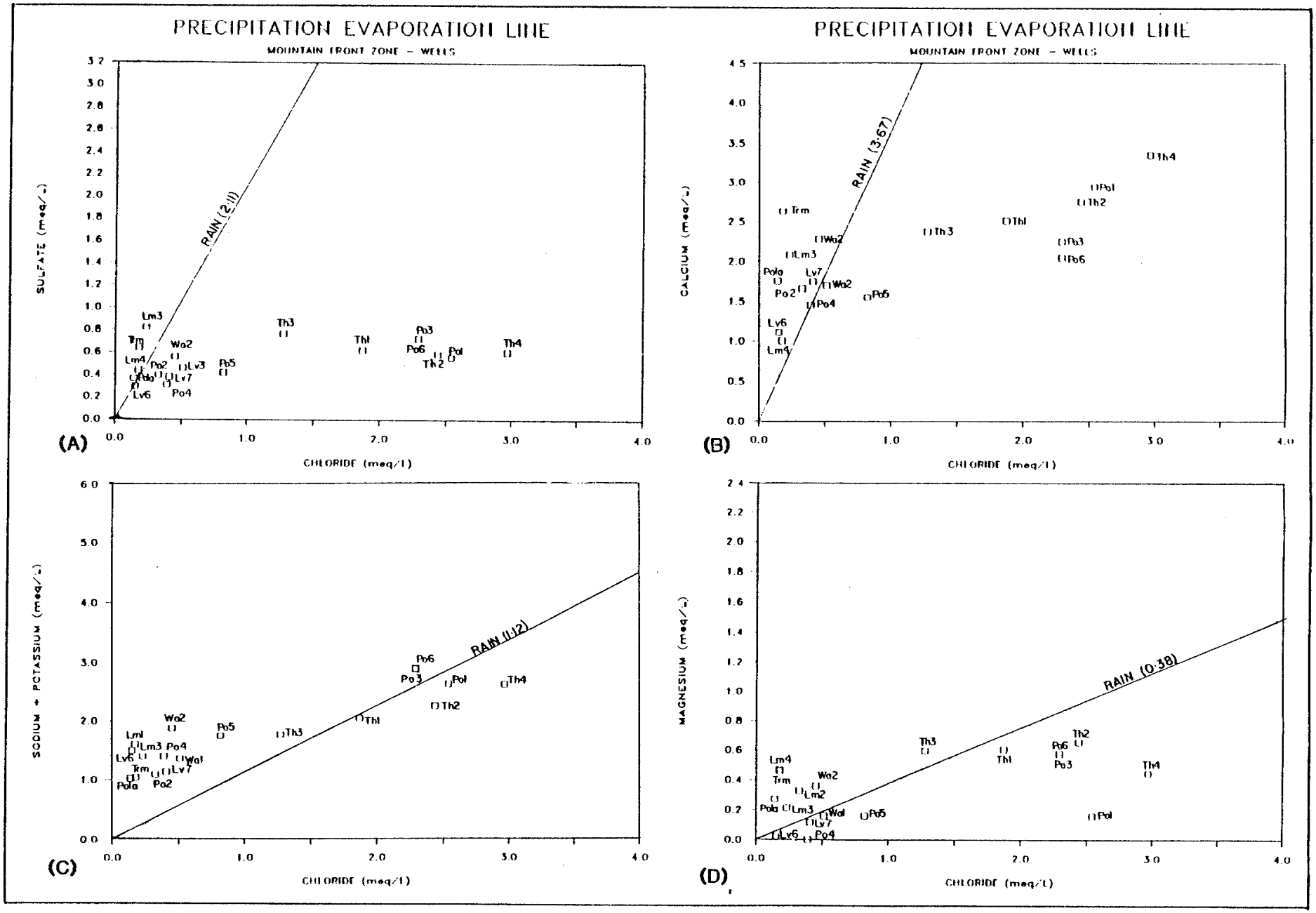

Figure 62: Major ion/chloride ratios in ground water are compared with the same ratio in precipitation, assuming all ions come from atmospheric input.

four major ions; sulfate, calcium, sodium*, and magnesium versus chloride for the MFZ shows the gain or lose of these ions in ground water with respect to atmospheric input.

Figure 62a and 56 both show sulfate in ground water near the recharge boundary follows the rain-evaporation line within ± ½ meq. Wells located further westward are depleted in sulfate. Absolute concentrations of sulfate (figure 42) show sulfate increasing westward from 15 to 37 mg/L, yet wells with the highest sulfate content are greatly depleted with respect to atmospheric input. The sulfate difference map (figure 56) shows most wells in the MFZ produce sulfate depleted ground water from - 0.5 to -5.6 meq/L (-24 to - 269 mg/L SO4) below atmospheric input.

Calcium (figure 62b and 57) depleted ground water is produced from the same wells depleted in sulfate. A large area, elongated north to south, of calcium and sulfate depleted ground water follows the mountain-front (figures 56 and 57). Two areas low in total calcium (mg/L) occur in the two eastern Na-HCO3 areas shown on the hydrogeochemical facies map (figure 28). Calcium concentrations range from 24 mg/L near the mountain recharge area to 67 mg/L over the high chloride area. Total calcium (mg/L) decreases in the high permeability area.

Ground-water sodium* ratios (figure 62c) follow the rain-evaporation line fairly well with some increase in sodium* in ground water low in TDS. Water high in TDS is chemically less aggressive than water low in TDS which may explain why only dilute waters show a relative increase in

sodium, magnesium, and calcium with respect to atmospheric input. The northern Na-HCO3 area (figure 28) shows elevated sodium* concentrations (figure 43) ranging from 32 mg/L to 79 mg/L over a short distance before concentrations decrease in the high permeability area. The sodium* difference map (figure 58) shows the high sodium area (figure 28) is within ± ½ meq/L (12 mg/L Na) of atmospheric input (figure 62c).

Ground-water magnesium (figure 62d) content in the MFZ agrees with the rain-evaporation line fairly well for some wells, two high chloride wells are magnesium depleted, and wells nearest the recharge area are enriched in magnesium.

Ground water produced by wells nearest the mountain-front are lower in total dissolved solids (TDS) than ground water associated with Tijeras Canyon inflow. TDS increases westward from 180 to 400 mg/L (figure 47). After reaching a high of 400 mg/L, TDS decreases westward toward the high permeability area.

Chloride concentrations are low near the MFZ recharge area (figure 41). Within about 3 km (≈2 mi) chloride increases from 5 to 105 mg/L. Two large high chloride areas are associated with the sulfate and calcium depleted areas shown on figures 56 and 57. High chloride concentrations are offset westward of high sodium* areas (figure 43).

Figure 63 is a trilinear plot of the average major ion reacting percentage for ground water in the MFZ. The initial recharge source, precipitation (P), and a well

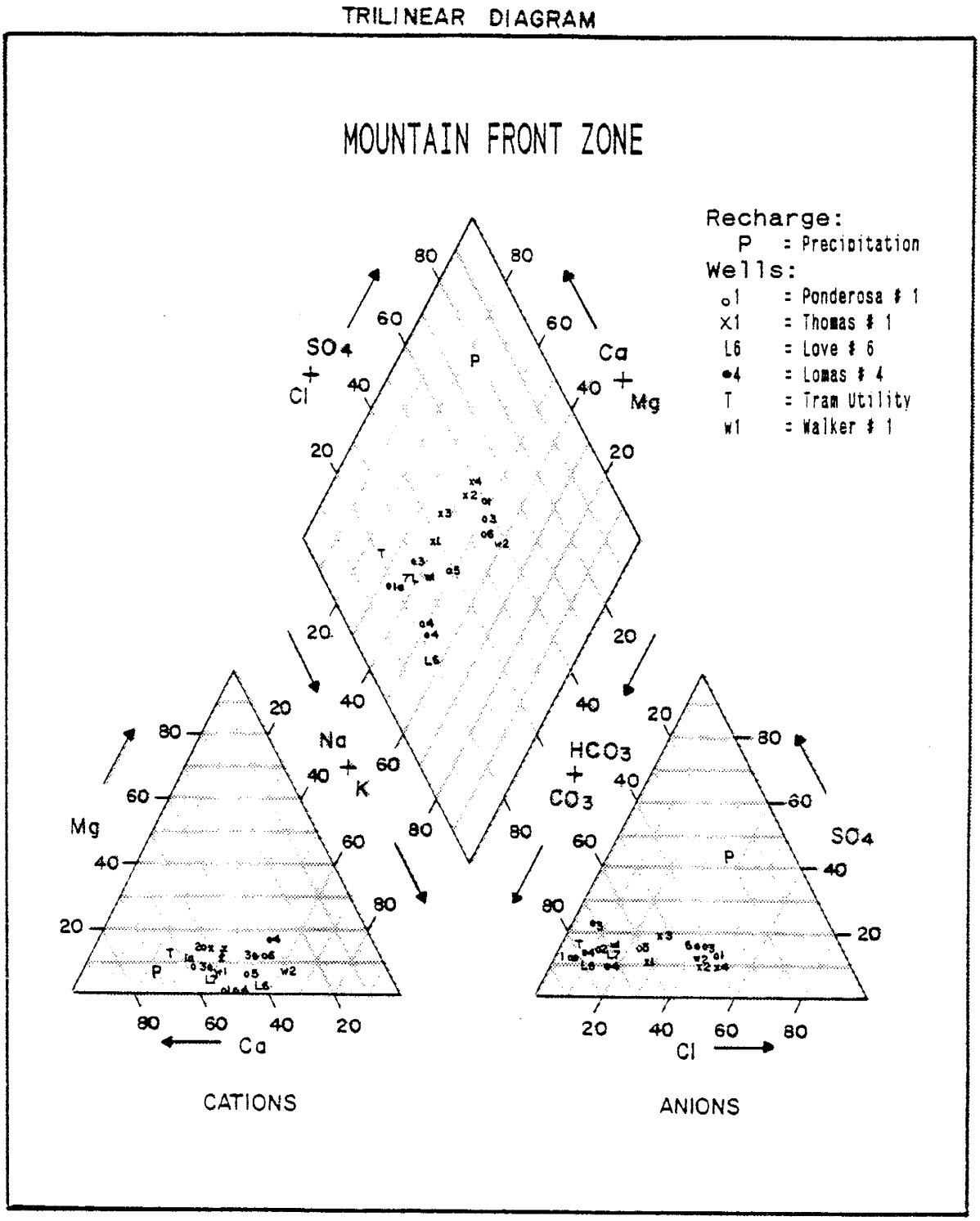

Figure 63: Cation and anion reacting percentages both show two trends with a mixing line in the diamond field.

receiving shallow alluvial inflow, Tramway Utility (T), are also shown as reference points for ion shifts along a flow path. Tramway well (T) seems to represent mountain-front recharge (exact well depth or location, within 8 mi^2, are unknown).

The cation field shows increasing sodium* with decreasing calcium typical of ion exchange. Cation sums along a MFZ flow path (figure 30) increase then decrease which indicates geochemical processes other than ion exchange are controlling the cation content of ground water in the area.

In the anion field, ground water plots in two areas, one area is low in sulfate and chloride and high in bicarbonate. The other area is low in sulfate and bicarbonate and high in chloride. Chloride increases from 10 to 60 percent of the total anions.

In the diamond field, two areas emerge, one with high chloride and the other with high bicarbonate reacting percentages. Ion shifts from the Tramway well down gradient show increasing sodium and chloride percentages.

Potassium (figure 64a) seems to be depleted in ground water with high chloride concentrations. This apparent depletion may only reflect increased chloride due to cyclic wetting/drying cycles. Nearly constant potassium levels in ground water may be controlled by secondary clay mineral formation of illite.

Deuterium and oxygen-18 ground-water content (figure 64b & 50) becomes isotopically lighter with distance from

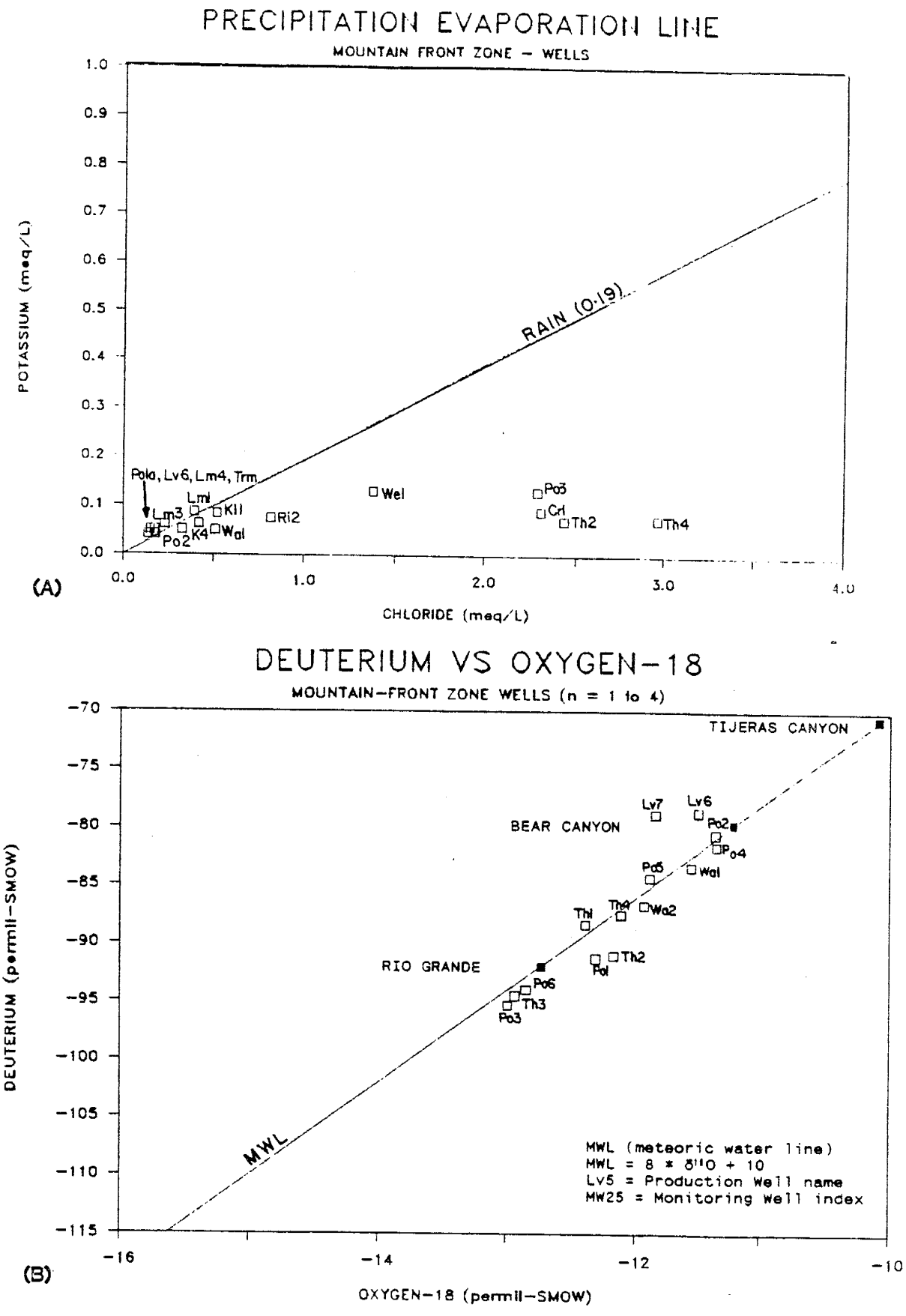

Figure 64: Potassium is nearly constant, concentrations may be contolled by illite formation (A); ground water isotopes scatter near the Bear Canyon recharge source but become lighter with distance from the recharge boundary (B).

the recharge area. These wells show a little less scatter about the MWL than the TCZ wells. Borehole mixing of younger isotopically heavier recent recharge with deeper older basin inflow would cause an apparent decrease in ground-water age in near-mountain-front wells (figures 50 & 51). Tritium units above the counting error of ±6 TU occur sporadically in ground water from deep wells in the MFZ which supports the assumption of borehole mixing of ground water of different ages (figure 53).

Ground water flowing from the northern mountain-front recharge area (N) is in equilibrium with kaolinite (figure 61a & 61b). Dissolved silica is nearly constant. Ground water from MFZ wells appear to be more evolved toward equilibrium with calcium smectite than ground-water associated with Tijeras Canyon inflow (T).

Thomas well 4 (Th4) produces the most geochemically anomalous ground water along the mountain front. Th4 is in the high permeability zone with warmer pumping temperatures than expected, highest chloride, lowest calcium and sulfate, and sodium and chloride are consistent with evaporation concentration of precipitation. Data inconsistencies are the high pumping temperature (deep source), yet apparent pedogenic enrichment (shallow source). Th4 isotopic content is consistent with surrounding wells and the ground water is in equilibrium with kaolinite. Which all suggest pedogenic enrichment rather than deep brine flow.

In summary, ground water flowing from the MFZ recharge

area seems to be more susceptible to cyclic wetting/drying cycles than recharge from the TCZ. A widespread, elongated front of calcium and sulfate depleted ground water covers most of the MFZ. Up gradient of the depleted zone, ground water is enriched or near concentrated atmospheric input for sodium and chloride. The Ca-Cl occurrences (figure 28), reflects the reaction percentage of chloride with respect to sulfate and bicarbonate, follow the rain-evaporation line very well. Ground water alterations due to cyclic wetting/drying cycles may be prevalent in the MFZ because of its broad alluvial fans (greater available surface area) and the network of coarse-grained highly permeable arroyos that provide the catchment for shallow-penetrating rains. In the TCZ, ground water flows through a relatively narrow canyon with restricted surface area where ground water is less susceptible to wetting/drying cycles. Isotopic evidence supports pedogenic rather than deep brine alteration of ground water in this area.

East Mesa Area

East Mesa area (EMA) ground-water chemistry, between the mountain and river recharge areas, poses several questions: (1) where is the geochemical boundary between west-flowing mountain-front and east-flowing river recharge? (2) how can total dissolved solids decrease in this area? (3) why do geochemical trends tend to reverse here? and (4) why are deuterium and oxygen-18 so light?

Before municipal pumpage lowered the water table, mountain-front recharge, apparently, flowed through the EMA toward the southwest. After the water table was lowered, present-day flow paths (figure 21) show recharge from the mountain front, Tijeras Canyon, and the Rio Grande flow into the EMA.

Hydraulic conductivities in the EMA vary from medium on the east and west boundaries to high in the central area (figure 17). Medium hydraulic conductivities range from 6.2 to 9.2 m/d (153-225 gpd/ft^2). The EMA is largely in the high hydraulic conductivity area which ranges from 12.3 to 50.6 m/d (301-1242 gpd/ft^2).

Ground-water temperatures are variable throughout the EMA. In the northern area, deep wells produce cooler than expected pumped ground-water temperatures. In the southern EMA, wells intercepting Tijeras Canyon inflow are cooler than expected. In contrast, two EMA wells intercepting water from the river (Mi1 & Ya3) are warmer than expected (figure 25).

Figure 65 shows the major ion content of EMA ground water with respect to both precipitation and Rio Grande evaporation lines. There is no clear-cut geochemical boundary between river and mountain recharge. Based on sulfate and sodium* ratios near the mountain front and in the flood plain, I will assume the precipitation evaporation line is the most appropriate for the EMA.

Ground water sulfate content is depleted in all wells (figure 65a) with respect to the river-evaporation line but

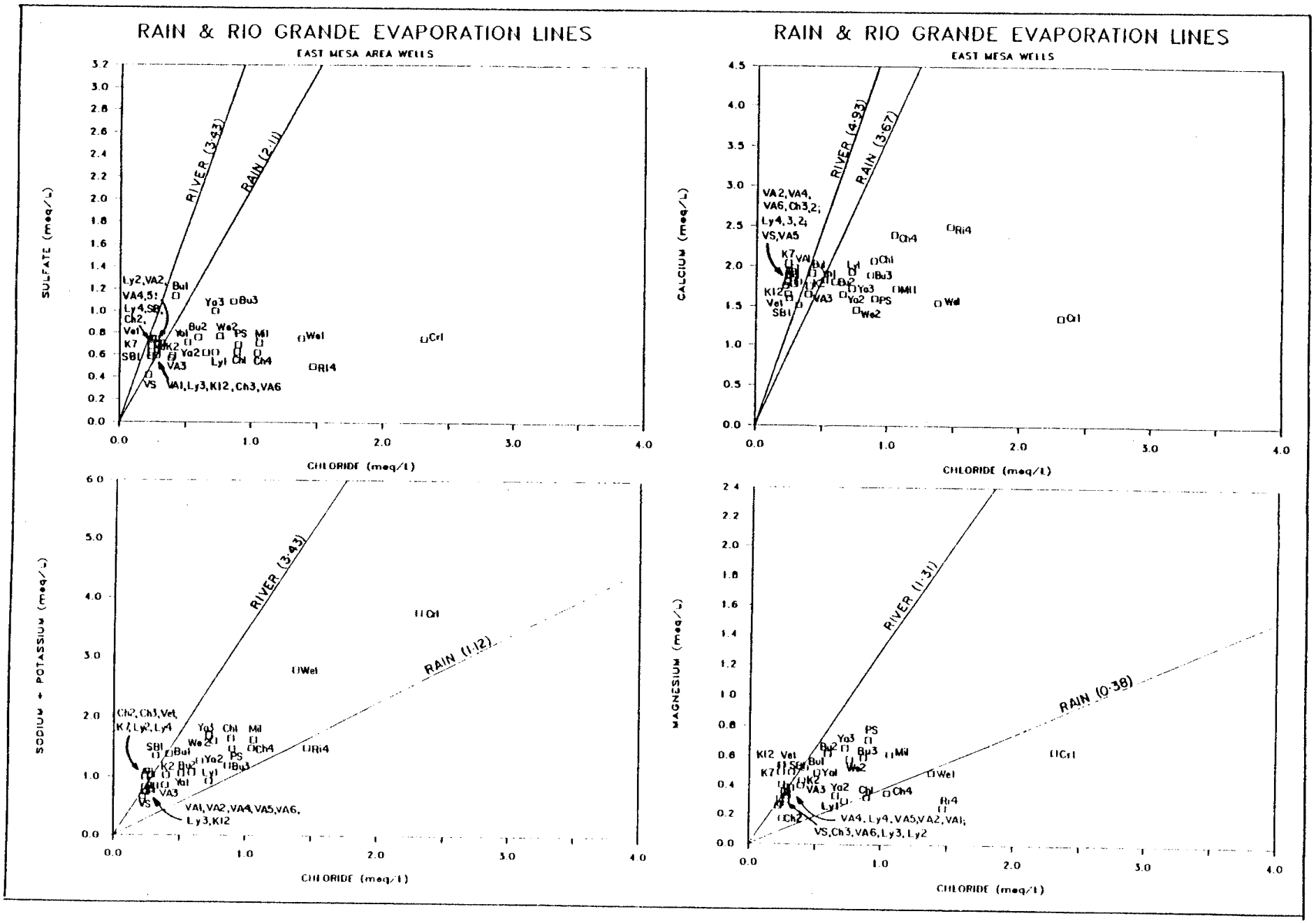

Figure 65: Major ion/chloride ratios in ground water are compared with the same ratio in precipitation and the river, assuming all ions come from either atmospheric input or river recharge.

data scatter on or below the rain-evaporation line. If I assume the only source of sulfate is atmospheric input and the only sink is soil wetting/drying cycles, then most of the data seems to fit the rain-evaporation line within ± ½ meq. A few wells in the far northern and southern EMA area produce water depleted in sulfate. The sulfate difference map for rain (figure 56) shows most wells have sulfate concentrations comparable to atmospheric input with the exception of a few wells in both the northern and southern areas. These sulfate depleted wells are near the EMA boundaries and are probably receiving a component of ground water altered by either the MFZ wetting/drying cycles or flood-plain evapotranspiration. In most EMA wells, absolute concentrations of sulfate are fairly consistent (figure 42), ranging from 20 to 55 mg/L but most ground water contains about 33 ± 7 mg/L sulfate.

Calcium/chloride ratios for both precipitation and the Rio Grande are close (figure 65b) to the ratios for most ground-water samples in the EMA. In an arid climate, a ground waters evolutionary history determines if calcium is either enriched or depleted. Consequently, either evaporation-line could be valid. Figure 57 shows calcium is depleted in the north and south areas and slightly enriched or near atmospheric input in the remaining ground water samples.

Sodium* (figure 65c) either follows (± ½ meq) or is enriched with respect to the rain-evaporation line. Figure 58 shows the distribution of sodium* differences for

atmospheric input. Absolute amounts of sodium* (figure 43) range from 12 to 42 mg/L with the average about 25 ± 7 mg/L.

Figure 65d shows the magnesium content of ground water in the EMA. There is no confirmed sink for magnesium. Some magnesium may exchange for sodium along with calcium but evidently the amount of magnesium removed by ion exchange is masked by additions from dissolution of biotite. Magnesium evaporation-line analyses is in agreement with sulfate in that mountain-front recharge is probably the primary source of water to these wells.

A central north-south band of low TDS ground water (figure 47) lies between areas higher in TDS inflowing from the three recharge sources (Tijeras Canyon, mountain front, and the Rio Grande). Northern EMA ground water is also lower in dissolved silica (figure 46) than surrounding areas.

Chloride is generally low, ranging from 8 to 14 mg/L throughout most of the area but with individual wells as high as 70 mg/L (figure 41). Ground water chloride concentrations are not monotonic but change from low to high to low to high along a presumed ancestral flow path.

Bicarbonate concentrations (mg/L) are lower in the EMA than areas to the east or west (Figure 45). North to south the concentrations increase from about 120 to 130 mg/L respectively.

Figures 66 and 67 are trilinear plots of ground water north and south of Interstate highway I-40 in the EMA.

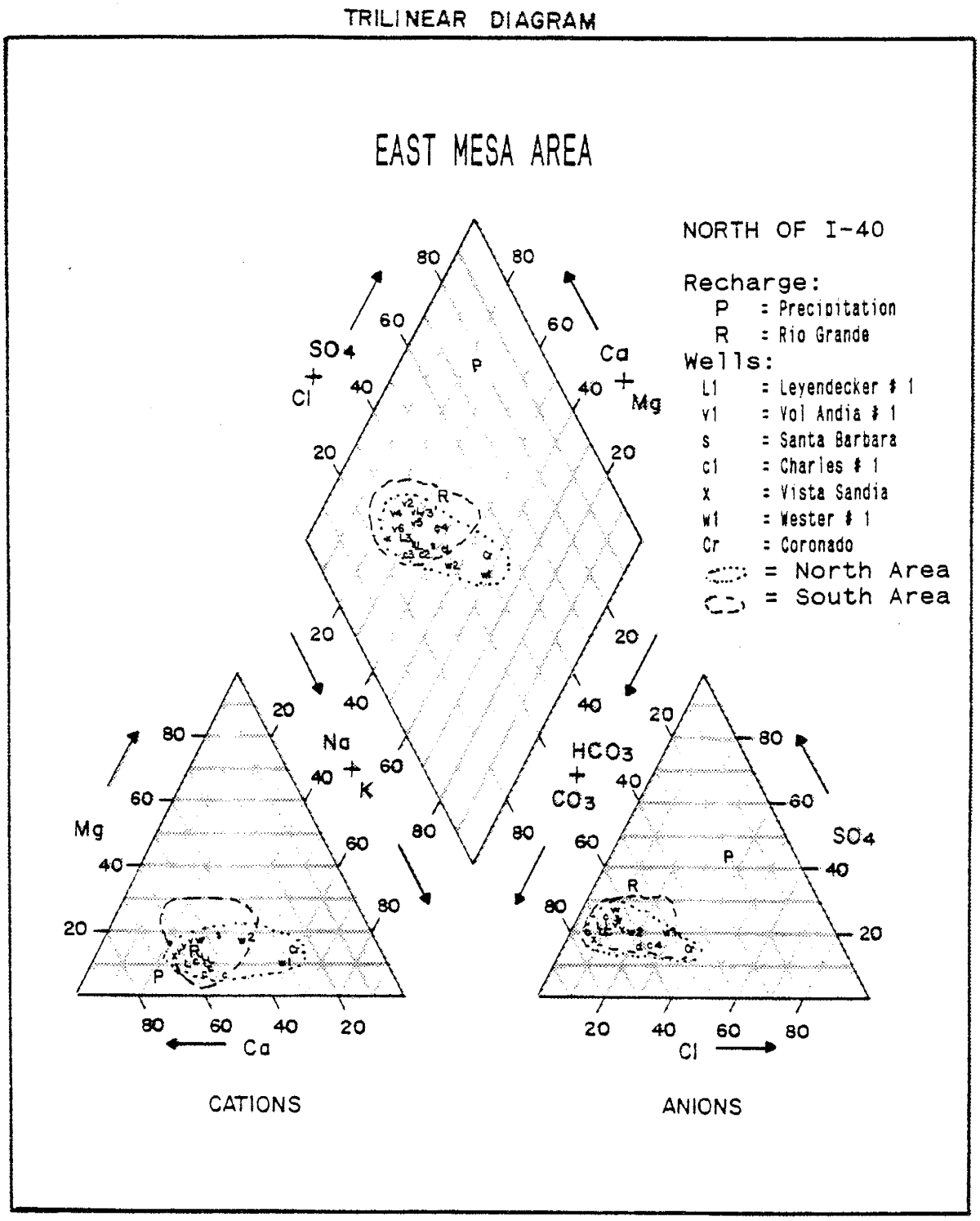

Figure 66: Ground water chemistry north of I-40 is more enriched in sodium but lower in magnesium. Some wells are higher in chloride.

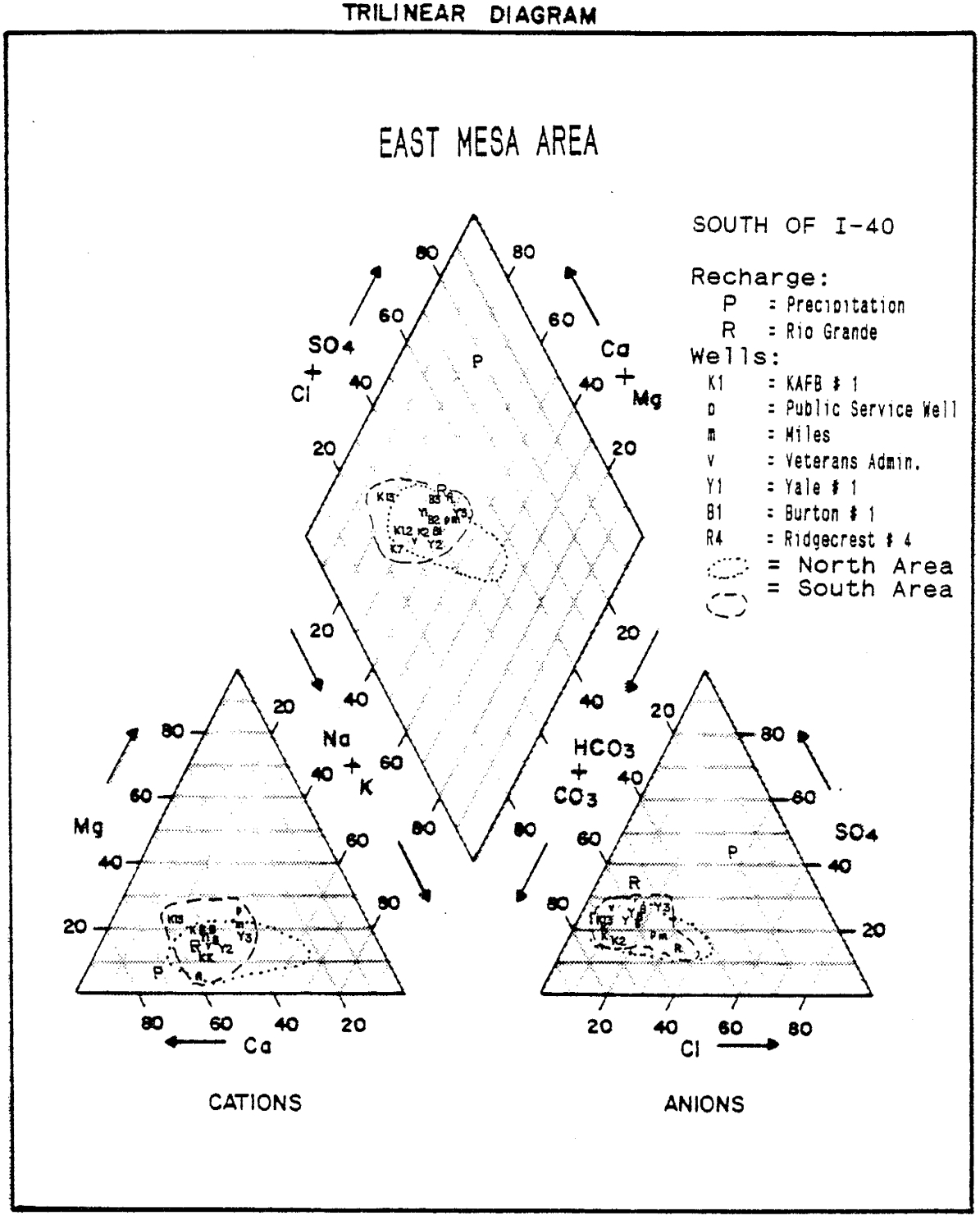

Figure 67: Ground waters in the southern area are enriched in sulfate while the northern area is enriched in chloride. Most ground waters are very similar in composition.

Recharge sources, the average Rio Grande (R) and precipitation (P), reacting percentages are included for comparing geochemical shifts.

In the cation field, ground water in both north and south areas are high in calcium. Ground water near the northern Na-HCO3 boundary (figure 28) shifts toward the sodium predominant field (We1, We2, & Cr1). In the northern EMA, the data cluster between the precipitation and the river reacting percentages (figure 66) while the southern EMA ground waters geochemically clusters near the river (figure 67).

Both north an south areas area similar in the anion field, both areas cluster on the high bicarbonate end. Southern wells nearest the southern high sodium area are increasing in chloride while wells nearest the western boundary are increasing in relative amounts of sulfate.

In the diamond field, geochemical trends associated with different recharge histories can be seen. The northern reacting percentages show more scatter while the southern well data cluster near the average river data. The low-TDS ground-water source or river and mountain-front recharge boundary cannot be determined from the trilinear plot.

Cation sums used to determine ion exchange (figure 30) are relatively constant. Apparently, ion exchange could be a possible process affecting calcium and sodium* concentrations from north to south through the EMA where changes in cation sums are small. Sodium* (figure 43)

appears to increase slightly and calcium (figure 44) decrease slightly from north to south but the changes are not systematic therefore ion exchange can not be verified unequivocally.

Potassium concentrations are low and cluster about both the precipitation and Rio Grande evaporation lines (figure 68a). The evaporation lines are too close at low concentrations to distinguish between them. Based on the magnesium data, with no sinks, (figure 65d) I will assume the rain line also represents the potassium data. Wells in the high chloride zones plot below the evaporation line indicating either ion exchange or formation of illite keep potassium concentrations relatively constant.

Figure 61 shows ground water flow along a present-day flow line from the Rio Grande toward the water-table depression (E). Ground water near the river is in equilibrium with Ca-smectite and plots on the line. Ground water at the end of the flow path, in the water-table depression, is in equilibrium with kaolinite. This suggests wells in the water-table depression may not be receiving river recharge yet or river recharge is a small component of water from several sources which are mixed in the borehole.

Stable isotopes in EMA ground water cluster in two groups about the meteoric water line (MWL) shown in figure 68b. The group lowest on the MWL are from the northern low TDS area while the group plotting higher on the MWL are the

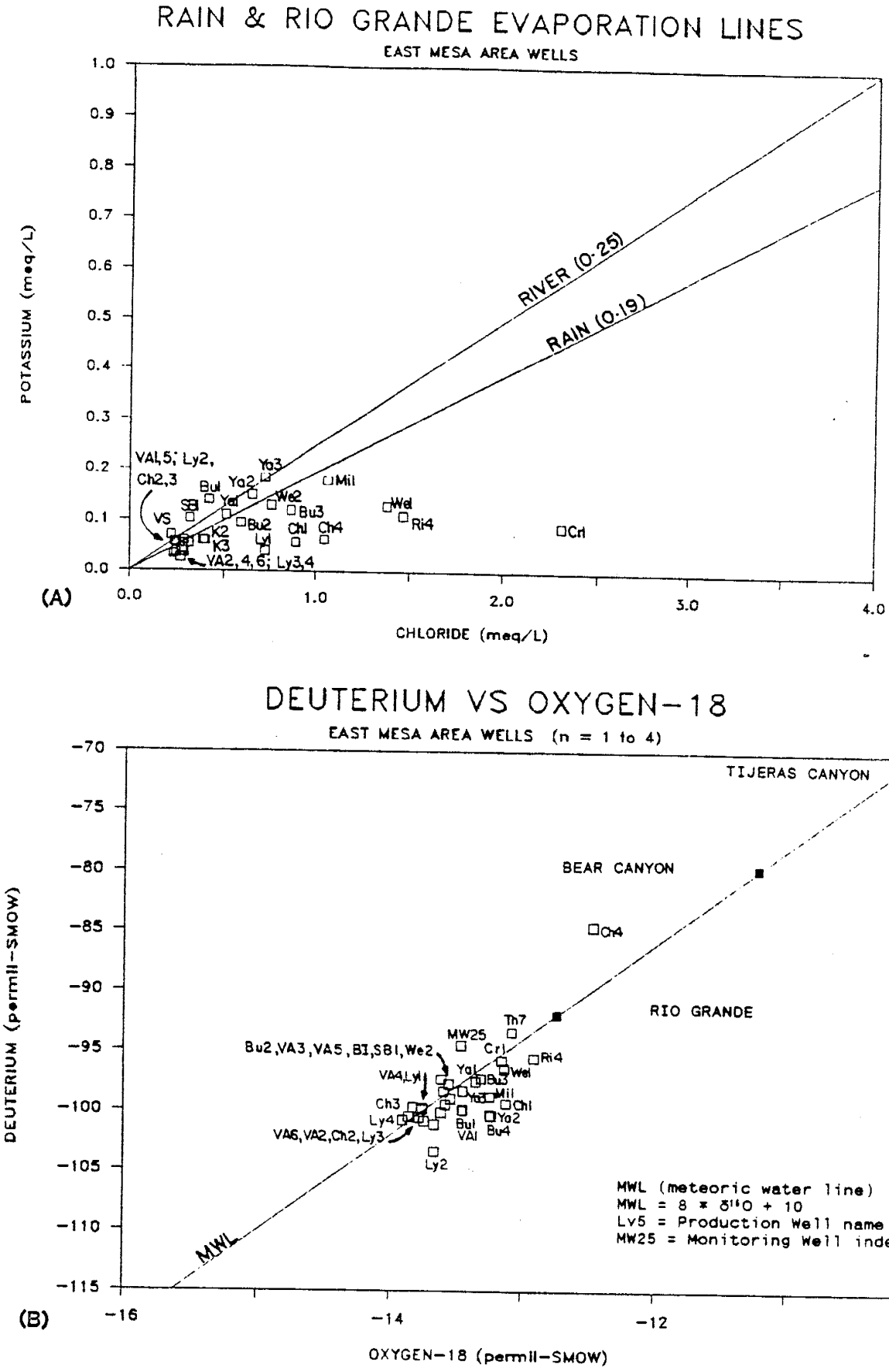

Figure 68: Potassium concentrations may be controlled by illite formation (A); deep and shallow well ground water isotopes are lighter than the average Rio Grande isotopes (B).

remaining wells in the EMA. All ground water in the EMA is lighter than the average isotopic concentration for the Rio Grande. Lighter isotopic content suggest a colder recharge source than the Rio Grande.

Figure 50 shows the average deuterium distribution in the EMA. In the northern area, light deuterium isopleths seem to follow high permeability boundaries but in the southern area the isopleths are skewed to the left presumably by isotopically heavier inflow from Tijeras Canyon. Oxygen-18 (figure 51) distribution is similar but isopleths form a broader area because of the change in scale and contour interval.

Tritium (figure 53) is found in various wells through out the area. Based on the calculated seepage velocities, tritium should have decayed before it reached the EMA from either the river or mountain-front recharge areas. Tritium may be introduced into the deep EMA wells by periodic storm waters infiltrating arroyos beds which traverse the East Mesa. Wells producing tritiated ground water are adjacent to arroyos or in densely foliated parks. Presumably, these periodic inputs of young, tritium enriched water reach the well through the gravel pack and are mixed in various proportions with older, deeper basin ground water. Tritium above 6 TU is a transient constituent in EMA wells.

In summary, water flowing into the EMA is either old (late Pleistocene) ground water or from a colder recharge area other than mountain-front or river recharge. If this ground water were late Pleistocene, I would expect it

to be thermally equilibrated with the local geothermal gradient - these waters are cooler than expected. If ground water originated from a colder recharge source, such as high elevation (Sandia Mountain) snowmelt, the low TDS, light isotopes, and cool water temperatures agree with expected inflow characteristics. The highly transmissive zone (figure 17) intercepting high-elevation inflow could be the mechanism for fast transport. Past and present water-table contours (figures 12 and 21) indicate the flow system moves from the northern mountains into the high permeability zone.

River Recharge Area

The river recharge area (RRA) is defined as the flood plain or inner-valley in this study. Water flowing through the Rio Grandes stream bed, MRGCD channels, and irrigation return flow are the principal sources of recharge to the shallow Quaternary alluvium. Ground water in the Rio Grande flood plain is contained in two water bearing units, the shallow Quaternary sediments and hydraulically connected deep basin-fill sediments. Most shallow domestic wells penetrate the younger more organic-rich Quaternary deposits. Water from this shallow water bearing unit is high in TDS, frequently contaminated by nitrates or electrochemically reduced due to the high density of septic tanks. Numerous areas are contaminated by organic solvents, and petroleum products from leaking storage

tanks, spills and dumping ponds.

Municipal water supply wells open to this shallow ground water have all been abandoned. Currently, municipal wells are cased from the surface, through the shallow unit, and opened to the lower basin-fill sediments which contain high quality water. The City abandoned a deep municipal well after shallow ground-water pollution infiltrated the deep basin aquifer through the well.

Ground water flows away from the river in the RRA. Near the river, water levels have remained essentially unchanged through the years but the direction of flow has shifted, on the east side of the river, from the southwest (figure 18a and 21) to southeast. Water-table gradients steepen with distance from the river. West of the river, water-table gradients not influence by large capacity wells have changed very little over the years.

Hydraulic conductivities are generally low to medium, ranging from 0.8 to 7.4 m/d (19 - 89 gpd/ft^2). Sediments in the RRA are fine-grained alluvial plain, playa, and distal fan deposits (figure 17).

Most wells near the river have low pumping temperatures for their depths which suggests a large component of pumped ground water is from river recharge with a short residence time. In the southern part of the RRA, wells have higher than expected water temperatures for their depth (figure 25). Figure 27 shows some of these ground-water temperatures are just below the minimum

expected temperature while others are near the mean annual temperature for the Rio Grande. In Atrisco well # 1 (At1), water temperatures fluctuate from 24 to 31°C from day to day. Other wells may also have widely variable ground water temperatures but I have data for only a few wells.

Total dissolved solids (TDS) increase from north to south (figure 47). The Duranes (Du) well field is higher in TDS than other wells probably because these wells intercept a proportionally greater amount of water from the shallow water bearing unit. The water table is 3 to 10 m (9-33 ft) from the surface in these wells.

Dissolved silica averages about 19 mg/L in the river and about 41 to 73 mg/L in the RRA ground water (figure 46). Silica increases westward in the deep basin aquifer from 21 to 73 mg/L which suggests the RRA ground water samples below 60 mg/L silica are probably mixing with river recharge which is lower in dissolved silica. Silica may also be removed by kaolinite or Ca-smectite formation.

Average chloride concentrations in the RRA wells are below the average chloride in the Rio Grande (figure 41). This may imply the volume of river recharge is probably not uniform through out the year. Spring run-off, lower in TDS, may contribute more to recharge because of the high river stage or the increase in seasonal pumpage may induce greater recharge during spring run-off. Wells further from the river are higher in chloride due to ion concentration by evapotranspiration by phreatophytes tapping the shallow RRA aquifer.

The hydrogeochemical facies changes from Ca-HCO3 in the north to Na-HCO3 in the south (figure 28). This cation shift is probably due to the changing lithology. Hydraulic conductivities are generally higher at Ca-HCO3 producing wells.

The average bicarbonate content (figure 45) seems to increase then decrease from north to south. This may be largely a reflection of the mixing ratio of river recharge, shallow ground water, and deep basin-fill ground water.

For the river-evaporation line analysis (figure 69), I am assuming most of the water produced by RRA wells comes from river recharge either directly from the river stream bed or the MRGCD channel system (figure 15). Differences of ± 1 standard deviation are essentially equal to the evaporation line.

Figure 69a shows the average sulfate concentration in ground water in the RRA. Most wells follow the river-evaporation line at low sulfate concentrations. As sulfate increases, the sulfate/chloride ratio increases. This could either mean trace amounts of pyrite are in the sediments forming the aquifer matrix or the average river sulfate content used to calculate the evaporation line is to low. All ground water except two San Jose wells are within one standard deviation of the evaporation line. San Jose wells 2 and 4 (SJ2 & SJ4) plot below the line which suggest sulfate has been removed. These wells are undersaturated with respect to gypsum yet are depleted in

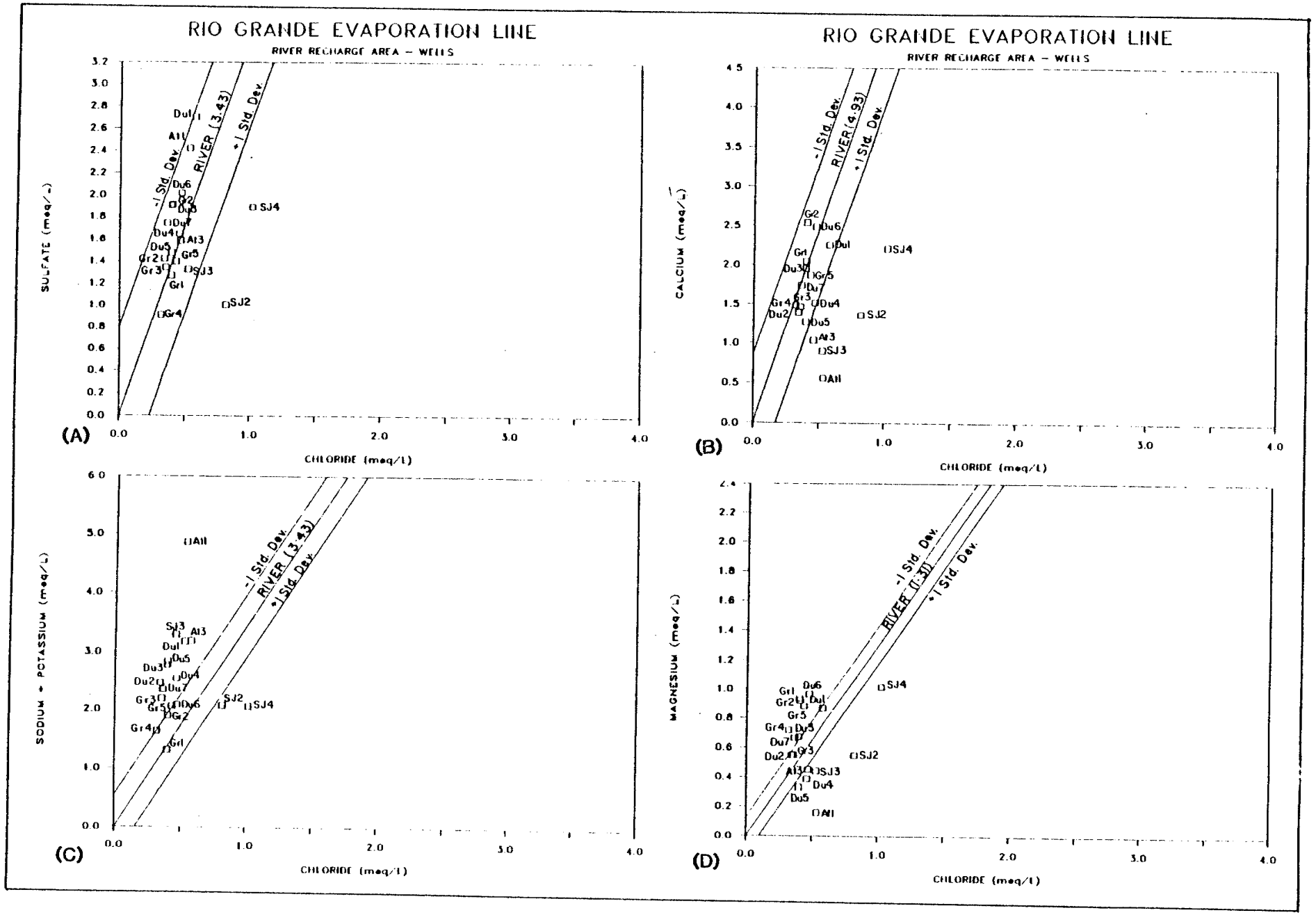

Figure 69: Major ion/chloride ratios in ground water are compared with the same ratio in the Rio Grande, assuming all ions come from river recharge.

both sulfate and calcium (PCWATEQ). SJ4 is contaminated with industrial solvents which may have increased the chloride thereby invalidating this analytical technique.

Figure 70 shows the areal distribution of the average sulfate difference with respect to the river-evaporation line. The San Jose wells (SJ) are depleted in sulfate while wells in the middle of the RRA are either near the evaporation line or are enriched in sulfate. Figure 42 shows two sulfate highs with a maximum sulfate content of 130 mg/L in the Duranes (Du) and Atrisco (At) well fields which can be explained by concentration due to evapotranspiration processes. The San Jose wells (SJ) also show a sulfate high (figure 41) but are depleted in sulfate with respect to the evaporation line. Water levels in the San Jose field are between 12 to 31 m (39-101 ft) below the surface, with nearby irrigation ditches that may contribute evaporation sulfate-depleted recharge to ground water.

Calcium concentrations are all within one standard deviation of the river evaporation line with the exception of five wells (figure 69b). The calcium-river difference map (figure 71) shows most of the wells are depleted in calcium. Three San Jose wells (SJ 2,3,4) and two Atrisco wells (At1,3) are notably depleted in calcium with respect to the evaporation line. All these wells are undersaturated with respect to gypsum but near equilibrium with respect to calcite (PCWATEQ). These wells are depleted in about twice the calcium as sulfate which implies the calcium may also be lost by calcite precipitation. Calcite is metastable

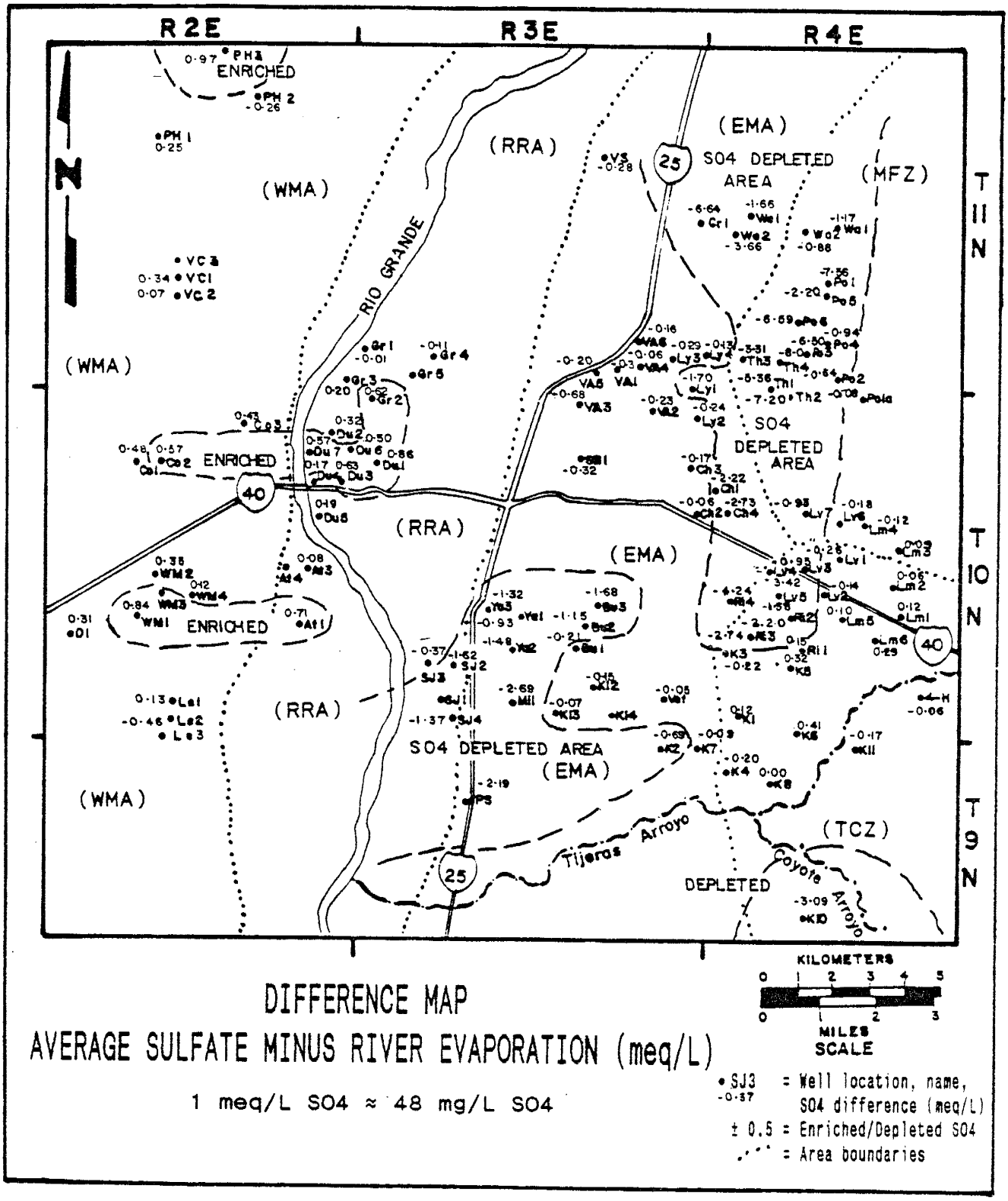

Figure 70: Areas enriched in sulfate are about one standard deviation (0.80 meq) from the river sulfate/chloride ratio This map areally represents graph A in figures 65, 69, and 75.

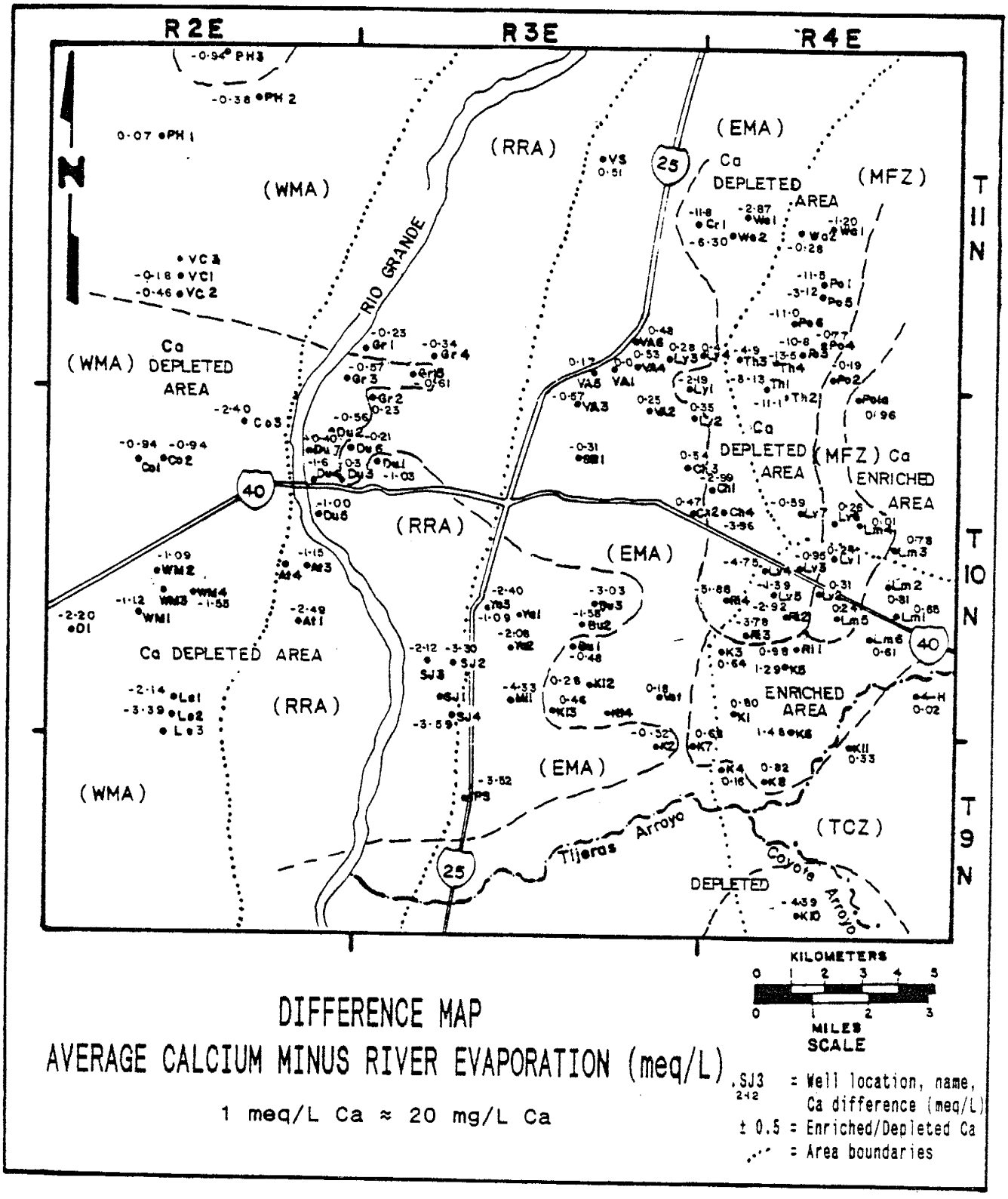

Figure 71: Areas enriched in calcium are about one standard deviation (0.86 meq) from the river calcium/chloride ratio This map areally represents graph B in figures 65, 69, and 75.

with respect to RRA ground water and may vary between under and oversaturated. Silica content is the highest in the area, therefore Ca-smectite formation is probably not a major factor in removing calcium.

Most sodium* concentrations are above one standard deviation of the evaporation line (figure 69c). Ground waters enriched in sodium* are probably due to dissolution of plagioclase. San Jose wells 2 and 4 (SJ2,SJ4) sodium* content falls below the river line but above the rain line (not shown) which may indicate these wells are producing water with a greater mixture of mountain front recharge, because of their proximity to the high permeability zone, than the other wells in the flood plain. A monotonic, east-to west, silica trend also supports this idea.

Figure 72 shows the distribution of sodium* minus the river-evaporation line. The difference map indicates the San Jose wells are depleted in sodium* with respect to the river and enriched with respect to rain (figure 58). Sodium sinks other than ion exchange are not documented in the literature for this area.

Magnesium scatters about the river-evaporation line (figure 69d). Magnesium is probably most commonly added to the ground water system by dissolving biotite which is found in trace amounts in the river sediments. No magnesium-rich secondary minerals have been verified in the literature. Therefore, the most probable explanations for the depletion of magnesium are ion exchange of magnesium in calcium-smectite, excess chloride decreasing the

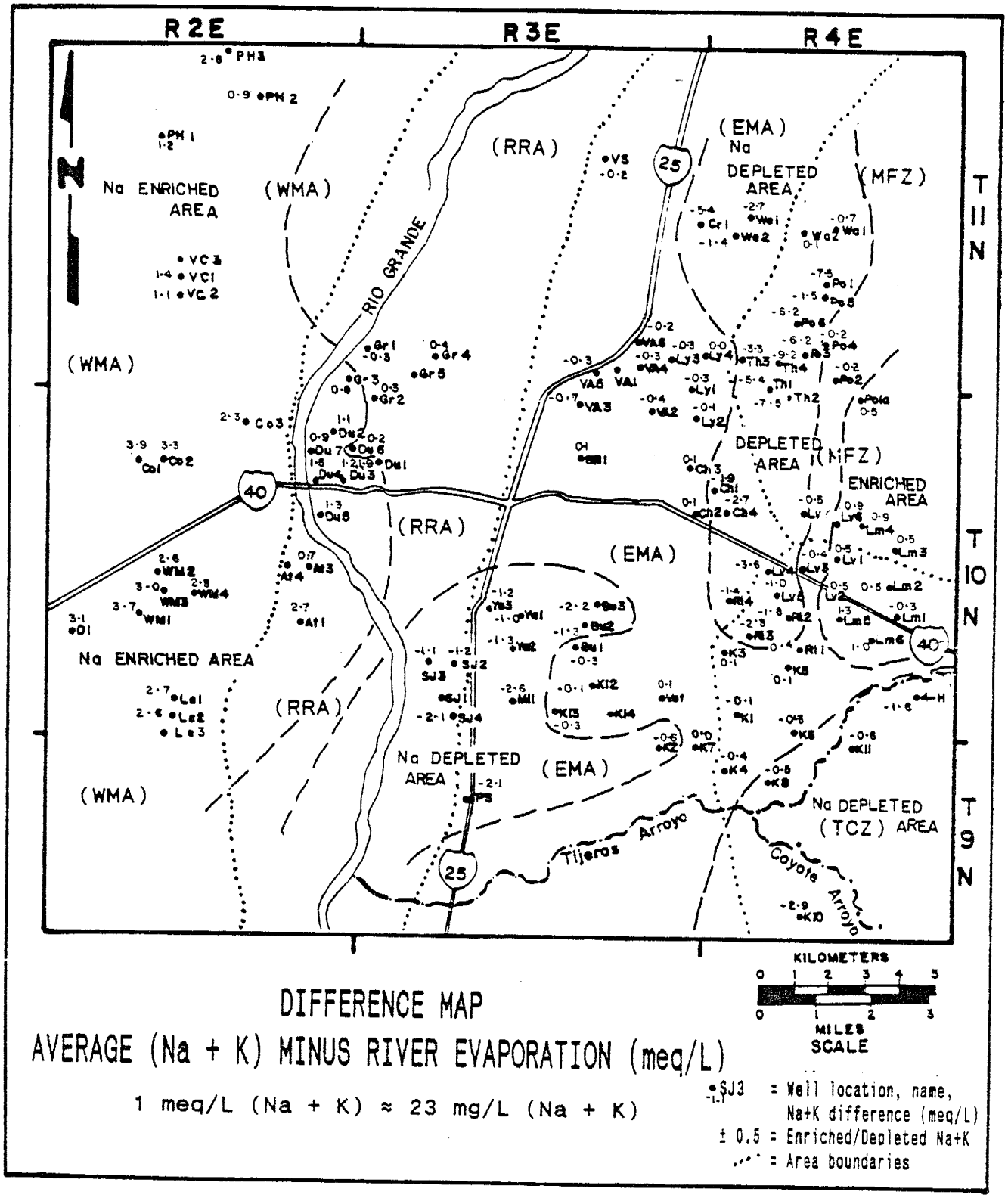

Figure 72: Areas enriched in sodium* are about one standard deviation (0.54 meq) from the river sodium*/chloride ratio This map areally represents graph C in figures 65, 69, and 75.

magnesium/chloride ratio, or errors in the analyses. All magnesium concentrations are above or nearly on the rain-evaporation line (not shown) which may indicate a greater percentage of mountain front recharge is intercepted by these deep wells.

The trilinear plot of the RRA ground water reacting percentages shows a lot of scatter (figure 73). In the cation field the San Jose wells (SJ 2,3,4) show a decrease in calcium and an increase in sodium from east to west. The Griegos wells (Gr) decrease in calcium from north to south. Duranes wells (Du) vary greatly but show a decreasing calcium trend. Atrisco wells 3 and 4 (At 3,4) cluster near each other while Atrisco well 1 (At1) is very depleted in calcium. Ground water analyses plots to the right of the average river composition which implies river recharge looses its calcium as it flows into the aquifer.

In the anion field most ground water clusters closely about the average river composition. The two San Jose wells (SJ 2,4) both plot to the right which gives support to the idea these two wells are receiving a greater component of deep mountain-front recharge (figure 67). These two wells are also warmer than expected for their depth which could indicate deep ground water flow.

In the diamond field, Atrisco well 1 (At1) plots to the extreme right of all the other wells indicating the water it intercepts is quite different in composition than the other wells in the RRA. A trend of increasing sodium* and decreasing calcium with relatively constant sulfate and

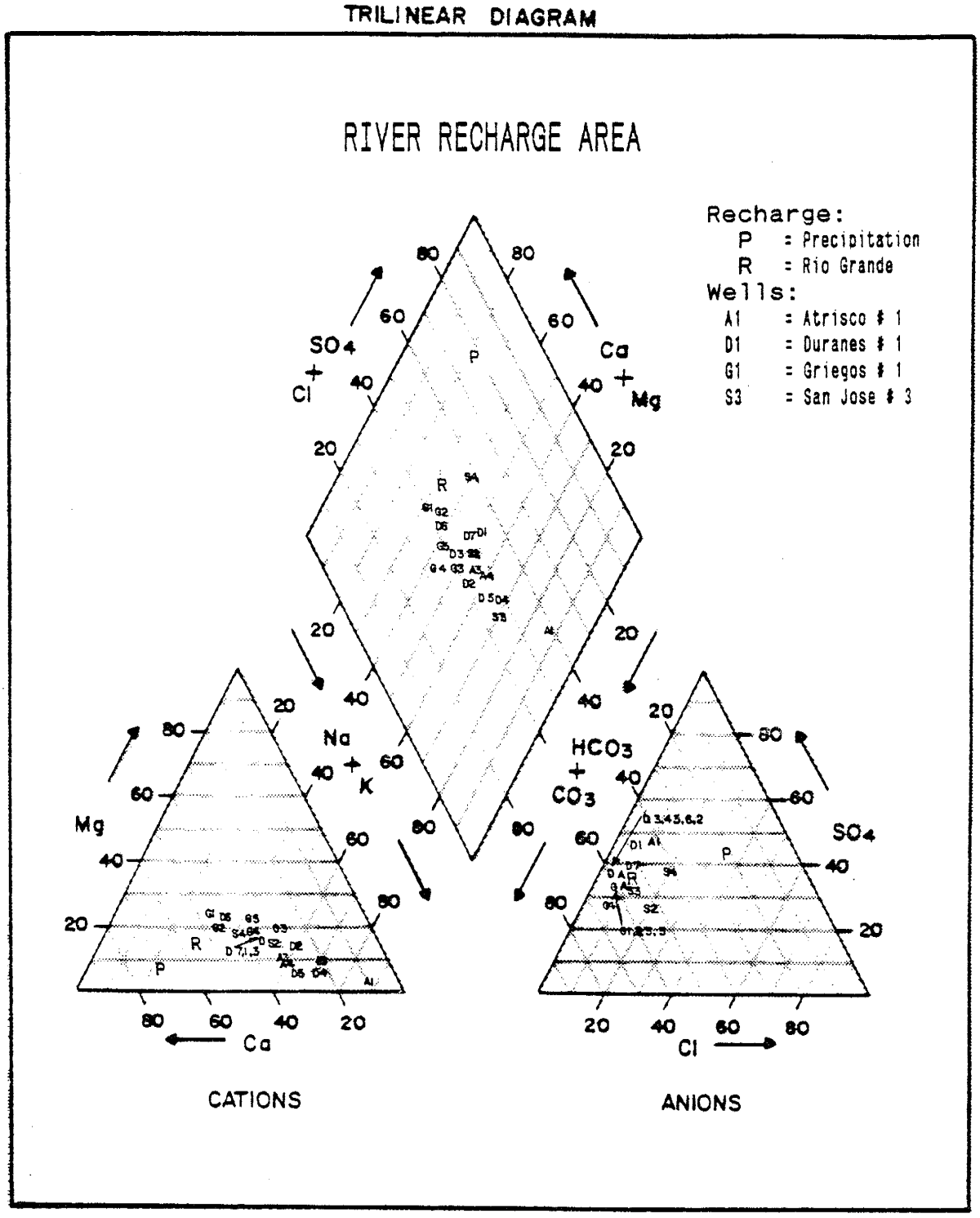

Figure 73: Cation reaction percentages show increasing sodium* and decreasing calcium which suggests cation exchange may control ground water quality in this area.

chloride as ground water flows away from the river can also be seen. This pattern usually implies ion exchange.

The cation sum map (figure 30) shows that more than ion exchange is occurring. The total cation concentrations are increasing from north to south and from east to west along most flow path projections.

Potassium in the RRA is enriched with respect to both the river and precipitation evaporation lines while most other ground water is either in agreement with evaporation or is depleted (figure 74a). Increased potassium may come from agricultural fertilizers reaching the shallow water table.

Deuterium and oxygen-18 isotopes in RRA ground water plot along the meteoric water line (MWL) between the minimum and maximum range for the Rio Grande (figure 74b). The San Jose wells plot low on the MWL in the East Mesa Area (EMA) between -14 to -13 $\delta^{18}O$. This also indicates these wells are receiving mountain front recharge. Water from shallow monitoring wells (MW1 & MW33) plot high on the MWL indicating these wells are intercepting seasonably warm river recharge.

Deuterium (figure 49) is relatively constant, in the range -96.4 ± -2.8 δD with the exception of the two shallow monitoring wells which tend to be isotopically heavier. An area of isotopically lighter oxygen-18 (figure 51) occurs in the Duranes and Griegos well fields (Du & Gr) which may indicate these wells are intercepting seasonally light recharge from cold spring snowmelt.

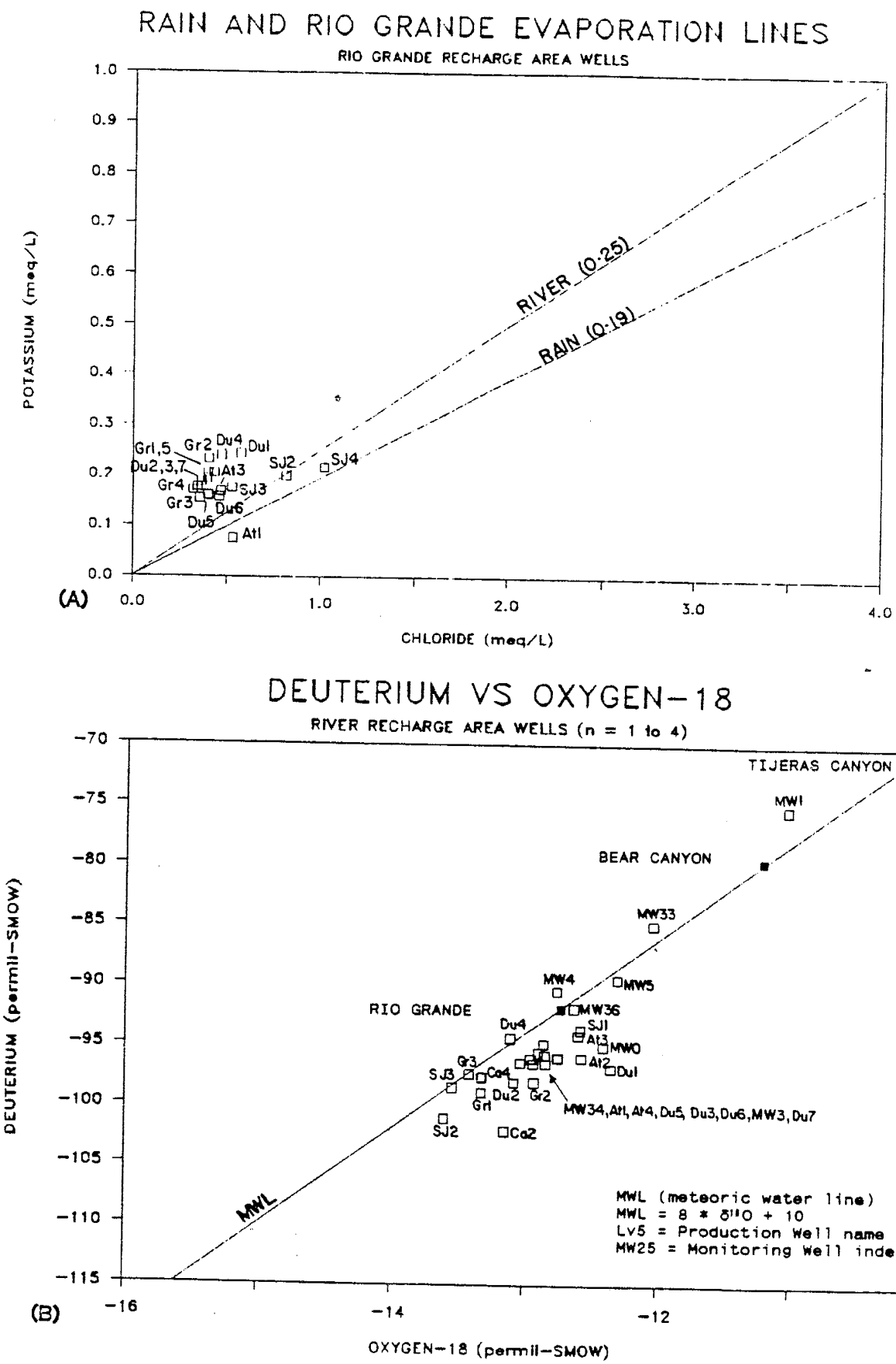

Figure 74: Increasing potassium may indicate agricultural chemical contamination (A); deep and shallow wells show a great deal of scatter with most lighter than average river isotopic content (B).

Most ground water in the RRA contains tritium but wells do not produce water with repeatable tritium counts. There does not seem to be a correlation between heavy deuterium and oxygen-18 content and tritium. Explanations for both the non-repeatability and non-correlation are the mixing proportions of deeper, presumably older, ground water with shallow, younger ground water and the extreme variability of tritium content in natural waters.

In summary, ground water flows from the Rio Grande, MRGCD channels, and irrigated areas into the shallow inner-valley fill. This highly mineralized water is induced into the deep basin fill wells by municipal pumpage where it is mixed in various proportions with mountain-front recharge and possibly deeper inflow from the northern basin. Evapotranspiration increases both sulfate and chloride in some areas. Irrigated areas increase the potassium and total dissolved solids in the shallow water-table areas. Wetting/drying cycles are less important a control on ground water geochemistry in the RRA but seem to play a role in the San Jose well field. Calcium and sulfate depletion in this area is not clear. These wells seem to receive a large portion of their water from Tijeras Canyon inflow with the geochemical characteristics of wetting/drying cycles.

West Mesa Area

Ground water flowing through the West Mesa area (WMA) is presumed to come from northern basin inflow, deep mountain-front recharge and the Rio Grande. Municipal wells are not as densely placed in the WMA as they are east of the river (figure 20). Municipal pumpage has distorted the original flow fields but without shallow well control the extent of the water-table depression can only be estimated (figure 21).

The aquifer matrix is composed of fine grained sediments laid down as alluvial plain, playa, and distal fan deposits. Hydraulic conductivities are low (figure 17), ranging from 0.8 to 3.5 m/d (20-86 gpd/ft^2).

Wells in the southern WMA produce ground water warmer than expected for their depths (figures 25 & 27). The geothermal gradient, assumed to be uniform, may be warmer in this area or deep ground-water flow may be convected upward along faults or buried low-permeability basin structures (figures 7,9, & 10).

Figure 75 shows the river-evaporation line with the average WMA ground water ion/chloride ratios for four major ions. The Rio Grande is assumed to be the primary source of recharge to the wells. Deep-basin inflow from the north and mountain front recharge from the east may flow below the wells screened intervals (figure 24).

All WMA ground-water sulfate concentrations plot within one standard deviation of the sulfate river

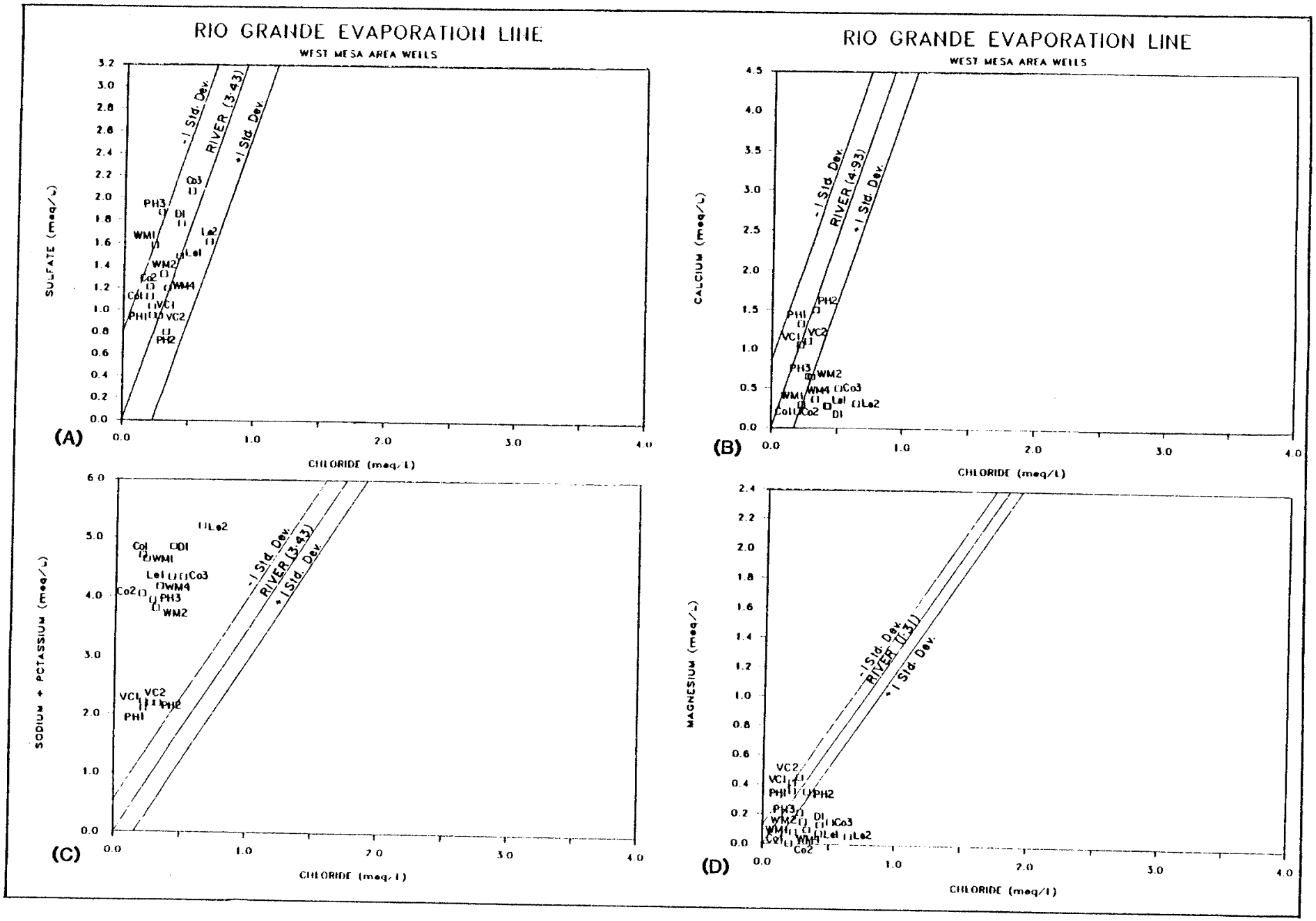

Figure 75: Major ion/chloride ratios in ground water are compared with the same ratio in the Rio Grande, assuming all ions come from river recharge.

evaporation line (figure 75a). Most wells plot above the line indicating either natural variability, a slight increase due to trace amounts of pyrite in the sediments, or concentration by evapotranspiration prior to flowing out of the shallow flood-plain deposits. Two wells produce ground water slightly lower in sulfate but within one standard deviation. With the exception of PH3, wells in the north are lower in sulfate than wells in the central and southern areas.

The sulfate-river difference map (figure 70) shows the distribution of wells with more than 0.5 meq of sulfate above the evaporation line. With the exception of WM1 and PH3, all these wells are within one standard deviation of the river-sulfate input. Differences in concentration suggest most wells receive most of their water from river recharge.

About half the calcium concentrations plot within one standard deviation of the river-evaporation line and the other half below the line (figure 75b). Calcium shows the opposite trend as sulfate in that the northern wells are higher in calcium than the southern wells. The northern wells plot along the line while the more southerly wells plot below the line. The calcium-river difference map (figure 71) and the average calcium distribution map (figure 44) show calcium decreasing from north to south.

Sodium* concentrations increases from east to west and from north to south in the WMA (figure 43). The sodium*-river difference map (figure 70) reflects this increasing

sodium* trend. Sodium* evaporation-line analyses (figure 75c) show the same bimodal distribution of the northern and southern wells observed on the magnesium and calcium evaporation lines.

Magnesium distribution tends to be bimodal (figure 75d). Wells in the northern WMA plot on the evaporation line while wells in the southern area plot below the line. Secondary magnesium minerals have not been reported in this area. Magnesium may substitute for calcium in ion exchange.

All ground-water types west of the Rio Grande are Na-HCO3 (figure 28). The concentration of total dissolved solids (TDS) generally increases along a north to southwest trend although the increasing trend is not uniform (figure 47). Relatively higher TDS seems to correlate with lower hydraulic conductivities which suggest the high TDS is due to lithology. Chloride concentrations in the WMA are lower than the average Rio Grande chloride content (figure 41) in most ground water samples. Bicarbonate increases from east to west. The average silica content decreases from east to west with very depleted area in the West Mesa (WM), Don (D1), and College (Co) well fields (figure 46).

Decreasing silica and calcium suggest the formation of Ca-smectite may be an important process in this area (figures 46 and 44). Figure 61 shows the WMA ground waters (W) are at or near equilibrium with Ca-smectite.

Figure 76 is a trilinear plot of the WMA ground water data showing the relationship between the samples and the average Rio Grande reacting percentages.

In the cation field, the northern and southern wells show a bimodal distribution, with the exception of Paradise Hills well #3 (PH3). Ground water increases in sodium and decreases in calcium and magnesium as it flows from the north to south. West Mesa Well 2 (WM2) appears to be a mixture of river recharge and older formation water.

The anion field shows the increasing bicarbonate trend seen on figure 45. Anions cluster indicating they are more stable than cations in this ground water system. Chloride reacting percentages are relatively constant. The percentage of sulfate decreases with increasing percentage of bicarbonate.

In the diamond field, ground waters bimodal composition and the mixing line for WM2 are apparent. Atrisco well # 1 (At1) (figure 71), in the RRA, plots in the same areas as the central and southern wells in the WMA. Even though At1 is near the river boundary, it is geochemically similar to ground water further to the west.

Ion exchange of sodium* for calcium is suggested by the sodium and calcium distribution maps, and trilinear plot (figures 43,44,76). The sum of the cations map (figure 30) shows increasing total cations from both north to south and east to west. In other words, the cation sum map indicates ion exchange is not the only process occurring.

Potassium shows the same trend characteristic as

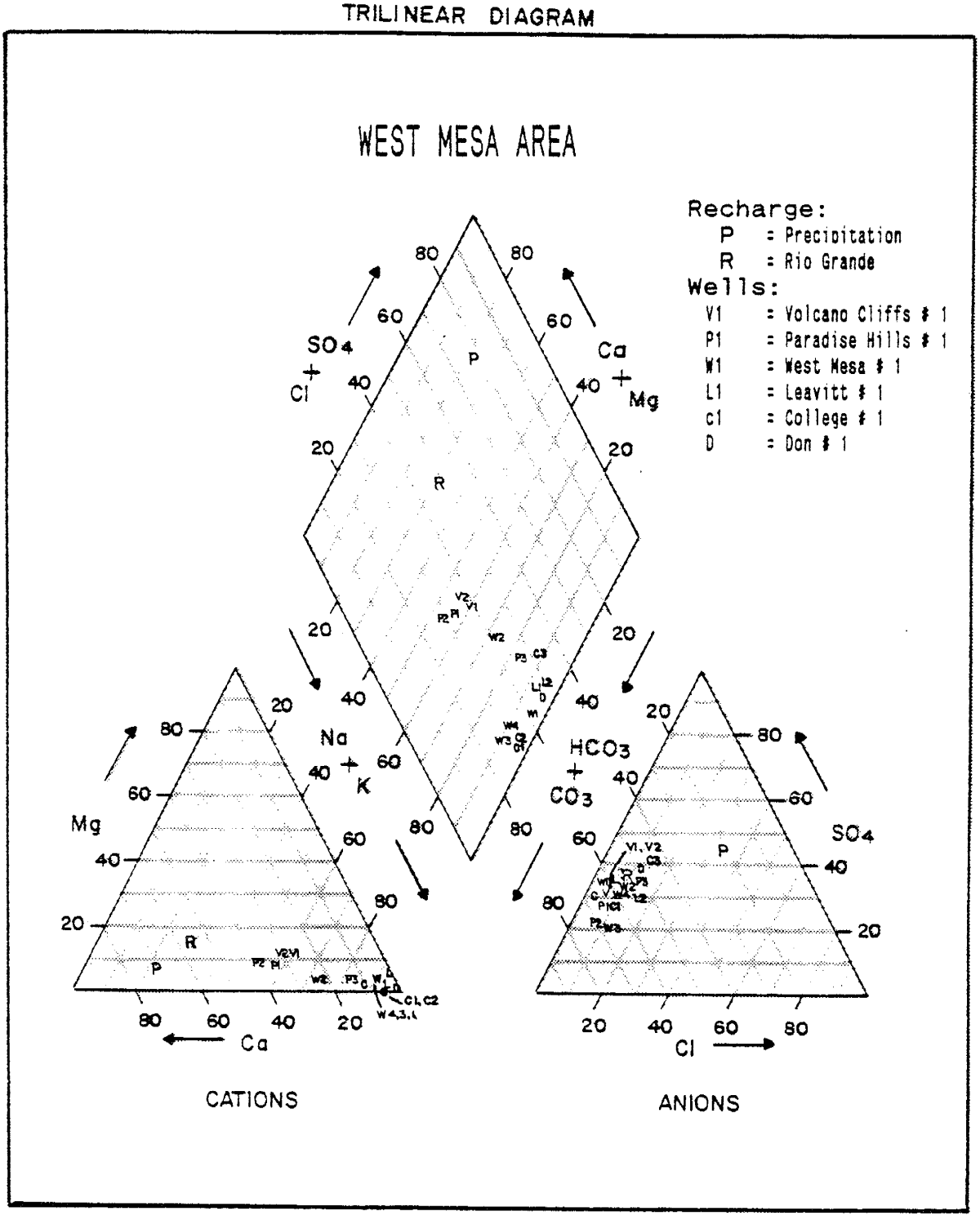

Figure 76: Cation reacting percentages show increasing sodium* and decreasing calcium while anions generally increase with respect to the river.

magnesium and calcium with the northern wells clustering above the evaporation line, the central wells near the line, and the southern wells below the line (figure 77a). Northern potassium enrichment indicates a component of river recharge is reaching these wells. Those wells depleted in potassium may reflect the high cation exchange capacity of surrounding sediments.

Deuterium and oxygen-18 in WMA ground water scatter up and down the meteoric water line (MWL) with three samples lighter than the minimum river deuterium (D1, WM1, and DE, figure 77b). These wells may be receiving the majority of their ground water from deep older basin flow. DE is Double Eagle II well located off the west map boundary about parallel with the Volcano Cliffs wells (VC). The three wells that plot above the average river deuterium content (Co1, WM2, and WM3) also contain tritium (figure 54) which suggest some component of the water they produce is probably recent river recharge.

In summary, the river influences ground-water chemistry outside the flood plain. Wells located in the northern WMA appear to receive a large component of river recharge. Calcium, magnesium, potassium, and sulfate are in excellent agreement with the river-evaporation line. The Volcano Cliff wells (VC1,2,3) plot on the MWL close to the average isotopic content of the river. West Mesa wells (WM2,3,4) and College wells (Co1,2,3) receive ground water from both the river and deep older ground water sources. The far southerly Leavitte wells (Le1,2,3) are isotopically

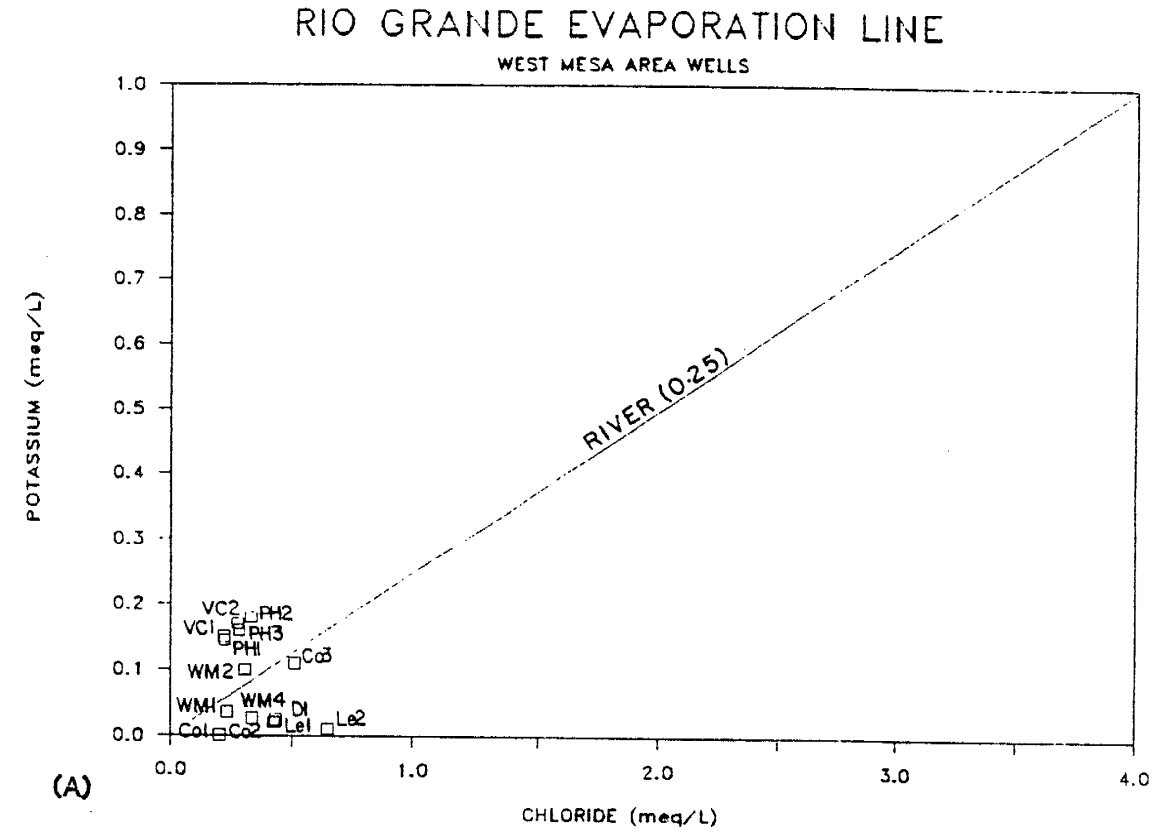

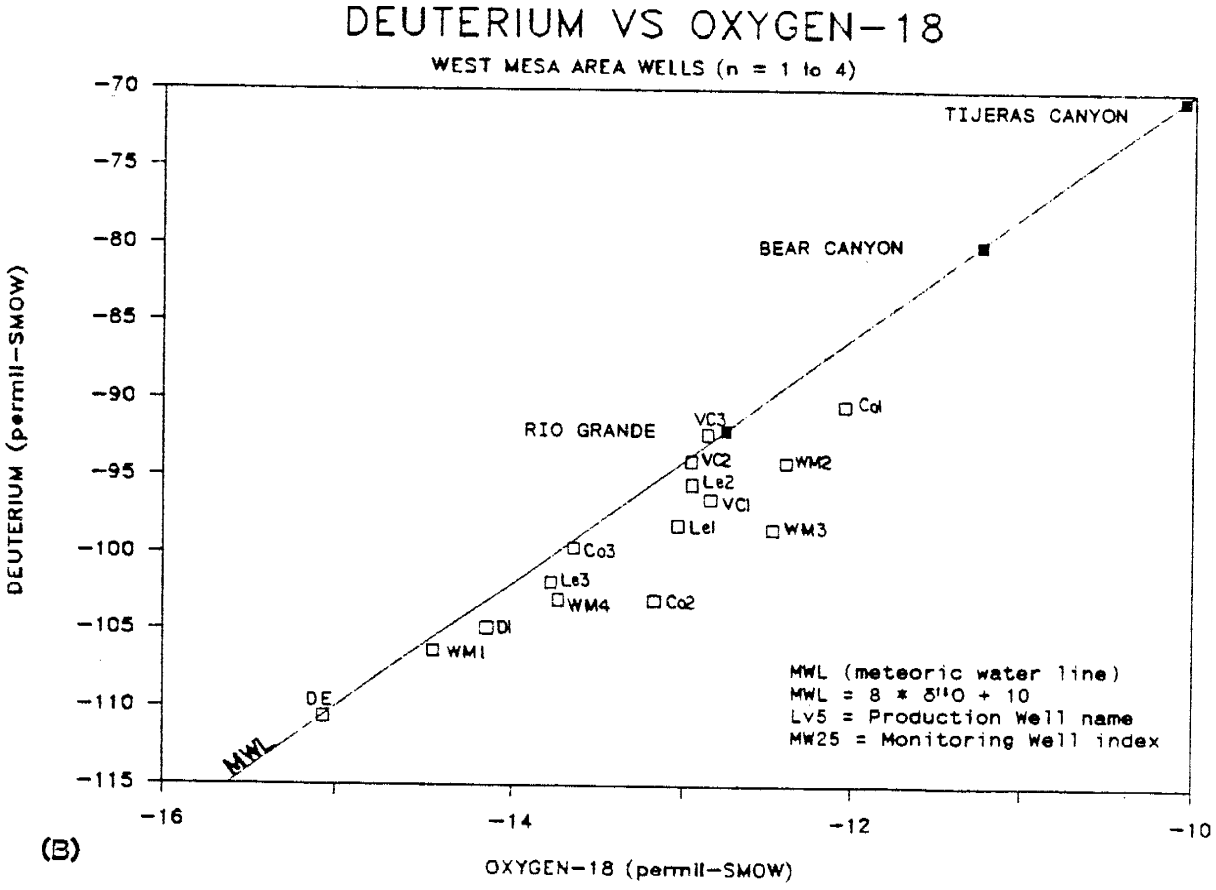

Figure 77: Potassium is higher in the northern wells than in the southern wells (A); isotopes generally scatter below the average river isotope content, the lightest ground water is farthest from the river.

similar to the river but are geochemically altered by intervening sediments.

Lithology exerts more influence on the WMA ground water chemistry than other areas. Calcium-smectite formation removes both calcium and silica from the ground water and ion exchange removes both calcium and potassium and inputs sodium. Wells with relatively high TDS have lower hydraulic conductivities than other nearby wells.

Wells with widely fluctuating water temperatures like At1 and intermittent tritium may be receiving river recharge during well recovery. This water is removed during the early stages of pumpage. Water becomes progressively warmer as pumpage continues indicating the well is producing from deeper, older formations with time.

Warmer than expected temperatures may be a reflection of a higher geothermal gradient in the WMA due to latent heat from past igneous activity.

Contradictions in Data Interpretations

Five major contradiction arose while analyzing the data: (1) estimated ground water velocities; (2) ground water temperatures; (3) geochemical disruptions midway along a flow path; (4) discontinuities in areas affected by wetting/drying cycles; (5) and tritium in ground water several kilometers from recharge boundaries. In this discussion I will briefly summarize the contradicting interpretations and determine which process I believe offers a viable explanation.

The first discrepancy in data interpretation is the order of magnitude difference between estimated ground water velocities using Darcy's Law and variations in deuterium. Seepage velocity calculations along a 1936 flow path (figure 23) suggest that ground water takes 25 years to flow from the mountain-recharge area to the deep basin margin under a high hydraulic gradient. Ground water takes an additional 1200 years to flow from the eastern deep-basin margin to the Rio Grande under a low hydraulic

gradient. By contrast, the areal distribution of deuterium and oxygen-18 indicate that, from east to west, ground water becomes isotopically lighter. Usually, isotopically light ground water ($\delta D < -100$ ‰) is thought to be associated with late Pleistocene recharge (Yapp, 1985). Seepage velocities suggested by decreasing deuterium imply ground water flow takes about 24,000 years to move from the mountain recharge area to the river.

To determine which ground water velocity represents the areas flow system, I compared all available hydrodynamic and geochemical data.

Low pumping-water-temperatures in wells several kilometers from either recharge area suggest cool ground-water recharge is moving at too rapid a rate to equilibrate with the geothermal gradient. These low-temperature wells are located in the EMA and TCZ high permeability areas (figures 17, 25). High-permeability-zone ground-water flow is much more rapid than the average seepage velocity along the 1936 flow path. Low ground-water temperatures also suggest recharge water is initially very cold in order to maintain its cool temperature over several kilometers. If recharge is cold, than deuterium and oxygen-18 would be light since storm temperature affects fractionation.

Isotopically-light ground water located between isotopically heavier ground water may be explained by studying Titus's (1961) water-level map (figure 78). Snowmelt or rain draining from high in the Sandia Mountains

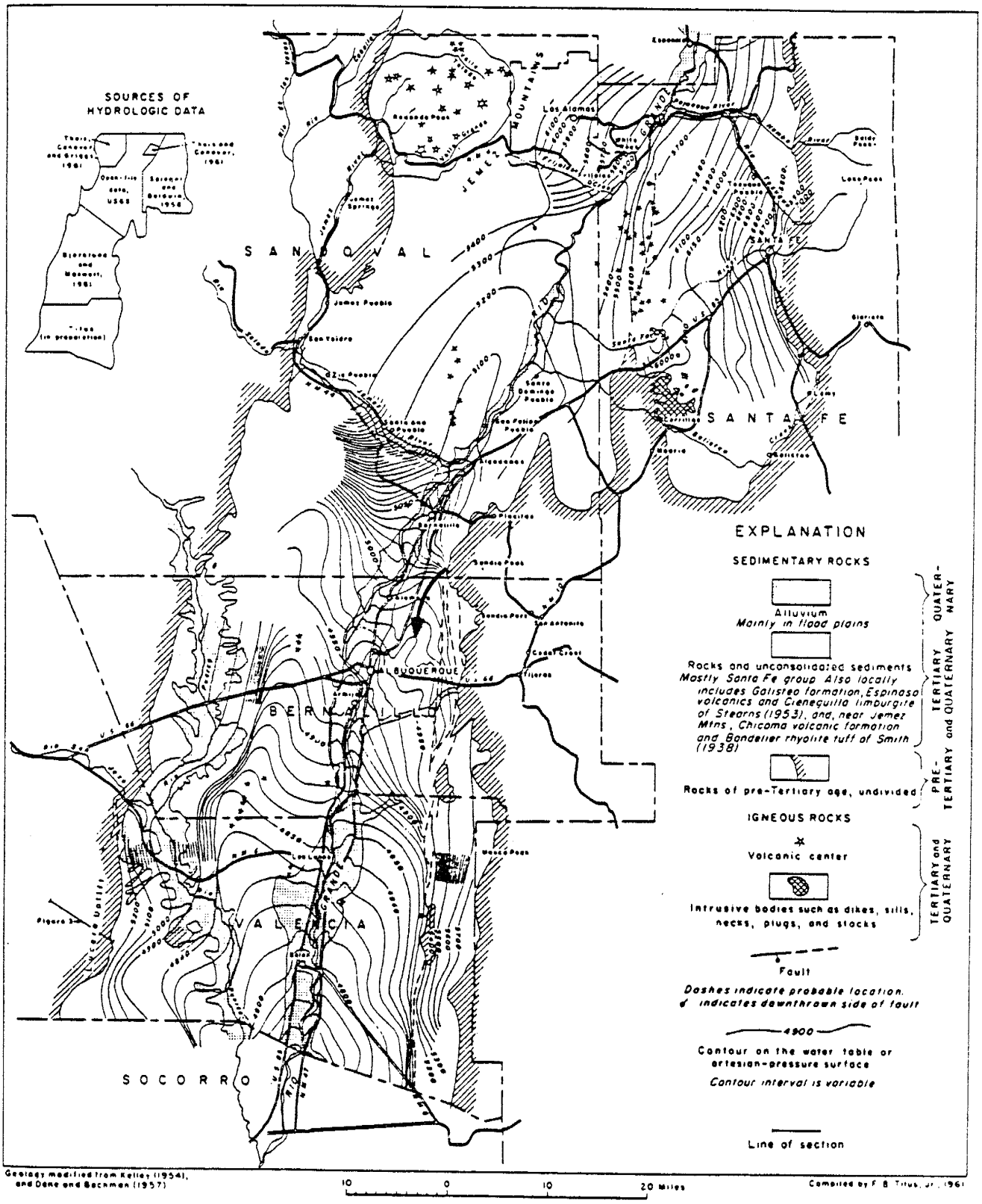

Figure 78: The arrow indicates the high-elevation recharge pathway into the high permeability zone (modified from Titus, 1961).

would follow the ground-water gradient into the high permeability zone (arrow on figure 78). The lightest deuterium from this zone (-108 δD) is equivalent to the average deuterium in precipitation falling at 2950 m (9700 ft). Isotopically-light ground water in the East Mesa area probably reflects the "elevation effect" on isotope fractionation and not late Pleistocene recharge.

Figure 78 also indicates river recharge could follow the hydraulic gradient into the high permeability zone. Geochemically these dilute ground waters could either come from the river (spring snowmelt) or precipitation. The primary difference between these two recharge sources is the lightness of deuterium and oxygen-18. Ground water isotopes represents the yearly average recharge isotopic content. High elevation precipitation would, consistently, be isotopically lighter than the Rio Grande.

Ground-water quality in the isotopically-light area is low in TDS, sulfate/chloride and calcium/chloride ratios increase above the rain-evaporation (figure 65a and 65b) which implies ground water is not subjected to soil wetting and drying cycles or evapotranspiration processes. Ground water from this area is geochemically very similar.

Cool temperature, isotopically light, the hydraulic gradients orientation, rain-evaporation line analyses, and anomalously low TDS all suggest these waters are probably inflow from higher elevations of the Sandia Mountains. Therefore, seepage velocity calculations based on Darcy's Law are probably a reasonable estimate.

The second discrepancy is with unexpected pumping temperatures in wells near recharge boundaries which have higher than expected temperatures and wells several kilometers from recharge boundaries which have cooler than expected temperatures.

The assumption ground water is in thermal equilibrium is dealt with, in part, in the preceding discussion. Wells near recharge boundaries may produce low temperature ground water which indicates a short residence time. Wells producing water warmer than expected for the local geothermal gradient may be intercepting ground water upwelling from depth or the assumption of a uniform geothermal gradient in the study area is not correct. In either case, ground water has not reached thermal equilibrium with the formation.

Deep high-capacity wells in the study area exhibit a variety of different characteristics which indicate general assumptions about temperature and producing intervals is not valid for all wells. Water temperature may increase with increased pumping time. Spinner survey logs I have studied for three different wells indicate the dominant producing interval starts near the top of the screen and moves down the well with time, thereby intercepting water with increased temperatures. Other temperature surveys show that some non-pumping wells increase in temperature with depth as long as the downward vertical flow component is small, as indicated by spinner surveys. One out-of-service

well, near the river, has an iron bacterial problem and had accumulated a thick organic ooze which generated heat 7C° degrees above the ambient ground water temperature. Temperature surveys showed the temperature changed from 24 to 31°C from top to bottom. Spinner surveys indicated a downward vertical flow for the top of the well and an upward vertical flow from the bottom of the well. In contrast, an out-of-service well near the mountain front intercepts the steep hydraulic gradient which imposes a large component of downward flow thereby creating a constant temperature from top to bottom.

Warm ground-water temperature interpretations may be misleading. Warm water may not necessarily be from a deep seated source - the temperature increase may be generated by bacteria, latent heat from an igneous intrusion in the area, or a non-uniform geothermal gradient. Cool temperatures may reflect a shallow production interval or rapid ground water movement through a high permeability zone such as the northern EMA wells and wells intercepting Tijeras Canyon inflow.

The third data interpretation inconsistency deals with disruptions in water quality trends which change from relatively high TDS to low TDS then back to a high TDS ground water along a flow path.

The north-south oriented high-permeability zone captures southwestward flowing dilute, low TDS, high-elevation inflow and relatively higher TDS recharge from Bear, Embudo, and Tijeras Canyons. Southeastward flowing

river recharge is also intercepted by this high permeability zone. Northern dilute ground water recharge moves rapidly through this zone, intercepting and mixing with higher TDS waters flowing across lithologic boundaries. Rapid flow and the aquifers heterogeneities mix ground waters with different characteristics thereby disrupting the expected geochemical trend.

Bjorklund and Maxwell (1961) mapped the water-level trough created by this high permeability zone. I suspect the ground-water gradient created by this trough has existed since the climate changed to arid, over ten thousand years ago. This implies the river was probably a losing stream at least during the seasonally dry months.

If the high permeability generated trough has existed for thousands of years then the estimated 1936 water-table map (Kelly, 1979) for the initial steady state case (figure 18a) may not be valid. I now suspect, a "smoothing" of Bjorklund and Maxwell's (1961) water-level map to remove pumpage effects, (figure 76) is closer to the steady state case. My cross section, based on a 1936 flow path (figure 22), is nearly coincident with a flow path through the 1961 high permeability trough after I adjusted equipotential lines for transmissivity.

Spatial variations in ground-water chemical characteristics seem to be "smeared" through the high permeability area toward the pumping-induced ground-water depression (figure 30). This shifting in ground water

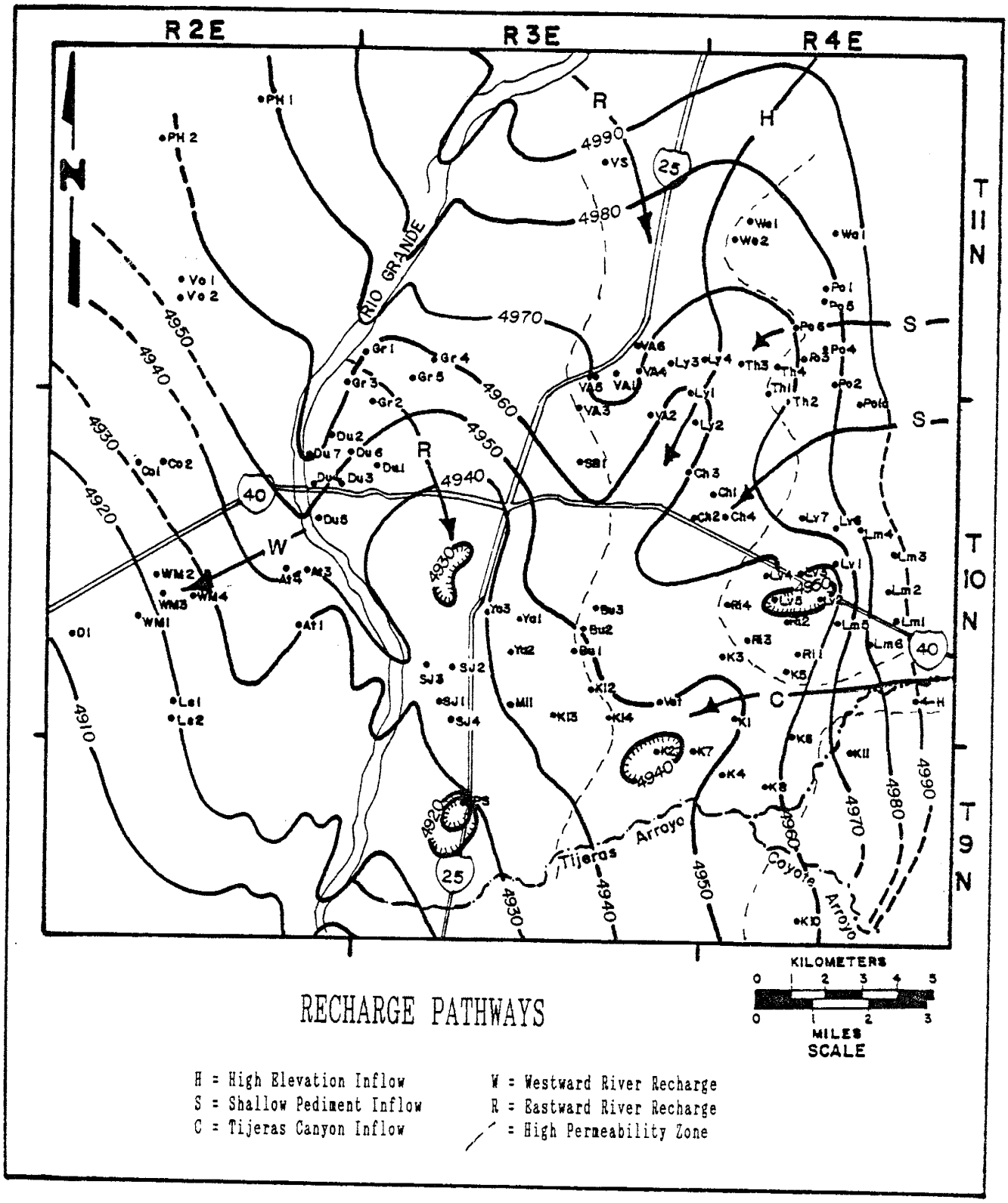

Figure 79: Flow paths showing high-permeability zone capture of four recharge areas and a flow path west of the Rio Grande (Modified from Bjorklund and Maxwell, 1961).

chemistry suggests ground water velocities may be greater than initial estimates.

The high permeability zone exerts a strong influence on past and present water-quality distribution across the East Mesa area.

The forth inconsistency is the areal persistence of ground water carrying the geochemical signature of soil wetting/drying cycles in some areas and not in others. Mountain-front zone (MFZ) ground water carries the high chloride and depleted sulfate and calcium "salt pulse" characteristics of soil wetting/drying cycles while Tijeras Canyon zone (TCZ) ground water generally does not.

I suspect the reason lies in the nature of the recharge areas. The MFZ recharge area is characterized by broad thin alluvial pediment covers which offer a large surface area as a catchment for small-volume storm waters which evaporate in the soil zone. Subsequent, periodic large-volume stormwaters flush these zones creating pulses of high-salt soil-zone altered recharge which discharges to the aquifers low to medium permeability zone (figure 17). Ground water flow is slow and salt-pulse characteristics are maintained over several kilometers.

The Tijeras Canyon zone (TCZ) is characterized by a narrow alluvium covered canyon which offers a smaller catchment for the wetting/drying process. Ground water draining the canyon probably flows through nearly the same pathway, keeping it flushed of accumulating salts. It is only very large-volume storms which produce enough water to

flush the salts accumulated in the alluvial fan at the mouth of the canyon. This salt-pulse discharges to the high permeability corridor where it rapidly disperses through subsurface heterogeneous mixing. Such an event is documented in the Kirtland well field (K) but is not discussed in detail in this study.

Apparently, catchment characteristics determine the importance of soil wetting/drying cycles to recharge water quality while the aquifers permeability determine the areal persistence of a high-salt pulse.

The fifth inconsistency is the occurrence of tritium in deep wells several kilometers from recharge sources (figures 53 & 54). Most of these wells have transient tritium - that is tritium does not always occur above the counting error in all samples. Pumpage induced ground water flow rates are higher than ambient rates but a reasonable rate would still exceed the life of tritiated water traveling several kilometers into the basin. Thus tritium must be coming from a nearby recharge source.

If flood-waters infiltrating arroyo bottoms were reaching the wells then flood-recharge should acquire the geochemical characteristic of soil wetting/ drying cycles, but all tritiated wells are not associated with this salt pulse. Eight tritiated wells near the mountain recharge area (Po3, Po6, Wa1, We1, Lv3, Lv4) produce water with a salt pulse while other tritiated wells near the large salt-pulse area do not (Lv1, Lv2, Lv6, Ch2, Ly2). West Mesa

tritiated wells also show characteristics of both sulfate enrichment (WM2, Co1) and sulfate depletion (Le1) associated with a salt pulse.

If wells located several kilometers from a recharge boundary contain transient tritium but are not associated with a salt pulse, then several processes may be occurring: (1) invalid sample (clerical or counting error); (2) large-volume stormwater event flushes the soil zone redissolving salts and subsequently diluting the salt-enriched recharge which is further diluted by wellbore mixing during pumpage. The probability of clerical error seems remote for the large number of samples with transient tritium. Some of these wells produce ground water near the counting error while others produce water more than twice the counting error. The second postulate of dilution seems like a complex set of events to produce tritium without increasing the TDS above the expected concentrations.

Several observations on individual wells may help explain the occurrence of transient tritium. Yapp (1985) studied deuterium in 5 municipal wells for 16 months (figure 80). During the low water demand months, West Mesa well 3 (WM3) produced water with average river deuterium. During the high production months, deuterium decreased by about -10 δD. This suggests young, shallow, river recharge may provide the largest volume of water during initial pumpage, but with time, pumpage depletes this water first before forcing production from the deeper, older formations. Shallow, tritiated river recharge may provide

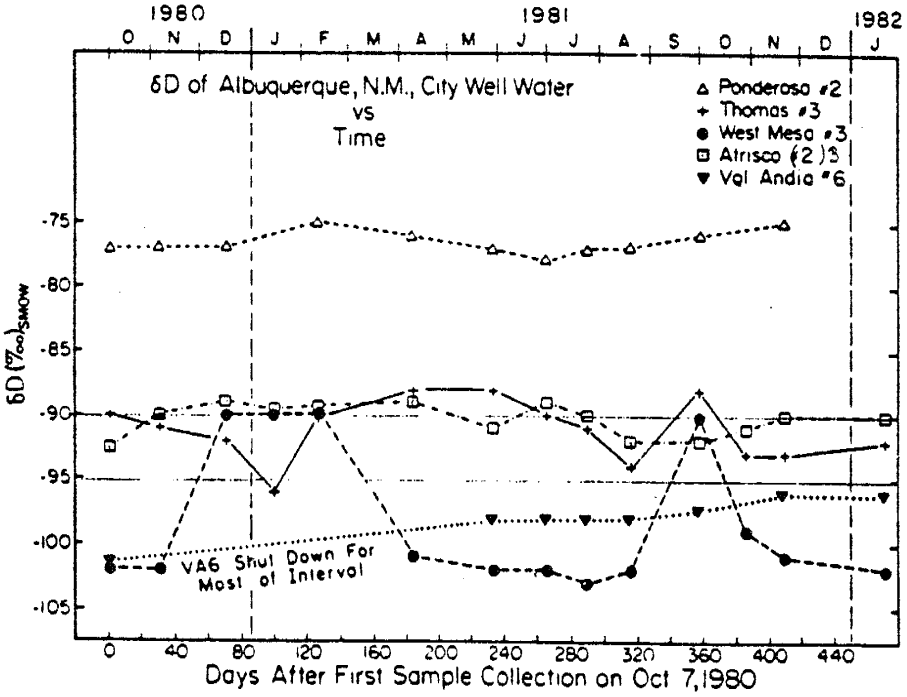

(A) Temporal variations in the δD-values of waters from five wells in the Albuquerque municipal water system. Note the apparent bimodal variation of West Mesa 3 δD-values

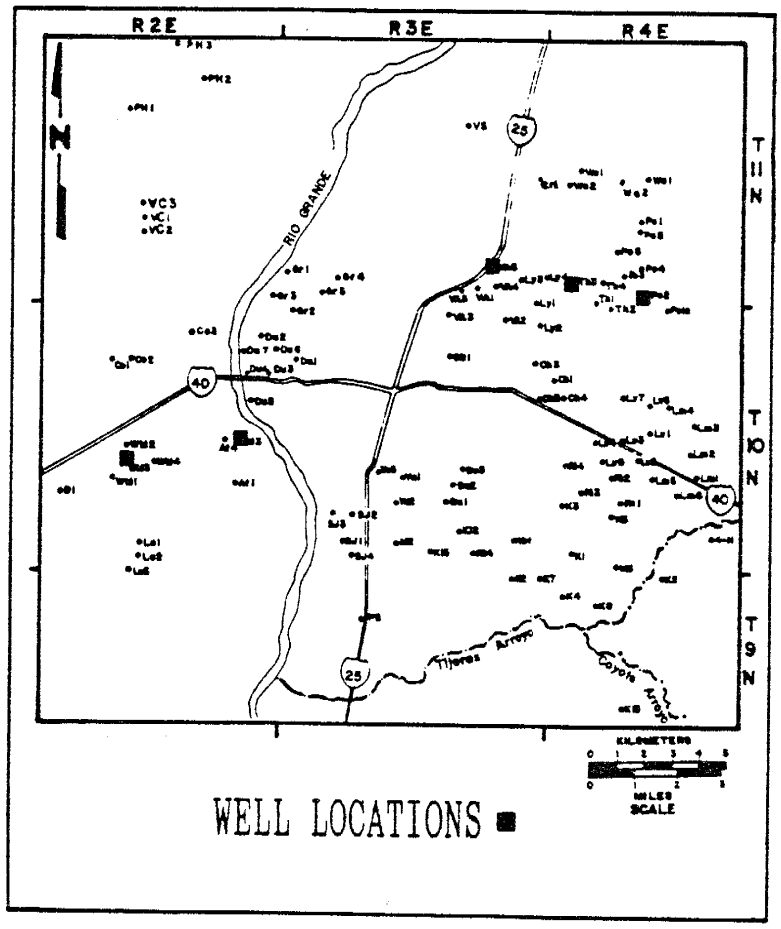

(B)

Figure 80: Temporal variations in deuterium in five City wells (A); well location map (B) (modified from Yapp, 1985).

the most available water during well recovery; downward vertical flow was verified with spinner log surveys of several wells in this area.

Figure 80 shows wells near the river and mountain-front recharge areas have relatively constant deuterium. Near the river recharge area, Atrisco well #3 (At3), formerly Atrisco 2, has a deuterium content ranging between the average Rio Grande value of -92 δD and -89 δD Tritium ranges between 12 and 28 ± 6TU. Deuterium and tritium both indicate At3 probably receives most of its production from river recharge even though the well is cased below the more permeable shallow aquifer unit. In the mountain-front recharge area, deuterium in Ponderosa well 2 (Po2) varies between -77 and -75 δD with the highest tritium count of 7 ± 6TU. Low tritium suggests Po2's mountain-front recharge is older than At3's river recharge. Both wells deuterium content is relatively constant indicating a consistent ground water source.

Wells several kilometers from either recharge boundary show greater variations in deuterium. This may indicate the wells intercept several flow regimes; shallow younger flow and deeper older flow. Deuterium increases while the wells are idle but decreases as the wells are pumped over long time periods. This suggests a wells recovery may come primarily from younger sources and as a well discharges with time, it draws increasingly older water from deeper in the well. Spinner logs and isotope content studies verified this process in several City wells (data from the

City and USGS).

In summary, a deep wells gravel pack may intercept tritiated, younger ground water from shallow, hydraulically connected overlying beds such as in the West Mesa and College well fields. Deep mid-mesa wells gravel packs may also intercept intermittent (arroyo recharge) and/or perched flow which produces transient tritium away from recharge boundaries.

Summary and Conclusions

When I started this study I wanted to understand what caused the geochemical shifts from east to west and, particularly, what caused the high sodium and chloride "islands" in a Ca-HCO3 ground water system. Previous investigators suggested geothermal fluids may have moved along deep seated faults or ground water flowed through buried salt beds to explain the increased total dissolved solids, specifically the high chloride and sodium. What I found after synthesizing all the available data is that shifts in the geochemical trends can all be explained with arid climate pedogenic processes and the hydrodynamic system.

As I studied the high chloride and sodium areas, I found these same ground waters were depleted in sulfate and calcium with respect to atmospheric input. In addition, mass balance calculations showed that silica was low, and calcium and sodium ratios did not agree with common minerals in the area. The significant result of this

investigation is that arid-climate soil wetting/drying cycle altered recharge and calcium smectite formation could account for all of the above observations.

Ground waters geochemical evolution, as it enters the hydrogeologic cycle, depends on its pathway. Water gains its initial chemical and isotopic composition from the atmosphere. As water moves into the soil zone it acquires dissolved solids from soil salts and rock mineral dissolution. Water flowing down below the zone of evaporation gains and loses ions by rock mineral dissolution, clay mineral formation, ion exchange and calcite precipitation and dissolution. Ground water flowing through low permeability sediments become more mineralized through the above processes and equilibrates with the geothermal gradient. Ground water flowing through high permeability sediments show very little chemical alteration and may not be in equilibrium with the geothermal gradient. Ground water flowing across high permeability boundaries and/or induced into pumping well fields is mixed either by subsurface heterogeneities or in the borehole with waters of different geochemical histories. This mixing obliterates clear geochemical boundaries along flow paths and near high-capacity well fields.

Isotopic evidence suggested contradicting flow histories. Ground water light in deuterium and oxygen-18 and low in total dissolved solids occurring mid-way along a

flow path suggested the wells were intercepting Pleistocene age ground water. This was supported by a very neat, east-to-west, and west-to-east monotonic decrease in ground waters isotopic content mid-way between the two recharge boundaries. Late Pleistocene ground water several kilometers from either recharge boundary suggested either a very slow seepage velocity or very old deep basin flow from the north was upwelling in this area. Contrary to the deuterium and oxygen-18 evidence are the seepage velocity calculations and tritium which periodically occurs in these ground waters. When I compared the areal distribution of isotopes, geochemistry, and ground water temperatures with the hydrodynamic system these discrepancies could all be answered by the elevation effect on isotopic fractionation and hydrodynamics.

If you were to trace the geochemical evolution of a recharge event from east-to-west the hydrodynamic cycle may take four slightly different routes before reaching the deep, basin-fill aquifer; high mountain inflow, shallow pediment or arroyo recharge, canyon inflow, and river recharge. Each route imprints a characteristic geochemical signature. The cycle begins with storm clouds from either the Pacific ocean or the Gulf of Mexico which bring moisture to the Albuquerque area.

Pathway one begins with high elevation recharge, as a storms air mass is topographically lifted by the Sandia Mountains, the cooled moisture precipitates with its temperature controlled isotopic content. Precipitation

falling in the high Sandia Mountains rapidly infiltrates to become recharge. Recharge probably occurs all year long for very little moisture leaves the mountains as surface runoff. Infiltrating moisture reacts with soil CO_2 thereby slightly enriching the waters initial chemical content contributed by the atmosphere. Soil enriched water moves below the zone of evaporation where it percolates downward into the fractured bedrock. Water flowing through the fractured bedrock either flows out of the mountainous area as inflow into the basin-fill deposits, through shallow pediment covers, or emanates as spring flow. Water discharging to the aquifer is captured by the north-south high permeability zone where it rapidly flows several kilometers without reaching geothermal equilibrium (figure 79, H). After capturing this dilute high-elevation recharge, the high permeability zone diverts its flow southward where it intercepts more mineralized water flowing away from the mountains, thereby disrupting the east-west geochemical trend. High elevation mountain-front inflow is generally low in total dissolved solids, cool, isotopically light, and geochemically follows the rain-evaporation line fairly well with some mineral enrichment.

Pathway two begins as shallow pediment or arroyo recharge which may originate as high mountain inflow or moisture falling at lower elevations onto the broad alluvial fans skirting the mountains. Low elevation moisture is usually from low-volume storms and is likely to

totally evaporate. Total evaporation of storm moisture in the soil zone leaves behind very soluble salts of sodium and chloride and less soluble salts of calcite and gypsum. Soil wetting/drying cycles followed by infrequent, large-volume storm events flush the soluble salts and some of the less soluble salts below the zone of evaporation forming a salt pulse which becomes recharge. Recharge from these broad shallow pediments discharge to low permeability sediments forming the deep-basin fill aquifer. A broad, elongated band of ground water characteristic of this salt pulse lies several kilometers away from the pediments along most of the mountain front area. The two areas enriched in Na-HCO3 and Ca-Cl were caused by this salt pulse.

The elongated salt pulse affected area is surrounded by ground water low in TDS and similar to atmospheric geochemical input which suggests that soil wetting/drying cycles may have been more important in the past than in the present. Apparently, between wetting/drying cycles, ground water recharge is geochemically very similar to concentrated atmospheric input with some rock-mineral dissolution enrichment. Westward flowing shallow pediment and arroyo recharge discharged to low permeability deep-basin sediments may be geochemically enriched as it flow slowly into the medium permeability area. As ground water reaches the high permeability area it is captured and diverted to the south (figure 79,S). Rapidly flowing dilute high-elevation recharge and mineralized shallow pediment recharge are mixed along the lithologic boundaries by

subsurface heterogeneities, consequently masking each waters geochemical characteristics. Shallow pediment recharge is higher in TDS than high-elevation recharge to the north.

Pathway three, Tijeras Canyon drainage, follows a slightly different route. Water flowing out of the Tijeras Canyon watershed drains the broad dip-slope of the eastward facing Sandia and Manzanita Mountains. Ground water is diverted through the narrow canyon-fill alluvium and shallow Tijeras stream where it flows westward. Tijeras Canyon drainage recharges the deep basin-fill aquifer as inflow or the stream flows out on the alluvial fan where it quickly infiltrates or completely evaporates. Shallow ground water flow is concentrated by evapotranspiration with some capillary wetting/drying cycles slightly depleting the sulfate. Tijeras Canyon flow discharges into a highly permeable east-west trending corridor which rapidly carries ground water with the Tijeras Canyon chemical signature far into the East Mesa area (figure 79,C). As Tijeras recharge flows basinward, subsurface heterogeneities and pumpage mix recharge with deeper more dilute flow. Occasional, large-volume storms may cause a salt-pulse, characteristic of wetting/drying cycles, to reach the deep basin aquifer. This salt-pulse rapidly moves through nearby wells but is dispersed within a year. Tijeras Canyon recharge is characterized by evaporatively concentrated ions, high TDS, isotopically

heavy, and cool temperatures. Tijeras Canyons influence can be seen on geochemical and temperature maps where fast moving ground water has not reached geothermal equilibrium.

Pathway four is eastward flowing river recharge. Recharge flows both east and westward through the shallow hydraulically connected sediments filling the inner-valley flood plain. Eastward moving river recharge is either captured by municipal well fields near the river or moves through the shallow upper part of the aquifer retaining its tritium for at least 6 km (4 mi) (figure 79,R). River recharge is a Ca-HCO3 water as it enters the alluvium where it is altered, probably by ion exchange, to a Na-HCO3 water. Phreatophyte transpiration and return irrigation flow concentrate sulfate and chlorides and add salts to the shallow ground water. Borehole mixing of shallow mineralized ground water with deeper, Ca-HCO3 basin flow or mixing near hydraulic boundaries may cause wells to geochemically shift back and forth from Na-HCO3 to Ca-HCO3 water types depending on the length of pumping time, season, or well interference. The present-day hydraulic gradient (figure 21) slopes toward the high permeability area, isotopic and geochemical evidence indicate eastward flowing river recharge is also captured by this high permeability zone.

All four recharge pathways with their particular geochemical signatures are captured by the mid-mesa high permeability zone. Rapid ground water movement through this zone mixes and quickly masks the geochemical histories

of captured flow. Years of municipal pumpage has created an extensive ground water low elongated through the high permeability zone. The high permeability zone exerts a profound influence on the chemical characteristics of ground water in the area. High-capacity municipal wells near lithologic boundaries produce ground water chemistry with characteristics of both rain and river recharge. Borehole mixing of ground water from medium and high permeability zones mask both the isotopic and geochemical characteristics of ground water produced near the lithologic boundaries.

River recharge moving westward has a different geochemical fate than eastward flowing ground water. West of the Rio Grande, aquifer permeability is low allowing river recharge reaching the older, basin-fill sediments time to equilibrate with the geothermal gradient. The fine grained, organic-rich shallow aquifer sediments rapidly alter the Ca-HCO3 river recharge to Na-HCO3 waters. Shallow inner-valley alluvium is more permeable than the underlying, hydraulically connected, older basin-fill alluvium. River recharge, high in TDS, isotopically heavy, cool temperatures, and with measurable tritium move rapidly through the thin alluvium (figure 79,W). Wells 4.5 km (3.7 mi) west of the river intercept the shallow flowing ground water and have measurable tritium. Borehole mixing of shallow, mineralized, tritiated ground water with deeper basin flow produces ground water with variable temperatures

and chemical composition depending on the wells pumping history. Lithology exerts geochemical control on ground water, high TDS is associated with low hydraulic conductivity areas while nearby wells lower in TDS have higher hydraulic conductivities. Calcium smectite formation creates decreasing silica and calcium trends from east to west. Ion exchange removes calcium and potassium and adds sodium as ground water flows westward.

Tritium found in deep wells near and several kilometers from recharge boundaries indicate these wells are short circuiting young, shallow ground water. Tritium in these deep wells is a strong indication of ground waters vulnerability to potential pollution in areas previously though to be protected by the wells depth and/or distance from recharge boundaries.

APPENDIX I: DEEP WELL CONSTRUCTION DATA

APPENDIX I: DEEP WELL CONSTRUCTION DATA

MAP CODE	WELL LOCATION	WELL NAME	WELL USE	SOU RCE	DRILLED DATE	WELL TYPE	SURFACE ELEV(ft)	DRILLED DEPTH	DIA. (in)	TOP (ft)	BOTT. (ft)	PERF. (ft)	DESIGN (gpm)	ORIG. SWL
At1	10-02-25-112	ATRISCO 1(II5)(5)	Pub	APW	1980	G. P.	4941	1270	18	255	1258	1003	3200	29.2
At2	10-02-24-312	ATRISCO 2(I1)(1)	Pub	APW	1950	Nat	4948	558					1050	
At3	10-02-24-112	ATRISCO 3(I2)(9)	Pub	SEO	1958	G. P.	4951	813	16	180	804	624	1600	12
At4	10-02-23-223	ATRISCO 4(I3)(13)	Pub	APW	1953	Nat	4950	500					1500	
Bu1	10-03-27-244	BURTON 1 (new)	Pub	APW	1985	G. P.	5321	1312		676	1292		3140	
Bu1a	10-03-27-243	BURTON 1 (not used)	Mon	SEO	1955	G. P.	5317	1000	14	452	1000	548	2250	365
Bu2	10-03-26-111	BURTON 2	Pub	APW	1962	G. P.	5282	857	18	425	845	420	2350	342
Bu3	10-03-23-314	BURTON 3	Pub	APW	1962	G. P.	5216	994	18	358	994	636	2840	276
Bu4	10-03-27-413	BURTON 4	Pub	APW	1988	G. P.	5274	1276					2925	
Ca1	10-03-04-333	CANDELARIA 1(21)	Mon	APW	1948	Nat	4973	578	14					
Ca2	10-03-04-331	CANDELARIA 2(22)	Mon	APW	1948	Nat	4970	288	13					
Ca3	10-03-04-332	CANDELARIA 3(23)	Mon	APW	1948	Nat	4976	310	14					
Ca4	10-03-05-444	CANDELARIA 4(24)	Mon	APW	1948	Nat	4972	296	14					
Ch1	10-04-07-321	CHARLES 1	Pub	SEO	1968	G. P.	5316	1060	16	456	1032	576	3730	378
Ch2	10-03-13-222	CHARLES 2	Pub	SEO	1968	G. P.	5266	1038	16	432	996	564	3460	324
Ch3	10-03-12-232	CHARLES 3	Pub	SEO	1968	G. P.	5266	1025	16	420	996	576	3400	330
Ch4	10-04-18-211	CHARLES 4	Pub	SEO	1968	G. P.	5325	1055	16	456	1032	576	3950	386
Ch5	10-03-12-331	CHARLES 5	Pub	APW	1988	G. P.	5219	3243	20	625	1385	760	3000	
Co1	10-02-09-114	COLLEGE 1	Pub	SEO	1978	G. P.	5337	1690	18	658	1663	1005	1600	397
Co2	10-02-09-232	COLLEGE 2	Pub	SEO	1978	G. P.	5227	1605	18	550	1564	1014	2100	291
Cr1	11-03-24-221	CORONADO 1 (Tracy 1)	Pub	APW	1974	G. P.	5288	1186	18	479	1184	705	2500	334
D1	10-02-29-113	DON 1	Mon	SEO	1963	G. P.	5336	1600	16	588	1440	852	1200	422
Du1	10-03-07-141	DURANES 1	Pub	SEO	1959	G. P.	4961	1000	16	204	924	720	2245	21
Du2	10-02-01-431	DURANES 2	Pub	SEO	1958	G. P.	4966	813	16	180	804	624	2000	16
Du3	10-02-12-412	DURANES 3	Pub	SEO	1953	G. P.	4961	1000	18-12	132	950	818	2700	10
Du4	10-02-12-312	DURANES 4	Pub	SEO	1953	G. P.	4957	950	18-12	144	954	810	2400	4
Du5	10-02-13-112	DURANES 5	Pub	SEO	1953	G. P.	4957	950	18-12	152	950	798	2000	4
Du6	10-02-12-222	DURANES 6	Pub	SEO	1953	G. P.	4964	950	18	156	540	384	2000	12
Du7	10-02-12-121	DURANES 7	Pub	SEO	1953	G. P.	4962	950	18-12	144	950	806	2120	4
Gr1	11-03-31-231	GRIEGOS 1	Pub	SEO	1955	G. P.	4972	824	14	232	802	570	2400	13
Gr2	10-03-06-121	GRIEGOS 2	Pub	SEO	1954	G. P.	4966	820	14	164	820	656	1800	10
Gr3	11-02-36-442	GRIEGOS 3	Pub	SEO	1954	G. P.	4971	916	14	260	916	656	1740	8
Gr4	11-03-32-143	GRIEGOS 4	Pub	SEO	1954	G. P.	4974	804	14	218	804	586	2050	13
Gr5	11-03-31-442	GRIEGOS 5	Pub	SEO	1958	G. P.	4972	813	16	180	804	624	2000	17
Le1	10-02-33-244	LEAVITT 1	Pub	APW	1973	G. P.	5082	1236	16	324	1224	900	1700	158
Le2	10-02-33-442	LEAVITT 2	Pub	APW	1973	G. P.	5069	1140	16	288	1128	840	1200	144
Le3	09-02-04-223	LEAVITT 3	Pub	SEO	1986	G. P.	5082	1520	18	514	1500	986	2560	
Lm1	10-04-22-342	LOMAS 1	Pub	APW	1962	G. P.	5597	1300	16	700	1300	600	1500	647
Lm2	10-04-22-132	LOMAS 2	Pub	APW	1973	G. P.	5578	1548	16	743	1539	796	500	673
Lm3a	10-04-15-314	LOMAS 3 abd.	Pub	APW	1973	G. P.	5631	1608	16	888	1596	708	500	663
Lm4a	10-04-16-241	LOMAS 4 abd.	Pub	APW	1973	G. P.	5575	1416	16	816	1416	600	700	648
Lm5	10-04-21-344	LOMAS 5(7)	Pub	SEO	1978	G. P.	5498	1707	18	830	1658	828	3000	600
Lm6	10-04-28-223	LOMAS 6(8)	Pub	SEO	1978	G. P.	5532	1710	18	880	1692	812	2680	644
Lv1	10-04-16-334	LOVE 1	Pub	SEO	1954	G. P.	5462	1150	14	596	1096	500	1200	483
Lv2	10-04-20-244	LOVE 2 (Parks)	PR	SEO	1958	G. P.	5444	1224	16	660	1224	564	1200	483
Lv3	10-04-20-212	LOVE 3	Pub	SEO	1958	G. P.	5402	1200	16	600	1260	660	1700	450
Lv4	10-04-20-111	LOVE 4	Pub	SEO	1958	G. P.	5364	1284	16	600	1284	684	1700	414
Lv5	10-04-20-143	LOVE 5	Pub	SEO	1958	G. P.	5397	1248	16	660	1248	588	1600	439
Lv6	10-04-16-123	LOVE 6	Pub	APW	1973	G. P.	5504	1512	16	756	1500	744	1050	588

APPENDIX I: DEEP WELL CONSTRUCTION DATA

MAP CODE	WELL LOCATION	WELL NAME	WELL USE	SOU RCE	DRILLED DATE	WELL TYPE	SURFACE ELEV(ft)	DRILLED DEPTH	DIA. (in)	TOP (ft)	BOTT. (ft)	PERF. (ft)	DESIGN (gpm)	ORIG. SWL
Lv7	10-04-08-434	LOVE 7	Pub	APW	1973	G. P.	5442	1488	16	648	1476	828	2230	519
Lv8	10-04-18-411	LOVE 8	Pub	APW	1989	G. P.	5318	3337	20	640	1440	800	3000	
Ly1	11-03-36-434	LEYENDECKER 1	Pub	SEO	1959	G. P.	5284	1000	18	468	996	528	2700	323
Ly2	10-03-01-244	LEYENDECKER 2	Pub	SEO	1959	G. P.	5298	1020	18	468	996	528	2450	341
Ly3	11-03-36-322	LEYENDECKER 3	Pub	SEO	1960	G. P.	5266	1018	18	456	996	540	2400	308
Ly4	11-03-36-422	LEYENDECKER 4	Pub	SEO	1960	G. P.	5327	1018	18	480	996	516	2400	365
Mi1	10-03-33-233	MILES 1	Pub	SEO	1974	G. P.	5147	1341	16	405	1165	760	2800	
Po1	11-04-28-111	PONDEROSA 1(9)	Pub	SEO	1979	G. P.	5647	1800	18	964	1693	729	2000	725
Po1a	10-04-04-212	PONDEROSA 1 aband.	Mon	APW	1962	G. P.	5676	1237	16	781	1237	456	325	718
Po2	11-04-33-332	PONDEROSA 2	Pub	APW	1973	G. P.	5600	1581	16	801	1569	768	1800	715
Po3	11-04-32-234	PONDEROSA 3	Pub	APW	1977	G. P.	5523	1685	18	870	1590	720	2300	596
Po4	11-04-33-113	PONDEROSA 4	Pub	APW	1979	G. P.	5627	1549	18	919	1532	613	1600	714
Po5	11-04-28-113	PONDEROSA 5(7)	Pub	APW	1978	G. P.	5630	1626	18	939	1613	674	1800	692
Po6	11-04-29-431	PONDEROSA 6	Pub	SEO	1979	G. P.	5556	1695	18	852	1662	810	2400	630
Ri1	10-04-29-232	RIDGECREST 1	Pub	SEO	1964	G. P.	5443	1260	16	636	1260	624	1500	511
Ri2	10-04-20-344	RIDGECREST 2	Pub	APW	1977	G. P.	5414	1512	18	730	1500	770	3200	505
Ri3	10-04-30-243	RIDGECREST 3	Pub	APW	1974	G. P.	5386	1475	16	620	1436	816	3200	475
Ri4	10-04-19-322	RIDGECREST 4	Pub	APW	1974	G. P.	5344	1424	16	572	1412	840	3000	434
SB1	10-03-10-224	SANTA BARBARA 1	Pub	SEO	1963	G. P.	5138	1000	16	312	984	672	3400	190
SJ1	10-03-32-231	SAN JOSE 1	Pub	B&M	1949		4950	306					1000	
SJ2	10-03-29-441	SAN JOSE 2(4)(7)	Pub	SEO	1959	G. P.	4991	1000	16	264	996	732	1500	64
SJ3	10-03-29-341	SAN JOSE 3(5)(8)	Pub	SEO	1963	G. P.	4945	1200	16	192	1032	840	2350	14
SJ3Ob	10-03-32-412	SAN JOSE 3 Observ.	Obs	B&M	1949		4952	504						
SJ4	10-03-32-414	SAN JOSE 4(6)(10)	Mon	SEO	1963	G. P.	4941	1200	16	180	912	732	2350	12
SJ9Ob	10-03-32-314	SAN JOSE 9 Observ.	Obs	SEO	1963		4940	1200	16	196	768	572		15
Th1	11-04-32-333	THOMAS 1	Pub	SEO	1959	G. P.	5442	1092	16	624	1092	468	1800	481
Th2	10-04-05-122	THOMAS 2	Pub	SEO	1958	G. P.	5486	1224	16	696	1224	528	1400	515
Th3	11-04-31-412	THOMAS 3	Pub	SEO	1958	G. P.	5412	1200	16	672	1200	528	1800	450
Th4	11-04-32-322	THOMAS 4	Pub	SEO	1958	G. P.	5484	1020	16	672	1020	348	1800	518
Th5	10-04-06-122	THOMAS 5	Pub	APW	1989	G. P.	5356	3376	20	722	1452	720	2000	
Th6	10-04-06-421	THOMAS 6	Pub	APW	1989	G. P.	5408		20	760	1520	760	1950	
Th7	10-04-06-341	THOMAS 7	Pub	APW	1989	G. P.	5341	1489	20	657	1460	723	2000	
VA1	11-03-35-324	VOL ANDIA 1	Pub	SEO	1960	G. P.	5142	1010	16	300	972	672	3860	180
VA2	10-03-01-131	VOL ANDIA 2	Pub	SEO	1960	G. P.	5208	1016	16	360	852	492	3580	249
VA3	10-03-03-224	VOL ANDIA 3	Pub	SEO	1960	G. P.	5110	1025	16	264	900	636	3600	145
VA4	11-03-35-424	VOL ANDIA 4	Pub	SEO	1960	G. P.	5201	1020	16	372	876	504	3100	242
VA5	11-03-35-313	VOL ANDIA 5	Pub	SEO	1960	G. P.	5111	1020	16	260	900	640	3000	149
VA6	11-03-35-232	VOL ANDIA 6	Pub	SEO	1960	G. P.	5177	1010	16	324	984	660	3000	216
VC1	11-02-28-222	VOLCANO CLIFFS 1	Pub	SEO	1968	G. P.	5335	1200	16	528	1056	528	2600	375
VC2	11-02-28-244	VOLCANO CLIFFS 2	Pub	SEO	1968	G. P.	5328	1200	16	528	876	348	2100	370
VC3	11-02-21-244	VOLCANO CLIFFS 3	Pub	Bov	1980		5344	1320		666	1310	644	3000	
VG1a	09-02-14-124	VALLEY GARDEN 1(A)abd		SEO	1963		4922	200	8	168	198	30		
VG2a	09-02-14-134	VALLEY GARDEN 2(B)abd		SEO	1963		4920	464	8	414	462	40		
Wa1	11-04-21-112	WALKER 1	Pub	APW	1980	G. P.	5699	1723	18	991	1711	720	1550	755
Wa2	11-04-20-221	WALKER 2	Pub	APW	1980	G. P.	5593	1785	18	852	1773	921	2500	651
We1	11-04-18-434	WEBSTER 1 (Alameda1)	Pub	APW	1977	G. P.	5436	1484	18	620	1345	725	2800	479
We2	11-04-19-142	WEBSTER 2 (Alameda2)	Pub	APW	1977	G. P.	5384	1450	18	608	1334	726	3400	436
WM1	10-02-21-343	WEST MESA 1	Pub	SEO	1958	G. P.	5179	1180	16	504	1176	672	500	250
WM2	10-02-21-213	WEST MESA 2	Pub	APW	1962	G. P.	5167	1402	16	394	1402	1008	1750	251

APPENDIX I: DEEP WELL CONSTRUCTION DATA

MAP CODE	WELL LOCATION	WELL NAME	WELL USE	SOU RCE	DRILLED DATE	WELL TYPE	SURFACE ELEV(ft)	DRILLED DEPTH	DIA. (in)	TOP (ft)	BOTT. (ft)	PERF. (ft)	DESIGN (gpm)	ORIG. SWL
WM3	10-02-21-412	WEST MESA 3	Pub	APW	1974	G. P.	5145	1364	16	404	1352	948	2500	239
WM4	10-02-22-312	WEST MESA 4	Pub	APW	1975	G. P.	5101	1286	16	386	1274	888	2500	189
Ya1	10-03-21-444	YALE 1(2)	Pub	SEO	1963	G. P.	5159	1000	16	336	960	624	2750	219
Ya2	10-03-28-243	YALE 2(3)	Pub	SEO	1973	G. P.	5126	1197	16	357	1185	828	3225	218
Ya3	10-03-21-341	YALE 3(4)	Pub	SEO	1973	G. P.	5080	1004	16	320	992	672	2500	159
4-H	10-04-34-214	4-HILLS C.C.	Pub	B&M	1957		5600	1200	18				1625	616
Co3	10-02-03-422	LADERA (College 3)	PR	Bov	1978		5180	1490	18	432	1440	1008	2600	164
DDII	11-01-24-334	DOUBLE EAGLE II	Pub	Bov	1985		5805	1800	8	1059	1702	Multi	200	682
K01	10-04-31-411	USAF 1	Pub	B&M	1949		5383	1200	12	550	1200	650	700	427
K02	09-03-01-112	USAF 2 (SANDIA 2)	Pub	B&M	1949		5318	1000	14	494	1000	506	855	365
K03	10-04-30-321	USAF 3 (SANDIA 3)	Pub	B&M	1949		5354	900	14	452	900	448	800	407
K04	09-04-06-322	USAF 4 (SANDIA 4)	Pub	B&M	1949		5362	1000	14	494	1000	506	760	407
K05	10-04-29-324	USAF 5 (SANDIA 5)	Pub	B&M	1952		5434	1004	14	504	1000	496	650	466
K06	10-04-32-433	USAF 6 (SANDIA 6)	Pub	B&M	1952		5421	1010	14	502	1010	508	590	458
K07	09-03-01-222	USAF 7 (SANDIA 7)	Pub	B&M	1954		5349	1010	16	449	976	527	1400	395
K08	09-04-05-332	USAF 8 (SANDIA 8)	Pub	B&M	1954		5378	1000	16	454	976	522	1000	400
K09	09-04-15-311	USAF 9 (MANZANO 9)	Pub	B&M	1948		5501	684	10	502	684	182	200	536
K10	09-04-20-221	USAF 10 (MANZANO 10)	Pub	B&M	1959		5425	1036	12				400	459
K11	09-04-04-211	USAF 11	Pub	B&M	1972		5468	1330	16	670	1330	660	2000	545
K12	10-03-35-111	USAF 12 (KAFB 1)	Pub	B&M	1952		5320	1030	16	491	1000	509	1500	358
K13	10-03-34-144	USAF 13 (KAFB 2)	Pub	B&M	1956		5303	1010	16	395	940	545	1400	358
K14	10-03-35-322	USAF 14	Pub	B&M										
MP1	09-03-11-242	POLICE FARM 1(Carter	IRR	USGS	1953		5165		17		330		1000	230
MP2	09-03-11-332	POLICE FARM 2(Carter	Dom	USGS				180	2		180		64	
MP3	09-03-11-444	POLICE FARM 3	Irr	APW	1968	G.P.	5144	302	8	248	288	40	200	210
MP4	09-03-11-420	MONTESSA PARK 1	Irr	USGS	1958			257		214	233			183
MP5	09-03-11-242	TONTO (Forest Serv.)	Pub	USGS	1982			462		305	410	Multi.		262
PH1	11-02-09-411	PARADISE HILLS 1	Pub	NMU	1960		5455	1095		645	1095	450		
PH2	11-02-02-343	PARADISE HILLS 2	Pub	NMU	1963		5320	1000		350	800	450		300
PH3	11-02-03-221	PARADISE HILLS 3	Pub	NMU	1980		5440	1360		650	1350	700		489
PS1	11-03-23-111	PUB.SRV. WELL 1	Ind	B&M	1957		5073	927	16				1400	93
PS4	09-03-09-113	PUB.SRV.PERSON 4	Ind	B&M	1956		5125	900	14	350	898	548	2000	182
Pvt	10-04-03-242	PRIVATE OWNED	Dom	B&M	1949		5850	320	6					255
RR1	12-03-31-243	RIO RANCHO 1	Pub	USGS	1961			350						
RR2	12-03-31-132	RIO RANCHO 2	Pub	USGS	1963		5260	750		508	751	243		
RR3	12-02-25-421	RIO RANCHO 3	Pub	USGS	1964		5370	823		584	820	236		
RR4	12-02-24-442	RIO RANCHO 4	Pub	USGS	1969		5415	990		670	990	320		
RR5	12-03-30-112	RIO RANCHO 5	Pub	USGS	1969		5385	980		380	975	595		
RR6	12-02-14-344	RIO RANCHO 6	Pub	USGS	1969		5610	1020		571	1000	429		
RR7	12-02-14-321	RIO RANCHO 7	Pub	USGS	1974		5650	1200		898	1180	282		
RR8	12-02-16-214	RIO RANCHO 8	Pub	USGS	1978		5825	1620		982	1600	618		
RR9	13-01-25-432	RIO RANCHO 9	Pub	USGS	1984			1540		1220	1520	300		
SAF	11-01-27-431	SOIL AMEND.FACILITY	Ind	APW	1989		5866	2489		1116	1429	313		
SP1	11-04-15-443	SANDIA PEAK UTIL. 1	Pub	USGS				520						372
SP2	11-04-10-332	SANDIA PEAK UTIL. 2	Pub	APW				1100						
SP3	11-04-09-431	SANDIA PEAK UTIL. 3	Pub	APW				1100						
UNM5	10-03-22-142	UNM 5	Pub	USGS										
UNM7	10-03-22-124	UNM 7	Pub	USGS										
Vet	10-03-36-132	VET. ADMIN.	Pub	USGS	1956		5341	997	14				860	400

APPENDIX I: DEEP WELL CONSTRUCTION DATA

MAP CODE	WELL LOCATION	WELL NAME	WELL USE	SOU RCE	DRILLED DATE	WELL TYPE	SURFACE ELEV(ft)	DRILLED DEPTH	DIA. (in)	TOP (ft)	BOTT. (ft)	PERF. (ft)	DESIGN (gpm)	ORIG. SWL
VS	11-03-11-334	VISTA SANDIA 2	Dom	USGS	1963		5070	810		720	800	80		91
WMA	11-01-24-240	WEST MESA AIR.(SHELL	Pub	SEO	1981		5780	1523	6	1020	1442	MULTI	60+	829
SBLF-1	09-03-22-311	S.BROADWAY LANDFILL-1	Dom	APW	1965		5300	551	20	479	539	MULTI		
ESYa1	10-03-34-3332	ENV. SERV. YALE 1	Mon.	SEO	1982			464	4.5	400	464	59		
ESYa2a	10-03-33-431	ENV. SERV. YALE 2 ab	Mon.	SEO	1982			305	4.5	250	300	50		
ESYa3	10-03-33-243	ENV. SERV. YALE 3	Mon.	APW										
ESYa4	10-03-34-313	ENV. SERV. YALE 4	Mon.	APW	1988		5306	443	2	398	438	40		
ESYa5	10-03-33-321	ENV. SERV. YALE 5	Mon.	APW										
USGS1A	10-01-22-144	USGS/CITY EXP.1-A	Obs.	SEO	1981		5798	1181	6	982	1181	MULTI		850
USGS-2	11-02-18-313	USGS/CITY EXP. 2	Obs.	SEO	1981		5730	1805	6	800	1795	MULTI		770
USGS-3	11-03-18-411	USGS/CITY EXP. 3	Obs.	SEO	1981		5000	1055	6	350	1050	MULTI		26

DATA SOURCES:
- APW = Albuquerque Public Works
- USGS = U. S. Geological Survey (reports & WATSTORE)
- Bov = Bovey Engineering
- Her = Herkenhoff
- B&M = Bjorklund and Maxwell 1961
- SEO = State Engineers Office completion reports

WELL USE: Usage may vary with time
- Pub = Public water supply well (Municipal and private suppliers)
- PR = Parks and recreation wells
- Dom = Domestic wells (not all private)
- Obs = observation wells
- Mon = Monitoring wells

WELL TYPE:
- G. P. = gravel pack
- Nat. = natural pack

MAP CODE:
- Atl = Atrisco Well No.1
- Bula = Burton Well No.1 abandoned

WELL LOCATION:
- 10-02-25-112 = Township 10 North, Range 2 East, Section 25, NE1/4,NW1/4,NW1/4

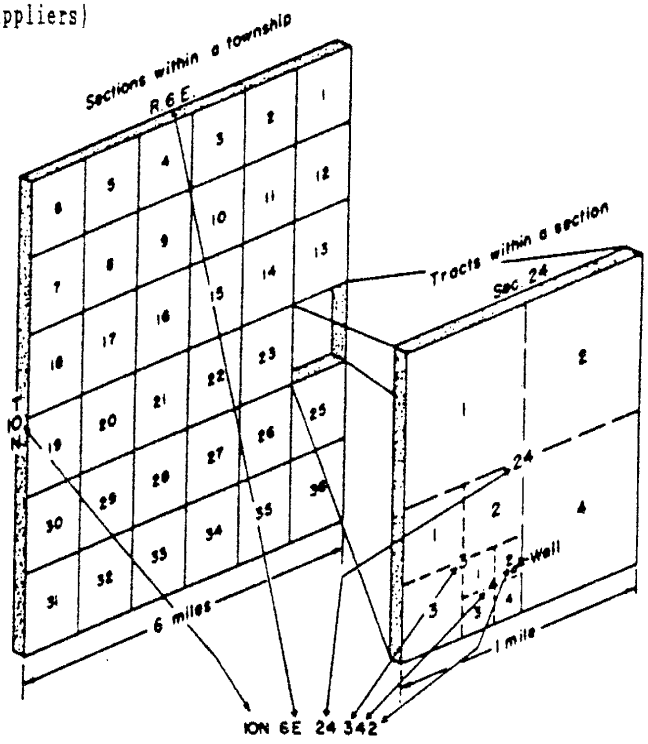

Figure 81: System of numbering wells and springs in New Mexico (modified from Titus, 1980)

APPENDIX II: SHALLOW WELL CONSTRUCTION DATA

APPENDIX II: SHALLOW WELL CONSTRUCTION AND WATER LEVELS FOR WINTER 1988-1989 (figure 21)

MAP INDEX	LOCATION	SURFACE ELEV.(ft)	WELL DEPTH	TOP PERF.	BOTTOM PERF.	WATER DEPTH	WATER ELEV.(ft)	DATE MEASURED	WELL TYPE	DATA SOURCE	COMMENTS
*	09N.03E.17.342	5001.14	106.5	86.5	106.5	98	4907	10/31/88	MONITOR	EID	ABQ FOREIGN AUTO
*	09N.03E.18.443	4968.52	73.9	53.9	73.9	60	4910	10/31/88	MONITOR	EID	PERFECTION TRUSS
*	09N.03E.19.223	4965.75	66	46	66	56	4909	10/31/88	MONITOR	EID	AMAFCA EASMENT
*	09N.03E.19.443	4979.23	90	70	85	76	4907	11/01/88	MONITOR	EID	McCATHERN DAIRY
*	09N.03E.20.432	5189				288	4901	8/15/89	MONITOR	AEHD	SOUTH BROADWAY LAND FILL
*	09N.03E.21.222	5311				409	4902	6/19/88	MONITOR	AEHD	SOUTH BROADWAY LAND FILL
*	09N.03E.29.142	5150				249	4901	8/15/89	MONITOR	AEHD	SOUTH BROADWAY LAND FILL
*	09N.03E.29.244	5330				430	4900	6/19/88	MONITOR	AEHD	SOUTH BROADWAY LAND FILL
*	09N.04E.29.443	5419	615	525	595	482	4937	10/10/88	MONITOR	SNL	SANDIA NATIONAL LAB
*	09N.04E.33.111	5435	528	445	495	478	4957	10/10/88	MONITOR	SNL	SANDIA NATIONAL LAB
*	10N.01E.22.322	5795		1139	1179	884	4911	9/ /88	PIEZOMETR	USGS	DEEP WELL OPEN 980-1121
*	10N.02E.12.241	4960		140	150	34	4926	9/ /88	OBSERV.	USGS	ABQ CITY OBSERVATION WELL
*	10N.03E.17.241	4959				50	4909		MONITOR	AEHD	BANES (NE CORNER)
*	10N.03E.32.111						4930		MONITOR	AEHD	
*	11N.01E.27.431	5866		1116	1429	917	4949		PRODUCTION	CITY	DEEP WELL OPEN 1116-1429
*	11N.02E.18.313	5730	800	955		768	4962	9/ /88	PIEZOMETR	USGS	DEEP WELL OPEN 800-955
*	11N.03E.31.214	4975	142	152		25	4950	9/ /88	OBSERV.	USGS	ABQ CITY OBSERVATION WELL
*	11N.03E.32.421	4875				38	4936		MONITOR	AEHD	PEERLESS NW CORNER
*	11N.03E.33.143	4980		140	150	46	4934	9/ /88	OBSERV.	USGS	ABQ CITY OBSERVATION WELL
*	11N.04E.18.124	5385	575			458	4927	9/ /88	OBSERV.	USGS	PRIVATE WELLS
*	12N.03E.30.112	5385	980	380	975	396	4989	9/ /88	PRODUCTION	USGS	DEEP WELL OPEN 380-975 mul
1	09N.03E.07.241	4926.76	49.3	44.3	49.3	7	4921	9/ /88	OBSERV.	USGS	USGS OBSERVATION WELL NEST
2	09N.03E.08.144	4933.33	49.3	44.3	49.3	17	4915	9/ /88	OBSERV.	USGS	USGS OBSERVATION WELL NEST
3	09N.03E.07.131	4929.19	48.6	43.6	48.6	8	4920	9/ /88	OBSERV.	USGS	USGS OBSERVATION WELL NEST
4	09N.02E.12.124	4931.28	39.2	33.4	38.4	9	4921	9/ /88	OBSERV.	USGS	USGS OBSERVATION WELL NEST
5	09N.02E.13.121	4926				11	4915	2/01/89	MONITOR	EID	ROBERTS ISLETTA & LAKEVIEW
6	09N.03E.18.431	4948.76	73	53	73	38	4911	11/03/88	MONITOR	EID	MOUNTAIN VIEW SCHOOL
7	09N.03E.17.344	5017.46	135.5	110	130	114	4906	10/31/88	MONITOR	EID	S. TIJERAS ARROYO
8	09N.03E.16.321	5047	170	145	165	143	4903	11/02/88	MONITOR	EID	HENSLEY PROPERTY
9	09N.03E.10.431	5102	225	200	220	203	4899	11/02/88	MONITOR	EID	IRA SPENCER RD.
10	09N.03E.11.242	5168	300	275	295	277	4891	11/02/88	MONITOR	EID	ABQ TREE FARM
11	09N.04E.20.143	5381	478	455	475	456	4925	1/09/89	MONITOR	SNL	SANDIA NATIONAL LAB
12	10N.02E.36.241						4941	1989	MONITOR	AEHD	
13	10N.02E.26.143	5006.44	97	71.88	91.70	76	4930	10/17/88	MONITOR	EID	PRONTO SERVICE
14	10N.03E.07.434	4960				31	4929	9/ /88	OBSERV.	USGS	PRIVATE WELL
15	10N.03E.18.221						4931		MONITOR	AEHD	
16	10N.03E.18.424						4933		MONITOR	AEHD	CHEVRON (NW CORNER)
17	10N.03E.17.232	4960	139	149		44	4916	9/ /88	OBSERV.	USGS	ABQ CITY OBSERVATION WELL
18	10N.03E.32.413	4936	17	6.5	16.5	15	4922	7/22/88	MONITOR	GTI	SUPERFUND SITE
19	10N.03E.20.211	4957	45	34.5	44.5	38	4919	10/19/88	MONITOR	AEHD	ABANDONED
20	10N.03E.20.344	4948	46	26	41	29	4920	5/18/88	MONITOR	AEHD	RAILROAD TIE TREATMENT
21	10N.03E.29.313						4931		MONITOR	AEHD	
22	10N.03E.32.112	4942				16	4926		MONITOR	AEHD	QUIKRETE
23	10N.03E.08.414	4966					4922		MONITOR	AEHD	
24	10N.03E.22.312	5169				280	4889		MONITOR	AEHD	VICKERS
24	10N.03E.34.313	5306.85	443	398	438	401	4906	11/01/88	MONITOR	AEHD	
26	10N.04E.32.422						4901		MONITOR	AEHD	EUBANK LAND FILL
27	10N.04E.26.333	5549				51	5498	12/06/88	MONITOR	AEHD	4 HILLS COUNTRY CLUB
28	11N.04E.15.321	5865	660			317	5548	9/ /88	OBSERV.	USGS	PRIVATE WELLS
29	11N.03E.13.242	5290		380	460	342	4952	9/ /88	OBSERV.	USGS	PRIVATE WELLS
30	11N.02E.14.131	5062		101	141	95	4968	9/26/88	MONITOR	AEHD	LOS ANGELES LAND FILL
31	11N.03E.14.331	5086.7		135	175	128	4958	9/20/88	MONITOR	AEHD	LOS ANGELES LAND FILL
32	11N.03E.33.433	4995	105	68	88	75	4921	10/17/88	MONITOR	AEHD	

APPENDIX II: SHALLOW WELL CONSTRUCTION AND WATER LEVELS FOR WINTER 1988-1989 (figure 21)

MAP INDEX	LOCATION	SURFACE ELEV.(ft)	WELL DEPTH	TOP PERF.	BOTTOM PERF.	WATER DEPTH	WATER ELEV.(ft)	DATE MEASURED	WELL TYPE	DATA SOURCE	COMMENTS
33	11N.03E.32.421	4974.68	50.2			34	4940	9/ /88	OBSERV.	USGS	USGS OBSERVATION WELL NEST
34	11N.03E.32.143	4972.49	49.8			23	4949	9/ /88	OBSERV.	USGS	USGS OBSERVATION WELL NEST
35	11N.03E.31.124	4969.84	39.7			10	4959	9/ /88	OBSERV.	USGS	USGS OBSERVATION WELL NEST
36	11N.02E.25.342	4975.08	48.4			8	4967	9/ /88	OBSERV.	USGS	USGS OBSERVATION WELL NEST
37	11N.02E.35.142	5110	250	230	245	148	4962	9/ /88	OBSERV.	USGS	PRIVATE WELLS
38	11N.02E.24.223	5065	274	259	274	100	4965	9/ /88	OBSERV.	USGS	PRIVATE WELLS
39	11N.03E.18.411	4995	840	710	790	27	4968	9/ /88	PIEZOMETR	USGS	DEEP WELL OPEN 350-590
40	11N.03E.07.442	5034.5				57	4977	6/16/89	MONITOR	AEHD	250'W OF COORS:N OF IRVING

MAP INDEX: Shallow well map code for figure 21
* = Data not shown on map but used in interpretation
AEHD = Albuquerque Environmental Health Department
EID = New Mexico State Environmental Improvement Division
USGS = United States Geological Survey
SNL = Sandia National Laboratory

APPENDIX III: GROUND-WATER QUALITY DATA

APPENDIX III: GROUND-WATER QUALITY DATA

MAP CODE	WELL LOCATION	WELL NAME	SAMPLE DATE	Ca (meq/L)	Mg (meq/L)	Na (meq/L)	K (meq/L)	Na+K-Na (meq/L)	HCO3 (meq/L)	SO4 (meq/L)	Cl (meq/L)	Hard. (meq/L)
4-H	10-04-34-214	4-HILLS C.C.	Sep-57	3.94	1.81			1.13	3.93	2.08	0.45	5.75
4-H	10-04-34-214	4-HILLS C.C.	Sep-73	3.99	1.56	1.17	0.09	1.26	4.10	2.08	0.48	5.55
4-H	10-04-34-214	4-HILLS C.C.	Dec-81	4.07	2.27	1.04	0.06	1.10	4.18	2.39	1.17	6.34
4-H	10-04-34-214	4-HILLS C.C.	Oct-87	2.30	1.19	0.49	0.02	0.51	3.43	2.71	1.80	3.48
At1	10-02-25-112	ATRISCO 1 (5)	May-80	0.31	0.07	5.22	0.05	5.27	2.00	2.71	0.59	0.38
At1	10-02-25-112	ATRISCO 1 (5)	Feb-87	0.80	0.25	4.35	0.10	4.45	2.50	2.14	0.48	1.04
At3	10-02-24-112	ATRISCO 3 (2:9)	Sep-73	1.50	0.40	2.40	0.17	2.57	2.62	1.55	0.59	1.90
At3	10-02-24-112	ATRISCO 3 (2:9)	Nov-73	1.78	0.64	2.10	0.19	2.29	2.56	1.56	0.40	2.42
At3	10-02-24-112	ATRISCO 3 (2:9)	Jan-76	1.38	0.37	2.80	0.16	2.96	2.51	1.82	0.49	1.75
At3	10-02-24-112	ATRISCO 3 (2:9)	Feb-87	1.40	0.41	2.18	0.15	2.33	2.46	1.39	0.39	1.81
Bu1a	10-03-27-243	BURTON 1 abd.	May-57	1.80	0.51			1.04	2.29	0.62	0.37	2.31
Bu1a	10-03-27-243	BURTON 1 abd.	Sep-73	2.02	0.53	1.60	0.14	1.74	2.38	1.65	0.47	2.55
Bu2	10-03-26-111	BURTON 2	Dec-65	1.60	0.60	0.74	0.06	0.80	2.06	0.65	0.28	2.20
Bu2	10-03-26-111	BURTON 2	Sep-73	1.80	0.55	1.00	0.09	1.09	2.25	0.96	0.47	2.35
Bu2	10-03-26-111	BURTON 2 +2	Jan-76	1.79	0.65	0.95	0.10	1.05	2.11	0.71	0.59	2.44
Bu2	10-03-26-111	BURTON 2	Feb-87	2.05	0.66	1.22	0.13	1.35	2.22	0.71	1.04	2.70
Bu3	10-03-23-314	BURTON 3 +3	Jan-76	1.94	0.60	1.07	0.11	1.18	2.16	0.90	0.63	2.54
Bu3	10-03-23-314	BURTON 3	Feb-87	1.85	0.58	1.09	0.13	1.22	2.10	1.27	1.10	2.42
Ch1	10-04-07-321	CHARLES 1	Oct-73	2.10	0.36	1.80	0.06	1.86	2.47	0.65	0.85	2.46
Ch1	10-04-07-321	CHARLES 1	Oct-77	2.12	0.35	1.50	0.06	1.56	2.35	0.55	0.95	2.47
Ch1	10-04-07-321	CHARLES 1	Feb-87	2.00	0.25	1.48	0.05	1.53	2.21	0.69	0.87	2.24
Ch2	10-03-13-222	CHARLES 2 +2	Jan-76	1.94	0.35	0.95	0.06	1.01	2.19	0.69	0.25	2.29
Ch2	10-03-13-222	CHARLES 2	May-85	1.85	0.00	1.13	0.05	1.18	2.08	0.79	0.25	1.85
Ch3	10-03-12-232	CHARLES 3	Oct-73	1.98	0.38	0.90	0.06	0.96	2.26	0.47	0.29	2.35
Ch3	10-03-12-232	CHARLES 3 +2	Jan-76	1.82	0.44	0.85	0.06	0.91	2.13	0.64	0.22	2.27
Ch3	10-03-12-232	CHARLES 3	May-85	1.85	0.00	1.17	0.05	1.22	2.13	0.65	0.20	1.85
Ch4	10-04-18-211	CHARLES 4	Oct-73	2.50	0.30	1.60	0.06	1.66	2.43	0.68	1.14	2.80
Ch4	10-04-18-211	CHARLES 4	Jan-76	2.43	0.40	1.30	0.07	1.37	2.34	0.64	1.04	2.82
Ch4	10-04-18-211	CHARLES 4	May-85	2.25	0.00	1.39	0.06	1.45	2.30	0.54	0.96	2.25
Co1	10-02-09-114	COLLEGE 1	Sep-78	0.18	0.03	4.79	0.04	4.83	3.20	1.19	0.16	0.22
Co1	10-02-09-114	COLLEGE 1	Feb-87	0.20	0.00	4.70	0.00	4.70	2.83	1.12	0.20	
Co2	10-02-09-232	COLLEGE 2	Dec-78	0.12	0.02	4.35	0.04	4.39	2.79	1.29	0.19	0.14
Co2	10-02-09-232	COLLEGE 2	Feb-87	0.20	0.00	4.05	0.00	4.05	2.74	1.21	0.20	0.20
Co3	10-02-03-422	LADERA(College3)	Sep-78	0.50	0.15	4.22	0.11	4.33	2.39	2.06	0.51	0.65
Cr1	11-03-24-221	CORONADO 1	May-85	1.36	0.64	3.60	0.09	3.69	2.56	0.75	2.31	2.00
Cr1	11-03-24-221	CORONADO 1	Oct-88	1.55	0.54	2.06	0.14	2.20	2.24	0.74	1.46	2.09
D1	10-02-29-113	DON 1	Jan-73	0.07	0.23	4.50	0.04	4.54	2.97	1.81	0.29	0.30
D1	10-02-29-113	DON 1	Jan-76	0.74	0.16	4.40	0.03	4.43	2.74	1.55	0.33	0.91
D1	10-02-29-113	DON 1	Feb-87	0.00	0.00	5.57	0.00	5.57	3.13	1.96	0.68	0.00
Du1	10-03-07-141	DURANES 1	Sep-73	2.18	0.74	2.90	0.23	3.13	2.94	2.45	0.56	2.92
Du1	10-03-07-141	DURANES 1 +2	Jan-76	2.04	0.95	2.80	0.24	3.04	2.80	2.44	0.52	2.99
Du1	10-03-07-141	DURANES 1	Feb-87	2.54	0.91	3.13	0.26	3.39	2.97	3.21	0.65	3.45
Du2	10-02-01-431	DURANES 2	Sep-73	1.25	0.55	2.70	0.18	2.88	2.56	1.39	0.34	1.80
Du2	10-02-01-431	DURANES 2 +2	Jan-76	1.39	0.61	2.15	0.17	2.32	2.49	1.54	0.32	2.00
Du2	10-02-01-431	DURANES 2	Feb-87	1.55	0.49	2.00	0.18	2.18	2.25	1.33	0.37	2.04
Du3	10-02-12-412	DURANES 3	May-57	1.80	0.63			2.70	2.97	1.81	0.34	2.42
Du3	10-02-12-412	DURANES 3	Sep-73	1.91	0.59	3.10	0.20	3.30	2.87	1.97	0.41	2.50
Du3	10-02-12-412	DURANES 3	Jan-76	2.11	0.81	2.30	0.20	2.50	2.78	2.05	0.42	2.92
Du3	10-02-12-412	DURANES 3	Feb-87	2.00	0.66	2.39	0.18	2.57	2.74	1.79	0.42	2.65
Du4	10-02-12-312	DURANES 4	Sep-73	1.06	0.36	3.90	0.16	4.06	2.66	1.83	0.46	1.42
Du4	10-02-12-312	DURANES 4 +2	Jan-76	1.25	0.56	2.84	0.16	3.00	2.30	1.68	0.47	1.81
Du4	10-02-12-312	DURANES 4	Feb-87	0.80	0.25	2.65	0.15	2.80	2.19	1.42	0.45	1.04
Du5	10-02-13-112	DURANES 5	Sep-73	1.57	0.14	3.20	0.17	3.37	2.63	1.56	0.39	1.71

APPENDIX III: GROUND-WATER QUALITY DATA

MAP CODE	WELL LOCATION	WELL NAME		SAMPLE DATE	Alka. (meq/L)	TDS (mg/L)	TDR (mg/L)	S.C. uS/cm	pH	Temp. (C)	SiO2 (mg/L)	WATER TYPE	DATA SOURCE
4-H	10-04-34-214	4-HILLS C.C.		Sep-57	3.93	400		636	7.3	14.0	20	CaHCO3	1
4-H	10-04-34-214	4-HILLS C.C.		Sep-73	4.10	410	369	630	7.6	15.5	20	CaHCO3	3
4-H	10-04-34-214	4-HILLS C.C.		Dec-81	4.18	460		585	7.3	14.0	19	CaHCO3	4
4-H	10-04-34-214	4-HILLS C.C.		Oct-87	3.43	576		890		23.0	23	CaHCO3	4
At1	10-02-25-112	ATRISCO 1 (5)		May-80	2.00	390		520	8.9	32.0	46	NaSO4	3
At1	10-02-25-112	ATRISCO 1 (5)		Feb-87	2.50	371		538	8.0	24.0	47	NaHCO3	4
At3	10-02-24-112	ATRISCO 3 (2:9)		Sep-73	2.62	330		443	7.8			NaHCO3	5
At3	10-02-24-112	ATRISCO 3 (2:9)		Nov-73	2.56	335		442	7.9			NaHCO3	7
At3	10-02-24-112	ATRISCO 3 (2:9)		Jan-76	2.51	305		490	8.1			NaHCO3	6
At3	10-02-24-112	ATRISCO 3 (2:9)		Feb-87	2.46	290		460	8.2	16.0	45	NaHCO3	4
Bu1a	10-03-27-243	BURTON 1 abd.		May-57	2.29	230	238	325	7.9	20.5	52	CaHCO3	1
Bu1a	10-03-27-243	BURTON 1 abd.		Sep-73	2.38		260	395	7.9			CaHCO3	5 & 7
Bu2	10-03-26-111	BURTON 2		Dec-65	2.06		210	295	8.2			CaHCO3	7
Bu2	10-03-26-111	BURTON 2		Sep-73	2.25		225	333	8.0			CaHCO3	5 & 7
Bu2	10-03-26-111	BURTON 2	+2	Jan-76	2.11		227	360	8.1			CaHCO3	6
Bu2	10-03-26-111	BURTON 2		Feb-87	2.22	264		471	8.1	21.0	43	CaHCO3	4
Bu3	10-03-23-314	BURTON 3	+3	Jan-76	2.15		239	379	8.0			CaHCO3	6
Bu3	10-03-23-314	BURTON 3		Feb-87	2.10	281		452	8.2	21.0	43	CaHCO3	4
Ch1	10-04-07-321	CHARLES 1		Oct-73	2.47		255	365	7.8			CaHCO3	5 & 7
Ch1	10-04-07-321	CHARLES 1		Oct-77	2.35		215	415	8.0			CaHCO3	6
Ch1	10-04-07-321	CHARLES 1		Feb-87	2.21	231		390	8.0	18.0	21	CaHCO3	4
Ch2	10-03-13-222	CHARLES 2	+2	Jan-76	2.19		218	316	8.0			CaHCO3	6
Ch2	10-03-13-222	CHARLES 2		May-85	2.08	209		304			33	CaHCO3	4
Ch3	10-03-12-232	CHARLES 3		Oct-73	2.26		225	294	7.8			CaHCO3	5 & 7
Ch3	10-03-12-232	CHARLES 3	+2	Jan-76	2.13		177	307	7.9			CaHCO3	6
Ch3	10-03-12-232	CHARLES 3		May-85	2.13	203		290			34	CaHCO3	4
Ch4	10-04-18-211	CHARLES 4		Oct-73	2.43		275	403	7.8			CaHCO3	5 & 7
Ch4	10-04-18-211	CHARLES 4		Jan-76	2.34		255	424	8.1			CaHCO3	6
Ch4	10-04-18-211	CHARLES 4		May-85	2.30	238					29	CaHCO3	4
Co1	10-02-09-114	COLLEGE 1		Sep-78	3.20	310		450	8.7	28	30	NaHCO3	8
Co1	10-02-09-114	COLLEGE 1		Feb-87					8.7	27.0	30	NaHCO3	4
Co2	10-02-09-232	COLLEGE 2		Dec-78	2.79	290		440	8.5	30	30	NaHCO3	3
Co2	10-02-09-232	COLLEGE 2		Feb-87	2.74	279			8.9	27.0	21	NaHCO3	4
Co3	10-02-03-422	LADERA(College3)		Sep-78	2.39	350		560	7.9	26	50	NaHCO3	3
Cr1	11-03-24-221	CORONADO 1		May-85	2.56	376		593	8.2	23	120	NaHCO3	8
Cr1	11-03-24-221	CORONADO 1		Oct-88	2.24	300			8.1		54	NaHCO3	3
D1	10-02-29-113	DON 1		Jan-73	2.97	348			8.2			NaHCO3	5
D1	10-02-29-113	DON 1		Jan-76	2.74	325			8.6			NaHCO3	6
D1	10-02-29-113	DON 1		Feb-87	3.13	370		615	8.6	28.0	24	NaHCO3	4
Du1	10-03-07-141	DURANES 1		Sep-73	2.94		425	581	7.7			NaHCO3	5 & 7
Du1	10-03-07-141	DURANES 1	+2	Jan-76	2.80		412	604	8.0			NaHCO3	6
Du1	10-03-07-141	DURANES 1		Feb-87	2.97	481		634	7.9	17.0	68	NaSO4	4
Du2	10-02-01-431	DURANES 2		Sep-73	2.56		295	406	7.9			NaHCO3	5 & 7
Du2	10-02-01-431	DURANES 2	+2	Jan-76	2.49		316	460	8.1			NaHCO3	6
Du2	10-02-01-431	DURANES 2		Feb-87	2.25	302		397	7.9	18.0	66	NaHCO3	4
Du3	10-02-12-412	DURANES 3		May-57	2.97	358		499	7.7	21.1	64	NaHCO3	1
Du3	10-02-12-412	DURANES 3		Sep-73	2.87		425	504	8.1			NaHCO3	5 & 7
Du3	10-02-12-412	DURANES 3		Jan-76	2.78		382	584	7.8			NaHCO3	6
Du3	10-02-12-412	DURANES 3		Feb-87	2.74	354		475	7.8	19.0	60	NaHCO3	4
Du4	10-02-12-312	DURANES 4		Sep-73	2.66		345	449	8.1			NaHCO3	5 & 7
Du4	10-02-12-312	DURANES 4	+2	Jan-76	2.30		335	490	8.1			NaHCO3	6
Du4	10-02-12-312	DURANES 4		Feb-87	2.19	300		490	8.3	19.0	49	NaHCO3	4
Du5	10-02-13-112	DURANES 5		Sep-73	2.63		305	432	8.1			NaHCO3	5 & 7

APPENDIX III: GROUND-WATER QUALITY DATA

MAP CODE	WELL LOCATION	WELL NAME	SAMPLE DATE	Ca (meq/L)	Mg (meq/L)	Na (meq/L)	K (meq/L)	Na+K-Na (meq/L)	HCO3 (meq/L)	SO4 (meq/L)	Cl (meq/L)	Hard. (meq/L)
Du5	10-02-13-112	DURANES 5	+2 Jan-76	1.30	0.53	2.65	0.16	2.81	2.54	1.51	0.42	1.83
Du5	10-02-13-112	DURANES 5	Feb-87	0.95	0.33	2.18	0.15	2.33	2.45	1.35	0.39	1.28
Du6	10-02-12-222	DURANES 6	Oct-73	3.39	1.20	2.30	0.28	2.58	3.62	2.42	0.52	4.59
Du6	10-02-12-222	DURANES 6	+2 Jan-76	2.40	1.03	1.80	0.24	2.04	3.18	1.88	0.45	3.43
Du6	10-02-12-222	DURANES 6	Feb-87	1.65	0.66	1.44	0.20	1.64	2.91	1.75	0.45	2.30
Du7	10-02-12-121	DURANES 7	Oct-73	2.05	0.55	2.50	0.20	2.70	2.53	2.00	0.38	2.60
Du7	10-02-12-121	DURANES 7	Jan-76	1.47	0.87	2.40	0.18	2.58	2.45	1.76	0.38	2.34
Du7	10-02-12-121	DURANES 7	Feb-87	1.70	0.58	1.57	0.18	1.75	2.22	1.46	0.34	2.27
Gr1	11-03-31-231	GRIEGOS 1	+2 Jan-76	2.09	0.96	1.18	0.21	1.39	2.41	1.35	0.41	3.05
Gr1	11-03-31-231	GRIEGOS 1	Feb-87	2.00	0.91	1.04	0.20	1.24	2.31	1.19	0.39	2.90
Gr2	10-03-06-121	GRIEGOS 2	Dec-65	2.15	0.33	1.26	0.18	1.44	2.74	1.69	0.31	2.48
Gr2	10-03-06-121	GRIEGOS 2	Oct-73	2.40	0.81	1.90	0.23	2.13	2.83	1.67	0.37	3.20
Gr2	10-03-06-121	GRIEGOS 2	+2 Jan-76	2.73	1.31	1.70	0.26	1.96	3.20	2.15	0.46	4.04
Gr2	10-03-06-121	GRIEGOS 2	Feb-87	2.84	1.23	1.78	0.26	2.04	3.34	2.14	0.48	4.08
Gr3	11-02-36-442	GRIEGOS 3	Sep-73	1.48	0.45	2.10	0.15	2.25	2.40	1.32	0.39	1.93
Gr3	11-02-36-442	GRIEGOS 3	Jan-76	1.46	0.72	2.00	0.18	2.18	2.41	1.42	0.34	2.18
Gr3	11-02-36-442	GRIEGOS 3	Feb-87	1.45	0.49	2.00	0.13	2.13	2.21	1.29	0.34	1.94
Gr4	11-03-32-143	GRIEGOS 4	+2 Jan-76	1.57	0.86	1.40	0.19	1.59	2.38	0.95	0.36	2.43
Gr4	11-03-32-143	GRIEGOS 4	Feb-87	1.40	0.58	1.52	0.15	1.67	2.34	0.87	0.28	1.97
Gr5	11-03-31-442	GRIEGOS 5	Sep-73	1.25	0.51	1.65	0.16	1.81	2.32	0.81	0.36	1.76
Gr5	11-03-31-442	GRIEGOS 5	+2 Jan-76	2.49	1.25	2.05	0.25	2.30	3.34	1.98	0.51	3.73
K1	10-04-31-411	KAFB 1	Mar-57	2.99	0.91			1.04	3.20	1.39	0.28	3.90
K1	10-04-31-411	KAFB 1	May-59	2.50	0.42			1.31	2.82	1.02	0.34	2.92
K1	10-04-31-411	KAFB 1	May-60	3.39	0.75			1.22	3.38	1.56	0.34	4.14
K1	10-04-31-411	KAFB 1	May-61	2.54	0.42			1.17	2.84	1.00	0.25	2.97
K1	10-04-31-411	KAFB 1	May-62	2.64	0.36			1.17	2.85	1.00	0.26	3.01
K1	10-04-31-411	KAFB 1	Nov-67	0.16	0.14	13.49	0.04	13.53	7.74	0.01	6.46	0.30
K1	10-04-31-411	KAFB 1	Nov-68	0.23	0.05	14.57	0.04	14.61	8.08	0.00	6.80	0.28
K1	10-04-31-411	KAFB 1	Sep-69	2.64	0.60			1.26	2.85	1.15	0.42	3.25
K1	10-04-31-411	KAFB 1	Sep-71	2.45	0.63	1.22	0.07	1.29	2.88	1.17	0.39	3.07
K1	10-04-31-411	KAFB 1	Dec-74	2.74	0.63	1.17	0.08	1.25	2.77	1.23	0.39	3.37
K1	10-04-31-411	KAFB 1	Nov-75	2.59	0.60	1.13	0.07	1.20	2.77	1.29	0.37	3.20
K2	09-03-01-112	KAFB 2	Mar-57	1.75	0.61			0.83	2.23	0.56	0.39	2.35
K2	09-03-01-112	KAFB 2	May-59	1.75	0.41			1.04	2.23	0.60	0.34	2.16
K2	09-03-01-112	KAFB 2	May-60	1.70	0.40			1.00	2.20	0.60	0.25	2.10
K2	09-03-01-112	KAFB 2	May-61	1.80	0.40			1.09	2.21	0.56	0.48	2.20
K2	09-03-01-112	KAFB 2	May-62	1.85	0.37			1.04	2.21	0.58	0.45	2.22
K2	09-03-01-112	KAFB 2	Jun-63	1.75	0.49			1.09	2.23	0.58	0.48	2.24
K2	09-03-01-112	KAFB 2	Jul-67	1.80	0.38			1.00	2.16	0.58	0.42	2.18
K2	09-03-01-112	KAFB 2	Sep-71	1.70	0.44	1.00	0.06	1.06	2.21	0.69	0.42	2.13
K2	09-03-01-112	KAFB 2	Oct-72	1.70	0.42	1.00	0.06	1.06	2.23	0.58	0.37	2.12
K3	10-04-30-321	KAFB 3	Mar-57	1.85	0.58			0.74	2.44	0.50	0.20	2.43
K3	10-04-30-321	KAFB 3	May-59	1.90	0.30			1.04	2.46	0.48	0.27	2.19
K3	10-04-30-321	KAFB 3	May-60	1.90	0.36			0.91	2.44	0.48	0.19	2.26
K3	10-04-30-321	KAFB 3	May-61	1.95	0.33			0.96	2.49	0.50	0.18	2.28
K3	10-04-30-321	KAFB 3	May-62	2.05	0.25			0.91	2.51	0.48	0.20	2.29
K3	10-04-30-321	KAFB 3	Jun-63	1.90	0.38			0.96	2.47	0.50	0.21	2.27
K3	10-04-30-321	KAFB 3	Jul-67	1.90	0.34			1.00	2.43	0.50	0.25	2.23
K3	10-04-30-321	KAFB 3	Nov-67	0.10	0.10	16.70	0.03	16.73	7.87	0.01	8.80	0.20
K3	10-04-30-321	KAFB 3	Nov-68	0.16	0.04	16.53	0.03	16.56	8.20	0.05	8.46	0.20
K3	10-04-30-321	KAFB 3	Sep-71	1.85	0.40	0.91	0.06	0.97	2.51	0.52	0.23	2.25
K3	10-04-30-321	KAFB 3	Oct-72	1.85	0.39	0.96	0.06	1.02	2.43	0.50	0.27	2.23
K4	09-04-06-322	KAFB 4	Mar-57	2.84	1.07			0.91	3.11	1.33	0.31	3.91

APPENDIX III: GROUND-WATER QUALITY DATA

MAP CODE	WELL LOCATION	WELL NAME	SAMPLE DATE	Alka. (meq/L)	TDS (mg/L)	TDR (mg/L)	S.C. uS/cm	pH	Temp. (C)	SiO2 (mg/L)	WATER TYPE	DATA SOURCE
Du5	10-02-13-112	DURANES 5	+2 Jan-76	2.54		333	488	8.2			NaHCO3	6
Du5	10-02-13-112	DURANES 5	Feb-87	2.46	278		483	8.1	19.0	45	NaHCO3	4
Du6	10-02-12-222	DURANES 6	Oct-73	3.62		450	624	8.2			CaHCO3	5 & 7
Du6	10-02-12-222	DURANES 6	+2 Jan-76	3.18		396	557	8.1			CaHCO3	6
Du6	10-02-12-222	DURANES 6	Feb-87	2.91	313		586	7.9	18.0	43	CaHCO3	4
Du7	10-02-12-121	DURANES 7	Oct-73	2.53		315	447	8.0			NaHCO3	5 & 7
Du7	10-02-12-121	DURANES 7	Jan-76	2.45		335	461	8.2			NaHCO3	6
Du7	10-02-12-121	DURANES 7	Feb-87	2.22	274		418	8.3	14.0	41	CaHCO3	4
Gr1	11-03-31-231	GRIEGOS 1	+2 Jan-76	2.41		302	440	8.1			CaHCO3	6
Gr1	11-03-31-231	GRIEGOS 1	Feb-87	2.31	284		375	7.7	18.0	60	CaHCO3	4
Gr2	10-03-06-121	GRIEGOS 2	Dec-65	2.74		342	455	8.0			CaHCO3	7
Gr2	10-03-06-121	GRIEGOS 2	Oct-73	2.83		325	468	8.3			CaHCO3	5 & 7
Gr2	10-03-06-121	GRIEGOS 2	+2 Jan-76	3.20		413	589	8.1			CaHCO3	6
Gr2	10-03-06-121	GRIEGOS 2	Feb-87	3.33	406		546	7.9	18.0	62	CaHCO3	4
Gr3	11-02-36-442	GRIEGOS 3	Sep-73	2.40		295	386	7.8			NaHCO3	5 & 7
Gr3	11-02-36-442	GRIEGOS 3	Jan-76	2.41		300	404	8.2			NaHCO3	6
Gr3	11-02-36-442	GRIEGOS 3	Feb-87	2.21	278		438	8.2	18.0	51	NaHCO3	4
Gr4	11-03-32-143	GRIEGOS 4	+2 Jan-76	2.38		280	399	8.1			CaHCO3	6
Gr4	11-03-32-143	GRIEGOS 4	Feb-87	2.34	253		403	8.0	18.0	53	NaHCO3	4
Gr5	11-03-31-442	GRIEGOS 5	Sep-73	2.32		270	335	7.8			NaHCO3	5 & 7
Gr5	11-03-31-442	GRIEGOS 5	+2 Jan-76	3.34		409	600	8.0			CaHCO3	6
K1	10-04-31-411	KAFB 1	Mar-57	3.20	297		474	7.7	14.4	27	CaHCO3	1
K1	10-04-31-411	KAFB 1	May-59	2.82	261	249	389	7.7		28	CaHCO3	2
K1	10-04-31-411	KAFB 1	May-60	3.38	324	333	504	7.5		28	CaHCO3	2
K1	10-04-31-411	KAFB 1	May-61	2.84	254	253	395	7.6		26	CaHCO3	2
K1	10-04-31-411	KAFB 1	May-62	2.85	257	252	395	7.8		27	CaHCO3	2
K1	10-04-31-411	KAFB 1	Nov-67	7.73	792	810	1410	7.9		12	NaHCO3	2
K1	10-04-31-411	KAFB 1	Nov-68	8.08	838	846	1490	8.0		10	NaHCO3	2
K1	10-04-31-411	KAFB 1	Sep-69	2.85	274	280	430	7.5		26	CaHCO3	2
K1	10-04-31-411	KAFB 1	Sep-71	2.88	277	274	428	7.7		29	CaHCO3	2
K1	10-04-31-411	KAFB 1	Dec-74	2.77	280	285	444	7.9		28	CaHCO3	2
K1	10-04-31-411	KAFB 1	Nov-75	2.77	275	269	450	8.0		25	CaHCO3	2
K2	09-03-01-112	KAFB 2	Mar-57	2.23	202		319	7.5	17.2	32	CaHCO3	1
K2	09-03-01-112	KAFB 2	May-59	2.23	208	200	297	7.8		34	CaHCO3	2
K2	09-03-01-112	KAFB 2	May-60	2.20	199	204	299	7.4		33	CaHCO3	2
K2	09-03-01-112	KAFB 2	May-61	2.21	209	211	320	7.7		32	CaHCO3	2
K2	09-03-01-112	KAFB 2	May-62	2.21	209	208	317	7.7		33	CaHCO3	2
K2	09-03-01-112	KAFB 2	Jun-63	2.23	213	214	316	7.4		34	CaHCO3	2
K2	09-03-01-112	KAFB 2	Jul-67	2.16	207	212	321	7.8		35	CaHCO3	2
K2	09-03-01-112	KAFB 2	Sep-71	2.21	216	212	321	7.6		36	CaHCO3	2
K2	09-03-01-112	KAFB 2	Oct-72	2.23	208	236	308	6.8			CaHCO3	2
K3	10-04-30-321	KAFB 3	Mar-57	2.44	193		310	7.7	14.4	26	CaHCO3	1
K3	10-04-30-321	KAFB 3	May-59	2.46	200	190	304	7.9		26	CaHCO3	2
K3	10-04-30-321	KAFB 3	May-60	2.44	194	206	308	7.6		26	CaHCO3	2
K3	10-04-30-321	KAFB 3	May-61	2.49	198	195	309	7.6		25	CaHCO3	2
K3	10-04-30-321	KAFB 3	May-62	2.51	198	192	306	7.8		26	CaHCO3	2
K3	10-04-30-321	KAFB 3	Jun-63	2.47	198	200	307	7.8		26	CaHCO3	2
K3	10-04-30-321	KAFB 3	Jul-67	2.43	204	204	315	7.6		31	CaHCO3	2
K3	10-04-30-321	KAFB 3	Nov-67	7.87	951	960	1670	8.0		13	NaHCO3	2
K3	10-04-30-321	KAFB 3	Nov-68	8.19	946	950	1650	7.9		11	NaHCO3	2
K3	10-04-30-321	KAFB 3	Sep-71	2.51	205	200	316	7.7		28	CaHCO3	2
K3	10-04-30-321	KAFB 3	Oct-72	2.43	202	208	305	6.8		27	CaHCO3	2
K4	09-04-06-322	KAFB 4	Mar-57	3.11	289		464	7.6	14.4	27	CaHCO3	1

APPENDIX III: GROUND-WATER QUALITY DATA

MAP CODE	WELL LOCATION	WELL NAME	SAMPLE DATE	Ca (meq/L)	Mg (meq/L)	Na (meq/L)	K (meq/L)	Na+K-Na (meq/L)	HCO3 (meq/L)	SO4 (meq/L)	Cl (meq/L)	Hard. (meq/L)
K4	09-04-06-322	KAFB 4	May-60	2.84	0.72			1.17	3.05	1.29	0.31	3.57
K4	09-04-06-322	KAFB 4	May-61	3.39	0.91			1.22	3.39	1.64	0.39	4.30
K4	09-04-06-322	KAFB 4	May-62	2.94	0.64			1.17	3.10	1.27	0.31	3.59
K4	09-04-06-322	KAFB 4	Jun-63	2.99	0.53			1.17	3.03	1.25	0.34	3.52
K4	09-04-06-322	KAFB 4	Jul-66	2.74	0.74			1.26	3.08	1.25	0.34	3.48
K4	09-04-06-322	KAFB 4	Nov-67	0.06	0.06	10.40	0.03	10.43	6.06	0.00	4.88	0.12
K4	09-04-06-322	KAFB 4	Nov-68	0.65	0.15	2.61	0.04	2.65	1.57	0.35	1.52	0.80
K4	09-04-06-322	KAFB 4	Sep-69	2.69	0.71			1.22	3.11	1.15	0.27	3.40
K4	09-04-06-322	KAFB 4	Sep-71	2.59	0.74	1.13	0.07	1.20	3.06	1.27	0.31	3.33
K4	09-04-06-322	KAFB 4	Oct-72	1.95	0.52	1.09	0.06	1.15	2.61	0.75	0.22	2.46
K4	09-04-06-322	KAFB 4	Dec-74	2.50	0.72	1.09	0.08	1.17	3.03	1.04	0.31	3.21
K5	10-04-29-324	KAFB 5	May-55	3.69	1.15			1.13	3.77	1.71	0.34	4.84
K5	10-04-29-324	KAFB 5	May-59	3.84	0.80			1.26	3.64	1.60	0.54	4.64
K5	10-04-29-324	KAFB 5	May-61	3.74	0.72			1.31	3.74	1.62	0.31	4.47
K5	10-04-29-324	KAFB 5	May-62	3.29	0.65			1.39	3.61	1.37	0.28	3.94
K5	10-04-29-324	KAFB 5	Jun-63	2.84	0.70			1.26	3.18	1.25	0.28	3.54
K5	10-04-29-324	KAFB 5	Jun-64	2.79	0.65			1.31	3.18	1.21	0.25	3.44
K5	10-04-29-324	KAFB 5	Jul-67	2.84	0.56			1.39	3.06	1.31	0.34	3.40
K5	10-04-29-324	KAFB 5	Nov-67	0.06	0.06	10.05	0.03	10.08	6.00	0.00	4.51	0.12
K5	10-04-29-324	KAFB 5	Nov-68	0.10	0.00	10.53	0.03	10.56	6.03	0.00	4.60	0.10
K5	10-04-29-324	KAFB 5	Nov-69	2.69	0.79			1.22	3.08	1.15	0.37	3.48
K6	10-04-32-433	KAFB 6	Mar-57	3.54	1.15			0.91	3.47	1.64	0.34	4.69
K6	10-04-32-433	KAFB 6	May-59	3.79	0.73			1.09	3.49	1.58	0.39	4.53
K6	10-04-32-433	KAFB 6	May-60	3.79	0.79			1.09	3.47	1.67	0.37	4.58
K6	10-04-32-433	KAFB 6	May-61	3.74	0.74			1.13	3.44	1.64	0.34	4.48
K6	10-04-32-433	KAFB 6	May-62	3.79	0.71			1.09	3.31	1.64	0.37	4.50
K6	10-04-32-433	KAFB 6	Jun-63	3.34	0.80			1.22	6.05	1.52	0.39	4.14
K6	10-04-32-433	KAFB 6	Nov-67	0.07	0.04	10.53	0.02	10.55	7.74	0.00	4.68	0.12
K6	10-04-32-433	KAFB 6	Nov-68	0.18	0.06	14.70	0.04	14.74	3.57	0.00	7.14	0.24
K6	10-04-32-433	KAFB 6	Nov-69	3.19	0.99			1.39	3.47	1.54	0.31	4.18
K6	10-04-32-433	KAFB 6	Sep-71	3.44	0.82	1.13	0.05	1.18	3.39	1.62	0.39	4.27
K6	10-04-32-433	KAFB 6	Oct-72	3.39	0.82	1.17	0.05	1.22	3.26	1.42	0.37	4.22
K6	10-04-32-433	KAFB 6	Nov-75	2.94	0.81	1.09	0.07	1.16	3.26	1.27	0.34	3.75
K7	09-03-01-222	KAFB 7	Mar-57	1.95	0.78			0.74	2.56	0.67	0.19	2.73
K7	09-03-01-222	KAFB 7	May-59	2.05	0.43			1.04	2.56	0.60	0.31	2.47
K7	09-03-01-222	KAFB 7	May-60	2.00	0.42			0.96	2.49	0.60	0.22	2.42
K7	09-03-01-222	KAFB 7	May-61	2.00	0.48			1.00	2.57	0.65	0.22	2.47
K7	09-03-01-222	KAFB 7	May-62	2.25	0.39			1.00	2.64	0.71	0.22	2.63
K7	09-03-01-222	KAFB 7	Jun-63	2.15	0.47			1.04	2.61	0.73	0.24	2.61
K7	09-03-01-222	KAFB 7	Jun-64	2.25	0.43			1.04	2.69	0.77	0.21	2.67
K7	09-03-01-222	KAFB 7	Jul-66	2.15	0.55			1.09	2.67	0.77	0.27	2.70
K7	09-03-01-222	KAFB 7	Nov-67	0.22	0.17	7.26	0.04	7.30	5.05	0.15	2.51	0.40
K7	09-03-01-222	KAFB 7	Nov-68	0.26	0.24	12.01	0.05	12.06	6.75	0.07	5.70	0.50
K7	09-03-01-222	KAFB 7	Sep-71	2.05	0.50	0.96	0.06	1.02	2.67	0.81	0.24	2.55
K7	09-03-01-222	KAFB 7	Oct-72	1.75	0.46	0.96	0.05	1.01	2.47	0.56	0.25	2.21
K7	09-03-01-222	KAFB 7	Nov-75	1.80	0.48	0.91	0.06	0.97	2.41	0.54	0.25	2.27
K8	09-04-05-332	KAFB 8	Mar-57	3.44	1.23			0.83	3.34	1.48	0.42	4.68
K8	09-04-05-332	KAFB 8	May-59	2.74	0.62			1.26	3.00	1.06	0.37	3.36
K8	09-04-05-332	KAFB 8	May-60	2.94	0.82			1.13	3.08	1.25	0.39	3.77
K8	09-04-05-332	KAFB 8	May-61	3.49	0.82			1.04	3.29	1.35	0.45	4.32
K8	09-04-05-332	KAFB 8	May-62	3.09	0.73			1.17	3.11	1.29	0.39	3.83
K8	09-04-05-332	KAFB 8	Jun-63	3.09	0.69			1.17	3.08	1.27	0.39	3.79
K8	09-04-05-332	KAFB 8	Jun-64	2.94	0.78			1.26	3.15	1.27	0.37	3.73

APPENDIX III: GROUND-WATER QUALITY DATA

MAP CODE	WELL LOCATION	WELL NAME	SAMPLE DATE	Alka. (meq/L)	TDS (mg/L)	TDR (mg/L)	S.C. uS/cm	pH	Temp. (C)	SiO2 (mg/L)	WATER TYPE	DATA SOURCE
K4	09-04-06-322	KAFB 4	May-60	3.05	288	290	449	7.5		28	CaHCO3	2
K4	09-04-06-322	KAFB 4	May-61	3.39	332	338	521	7.4		26	CaHCO3	2
K4	09-04-06-322	KAFB 4	May-62	3.10	289	290	450	7.7		27	CaHCO3	2
K4	09-04-06-322	KAFB 4	Jun-63	3.03	287	295	444	7.6		27	CaHCO3	2
K4	09-04-06-322	KAFB 4	Jul-66	3.08	287	302	452	7.5		27	CaHCO3	2
K4	09-04-06-322	KAFB 4	Nov-67	6.06	610	630	1080	7.9		12	NaHCO3	2
K4	09-04-06-322	KAFB 4	Nov-68	1.57	206	206	369	7.2		10	NaHCO3	2
K4	09-04-06-322	KAFB 4	Sep-69	3.11	277	280	432	7.7		26	CaHCO3	2
K4	09-04-06-322	KAFB 4	Sep-71	3.06	287	284	447	7.7		29	CaHCO3	2
K4	09-04-06-322	KAFB 4	Oct-72	2.61	226	224	341	7.0		28	CaHCO3	2
K4	09-04-06-322	KAFB 4	Dec-74	3.03	272	274	434	8.4		29	CaHCO3	2
K5	10-04-29-324	KAFB 5	May-55	3.77	354	354	555	7.6	21.5	27	CaHCO3	3
K5	10-04-29-324	KAFB 5	May-59	3.64	353	350	556	7.4		26	CaHCO3	2
K5	10-04-29-324	KAFB 5	May-61	3.74	345	351	542	7.4		25	CaHCO3	2
K5	10-04-29-324	KAFB 5	May-62	3.61	320	316	491	7.7		26	CaHCO3	2
K5	10-04-29-324	KAFB 5	Jun-63	3.18	290	300	455	7.4		26	CaHCO3	2
K5	10-04-29-324	KAFB 5	Jun-64	3.18	286	286	447	7.6		26	CaHCO3	2
K5	10-04-29-324	KAFB 5	Jul-67	3.06	292	300	448	7.5		26	CaHCO3	2
K5	10-04-29-324	KAFB 5	Nov-67	6.00	587	600	1040	7.4		12	NaHCO3	2
K5	10-04-29-324	KAFB 5	Nov-68	6.03	598	606	1080	7.7		7	NaHCO3	2
K5	10-04-29-324	KAFB 5	Nov-69	3.08	283	286	440	8.1		27	CaHCO3	2
K6	10-04-32-433	KAFB 6	Mar-57	3.47	334		534	7.6	16.7	24	CaHCO3	1
K6	10-04-32-433	KAFB 6	May-59	3.49	337	350	527	7.7		25	CaHCO3	2
K6	10-04-32-433	KAFB 6	May-60	3.47	341	354	538	7.4		25	CaHCO3	2
K6	10-04-32-433	KAFB 6	May-61	3.44	338	344	532	7.4		24	CaHCO3	2
K6	10-04-32-433	KAFB 6	May-62	3.31	338	348	535	7.7		25	CaHCO3	2
K6	10-04-32-433	KAFB 6	Jun-63	6.05	323	338	506	7.4		25	CaHCO3	2
K6	10-04-32-433	KAFB 6	Nov-67	7.73	616	647	1120	8.0		12	NaHCO3	2
K6	10-04-32-433	KAFB 6	Nov-68	3.57	841	841	1510	7.8		9	NaCl	2
K6	10-04-32-433	KAFB 6	Nov-69	3.47	336	322	499	7.8		27	CaHCO3	2
K6	10-04-32-433	KAFB 6	Sep-71	3.39	342	342	541	7.5		26	CaHCO3	2
K6	10-04-32-433	KAFB 6	Oct-72	3.26	327	342	507	6.9		26	CaHCO3	2
K6	10-04-32-433	KAFB 6	Nov-75	3.26	302	287	494	7.7		24	CaHCO3	2
K7	09-03-01-222	KAFB 7	Mar-57	2.56	212		341	7.8	16.7	28	CaHCO3	1
K7	09-03-01-222	KAFB 7	May-59	2.56	217	210	328	8.0		27	CaHCO3	2
K7	09-03-01-222	KAFB 7	May-60	2.49	210	212	325	7.6		28	CaHCO3	2
K7	09-03-01-222	KAFB 7	May-61	2.57	214	210	330	7.7		27	CaHCO3	2
K7	09-03-01-222	KAFB 7	May-62	2.64	223	222	345	7.9		27	CaHCO3	2
K7	09-03-01-222	KAFB 7	Jun-63	2.61	225	228	348	7.7		28	CaHCO3	2
K7	09-03-01-222	KAFB 7	Jun-64	2.69	231	238	354	7.8		28	CaHCO3	2
K7	09-03-01-222	KAFB 7	Jul-66	2.67	232	244	357	7.7		28	CaHCO3	2
K7	09-03-01-222	KAFB 7	Nov-67	5.05	443	444	755	7.6		19	NaHCO3	2
K7	09-03-01-222	KAFB 7	Nov-68	6.75	710	710	1260	7.9		15	NaHCO3	2
K7	09-03-01-222	KAFB 7	Sep-71	2.67	233	228	355	7.7		30	CaHCO3	2
K7	09-03-01-222	KAFB 7	Oct-72	2.47	205	202	313	7.1		28	CaHCO3	2
K7	09-03-01-222	KAFB 7	Nov-75	2.41	200	221	318	7.9		25	CaHCO3	2
K8	09-04-05-332	KAFB 8	Mar-57	3.34	333		576	7.7	16.7	28	CaHCO3	1
K8	09-04-05-332	KAFB 8	May-59	3.00	285	290	439	7.8		29	CaHCO3	2
K8	09-04-05-332	KAFB 8	May-60	3.08	301	311	472	7.5		28	CaHCO3	2
K8	09-04-05-332	KAFB 8	May-61	3.29	327	338	521	7.5		26	CaHCO3	2
K8	09-04-05-332	KAFB 8	May-62	3.11	305	302	476	7.7		27	CaHCO3	2
K8	09-04-05-332	KAFB 8	Jun-63	3.08	303	312	474	7.6		27	CaHCO3	2
K8	09-04-05-332	KAFB 8	Jun-64	3.15	304	312	471	7.7		27	CaHCO3	2

APPENDIX III: GROUND-WATER QUALITY DATA

MAP CODE	WELL LOCATION	WELL NAME	SAMPLE DATE	Ca (meq/L)	Mg (meq/L)	Na (meq/L)	K (meq/L)	Na+K-Na (meq/L)	HCO3 (meq/L)	SO4 (meq/L)	Cl (meq/L)	Hard. (meq/L)
K8	09-04-05-332	KAFB 8	Jul-66	3.19	0.99			1.22	3.26	1.35	0.48	4.18
K8	09-04-05-332	KAFB 8	Sep-68	3.29	0.91			1.22	3.34	1.35	0.39	4.20
K8	09-04-05-332	KAFB 8	Nov-69	3.19	0.99			1.22	3.38	1.35	0.39	4.18
K8	09-04-05-332	KAFB 8	Sep-71	3.14	0.99	1.13	0.07	1.20	3.34	1.44	0.45	4.13
K8	09-04-05-332	KAFB 8	Oct-72	3.19	0.91	1.17	0.07	1.24	3.38	1.27	0.42	4.10
K10	09-04-20-221	KAFB 10	Jul-57	3.29	1.56			2.52	4.59	1.23	1.35	4.85
K11	09-04-04-211	KAFB 11	Mar-72	3.24	0.99	1.52	0.08	1.60	3.11	1.71	0.56	4.23
K11	09-04-04-211	KAFB 11	Dec-74	3.14	0.99	1.52	0.09	1.61	3.25	1.58	0.56	4.13
K11	09-04-04-211	KAFB 11	Nov-75	3.54	1.07	1.22	0.08	1.30	3.47	1.23	0.45	4.61
K12	10-03-35-111	KAFB 12 (1)	Jul-57	1.65	0.54			0.83	2.13	0.62	0.24	2.19
K13	10-03-34-144	KAFB 13 (2)	Jan-57	1.65	0.67			0.52	2.00	0.60	0.21	2.31
Le1	10-02-33-244	LEAVITT 1	Jan-76	0.36	0.14	3.80	0.04	3.84	2.62	1.26	0.40	0.50
Le1	10-02-33-244	LEAVITT 1	Feb-87	0.20	0.00	4.83	0.00	4.83	2.25	1.71	0.45	0.20
Le2	10-02-33-442	LEAVITT 2	Jan-76	0.42	0.11	5.45	0.02	5.47	2.56	1.98	0.76	0.53
Le2	10-02-33-442	LEAVITT 2	Feb-87	0.20	0.00	4.92	0.00	4.92	2.66	1.25	0.54	0.20
Lm1	10-04-22-342	LOMAS 1	Apr-65	2.94	0.74			1.22	3.15	1.31	0.31	3.68
Lm1	10-04-22-342	LOMAS 1	Oct-73	2.99	0.70	1.20	0.08	1.28	3.10	1.33	0.45	3.69
Lm1	10-04-22-342	LOMAS 1	Jan-76	3.13	0.77	1.20	0.10	1.30	3.19	1.39	0.37	3.91
Lm1	10-04-22-342	LOMAS 1	Feb-87	3.34	0.82	1.17	0.08	1.25	3.05	1.50	0.45	4.17
Lm2	10-04-22-132	LOMAS 2	Jan-76	1.96	0.29	1.30	0.06	1.36	2.32	0.75	0.28	2.24
Lm2	10-04-22-132	LOMAS 2	Apr-85	2.40	0.00	1.44	0.06	1.50	2.55	0.90	0.20	2.40
Lm3	10-04-15-314	LOMAS 3	? Oct-73	1.85	0.27	1.22	0.06	1.28	2.46	0.69	0.19	2.12
Lm3	10-04-15-314	LOMAS 3	+2 Jan-76	2.04	0.37	1.35	0.06	1.41	2.41	0.94	0.24	2.41
Lm4	10-04-16-241	LOMAS 4	Nov-73	0.95	0.07	1.78	0.05	1.83	2.29	0.44	0.15	1.02
Lm4	10-04-16-241	LOMAS 4	+2 Jan-76	1.06	0.87	1.30	0.05	1.35	2.41	0.44	0.20	1.93
Lm5	10-04-21-344	LOMAS 5 (7)	Feb-79	1.30	0.30	1.61	0.07	1.68	2.20	0.71	0.21	1.60
Lm5	10-04-21-344	LOMAS 5 (7)	May-85	1.35	0.00	2.31	0.06	2.37	2.48	0.71	0.17	1.35
Lm6	10-04-28-223	LOMAS 6 (8)	Mar-79	1.95	0.45	1.61	0.08	1.69	2.39	1.10	0.27	2.40
Lm6	10-04-28-223	LOMAS 6 (8)	Apr-85	1.95	0.00	2.09	0.07	2.16	2.87	0.98	0.20	1.95
Lv1	10-04-16-334	LOVE 1	May-57	1.40	0.23			1.26	2.13	0.42	0.23	1.63
Lv1	10-04-16-334	LOVE 1	Oct-73	1.40	0.35	1.40	0.05	1.45	2.20	0.58	0.28	1.75
Lv1	10-04-16-334	LOVE 1	+2 Jan-76	1.63	0.49	1.94	0.05	1.99	2.42	1.05	0.43	2.11
Lv1	10-04-16-334	LOVE 1	May-85	1.55	0.00	1.91	0.05	1.96	2.23	0.81	0.28	1.55
Lv2	10-04-20-244	LOVE 2	Dec-65	1.70	0.40	1.31	0.05	1.36	2.46	0.75	0.20	2.10
Lv2	10-04-20-244	LOVE 2	Oct-73	1.70	0.26	1.40	0.06	1.46	2.25	0.58	0.30	1.95
Lv2	10-04-20-244	LOVE 2	+2 Jan-76	1.52	0.26	1.40	0.07	1.47	2.36	0.48	0.20	1.77
Lv3	10-04-20-212	LOVE 3	Oct-73	1.60	0.30	1.10	0.06	1.16	2.16	0.42	0.46	1.90
Lv3	10-04-20-212	LOVE 3	+2 Jan-76	1.33	0.65	1.05	0.06	1.11	2.16	0.35	0.34	1.98
Lv3	10-04-20-212	LOVE 3	May-85	1.50	0.00	1.52	0.06	1.58	1.78	0.46	0.48	1.50
Lv4	10-04-20-111	LOVE 4	Aug-58	2.00	0.10			1.13	2.13	0.40	0.62	2.10
Lv4	10-04-20-111	LOVE 4	Oct-74	2.00	0.55	1.20	0.07	1.27	2.28	0.57	1.05	2.55
Lv4	10-04-20-111	LOVE 4	Jan-76	2.24	0.49	1.10	0.07	1.17	2.13	0.45	1.12	2.73
Lv4	10-04-20-111	LOVE 4	Feb-87	2.54	0.16	1.48	0.08	1.56	1.83	0.50	2.09	2.71
Lv5	10-04-20-143	LOVE 5	Oct-73	1.75	0.35	1.10	0.07	1.17	2.06	0.42	0.63	2.10
Lv5	10-04-20-143	LOVE 5	+2 Jan-76	1.78	0.40	1.00	0.07	1.07	2.14	0.36	0.55	2.18
Lv5	10-04-20-143	LOVE 5	May-85	1.75	0.00	1.31	0.07	1.38	2.06	0.40	0.48	1.75
Lv6	10-04-16-123	LOVE 6	Jan-76	1.22	0.04	1.40	0.05	1.45	2.08	0.26	0.16	1.26
Lv6	10-04-16-123	LOVE 6	May-85	1.00	0.00	1.48	0.05	1.53	1.99	0.33	0.14	1.00
Lv7	10-04-08-434	LOVE 7	Jan-74	1.60	0.08	1.04	0.06	1.10	1.97	0.40	0.37	1.68
Lv7	10-04-08-434	LOVE 7	+2 Jan-76	1.74	0.27	1.00	0.06	1.06	2.09	0.37	0.41	2.01
Lv7	10-04-08-434	LOVE 7	May-85	1.90	0.00	1.17	0.06	1.23	2.02	0.37	0.45	1.90
Ly1	11-03-36-434	LEYENDECKER 1	Dec-65	1.90	0.42	0.87	0.05	0.92	2.24	0.62	0.27	2.32
Ly1	11-03-36-434	LEYENDECKER 1	Oct-73	2.05	0.26	0.90	0.05	0.95	2.27	0.62	2.06	2.30

APPENDIX III: GROUND-WATER QUALITY DATA

MAP CODE	WELL LOCATION	WELL NAME	SAMPLE DATE	Alka. (meq/L)	TDS (mg/L)	TDR (mg/L)	S.C. uS/cm	pH	Temp. (C)	SiO2 (mg/L)	WATER TYPE	DATA SOURCE
K8	09-04-05-332	KAFB 8	Jul-66	3.26	327	345	509	7.6		27	CaHCO3	2
K8	09-04-05-332	KAFB 8	Sep-68	3.34	327	330	508	7.7		26	CaHCO3	2
K8	09-04-05-332	KAFB 8	Nov-69	3.38	332	333	502	8.1		30	CaHCO3	2
K8	09-04-05-332	KAFB 8	Sep-71	3.34	336	332	523	7.6		30	CaHCO3	2
K8	09-04-05-332	KAFB 8	Oct-72	3.38	326	374	505	7.0		28	CaHCO3	2
K10	09-04-20-221	KAFB 10	Jul-57	4.59	425	427	704	7.6	23.0	28	CaHCO3	1
K11	09-04-04-211	KAFB 11	Mar-72	3.11	370	368	569	7.5	22.5	28	CaHCO3	2
K11	09-04-04-211	KAFB 11	Dec-74	3.24	358	354	569	8.2		28	CaHCO3	2
K11	09-04-04-211	KAFB 11	Nov-75	3.47	360	352	589	7.6		26	CaHCO3	2
K12	10-03-35-111	KAFB 12 (1)	Jul-57	2.13	200	200	292	7.9		38	CaHCO3	1
K13	10-03-34-144	KAFB 13 (2)	Jan-57	2.00	197		284	7.6		47	CaHCO3	1
Le1	10-02-33-244	LEAVITT 1	Jan-76	2.62	296		458	8.5			NaHCO3	6
Le1	10-02-33-244	LEAVITT 1	Feb-87	2.25	331		504	8.9	29.0	39	NaHCO3	4
Le2	10-02-33-442	LEAVITT 2	Jan-76	2.56	406		619	8.7			NaHCO3	6
Le2	10-02-33-442	LEAVITT 2	Feb-87	2.66	318		473	8.8	24.0	32	NaHCO3	4
Lm1	10-04-22-342	LOMAS 1	Apr-65	3.15	300	308	472	7.7	23.5	25	CaHCO3	3
Lm1	10-04-22-342	LOMAS 1	Oct-73	3.10		325	466	7.6			CaHCO3	5 & 7
Lm1	10-04-22-342	LOMAS 1	Jan-76	3.19		313	520	7.9			CaHCO3	6
Lm1	10-04-22-342	LOMAS 1	Feb-87	3.05	318		486	7.8	22.0	19	CaHCO3	4
Lm2	10-04-22-132	LOMAS 2	Jan-76	2.32		229	368	7.7			CaHCO3	6
Lm2	10-04-22-132	LOMAS 2	Apr-85	2.54	244		390			27	CaHCO3	4
Lm3	10-04-15-314	LOMAS 3 ?	Oct-73	2.46	210	266	339	8.0	24.5	24	CaHCO3	3
Lm3	10-04-15-314	LOMAS 3 +2	Jan-76	2.41		230	374	8.0			CaHCO3	6
Lm4	10-04-16-241	LOMAS 4	Nov-73	2.29	190	187	283	8.2	25.0	34	NaHCO3	3
Lm4	10-04-16-241	LOMAS 4 +2	Jan-76	2.41		182	311	8.0			NaHCO3	6
Lm5	10-04-21-344	LOMAS 5 (7)	Feb-79	2.20	210		350	7.6	26.5	26	NaHCO3	3
Lm5	10-04-21-344	LOMAS 5 (7)	May-85	2.48	229		368			30	NaHCO3	4
Lm6	10-04-28-223	LOMAS 6 (8)	Mar-79	2.39	250		400	7.6	25.0	26	CaHCO3	3
Lm6	10-04-28-223	LOMAS 6 (8)	Apr-85	2.87	260		411			27	NaHCO3	4
Lv1	10-04-16-334	LOVE 1	May-57	2.13	184	187	283	7.9	24.0	29	CaHCO3	1
Lv1	10-04-16-334	LOVE 1	Oct-73	2.30		210	292	8.5			CaHCO3	5 & 7
Lv1	10-04-16-334	LOVE 1 +2	Jan-76	2.42		219		8.1			NaHCO3	6
Lv1	10-04-16-334	LOVE 1	May-85	2.23	224					28	NaHCO3	4
Lv2	10-04-20-244	LOVE 2	Dec-65	2.46		220	335	8.3			CaHCO3	7
Lv2	10-04-20-244	LOVE 2	Oct-73	2.40		215	313	8.5			CaHCO3	5 & 7
Lv2	10-04-20-244	LOVE 2 +2	Jan-76	2.36		200	324	8.1			CaHCO3	6
Lv3	10-04-20-212	LOVE 3	Oct-73	2.16		190	281	8.4			CaHCO3	7
Lv3	10-04-20-212	LOVE 3 +2	Jan-76	2.16		172	299	8.1			CaHCO3	6
Lv3	10-04-20-212	LOVE 3	May-85	1.78	193		301			31	NaHCO3	4
Lv4	10-04-20-111	LOVE 4	Aug-58	2.13	200	206	315	7.9	21.5	28	CaHCO3	1
Lv4	10-04-20-111	LOVE 4	Oct-74	2.28			375	8.1			CaHCO3	5 & 7
Lv4	10-04-20-111	LOVE 4	Jan-76	2.13		250	388	8.1			CaHCO3	6
Lv4	10-04-20-111	LOVE 4	Feb-87	1.83	269		478		23.0	26	CaCl	4
Lv5	10-04-20-143	LOVE 5	Oct-73	2.19		215	308	8.4			CaHCO3	7
Lv5	10-04-20-143	LOVE 5 +2	Jan-76	2.14		165	321	8.2			CaHCO3	6
Lv5	10-04-20-143	LOVE 5	May-85	2.06	197		320			29	CaHCO3	4
Lv6	10-04-16-123	LOVE 6	Jan-76	2.08		142	270	8.1			NaHCO3	6
Lv6	10-04-16-123	LOVE 6	May-85	1.99	171					33	NaHCO3	4
Lv7	10-04-08-434	LOVE 7	Jan-74	1.97	183	182	284	7.9	24.0	32	CaHCO3	3
Lv7	10-04-08-434	LOVE 7 +2	Jan-76	2.09		160	297	8.1			CaHCO3	6
Lv7	10-04-08-434	LOVE 7	May-85	2.02	196					33	CaHCO3	4
Ly1	11-03-36-434	LEYENDECKER 1	Dec-65	2.24		207	315	8.1			CaHCO3	7
Ly1	11-03-36-434	LEYENDECKER 1	Oct-73	2.27		200	327	7.6			CaHCO3	5 & 7

MAP CODE	WELL LOCATION	WELL NAME	SAMPLE DATE	Ca (meq/L)	Mg (meq/L)	Na (meq/L)	K (meq/L)	Na+K-Na (meq/L)	HCO3 (meq/L)	SO4 (meq/L)	Cl (meq/L)	Hard. (meq/L)
Ly1	11-03-36-434	LEYENDECKER 1 +2	Jan-76	1.98	0.26	0.80	0.06	0.86	2.21	0.63	0.26	2.25
Ly1	11-03-36-434	LEYENDECKER 1	Feb-87	1.80	0.25	0.96	0.00	0.96	2.11	0.62	0.31	2.04
Ly2	10-03-01-244	LEYENDECKER 2	Nov-73	2.00	0.30	1.00	0.07	1.07	2.35	0.68	0.38	2.30
Ly2	10-03-01-244	LEYENDECKER 2 +2	Jan-76	1.98	0.44	0.95	0.06	1.01	2.35	0.74	0.23	2.41
Ly2	10-03-01-244	LEYENDECKER 2	Feb-87	1.95	0.25	0.96	0.05	1.01	2.15	0.62	0.25	2.19
Ly3	11-03-36-322	LEYENDECKER 3	Nov-73	2.00	0.20	0.70	0.06	0.76	2.19	0.55	0.37	2.19
Ly3	11-03-36-322	LEYENDECKER 3 +2	Jan-76	1.87	0.47	0.75	0.05	0.80	2.12	0.66	0.21	2.34
Ly3	11-03-36-322	LEYENDECKER 3	Feb-87	1.70	0.25	0.83	0.00	0.83	2.02	0.56	0.25	1.94
Ly4	11-03-36-422	LEYENDECKER 4 +2	Jan-76	1.97	0.47	1.05	0.05	1.10	2.33	0.78	0.26	2.43
Ly4	11-03-36-422	LEYENDECKER 4	Feb-87	1.90	0.25	1.09	0.00	1.09	2.35	0.69	0.28	2.14
Mi1	10-03-33-233	MILES 1	Jan-76	1.82	0.67	1.30	0.18	1.48	2.17	0.62	1.13	2.48
Mi1	10-03-33-233	MILES 1	Jun-80	1.70	0.59	1.44	0.18	1.62	2.20	0.71	0.99	2.29
Mi1	10-03-33-233	MILES 1	Feb-87	1.65	0.58	1.61	0.18	1.79	2.05	0.79	1.07	2.22
PH1	11-02-09-411	PARADISE HILL 1	Jan-73	1.61	0.31	1.70	0.14	1.84	2.54	0.96	0.25	1.92
PH1	11-02-09-411	PARADISE HILL 1	Jan-76	1.04	0.40	2.20	0.15	2.35	2.46	0.94	0.19	1.45
PH2	11-02-02-343	PARADISE HILL 2	Jan-73	1.50	0.35	2.00	0.18	2.18	2.75	0.80	0.33	1.85
PH3	11-02-03-221	PARADISE HILL 3	May-80	0.65	0.21	3.78	6.16	3.94	2.59	1.87	0.28	43.16
Po1	11-04-28-111	PONDEROSA 1(9)	Jun-79	2.20	0.15	1.87	0.10	1.97	2.18	0.65	1.72	2.35
Po1	11-04-28-111	PONDEROSA 1(9)	Feb-87	2.94	0.16	2.52	0.10	2.62	2.07	0.56	2.54	3.11
Po1a	10-04-04-212	PONDEROSA 1 abd.	Jan-73	1.80	0.15	1.00	0.04	1.04	2.40	0.36	0.12	1.95
Po1a	10-04-04-212	PONDEROSA 1 abd.+3	Jan-76	1.71	0.40	0.97	0.04	1.01	2.36	0.37	0.16	2.10
Po2	11-04-33-332	PONDEROSA 2	Feb-74	1.50	0.12	1.13	0.05	1.18	2.28	0.31	0.18	1.16
Po2	11-04-33-332	PONDEROSA 2 +2	Jan-76	1.47	0.50	0.95	0.05	1.00	2.20	0.39	0.20	1.97
Po2	11-04-33-332	PONDEROSA 2	Feb-87	1.85	0.16	1.13	0.05	1.18	2.06	0.40	0.45	2.01
Po3	11-04-32-234	PONDEROSA 3	Feb-87	2.25	0.58	2.74	0.13	2.87	2.42	0.73	2.29	2.82
Po4	11-04-33-113	PONDEROSA 4	Jun-79	1.40	0.12	1.35	0.03	1.38	2.20	0.35	0.20	1.52
Po4	11-04-33-113	PONDEROSA 4	Feb-87	1.45	0.00	1.39	0.00	1.39	2.31	0.31	0.39	1.45
Po5	11-04-28-113	PONDEROSA 5 (7)	Feb-87	1.55	0.16	1.74	0.00	1.74	2.06	0.42	0.82	1.71
Po6	11-04-29-431	PONDEROSA 6	Feb-87	2.05	0.58	2.74	0.15	2.89	2.50	0.73	2.29	2.62
PS	09-03-09-113	PUB.SRV.PERSON 3	May-56	1.60	0.71			1.48	2.13	0.69	0.90	2.30
Ri1	10-04-29-232	RIDGECREST 1	Jan-73	2.37	0.58	1.30	0.07	1.37	2.84	0.88	0.28	2.95
Ri1	10-04-29-232	RIDGECREST 1 +2	Jan-76	2.50	0.59	1.15	0.06	1.21	2.82	1.09	0.28	3.09
Ri1	10-04-29-232	RIDGECREST 1	Apr-85	2.69	0.41	1.65	0.07	1.72	2.90	1.06	0.25	3.11
Ri2	10-04-20-344	RIDGECREST 2	Jan-76	1.80	0.45	1.10	0.07	1.17	2.09	0.42	0.77	2.25
Ri2	10-04-20-344	RIDGECREST 2	May-85	1.70	0.00	1.65	0.08	1.73	1.82	0.42	0.87	1.70
Ri3	10-04-30-243	RIDGECREST 3	Jan-76	2.08	0.26	1.10	0.09	1.19	2.27	0.55	0.80	2.34
Ri3	10-04-30-243	RIDGECREST 3	Feb-87	1.80	0.33	1.17	0.05	1.22	1.79	0.40	1.21	2.13
Ri4	10-04-19-322	RIDGECREST 4	May-85	2.50	0.25	1.39	0.11	1.50	1.98	0.50	1.47	2.74
SB1	10-03-10-224	SANTA BARBARA 1	Jan-73	1.55	0.50	1.10	0.09	1.19	2.16	0.67	0.39	2.05
SB1	10-03-10-224	SANTA BARBARA 1 +2	Jan-76	1.54	0.56	1.05	0.09	1.14	2.12	0.66	0.29	2.10
SB1	10-03-10-224	SANTA BARBARA 1	Feb-87	1.45	0.41	1.61	0.13	1.74	3.06	0.77	0.28	1.86
SJ2	10-03-29-441	SAN JOSE 2(4:7)	Jan-73	1.10	0.40	2.10	0.18	2.28	2.18	0.87	0.81	1.50
SJ2	10-03-29-441	SAN JOSE 2(4:7) +2	Jan-76	1.59	0.76	1.65	0.22	1.87	2.19	1.02	0.83	2.34
SJ2	10-03-29-441	SAN JOSE 2(4:7)	Feb-87	1.40	0.49	1.87	0.20	2.07	1.95	1.12	0.82	1.89
SJ3	10-03-29-341	SAN JOSE 3(5:8)	Jan-73	0.80	0.40	3.40	0.17	3.57	2.77	1.30	0.52	1.20
SJ3	10-03-29-341	SAN JOSE 3(5:8) +2	Jan-76	1.00	0.49	2.60	0.18	2.78	2.24	1.35	0.54	1.48
SJ3	10-03-29-341	SAN JOSE 3(5:8)	Feb-87	1.05	0.41	2.61	0.18	2.79	2.13	1.39	0.42	1.46
SJ4	10-03-32-414	SAN JOSE 4(6:10)	Jan-73	1.61	0.56	2.25	0.19	2.44	2.21	1.27	0.95	2.17
SJ4	10-03-32-414	SAN JOSE 4(6:10) +2	Jan-76	3.32	1.88	1.20	0.25	1.45	2.58	3.05	1.09	5.19
SJ4	10-03-32-414	SAN JOSE 4(6:10)	Jun-80	1.70	0.60	2.09	0.21	2.30	1.88	1.35	1.02	2.30
Th1	11-04-32-333	THOMAS 1	May-65	2.74	0.30			2.04	2.64	0.62	1.81	3.04
Th1	11-04-32-333	THOMAS 1 +2	Jan-76	1.80	1.19	1.70	0.06	1.76	2.61	0.54	1.57	2.98
Th1	11-04-32-333	THOMAS 1	Feb-87	2.99	0.33	2.26	0.05	2.31	2.46	0.71	2.23	3.32

APPENDIX III: GROUND-WATER QUALITY DATA

MAP CODE	WELL LOCATION	WELL NAME	SAMPLE DATE	Alka. (meq/L)	TDS (mg/L)	TDR (mg/L)	S.C. uS/cm	pH	Temp. (C)	SiO2 (mg/L)	WATER TYPE	DATA SOURCE
Ly1	11-03-36-434	LEYENDECKER 1 +2	Jan-76	2.21		204	315	8.0			CaHCO3	6
Ly1	11-03-36-434	LEYENDECKER 1	Feb-87	2.11	194		341	8.0	18.0	28	CaHCO3	4
Ly2	10-03-01-244	LEYENDECKER 2	Nov-73	2.35		220	315	7.8			CaHCO3	5 & 7
Ly2	10-03-01-244	LEYENDECKER 2 +2	Jan-76	2.35		216	333	8.0			CaHCO3	6
Ly2	10-03-01-244	LEYENDECKER 2	Feb-87	2.15	196		351	8.0	19.0	26	CaHCO3	4
Ly3	11-03-36-322	LEYENDECKER 3	Nov-73	2.19		185	297	7.8			CaHCO3	5 & 7
Ly3	11-03-36-322	LEYENDECKER 3 +2	Jan-76	2.12		195	303	7.9			CaHCO3	6
Ly3	11-03-36-322	LEYENDECKER 3	Feb-87	2.02	177		325	8.0	18.0	24	CaHCO3	4
Ly4	11-03-36-422	LEYENDECKER 4 +2	Jan-76	2.33		221	342	7.8			CaHCO3	6
Ly4	11-03-36-422	LEYENDECKER 4	Feb-87	2.35	206		367	8.0	19.0	26	CaHCO3	4
Mi1	10-03-33-233	MILES 1	Jan-76	2.17		282	420	8.0			CaHCO3	6
Mi1	10-03-33-233	MILES 1	Jun-80	2.20	290		400	7.5	25.0	71	CaHCO3	3
Mi1	10-03-33-233	MILES 1	Feb-87	2.05	295		410	7.9	26.0	71	CaHCO3	4
PH1	11-02-09-411	PARADISE HILL 1	Jan-73	2.54	290		348	7.8			NaHCO3	5
PH1	11-02-09-411	PARADISE HILL 1	Jan-76	2.46	254		373	8.0			NaHCO3	6
PH2	11-02-02-343	PARADISE HILL 2	Jan-73	2.75	305		364	8.0			NaHCO3	5
PH3	11-02-03-221	PARADISE HILL 3	May-80	2.59	350		485	7.7	23	66	NaHCO3	3
Po1	11-04-28-111	PONDEROSA 1(9)	Jun-79	2.18	270		422	7.7	26	30	CaHCO3	3
Po1	11-04-28-111	PONDEROSA 1(9)	Feb-87	2.07	331		623	8.1	26.0	28	CaCl	4
Pola	10-04-04-212	PONDEROSA 1 abd.	Jan-73	2.40		185	281	7.8			CaHCO3	5
Pola	10-04-04-212	PONDEROSA 1 abd.+3	Jan-76	2.36		178	295	8.0			CaHCO3	6
Po2	11-04-33-332	PONDEROSA 2	Feb-74	2.28	180		275	7.9	25.5	32	CaHCO3	3
Po2	11-04-33-332	PONDEROSA 2 +2	Jan-76	2.20		185	282	8.2			CaHCO3	6
Po2	11-04-33-332	PONDEROSA 2	Feb-87	2.06	193		305	7.8	26.0	28	CaHCO3	4
Po3	11-04-32-234	PONDEROSA 3	Feb-87	2.42	340		633	8.0	28.0	30	NaHCO3	4
Po4	11-04-33-113	PONDEROSA 4	Jun-79	2.20	180			7.6	26	30	CaHCO3	3
Po4	11-04-33-113	PONDEROSA 4	Feb-87	2.31	184		339	8.0	26.0	24	CaHCO3	4
Po5	11-04-28-113	PONDEROSA 5 (7)	Feb-87	2.06	216		353	8.1	26.0	30	NaHCO3	4
Po6	11-04-29-431	PONDEROSA 6	Feb-87	2.49	341		607	8.0	29.0	32	NaHCO3	4
PS	09-03-09-113	PUB.SRV.PERSON 3	May-56	2.13	270	292	389	7.7	25.0	69	CaHCO3	1 & 3
Ri1	10-04-29-232	RIDGECREST 1	Jan-73	2.84		250	400	7.7			CaHCO3	5
Ri1	10-04-29-232	RIDGECREST 1 +2	Jan-76	2.82		264	457	8.0			CaHCO3	6
Ri1	10-04-29-232	RIDGECREST 1	Apr-85	2.90	279		427			28	CaHCO3	4
Ri2	10-04-20-344	RIDGECREST 2	Jan-76	2.09		209	349	8.0			CaHCO3	6
Ri2	10-04-20-344	RIDGECREST 2	May-85	1.82	211		349			30	CaHCO3	4
Ri3	10-04-30-243	RIDGECREST 3	Jan-76	2.27	234	391		7.9			CaHCO3	6
Ri3	10-04-30-243	RIDGECREST 3	Feb-87	1.79	211		395	8.0	23.0	26	CaHCO3	4
Ri4	10-04-19-322	RIDGECREST 4	May-85	1.98	272					42	CaHCO3	4
SB1	10-03-10-224	SANTA BARBARA 1	Jan-73	2.16		220	302	8.5			CaHCO3	5
SB1	10-03-10-224	SANTA BARBARA 1 +2	Jan-76	2.12		213	312	8.1			CaHCO3	6
SB1	10-03-10-224	SANTA BARBARA 1	Feb-87	3.05	261		362	8.1	20.0	45	NaHCO3	4
SJ2	10-03-29-441	SAN JOSE 2(4:7)	Jan-73	2.18		300	385	8.1			NaHCO3	5
SJ2	10-03-29-441	SAN JOSE 2(4:7) +2	Jan-76	2.19		256	426	8.0			NaHCO3	6
SJ2	10-03-29-441	SAN JOSE 2(4:7)	Feb-87	1.95	303		408	7.9	24.0	73	NaHCO3	4
SJ3	10-03-29-341	SAN JOSE 3(5:8)	Jan-73	2.77		330	407	8.3			NaHCO3	5
SJ3	10-03-29-341	SAN JOSE 3(5:8) +2	Jan-76	2.24		301	436	8.2			NaHCO3	6
SJ3	10-03-29-341	SAN JOSE 3(5:8)	Feb-87	2.13	313		420	8.1	22	71	NaHCO3	4
SJ4	10-03-32-414	SAN JOSE 4(6:10)	Jan-73	2.21		345	426	8.2			NaHCO3	5
SJ4	10-03-32-414	SAN JOSE 4(6:10)+2	Jan-76	2.58		475	690	8.0			CaSO4	6
SJ4	10-03-32-414	SAN JOSE 4(6:10)	Jun-80	1.88	330		465	7.4	26.0	71	NaHCO3	3
Th1	11-04-32-333	THOMAS 1	May-65	2.64		318	518	7.8	23.0	30	CaHCO3	3
Th1	11-04-32-333	THOMAS 1 +2	Jan-76	2.61		294	493	8.0			CaHCO3	6
Th1	11-04-32-333	THOMAS 1	Feb-87	2.46	338		567	7.7	23.0	32	CaHCO3	4

APPENDIX III: GROUND-WATER QUALITY DATA

MAP CODE	WELL LOCATION	WELL NAME		SAMPLE DATE	Ca (meq/L)	Mg (meq/L)	Na (meq/L)	K (meq/L)	Na+K-Na (meq/L)	HCO3 (meq/L)	SO4 (meq/L)	Cl (meq/L)	Hard. (meq/L)
Th2	10-04-05-122	THOMAS 2		Jan-73	2.84	0.65	2.00	0.07	2.07	2.43	0.54	2.10	3.49
Th2	10-04-05-122	THOMAS 2		Jan-76	2.11	0.99	2.00	0.06	2.06	2.43	0.56	2.11	3.09
Th2	10-04-05-122	THOMAS 2		Feb-87	3.29	0.33	2.52	0.08	2.60	2.38	0.67	3.10	3.62
Th3	11-04-31-412	THOMAS 3		Jan-73	2.78	0.31	1.80	0.06	1.86	2.76	0.69	1.53	3.10
Th3	11-04-31-412	THOMAS 3		Jan-76	2.04	1.15	1.70	0.06	1.76	2.46	0.82	1.50	3.18
Th3	11-04-31-412	THOMAS 3		Feb-87	2.30	0.33	1.61	0.05	1.66	2.54	0.79	0.79	2.63
Th4	11-04-32-322	THOMAS 4		Jan-73	3.09	0.40	2.40	0.07	2.47	2.57	0.60	2.52	3.50
Th4	11-04-32-322	THOMAS 4	+2	Jan-76	3.17	0.53	2.50	0.07	2.57	2.57	0.61	2.99	3.70
Th4	11-04-32-322	THOMAS 4		Feb-87	3.79	0.41	2.70	0.08	2.78	2.45	0.62	3.39	4.21
TRM	11-04-10-314	TRAMWAY UT.		Jan-76	2.63	0.46	1.00	0.04	1.04	3.16	0.64	0.18	3.10
VA1	11-03-35-324	VOL ANDIA 1		Jan-73	1.62	0.33	0.70	0.06	0.76	1.95	0.54	0.16	1.95
VA1	11-03-35-324	VOL ANDIA 1	+2	Jan-76	1.70	0.41	0.80	0.05	0.85	1.95	0.62	0.22	2.11
VA1	11-03-35-324	VOL ANDIA 1		Feb-87	2.10	0.41	0.87	0.05	0.92	1.99	0.83	0.56	2.51
VA2	10-03-01-131	VOL ANDIA 2		Jan-73	2.16	0.35	0.80	0.06	0.86	2.16	0.82	0.41	2.52
VA2	10-03-01-131	VOL ANDIA 2	+2	Jan-76	1.85	0.44	0.70	0.05	0.75	1.99	0.68	0.21	2.29
VA2	10-03-01-131	VOL ANDIA 2		Feb-87	1.70	0.25	0.70	0.00	0.70	1.91	0.58	0.25	1.94
VA3	10-03-03-224	VOL ANDIA 3		Jan-73	1.65	0.40	0.80	0.06	0.86	1.94	0.57	0.39	2.05
VA3	10-03-03-224	VOL ANDIA 3		Jan-74	1.65	0.40	0.80	0.06	0.86	1.94	0.57	0.39	2.05
VA4	11-03-35-424	VOL ANDIA 4		Jan-73	1.88	0.37	0.70	0.06	0.76	2.03	0.81	0.21	2.25
VA4	11-03-35-424	VOL ANDIA 4	+2	Jan-76	1.82	0.44	0.70	0.05	0.75	1.97	0.60	0.22	2.27
VA4	11-03-35-424	VOL ANDIA 4		Feb-87	2.10	0.41	0.70	0.00	0.70	2.15	0.79	0.31	2.51
VA5	11-03-35-313	VOL ANDIA 5		May-65	1.70	0.32			0.83	2.02	0.60	0.21	2.02
VA5	11-03-35-313	VOL ANDIA 5		Jan-73	1.80	0.45	0.80	0.05	0.85	1.98	0.62	0.35	2.25
VA5	11-03-35-313	VOL ANDIA 5	+2	Jan-76	1.76	0.47	0.75	0.06	0.81	1.94	0.73	0.23	2.23
VA5	11-03-35-313	VOL ANDIA 5		Feb-87	1.86	0.33	0.83	0.05	0.88	1.93	0.85	0.34	2.13
VA6	11-03-35-232	VOL ANDIA 6		Oct-60	1.90	0.08			0.74	1.97	0.54	0.17	1.98
VA6	11-03-35-232	VOL ANDIA 6		Jan-73	1.80	0.40	0.70	0.05	0.75	1.96	0.53	0.32	2.20
VA6	11-03-35-232	VOL ANDIA 6	+2	Jan-76	1.81	0.43	0.70	0.05	0.75	2.12	0.65	0.19	2.23
VA6	11-03-35-232	VOL ANDIA 6		Feb-87	1.70	0.33	0.74	0.00	0.74	1.95	0.62	0.25	2.03
Vet	10-03-36-132	VET. ADMIN.		May-56	1.60	0.54			1.09	2.13	0.75	0.25	2.14
VC1	11-02-28-222	VOLCANO CLIFF 1		Jan-73	1.14	0.49	1.70	0.15	1.85	2.25	1.12	0.23	1.62
VC1	11-02-28-222	VOLCANO CLIFF 1		Jan-76	1.01	0.41	2.15	0.15	2.30	2.35	1.01	0.22	1.42
VC1	11-02-28-222	VOLCANO CLIFF 1		Feb-87	1.00	0.33	2.35	0.15	2.50	2.29	0.96	0.20	1.33
VC2	11-02-28-244	VOLCANO CLIFF 2		Jan-73	1.05	0.35	2.30	0.15	2.45	2.45	1.03	0.27	1.40
VC2	11-02-28-244	VOLCANO CLIFF 2		Jan-76	1.20	0.58	1.60	0.18	1.78	2.16	0.84	0.27	1.78
VC2	11-02-28-244	VOLCANO CLIFF 2		Feb-87	1.05	0.41	2.13	0.18	2.31	2.21	0.96	0.28	1.46
VS	11-03-11-334	VISTA SANDIA 2		Jan-76	1.76	0.26	0.60	0.07	0.67	1.96	0.42	0.22	2.02
Wa1	11-04-21-112	WALKER 1		Feb-87	1.70	0.16	1.31	0.05	1.36	2.06	0.46	0.51	1.86
Wa2	11-04-20-221	WALKER 2		Mar-80	1.85	0.45	3.22	0.15	3.37	2.59	0.77	2.43	2.30
We1	11-04-18-434	WEBSTER-ALA. 1		Feb-87	1.55	0.49	2.65	0.13	2.78	2.39	0.75	1.38	2.04
We2	11-04-19-142	WEBSTER-ALA. 2		Feb-87	1.45	0.58	1.48	0.13	1.61	2.44	0.77	0.76	2.02
WM1	10-02-21-343	WEST MESA 1		Jan-73	0.41	0.08	4.50	0.05	4.55	2.99	1.50	0.21	0.49
WM1	10-02-21-343	WEST MESA 1		Jan-76	0.17	0.07	4.59	0.02	4.61	2.71	1.51	0.25	0.25
WM1	10-02-21-343	WEST MESA 1		Feb-87	0.00	0.00	4.74	0.00	4.74	2.87	1.73	0.23	0.00
WM2	10-02-21-213	WEST MESA 2		Jan-76	1.09	0.15	3.25	0.10	3.35	2.74	1.67	0.38	1.24
WM2	10-02-21-213	WEST MESA 2		Feb-87	0.20	0.00	4.26	0.00	4.26	2.71	0.98	0.23	0.20
WM3	10-02-21-412	WEST MESA 3		Jan-76	0.25	0.15	3.90	0.04	3.94	2.82	0.88	0.23	0.40
WM4	10-02-22-312	WEST MESA 4		Jan-76	0.42	0.19	3.90	0.05	3.95	2.71	1.16	0.33	0.61
WM4	10-02-22-312	WEST MESA 4		Feb-87	0.30	0.00	4.39	0.00	4.39	2.67	1.23	0.34	0.30
Ya1	10-03-21-444	YALE 1 (2)		Jan-73	1.97	0.38	0.90	0.10	1.00	2.06	0.66	0.43	2.35
Ya1	10-03-21-444	YALE 1 (2)		Oct-77	1.77	0.60	0.85	0.10	0.95	1.94	0.76	0.52	2.37
Ya1	10-03-21-444	YALE 1 (2)		Feb-87	1.75	0.49	1.09	0.13	1.22	1.97	0.71	0.59	2.24
Ya2	10-03-28-243	YALE 2 (3)		Oct-77	1.55	0.09	0.80	0.12	0.92	1.85	0.51	0.27	1.64

APPENDIX III: GROUND-WATER QUALITY DATA

MAP CODE	WELL LOCATION	WELL NAME		SAMPLE DATE	Alka. (meq/L)	TDS (mg/L)	TDR (mg/L)	S.C. uS/cm	pH	Temp. (C)	SiO2 (mg/L)	WATER TYPE	DATA SOURCE
Th2	10-04-05-122	THOMAS 2		Jan-73	2.43		355	520	7.7			CaHCO3	5
Th2	10-04-05-122	THOMAS 2		Jan-76	2.43		312	548	8.1			CaHCO3	6
Th2	10-04-05-122	THOMAS 2		Feb-87	2.38	375		624	7.9	25.0	30	CaCl	4
Th3	11-04-31-412	THOMAS 3		Jan-73	2.76		325	499	7.8			CaHCO3	5
Th3	11-04-31-412	THOMAS 3		Jan-76	2.46		310	500	8.1			CaHCO3	6
Th3	11-04-31-412	THOMAS 3		Feb-87	2.54	268		407	7.7	21.0	36	CaHCO3	4
Th4	11-04-32-322	THOMAS 4		Jan-73	2.57		450	593	7.7			CaHCO3	5
Th4	11-04-32-322	THOMAS 4	+2	Jan-76	2.57		395	693	8.1			CaCl	6
Th4	11-04-32-322	THOMAS 4		Feb-87	2.45	402		684	7.7	25.0	32	CaCl	4
TRM	11-04-10-314	TRAMWAY UT.		Jan-76	3.16	215		390	8.2			CaHCO3	6
VA1	11-03-35-324	VOL ANDIA 1		Jan-73	1.95		205	255	8.0			CaHCO3	5
VA1	11-03-35-324	VOL ANDIA 1	+2	Jan-76	1.95		183	289	7.8			CaHCO3	6
VA1	11-03-35-324	VOL ANDIA 1		Feb-87	1.99	223		470	8.2	17.0	24	CaHCO3	4
VA2	10-03-01-131	VOL ANDIA 2		Jan-73	2.16		230	373	7.8			CaHCO3	5
VA2	10-03-01-131	VOL ANDIA 2	+2	Jan-76	1.99		193	296	8.1			CaHCO3	6
VA2	10-03-01-131	VOL ANDIA 2		Feb-87	1.91	175		286	8.0	18.0	26	CaHCO3	4
VA3	10-03-03-224	VOL ANDIA 3		Jan-73	1.94		205	280	7.9			CaHCO3	5
VA3	10-03-03-224	VOL ANDIA 3		Jan-74	1.94		165	280	7.9			CaHCO3	6
VA4	11-03-35-424	VOL ANDIA 4		Jan-73	2.03		200	281	7.7			CaHCO3	5
VA4	11-03-35-424	VOL ANDIA 4	+2	Jan-76	1.97		181	292	8.1			CaHCO3	6
VA4	11-03-35-424	VOL ANDIA 4		Feb-87	2.15	206		331	7.9	17.0	26	CaHCO3	4
VA5	11-03-35-313	VOL ANDIA 5		May-65	2.02		192	278	8.0	17.0	33	CaHCO3	3
VA5	11-03-35-313	VOL ANDIA 5		Jan-73	1.98		230	280	7.7			CaHCO3	5
VA5	11-03-35-313	VOL ANDIA 5	+2	Jan-76	1.94		207	294	8.1			CaHCO3	6
VA5	11-03-35-313	VOL ANDIA 5		Feb-87	1.93	198		326	8.1	17.0	26	CaHCO3	4
VA6	11-03-35-232	VOL ANDIA 6		Oct-60	1.97	180	188	263	8.0	16.5	32	CaHCO3	3
VA6	11-03-35-232	VOL ANDIA 6		Jan-73	1.96		185	280	7.9			CaHCO3	5
VA6	11-03-35-232	VOL ANDIA 6	+2	Jan-76	2.12		188	291	7.9			CaHCO3	6
VA6	11-03-35-232	VOL ANDIA 6		Feb-87	1.95	177		308	7.9	17.0	24	CaHCO3	4
Vet	10-03-36-132	VET. ADMIN.		May-56	2.13	210	231	318	7.8	20.0	38	CaHCO3	1
VC1	11-02-28-222	VOLCANO CLIFF 1		Jan-73	2.25	288		330	7.6			NaHCO3	5
VC1	11-02-28-222	VOLCANO CLIFF 1		Jan-76	2.35			410	8.1			NaHCO3	6
VC1	11-02-28-222	VOLCANO CLIFF 1		Feb-87	2.29	282		371	8.1	23.0	68	NaHCO3	4
VC2	11-02-28-244	VOLCANO CLIFF 2		Jan-73	2.45	335		374	8.0			NaHCO3	5
VC2	11-02-28-244	VOLCANO CLIFF 2		Jan-76	2.16	250		386	8.0			NaHCO3	6
VC2	11-02-28-244	VOLCANO CLIFF 2		Feb-87	2.21	280		346	8.0	23.0	66	NaHCO3	4
VS	11-03-11-334	VISTA SANDIA 2		Jan-76	1.96	163		273	8.2			CaHCO3	6
Wa1	11-04-21-112	WALKER 1		Feb-87	2.06	203		316	8.1	26.0	30	CaHCO3	4
Wa2	11-04-20-221	WALKER 2		Mar-80	2.59	370		580	7.7	29	41	NaHCO3	3
We1	11-04-18-434	WEBSTER-ALA. 1		Feb-87	2.39	313		450	7.8	23.0	51	NaHCO3	4
We2	11-04-19-142	WEBSTER-ALA. 2		Feb-87	2.44	262		363	7.9	22.0	49	NaHCO3	4
WM1	10-02-21-343	WEST MESA 1		Jan-73	2.99	356		445	8.2			NaHCO3	5
WM1	10-02-21-343	WEST MESA 1		Jan-76	2.71	315		509	8.8			NaHCO3	6
WM1	10-02-21-343	WEST MESA 1		Feb-87	2.87	305			9.0	27.0	15	NaHCO3	4
WM2	10-02-21-213	WEST MESA 2		Jan-76	2.89	325		493	8.4			NaHCO3	6
WM2	10-02-21-213	WEST MESA 2		Feb-87	2.71	278			8.8	24.0	26	NaHCO3	4
WM3	10-02-21-412	WEST MESA 3		Jan-76	2.88	266		422	8.5			NaHCO3	6
WM4	10-02-22-312	WEST MESA 4		Jan-76	2.71	292		492	8.0			NaHCO3	6
WM4	10-02-22-312	WEST MESA 4		Feb-87	2.67	293			8.5	24.0	26	NaHCO3	4
Ya1	10-03-21-444	YALE 1 (2)		Jan-73	2.06		235	307	7.9			CaHCO3	5
Ya1	10-03-21-444	YALE 1 (2)		Oct-77	1.94		205	329	8.2			CaHCO3	6
Ya1	10-03-21-444	YALE 1 (2)		Feb-87	1.97	239		337	8.0	21.0	51	CaHCO3	4
Ya2	10-03-28-243	YALE 2 (3)		Oct-77	1.85		239	297	8.1			CaHCO3	6

APPENDIX III: GROUND-WATER QUALITY DATA

MAP CODE	WELL LOCATION	WELL NAME	SAMPLE DATE	Ca (meq/L)	Mg (meq/L)	Na (meq/L)	K (meq/L)	Na+K-Na (meq/L)	HCO3 (meq/L)	SO4 (meq/L)	Cl (meq/L)	Hard. (meq/L)
Ya2	10-03-28-243	YALE 2 (3)	Feb-87	1.75	0.58	1.44	0.18	1.62	2.82	0.73	1.04	2.32
Ya3	10-03-21-341	YALE 3 (4)	+2 Jan-76	1.55	0.65	1.35	0.17	1.52	2.23	0.81	0.58	2.20
Ya3	10-03-21-341	YALE 3 (4)	Feb-87	1.90	0.66	1.65	0.20	1.85	2.14	1.19	0.87	2.55

APPENDIX III: GROUND-WATER QUALITY DATA

MAP CODE	WELL LOCATION	WELL NAME		SAMPLE DATE	Alka. (meq/L)	TDS (mg/L)	TDR (mg/L)	S.C. uS/cm	pH	Temp. (C)	SiO2 (mg/L)	WATER TYPE	DATA SOURCE
Ya2	10-03-28-243	YALE 2 (3)		Feb-87	2.82	306		380	7.9	24.0	64	CaHCO3	4
Ya3	10-03-21-341	YALE 3 (4)	+2	Jan-76	2.23		272	382	8.1			CaHCO3	6
Ya3	10-03-21-341	YALE 3 (4)		Feb-87	2.14	317		420	8.0	24.0	68	CaHCO3	4

DATA SOURCES:
1 = Bjorklund and Maxwell 1961
2 = Science Applications Inc. 1985
3 = USGS WATSTORE (Water Quality Database)
4 = Albuquerque Public Works (Wilson Labs)
5 = NMEID 1974 (If date unknown used Jan-74 as dummy date)
6 = NMEID 1980 (If date unknown used Jan-76 as dummy date)
7 = AEHD 1986
8 = Albuquerque Public Works (APW)
+2 = average of 2 analyses

APPENDIX IV: SPRING WATER QUALITY DATA

APPENDIX IV: SPRING WATER QUALITY DATA

MAP CODE	SPRING LOCATION	SPRING NAME	SAMPLE DATE	Ca (meq/L)	Mg (meq/L)	Na+K-Na (meq/L)	Na (meq/L)	K (meq/L)	HCO3 (meq/L)	SO4 (meq/L)	Cl (meq/L)	Hard (meq/L)
1	09-04-24-2114-S	COYOTE SPRING-1	Jul-45	13.97	5.35	17.40			20.16	2.71	13.82	19.31
2	09-04-24-112-S	COYOTE SPRING-2	Jul-45	9.48	3.62	8.26			12.29	1.62	7.33	13.09
3	09-04-24-113-S	COYOTE SPRING-3	Jul-45	10.98	4.20	12.62			15.73	2.08	9.87	15.17
4	10-04-26-3211-A	TIJERAS ARROYO	Oct-88	5.49	2.22		1.96	0.10	4.26	2.50	2.40	7.71
4	10-04-26-3211-A	TIJERAS ARROYO	Jan-89	5.49	2.22		2.00	0.09	4.38	2.50	2.54	7.71
4	10-04-26-3211-A	TIJERAS ARROYO	May-89	4.99	2.22		2.00	0.10	4.00	2.71	2.54	7.21
5	10-05-30-322-S	McDANIEL-SPRG.	Jun-77	4.63	1.97	1.35	1.30	0.05	3.67	2.54	1.68	6.59
6	10-05-30-322-S	McDANIEL-POND	Jun-77	4.83	1.93	1.30	1.30	0.05	4.21	2.48	1.62	6.75
7	10-04-13-242-S	EMBUDO SPRING	May-56	7.44	2.55	1.26			8.15	2.52	0.51	9.98
8	10-05-10-434-S	HOBBIE SPRING	Aug-62	3.84	0.60	0.37	0.34	0.00	4.21	0.37	0.09	4.44
9	12-05-33-214-S	HOUSE SPRING	Jul-62	4.24	0.56	0.11	0.09	0.02	4.59	0.29	0.33	4.80
10	12-05-33-141-S	HEAD SPRING	Jul-63	4.89	0.21	0.07			4.72	0.27	0.07	5.11
11	10-05-21-412-S	7-SPRINGS-1	Jun-62	5.29	1.23	0.96			4.59	2.37	0.48	6.52
12	13-05-33-342-S	PLACITAS-1	Aug-62	3.44	0.36	0.18	0.16	0.02	3.36	0.33	0.06	3.81
13	13-05-15-241-S	PLACITAS-2	Nov-62	3.69	0.79	2.04			5.39	0.79	0.25	4.48
14	10-06-10-433-S	BRICKNER SPRING	Jan-64	5.09	1.73	1.04	1.00	0.04	4.57	2.42	0.62	6.82
15	11-04-01-313-S	LA CUEVA	May-56	2.10	0.61	0.52			2.67	0.33	0.16	2.70
16	10-05-21-223-S	7-SPRING-2	Feb-58	5.09	0.78	0.44			5.05	1.15	0.11	5.87

MAP CODE	SPRING LOCATION	SPRING NAME	SAMPLE DATE	Alka (meq/L)	TDS (mg/L)	SC-Lab (uS/cm)	SC-Fld (uS/cm)	Temp. (C)	SiO2 (mg/L)	DATA SOURCE
1	09-04-24-2114-S	COYOTE SPRING-1	Jul-45	20.16	2000		3400	16.0	15	1:2
2	09-04-24-112-S	COYOTE SPRING-2	Jul-45	12.29	1200				18	1
3	09-04-24-113-S	COYOTE SPRING-3	Jul-45	15.73	1500		2540	17.0	16	1
4	10-04-26-3211-A	TIJERAS ARROYO	Oct-88	4.26			910	11.5	18	4
4	10-04-26-3211-A	TIJERAS ARROYO	Jan-89	4.38			910	11.0	17	4
4	10-04-26-3211-A	TIJERAS ARROYO	May-89	4.00			925	19.0	15	4
5	10-05-30-322-S	McDANIEL-SPRG.	Jun-77	3.67	470	756				3
6	10-05-30-322-S	McDANIEL-POND	Jun-77	4.21	475	771				3
7	10-04-13-242-S	EMBUDO SPRING	May-56	8.14	628		963	13.0	34	1:2
8	10-05-10-434-S	HOBBIE SPRING	Aug-62	4.21	246				24	2
9	12-05-33-214-S	HOUSE SPRING	Jul-62	4.59			459	9.0		2
10	12-05-33-141-S	HEAD SPRING	Jul-63	4.72			470	7.0		2
11	10-05-21-412-S	7-SPRINGS-1	Jun-62	4.59	470		692	11.0	18	2
12	13-05-33-342-S	PLACITAS-1	Aug-62	3.36	198		350	14.0	14	2
13	13-05-15-241-S	PLACITAS-2	Nov-62	5.39	360		590	23.0	16	2
14	10-06-10-433-S	BRICKNER SPRING	Jan-64	4.57	465		720			2:3
15	11-04-01-313-S	LA CUEVA	May-56	2.67	186	297		17.0	20	2
16	10-05-21-223-S	7-SPRING-2	Feb-58	5.05	352	567		14.0	16	2

DATA SOURCES:
1 = USGS WATSTORE (Water Quality Database)
2 = Titus 1980
3 = New Mexico Department of Public Health
4 = USGS Albuquerque Office

APPENDIX V: RIO GRANDE WATER QUALITY

APPENDIX V: Rio Grande Water Quality

SAMPLE SITE	DATE	Ca (mg/L)	n = (#)	Mg (mg/L)	n = (#)	Na (mg/L)	n = (#)	K (mg/L)	n = (#)	Na+K-Na (mg/L)	n = (#)	HCO3 (mg/L)	n = (#)	SO4 (mg/L)	n = (#)
Isleta	1936-1937	54.5	(10)	9.2	(10)	41.6	(10)	4.69	(10)			160.5	(10)	101.8	(10)
Albuquerque	10/ /37	62	(9)	11	(9)	49	(9)			49	(9)	168	(9)	127	(9)
Albuquerque	6/ /38	24	(10)	6.6	(10)									34	(10)
Albuquerque	1966-1976	65.9	(2)	9.1	(2)	47.9	(2)	5.9	(1)					150.0	(1)
Albuquerque	1976-1986	40.9	(24)	6.9	(24)	24.3	(24)	3.15	(24)					65.9	(24)
Isleta	1969-1982	47.9	(96)	7.7	(96)	33.5	(96)			29.2	(11)	148	(87)	80	(96)
ABQ-Baralas	11/03/83	51.7	(1)	7.7	(1)	32.2	(1)	3.51	(1)			173	(1)	78	(1)
ABQ-Rio Bravo	11/03/83	50.3	(1)	9.4	(1)	29.9	(1)	3.9	(1)			172	(1)	73	(1)
Isleta Dam	11/03/83	49.5	(1)	10.6	(1)	39.1	(1)	5.07	(1)			169	(1)	74	(1)
ABQ-Rio Bravo	12/ /83													63.4	(16)
ABQ-I25	12/ /83													65.7	(16)
ABQ-Barales	12/ /83													63.0	(16)
Isleta Dam	12/ /83													67.1	(16)
ABQ-Rio Bravo	1/ /84													56.7	(16)
ABQ-I25	1/ /84													58.2	(16)
ABQ-Barales	1/ /84													55.9	(16)
Isleta Dam	1/ /84													60.5	(16)
ABQ-Rio Bravo	2/ /84													54.9	(16)
ABQ-I25	2/ /84													57.6	(16)
ABQ-Barales	2/ /84													55.7	(16)
Isleta Dam	2/ /84													59.3	(16)
ABQ-Rio Bravo	3/ /84													50.8	(16)
ABQ-I25	3/ /84													52.8	(16)
ABQ-Barales	3/ /84													49.5	(16)
Isleta Dam	3/ /84													52.3	(16)
ABQ-Rio Bravo	8/27/84	81.6	(1)	7.8	(1)	62.1	(1)	5.46	(1)			159	(1)	193	(1)
ABQ-I25	8/27/84	75.2	(1)	10.7	(1)	51.5	(1)	5.46	(1)			162	(1)	182	(1)
Isleta Dam	8/27/84	80	(1)	7.3	(1)	50.6	(1)	5.46	(1)			173	(1)	161	(1)

	Ca	Mg	Na	K	Na+K	HCO3	SO4
n (#) =	(157)	(157)	(147)	(41)	(20)	(112)	(412)
Mean (mg)=	56.96	8.67	41.97	4.73	39.10	164.94	80.11
Mean(meq)=	2.84	0.72	1.83	0.12	1.70	2.70	1.67
s (mg) =	16.17	1.48	10.82	0.93	9.90	7.86	41.44
s (meq) =	0.81	0.12	0.47	0.02	0.43	0.13	0.86

APPENDIX V: Rio Grande Water Quality

SAMPLE SITE	DATE	Cl (mg/L)	n = (#)	NO3-N	n = (#)	F (mg/L)	n = (#)	TDS (mg/L)	n = (#)	SiO2 (mg/L)	n = (#)	pH	n = (#)	TEMP (C)	n = (#)	SOURCE
Isleta	1936-1937	21.6	(10)	0.42	(10)			343	(10)	25	(1)					1
Albuquerque	10/ /37	26	(9)													2
Albuquerque	6/ /38	35	(10)													2
Albuquerque	1966-1976	37.0	(1)	1.60	(1)	0.70	(1)			28.0	(1)	7.85	(2)	14.92	(188)	3
Albuquerque	1976-1986	10.3	(24)	0.08	(5)	0.35	(24)			19.08	(24)	8.05	(36)	14.06	(270)	3
Isleta	1969-1982	17.2	(96)					292	(87)							4
ABQ-Baralas	11/03/83	17	(1)	0.15	(1)			336	(1)			8.25	(15)	8.85	(15)	5
ABQ-Rio Bravo	11/03/83	14	(1)	1.08	(1)			320	(1)			8.13	(15)	9.4	(15)	5
Isleta Dam	11/03/83	25	(1)	0.20	(1)			358	(1)			7.75	(10)	10.02	(10)	5
ABQ-Rio Bravo	12/ /83	12.6	(16)	0.07	(16)			320	(16)			8.07	(10)	2.8	(16)	6
ABQ-I25	12/ /83	17.6	(16)	0.13	(16)			324	(16)			7.97	(10)	3.0	(16)	6
ABQ-Barales	12/ /83	11.4	(16)	0.08	(16)			328	(16)					2.2	(16)	6
Isleta Dam	12/ /83	20.6	(16)	0.26	(16)			316	(16)			7.75	(10)	3.6	(16)	6
ABQ-Rio Bravo	1/ /84	11.6	(16)	0.08	(16)			279	(16)					0.9	(16)	6
ABQ-I25	1/ /84	15.8	(16)	0.13	(16)			293	(16)					-1.1	(16)	6
ABQ-Barales	1/ /84	11.8	(16)	0.05	(16)			274	(16)					0.4	(16)	6
Isleta Dam	1/ /84	17.4	(16)	0.07	(16)			299	(16)					2.4	(16)	6
ABQ-Rio Bravo	2/ /84	11.5	(16)	0.05	(16)			261	(16)					4.0	(16)	6
ABQ-I25	2/ /84	13.2	(16)	0.07	(16)			278	(16)					4.9	(16)	6
ABQ-Barales	2/ /84	8.2	(16)	0.05	(16)			256	(16)					3.9	(16)	6
Isleta Dam	2/ /84	16.4	(16)	0.13	(16)			285	(16)					5.2	(16)	6
ABQ-Rio Bravo	3/ /84	10.7	(16)	0.11	(16)			225	(16)			8.3	(5)	7.6	(16)	6
ABQ-I25	3/ /84	12.9	(16)	0.16	(16)			243	(16)			8.0	(5)	8.5	(16)	6
ABQ-Barales	3/ /84	11.8	(16)	0.10	(16)			223	(16)			8.3	(5)	7.8	(16)	6
Isleta Dam	3/ /84	16	(16)	0.20	(16)			245	(16)			8.1	(5)	8.6	(16)	6
ABQ-Rio Bravo	8/27/84	35	(1)	0.15	(1)			543	(1)			8.2	(2)	22.1	(2)	7
ABQ-I25	8/27/84	32	(1)	0.48	(1)			805	(1)			7.7	(2)	22.5	(5)	7
Isleta Dam	8/27/84	31	(1)	0.55	(1)			460	(1)			7.8	(2)	23.1	(5)	7

	Cl	NO3-N	F	TDS	SiO2	pH	TEMP
n (#) =	(412)	(278)	(25)	(359)	(26)	(134)	(888)
Mean (mg)=	18.59	0.26	0.53	329	24.03	8.01	8.2
Mean(meq)=	0.52	0.02	0.03				
s (mg) =	8.34	0.35	0.17	121	3.71	0.20	6.8
s (meq) =	0.24	0.02	0.01				

CODE = DATA SOURCE
1 = Scofield 1938
2 = Bjorklund & Maxwell 1961
3 = USGS-WATSTORE
4 = Anderholm 1988 (WATSTORE)
5 = EID-Potter-11/30/84
6 = City in EID-Potter-11/84
7 = EID-Potter-12/31/84

APPENDIX VI: TRANSMISSIVITY DATA

APPENDIX VI: HYDRAULIC CONDUCTIVITY (K) = TRANSMISSIVITY (T) / SATURATED THICKNESS

MAP CODE	WELL FIELD and WELL NUMBER	B & M 1961 TRANSMISS. T(gpd/ft)	COE/78-SAI/81 TRANSMISS. T(gpd/ft)	LAYNE-85 TRANSMISS. T(gpd/ft)	GW-MGT-87 TRANSMISS. T(gpd/ft)	1961 HYD.CON. (m/d)	78-81 HYD.CON. (m/d)	1985 HYD.CON. (m/d)	1987 HYD.CON. (m/d)
At1	ATRISCO 1(II5)(5)				47500				1.6
At3	ATRISCO 3(I2)(9)	60000			26000	3.0			1.3
At4	ATRISCO 4(I3)(13)				24000				2.0
Bu2	BURTON 2				157000				13.9
Bu3	BURTON 3				189000				12.3
Ca2	CANDELARIA 2(22)				41000				7.4
Ca3	CANDELARIA 3(23)				23000				3.6
Ch1	CHARLES 1				444000				29.0
Ch2	CHARLES 2			420000				26.1	
Ch3	CHARLES 3			500000 OB				32.4	
Ch4	CHARLES 4			420000				28.1	
Co1	COLLEGE 1				49000				1.6
Co2	COLLEGE 2				110000				3.5
Cr1	CORONADO 1 (Tracie1)		78000				3.7		
D1	DON 1				65000				2.3
Du1	DURANES 1	75000			38000	3.1			1.6
Du2	DURANES 2	62000			94000	3.2			4.9
Du3	DURANES 3				80000				3.4
Du4	DURANES 4				24000				1.1
Du5	DURANES 5				35000				1.5
Du6	DURANES 6				41000				1.8
Du7	DURANES 7				55000				2.4
Gr1	GRIEGOS 1				80000				4.1
Gr2	GRIEGOS 2				88000				4.5
Gr3	GRIEGOS 3				28000				1.3
Gr4	GRIEGOS 4				65000				3.5
Gr5	GRIEGOS 5	90000				4.6			
Le1	LEAVITT 1				82000				3.2
Le2	LEAVITT 2				19000				0.8
Ly1	LEYENDECKER 1	530000			412000	31.9			52.1
Ly2	LEYENDECKER 2	400000			303000	23.8			20.3
Ly3	LEYENDECKER 3	600000			418000	34.1			26.3
Ly4	LEYENDECKER 4	520000			366000	32.2			25.4
Lm1	LOMAS 1				127000				5.6
Lm2	LOMAS 2			8000				0.4	
Lm5	LOMAS 5(7)			110000 OB				4.2	
Lm6	LOMAS 6(8)			100000 OB				3.9	
Lv1	LOVE 1			45000				3.3	
Lv2	LOVE 2	75000				4.2			
Lv3	LOVE 3	110000		210000 OB		6.0		12.8	
Lv4	LOVE 4	240000			177000	11.2			9.3
Lv5	LOVE 5	180000		110000		9.1		6.2	
Lv6	LOVE 6			35000				1.6	
Lv7	LOVE 7			140000				6.1	
Mi1	MILES 1				72000				2.7
Po1	PONDEROSA 1(9)				72000				2.8
Po2	PONDEROSA 2				54000				2.5
Po3	PONDEROSA 3				143000				5.5
Po4	PONDEROSA 4				36000				1.8
Po5	PONDEROSA 5(7)				48000				2.2
Po6	PONDEROSA 6				318000				12.4
Ri1	RIDGECREST 1			45000 OB				2.7	

APPENDIX VI: HYDRAULIC CONDUCTIVITY (K) = TRANSMISSIVITY (T) / SATURATED THICKNESS

MAP CODE	WELL FIELD and WELL NUMBER	B & M 1961 TRANSMISS. T(gpd/ft)	COE/78-SAI/81 TRANSMISS. T(gpd/ft)	LAYNE-85 TRANSMISS. T(gpd/ft)	GW-MGT-87 TRANSMISS. T(gpd/ft)	1961 HYD.CON. (m/d)	78-81 HYD.CON. (m/d)	1985 HYD.CON. (m/d)	1987 HYD.CON. (m/d)
Ri2	RIDGECREST 2			170000 OB				7.1	
Ri3	RIDGECREST 3				249000				10.5
Ri4	RIDGECREST 4			280000				11.9	
SJ1	SAN JOSE 1				5000				0.8
SJ2	SAN JOSE 2(4)(7)	50000			45000	2.2			2.0
SJ3	SAN JOSE 3(5)(8)				46000				1.6
SB1	SANTA BARBARA 1				171000				9.2
Th1	THOMAS 1	400000			216000	26.6			15.3
Th2	THOMAS 2	100000			136000	5.8			8.9
Th3	THOMAS 3	280000			326000	15.3			19.6
Th4	THOMAS 4	200000			299000	16.2			28.3
VA1	VOL ANDIA 1				415000				22.0
VA2	VOL ANDIA 2				487000				28.4
VA4	VOL ANDIA 4				433000				24.7
VA5	VOL ANDIA 5				302000				15.2
VA6	VOL ANDIA 6				383000				21.2
VC1	VOLCANO CLIFFS 1				67000				3.5
VC2	VOLCANO CLIFFS 2				65000				3.3
Wa1	WALKER 1				30000				1.3
We1	WEBSTER 1 (Alameda1)				314000				13.2
We2	WEBSTER 2 (Alameda2)				149000				6.2
WM1	WEST MESA 1				27000				1.2
WM2	WEST MESA 2				70000				2.5
WM4	WEST MESA 4				81000				2.4
Ya1	YALE 1(2)				114000				6.4
Ya2	YALE 2(3)				146000				6.2
Ya3	YALE 3(4)				60000				3.0
PUBLIC WELLS									
4-H	4-HILLS C.C.	280000				19.5			
K01	USAF 1 (SANDIA 1)	450000				24.0			
K04	USAF 4 (SANDIA 4)		678000				50.6		
K08	USAF 8 (SANDIA 8)		344000				26.3		
K10	USAF 10 (MANZANO 10)	7500				0.5			
K11	USAF 11		23500				1.3		
K13	USAF 13 (KAFB 2)	100000				6.2			
PS1	PUB.SRV. WELL 1	150000				7.3			
SS	SANDIA SUB.(LOVE)		380000				104.6		
Vet	VET. ADMIN.	320000				21.6			
GS-3	USGS/CITY EXP. 3			29000 *					

PUMP TEST DATA IS FROM THE FOLLOWING PUBLISHED AND UNPUBLISHED REPORTS:

B & M = BJORKLUND AND MAXWELL 1961
COE-78 = USACOE, 1978
SAI-85 = SCIENCE APPLICATION INC. 1985
LAYNE-85 = LAYNE-WESTERN 1985
GW-MGT-87 = GROUNDWATER MANAGEMENT 1987
* = USGS WRI RPT 86-4185 1987
OB = TRANSMISSIVITY MEASURED USING A PRODUCTION WELL AS AN OBSERVATION WELL

APPENDIX VII: ENVIRONMENTAL ISOTOPES

APPENDIX VII: ENVIRONMENTAL ISOTOPES

WELL NAME	Aug.1981 DEL-D 81	Jan.1982 DEL-D 82	Feb.1987 DEL-D 87	Jan.1988 DEL-D 88	July 1988 DEL-D 88	Mar.1989 DEL-D 89	June 1989 DEL-D 89	Feb.1987 DEL-O 87	Jan.1988 DEL-O 88	July 1988 DEL-O 88	Mar.1989 DEL-O 89	June 1989 DEL-O 89
ATRISCO 1(5)			-102.10		-94.64		-92.9	-12.94		-12.76		
ATRISCO 2(1)			-99.30	-92.97	-95.96			-11.99	-12.78	-12.98		
ATRISCO 3(2:9)	-92	-90	-98.70	-92.41	-96.06		-96.03	-12.79	-12.54	-13.03		
ATRISCO 4(3:13)		-90	-99.30		-96.00		-98.08	-12.69		-13.02		
BURTON 1 (new)					-97.13	-96.97	-99.48			-13.51	-13.42	-13.40
BURTON 2		-95	-98.90		-97.36	-99.97	-103.50	-13.31		-13.54	-13.72	-13.58
BURTON 3	-96	-95	-101.10		-96.47	-97.77		-13.00		-13.45		-13.47
BURTON 4 (new)					-100.40					-13.23		
CANDELARIA 1	-94											
CANDELARIA 2			-102.20					-13.15				
CANDELARIA 4	-94		-101.50					-13.32				
CHARLES 1			-102.30		-96.40			-12.97		-13.27		
CHARLES 2					-99.90	-96.86	-101.20			-13.85	-13.82	-13.66
CHARLES 3					-100.20	-101.30				-13.92	-13.88	
CHARLES 4		-83			-86.10					-12.48		
COLLEGE 1		-90	-96.20		-89.28	-86.34		-11.81		-12.15	-12.17	
COLLEGE 2			-106.30		-96.27		-106.50	-13.62		-12.71		
COLLEGE 3 (LADERA)					-99.65					-13.64		
CORONADO 1					-97.95		-93.55			-13.15	-13.16	
DON 1	-104	-103	-107.60					-14.14				
DURANES 1			-97.60		-96.22			-12.24		-12.48		
DURANES 2			-101.90		-96.66		-95.85	-12.92		-13.24		
DURANES 3			-100.40		-94.99		-91.60	-12.70		-13.11		
DURANES 4	-92	-92	-100.90		-93.84		-93.38	-12.89		-13.33		
DURANES 5			-99.70		-91.56		-93.47	-12.70		-13.03		
DURANES 6			-100.00		-95.93		-93.67	-12.83		-13.05		
DURANES 7			-101.60		-93.93		-93.99	-12.86		-13.21		
GRIEGOS 1			-100.00		-97.99			-13.06		-13.58		
GRIEGOS 2			-99.40		-96.77			-12.70		-13.17		
GRIEGOS 3			-99.90		-100.40		-92.10	-13.30		-13.53		
GRIEGOS 4	-96	-95	-101.50		-98.29	-95.39	-100.10	-13.20		-13.31	-13.43	
LEAVITT 1	-103	-102	-107.20		-88.90	-94.09	-93.97	-13.69		-12.64	-12.76	
LEAVITT 2			-99.70		-92.62		-94.19	-12.78		-13.12		
LEAVITT 3					-101.50	-103.30	-100.80			-13.74	-13.81	
LEYENDECKER 1			-102.80		-99.25	-100.50		-13.62		-13.86		
LEYENDECKER 2			-104.60		-103.20		-102.30	-13.66		-13.70		-13.62
LEYENDECKER 3		-98	-103.10		-99.64		-97.93	-13.68		-13.97		
LEYENDECKER 4	-98		-105.90		-98.98		-99.11	-13.81		-13.80		-13.96
LOMAS 1			-82.70		-77.07		-78.22	-10.65		-10.73		
LOMAS 2	-78	-77										
LOMAS 4							-79.84					
LOMAS 5					-79.47		-75.87			-11.27		
LOMAS 6					-81.10		-79.10			-11.51		
LOVE 1				-83.24	-87.57	-83.12	-87.80		-11.99	-12.00	-11.84	-12.10
LOVE 2 (LOS ALTOS)					-78.95		-75.41			-11.26		
LOVE 3	-80	-80			-81.35		-81.00			-11.75		
LOVE 4			-99.60		-88.97		-83.95	-12.84		-12.40		

APPENDIX VII: ENVIRONMENTAL ISOTOPES

WELL NAME	Feb.1987 TRITIUM	Jul.1988 TRITIUM	Dec.1988 TRITIUM	Jun.1989 TRITIUM
ATRISCO 1(5)	< 6	15		< 6
ATRISCO 2(1)	24	69		22
ATRISCO 3(2:9)	17	28		12
ATRISCO 4(3:13)	24	15		< 6
BURTON 1 (new)		< 6	9	< 6
BURTON 2	30	8		< 6
BURTON 3	19	< 6		< 6
BURTON 4 (new)		< 6		< 6
CANDELARIA 1				
CANDELARIA 2	< 6			
CANDELARIA 4	< 6			
CHARLES 1	7	< 6		< 6
CHARLES 2		< 6	< 6	12
CHARLES 3		< 6		< 6
CHARLES 4		< 6		< 6
COLLEGE 1	15	< 6		< 6
COLLEGE 2	< 6	< 6		< 6
COLLEGE 3 (LADERA		< 6		< 6
CORONADO 1		< 6	< 6	< 6
DON 1	< 6			
DURANES 1	23	< 6		24
DURANES 2	27	7		28
DURANES 3	34	10		24
DURANES 4	13	10		16
DURANES 5	31	12		19
DURANES 6	22	24		12
DURANES 7	35	37		27
GRIEGOS 1	26	12		16
GRIEGOS 2	55	9		7
GRIEGOS 3	16	< 6		16
GRIEGOS 4	< 6	< 6		8
LEAVITT 1	< 6	< 6		< 6
LEAVITT 2	< 6	< 6		< 6
LEAVITT 3		11	< 6	11
LEYENDECKER 1	< 6	< 6		< 6
LEYENDECKER 2	15	< 6		< 6
LEYENDECKER 3	< 6	< 6		< 6
LEYENDECKER 4	< 6	< 6		< 6
LOMAS 1	18	< 6		< 6
LOMAS 2				< 6
LOMAS 4				< 6
LOMAS 5		< 6		8
LOMAS 6		< 6		8
LOVE 1		< 6	< 6	< 6
LOVE 2 (LOS ALTOS		8		< 6
LOVE 3		9		8
LOVE 4	< 6	< 6		7

APPENDIX VII: ENVIRONMENTAL ISOTOPES

WELL NAME	Aug.1981 DEL-D 81	Jan.1982 DEL-D 82	Feb.1987 DEL-D 87	Jan.1988 DEL-D 88	July 1988 DEL-D 88	Mar.1989 DEL-D 89	June 1989 DEL-D 89	Feb.1987 DEL-O 87	Jan.1988 DEL-O 88	July 1988 DEL-O 88	Mar.1989 DEL-O 89	June 1989 DEL-O 89
LOVE 5				-83.69		-81.26			-11.89			
LOVE 6				-81.36		-75.99			-11.51			
LOVE 7	-79	-79		-76.79		-80.58			-11.85			
MILES 1			-101.00	-97.56		-97.77	-13.00		-13.43	-13.30		
PARADISE HILLS 3		-96										
PONDEROSA 2	-77		-85.00	-80.41	-79.84		-10.79		-11.58	-11.72		
PONDEROSA 3			-98.50	-94.06	-93.75	-95.04	-12.86		-12.86	-13.08		-13.18
PONDEROSA 4			-83.80	-79.52	-81.45	-81.63	-11.11		-11.39	-11.56		
PONDEROSA 5(7)			-87.80	-83.22		-81.96	-11.89		-11.90			
PONDEROSA 6			-98.90	-91.93	-92.51	-92.54	-12.58		-12.89	-13.00		-12.95
PONDEROSA 1(9)			-95.40	-91.43		-86.93	-12.29		-12.36			
RIDGECREST 1				-83.30		-85.02			-11.16			
RIDGECREST 2				-85.33		-80.48			-11.84			
RIDGECREST 3	-82		-94.30	-87.39		-85.27	-12.31		-12.12			-11.97
RIDGECREST 4				-97.26		-93.87			-12.94			-12.89
SAN JOSE 1			-96.70	-92.71		-91.72	-12.52		-12.60			-12.66
SAN JOSE 2(4:7)			-103.60	-102.20		-97.82	-13.31		-13.90			
SAN JOSE 3(5:8)	-98	-96	-101.50	-99.64		-97.84	-13.45		-13.64			
SANTA BARBARA 1		-96	-102.60	-98.43	-99.90	-100.50	-13.17		-13.74	-13.64		-13.76
THOMAS 1			-98.10	-85.66		-81.33	-12.77		-12.04			
THOMAS 2			-96.90	-85.10			-12.28		-12.08			
THOMAS 3	-94	-92	-101.20	-90.92			-13.13		-12.75			
THOMAS 4	-87	-86	-96.40	-86.45		-81.65	-12.25		-11.99			
THOMAS 7 (new)					-93.39				-13.08			
TRAM (est.all)	-77											
UNM 5												
UNM 7												
VALLEY GRDENS 1		-92										
VOL ANDIA 1			-104.40	-99.57	-100.00	-95.54	-13.26		-13.53	-13.54		
VOL ANDIA 2			-104.70	-97.08		-97.78	-13.77		-13.73			
VOL ANDIA 3				-97.57	-97.15				-13.66	-13.56		
VOL ANDIA 4			-103.90	-100.80	-99.52	-100.30	-13.47		-13.72	-13.79		
VOL ANDIA 5			-103.10	-98.38		-98.84	-13.63		-13.52			-13.67
VOL ANDIA 6	-98	-96	-105.10	-99.98		-99.56	-13.59		-13.68			-13.98
VOLCANO CLIFFS 1			-99.10	-96.69	-93.72		-12.60		-12.86	-13.06		
VOLCANO CLIFFS 2	-94	-90	-99.90	-93.43		-92.79	-12.84		-13.07			
VOLCANO CLIFFS 3				-92.62		-91.90			-12.86			
WALKER-1			-86.50	-86.16		-77.50	-11.31		-11.82			
WALKER-2				-86.72					-11.94			
WEBSTER 1		-92	-99.10	-96.91	-98.95	-95.26	-12.72		-13.36	-13.14		-13.32
WEBSTER 2			-103.50	-96.71		-93.04	-13.38		-13.72			
WEST MESA 1			-104.70	-106.80	-107.50		-13.68		-14.64	-14.99		
WEST MESA 2			-98.80	-92.40		-91.05	-12.25		-12.54			
WEST MESA 3	-102	-102		-93.81		-95.83			-12.53			-12.42
WEST MESA 4			-102.00	-105.80	-101.20		-12.88		-14.10	-14.21		
YALE 1(2)	-96	-95	-102.80	-98.94		-94.85	-13.37		-13.32			
YALE 2(3)			-101.60	-99.39		-100.00	-12.86		-13.39			-13.48

APPENDIX VII: ENVIRONMENTAL ISOTOPES

WELL NAME	Feb.1987 TRITIUM	Jul.1988 TRITIUM	Dec.1988 TRITIUM	Jun.1989 TRITIUM
LOVE 5		< 6		< 6
LOVE 6		7		< 6
LOVE 7		< 6		< 6
MILES 1	< 6	< 6		< 6
PARADISE HILLS 3				
PONDEROSA 2	< 6	< 6	7	< 6
PONDEROSA 3	< 6	< 6	16	< 6
PONDEROSA 4	< 6	< 6		8
PONDEROSA 5(7)	< 6	< 6		7
PONDEROSA 6	< 6	< 6	9	19
PONDEROSA 1(9)	< 6	< 6		< 6
RIDGECREST 1		< 6		< 6
RIDGECREST 2		< 6		< 6
RIDGECREST 3	< 6	< 6		< 6
RIDGECREST 4		< 6		< 6
SAN JOSE 1	58	51	40	38
SAN JOSE 2(4:7)	< 6	< 6		7
SAN JOSE 3(5:8)	21	12		< 6
SANTA BARBARA 1	< 6	12	< 6	< 6
THOMAS 1	< 6	< 6		< 6
THOMAS 2	< 6	< 6		< 6
THOMAS 3	< 6	< 6		< 6
THOMAS 4	< 6	< 6		< 6
THOMAS 7 (new)			< 6	
TRAM (est.all)				
UNM 5				7
UNM 7				< 6
VALLEY GRDENS 1				
VOL ANDIA 1	< 6	< 6	10	< 6
VOL ANDIA 2	< 6	< 6		7
VOL ANDIA 3		< 6	< 6	
VOL ANDIA 4	< 6	< 6	< 6	< 6
VOL ANDIA 5	< 6	< 6		< 6
VOL ANDIA 6	< 6	< 6		9
VOLCANO CLIFFS 1	< 6	< 6		< 6
VOLCANO CLIFFS 2	< 6	< 6		< 6
VOLCANO CLIFFS 3		< 6		< 6
WALKER-1	< 6	< 6		15
WALKER-2		11		< 6
WEBSTER 1	< 6	12		< 6
WEBSTER 2	< 6	< 6		< 6
WEST MESA 1	< 6	< 6		< 6
WEST MESA 2	29	8		< 6
WEST MESA 3		9		< 6
WEST MESA 4	< 6	< 6		< 6
YALE 1(2)	8	8		< 6
YALE 2(3)	< 6	10		< 6

APPENDIX VII: ENVIRONMENTAL ISOTOPES

WELL NAME	Aug.1981 DEL-D 81	Jan.1982 DEL-D 82	Feb.1987 DEL-D 87	Jan.1988 DEL-D 88	July 1988 DEL-D 88	Mar.1989 DEL-D 89	June 1989 DEL-D 89	Feb.1987 DEL-O 87	Jan.1988 DEL-O 88	July 1988 DEL-O 88	Mar.1989 DEL-O 89	June 1989 DEL-O 89
YALE 3(4)			-101.80		-98.93		-99.04	-13.34		-13.57		-13.44
BIG-I (IRR-WELL)					-98.34					-13.59		
DOUBLE EAGLE 2					-110.60					-15.07		
4-HILL GC					-74.40		-75.41			-10.32		
MONTANO 1 (SHAL)					-91.93					-12.64		
MONTANO 3 (SHAL)					-96.04					-12.76		
MONTANO 4 (SHAL)					-84.97					-12.05		
RIO BRAVO 1 (SHAL)					-75.32					-11.04		
RIO BRAVO 2 (SHAL)					-96.11					-12.96		
RIO BRAVO 3 (SHAL)					-90.52					-12.77		
RIO BRAVO 4 (SHAL)					-89.51					-12.32		
MWUNM					-94.49					-13.46		
OWCOCO01					-95.13					-12.42		

Sample dates may be approximate within three months

APPENDIX VII: ENVIRONMENTAL ISOTOPES

WELL NAME	Feb.1987 TRITIUM	Jul.1988 TRITIUM	Dec.1988 TRITIUM	Jun.1989 TRITIUM
YALE 3(4)	10	< 6		7
BIG-I (IRR-WELL)		12		13
DOUBLE EAGLE 2		< 6		< 6
4-HILL GC		19		8
MONTANO 1 (SHAL)		41		
MONTANO 3 (SHAL)		27		
MONTANO 4 (SHAL)		27		
RIO BRAVO 1 (SHAL		18		
RIO BRAVO 2 (SHAL		30		
RIO BRAVO 3 (SHAL		48		
RIO BRAVO 4 (SHAL		10		
MWUNM		< 6		
OWCOC001			< 6	

APPENDIX VIII: DARCY'S LAW SEEPAGE VELOCITY CALCULATIONS

APPENDIX VIII: DARCY'S LAW SEEPAGE CALCULATIONS

Seepage Velocity:

The flowpath used for seepage velocity calculations is interpreted from a flownet drawn on a modified version of figure 18a. Equations are from Todd (1980), and Driscoll (1986) with respect to flow through a tube.

$$\text{Seepage Velocity } (V) = dx/dt = q/n = (K/n)*(dh/ds)$$

$$\text{Travel time } (dt) = (n * ds_i^2)/Kdh$$

q = specific discharge = K*(dh/dx)
dx = ds = length of flow line between potential lines
n = porosity (assumed value = 0.2)
K = geometric mean of hydraulic conductivities along flowpath
dh = change in head between potential lines

APPENDIX IX: MINERAL EQUILIBRIA EQUATIONS

APPENDIX IX: MINERAL EQUILIBRIUM EQUATIONS

Thermodynamic data used to calculate mineral equilibria are from PCWATEQ which is derived from the USGS program WATEQ. Equations are from Truesdale and Jones (1974), Stumm and Morgan (1981), Drever (1982), and Rogers (1989).

Equation 1: Calcium Smectite to Kaolinite

$$6[Ca_{.167}Al_{2.33}Si_{3.67}O_{10}(OH)_2 + 12H_2O = 0.17Ca^{+2} + 2.33Al(OH)_4^- + 2H^+ + 3.67H_4SiO_4]$$

$$7[2Al(OH)_4^- + 2H_4SiO_4 + 2H^+ = Al_2Si_2O_5(OH)_4 + 7H_2O]$$

$$6Ca_{.167}Al_{2.33}Si_{3.67}O_{10}(OH)_2 + 2H^+ + 23H_2O = 7Al_2Si_2O_5(OH)_4 + Ca^{+2} + 8H_4SiO_4$$

Equilibrium Constant (Log K):

Ca-Smectite Log K_{Cs} = 6(- 45.00)

Kaolinite Log K_{Ka} = -7(- 36.91)

Log K_{Cs-Ka} = - 11.63

Equation 2: Sodium Smectite to Kaolinite:

$$3[Na_{.33}Al_{2.33}Si_{3.67}O_{10}(OH)_2 + 12H_2O = 0.33Na^+ + 2.33Al(OH)_4^- + 3.67H_4SiO_4 + 2H^+]$$

$$3.5[2Al(OH)_4^- + 2H_4SiO_4 + 2H^+ = Al_2Si_2O_5(OH)_4 + 7H_2O]$$

$$3Na_{.33}Al_{2.33}Si_{3.67}O_{10}(OH)_2 + H^+ + 11.5H_2O = Na^+ + 3.5Al_2Si_2O_5(OH)_4 + 4H_4SiO_4$$

Equilibrium Constant (Log K):

Na-Smectite K_{Ns} = 3(-45.26)

Kaolinite K_{Ka} = - 3.5(-36.91)

Log K_{Ns-Ka} = - 6.595

Equation 3: Illite to Kaolinite:

$K_{.6}Mg_{.25}Al_{2.3}Si_{3.5}O_{10}(OH)_2 + 11.2H_2O = .6K^+ + .25Mg^{+2} + 3.5H_4SiO_4 + 2.3Al(OH)_4^- + 1.2H^+$

$1.15[2Al(OH)_4^- + 2H_4SiO_4 + 2H^+ = Al_2Si_2O_5(OH)_4 + 7H_2O]$

$K_{.6}Mg_{.25}Al_{2.3}Si_{3.5}O_{10}(OH)_2 + 3.15H_2O + 1.1H^+ =$

$.6K^+ + .25Mg^{+2} + 1.2H_4SiO_4 + 1.15Al_2Si_2O_5(OH)_4$

Equilibrium Constant (Log K):

$\text{Log } K_{Ill} = 1(-40.31)$

$\text{Log } K_{Kao} = -1.15(-36.91)$

$\text{Log } K_{Ill\text{-}Kao} = 2.137$

Equation 4: Calcite to dissolved Calcium at prescribed P_{CO_2}:

$CaCO_3 = Ca^{+2} + CO_3^{-2}$

$\text{Log } K_{CaCO_3} = -8.48$

$\text{Log } K_D = K_{CO_2} = -1.47$

$\text{Log } K_1' = -6.3$

$\text{Log } K_2 = -10.33$

$P_{CO_2} = -3.0$

$K_{eq} = [Ca]K_{CO_2}K_1'K_2P_{CO_2} / [H]^2$

$[Ca]/[H]^2 = K_{eq} / K_{CO_2}K_1'K_2P_{CO_2}$

Equation 5: Solid Quartz to Dissolved Silica:

$$SiO_{2(s)} + 2H_2O = H_4SiO_{4(aq)}$$

$$\text{Log } K_{SiO_2} = -4.005$$

Equation 6: Amorphous Silica to Dissolved Silica:

$$SiO_{2(a)} + 2H_2O = H_4SiO_{4(aq)}$$

$$\text{Log } K_{SiO_2} = -2.7$$

Equation 7: Reaction Quotient (Q) for Calcium Smectite

$$6Ca_{.167}Al_{2.33}Si_{3.67}O_{10}(OH)_2 + 2H^+ + 23H_2O = 7Al_2Si_2O_5(OH)_4 + Ca^{+2} + 8H_4SiO_4$$

$$Q = \frac{[Ca][SiO_2]^8}{[H]^2}$$

$$Q = \text{Log } m_{Ca} + 8\text{Log } m_{SiO_2} + 2pH$$

REFERENCES

AEHD, (1986), Summarization of water quality data, Bernalillo County 1960-1976: City of Albuquerque Environmental Health Department, unpublished report compiled by Chester Rail.

Affholter, Kathleen, (1979), Petrogenesis of Orbicular Rock, Tijeras Canyon, Sandia Mountains, New Mexico: M.S. thesis, University of New Mexico, p.

Albuquerque Journal, 10 July 1988, p.1.

Anderholm, S. A., (1985), Clay-size fraction and powdered whole-rock x-ray analyses of allluvial basin deposits in central and southern New Mexico: U.S. Geol. Survey Open-File Report 85-173, 18p.

Anderholm, S. A., (1988), Ground-water geochemistry of the Albuquerque-Belen Basin, Central New Mexico: U. S. Geol. Survey Water-Resources Investigation Rpt. 86-4094, 110 p.

Black, Bruce A.,(1982), Oil and gas exploration in the Albuquerque Basin: in New Mexico Geol. Society Guidebook, 33rd Field Conf. Albuquerque County II, p. 313-324.

Birch, F. S., (1980), Geophysical evolution of basin hydrologic characteristics in the central Rio Grande. Part 1: Gravity models of the Albuquerque-Belen Basin: Report submitted to U.S Geol. Survey. contract No. 14-08-0001-17879, 30 p.

Bjorklund, L.J., and B. W. Maxwell. (1961). Availability of ground water in the Albuquerque area, Bernalillo and Sandoval Counties, New Mexico: U.S. Geol. Surv. and N.M. State Engineer, Santa Fe, Technical Report 21, 117p.

Brutsaert, W. F., and T. G. Gebhard, Jr., (1975), Conjunctive availability of surface and ground water in the Albuquerque area, New Mexico: a modeling approach: Ground Water, v. 13, no. 4, pp. 345-353.

Bryan, Kirk, (1909), Geology of the vicinity of Albuquerque: New Mexico University, Albuquerque, Bull. 51, Geol. Ser. 3, no. 1, 24 p.

Bureau of the Census, U. S. Department of Commerce,

Busenberg, E., and C. V. Clemency, (1976), The dissolution kinetics of feldspars at 25°C and 1 atm CO_2 partial pressure: Geochimica et Cosmochimica Acta, v.40, pp.41-49.

Devore, Jay L., (1982), Probability and Statistics for Engineering and the Sciences: Brooks/Cole Publishing Co., Monterey, California, 640 p.

Drever, J. I., (1982), The Geochemistry of Natural Waters, Prentice-Hall Inc., Englewood Cliffs, N. J., 388 p.

Driscoll, Fletcher G., (1986), Groundwater and Wells: Johnson Division, 1089p.

Einerson, J. H., and P. C. Pei, (1988), A comparison of laboratory performances: Sandia National Lab., Environ. Programs Div., SAND 88-0226C, unpublished report, p. 43.

Fetter, C. W., Jr., (1980), Applied Hydrology, Charles E. Merrill Publishing Co., Columbus, Ohio, 488 p.

Freeze, R. A., and J. A. Cherry, (1979), Groundwater: Prentice-Hall Inc., Englewood Cliffs, N. J., 604 p.

Garrels, R. M., and F. T. Mackenzie, (1967), Origin of the chemical composition of some springs and lakes: Equilibrium Concepts in Natural Water Systems, ed. W. Stumm Wash. D.C. American Chemical Society Series # 67, p.222-242.

Garrels, R. M., and F. T. Mackenzie, (1971), Evolution of Sedimentary Rocks: W. W. Norton & Co., New York, 397p.

Grant, P. R., (1982), Geothermal potential in the Albuquerque area, New Mexico: New Mexico Geol. Society Guidebook, 33rd Field Conf. Albuquerque County II, p. 325-331.

Hem, J. D., (1970), Study and interpretation of the chemical characteristics of natural water: U. S. Geol. Survey Water Supply Paper 1473, 363 p.

Hiss, W., F. W. Trainer, B.S. Black, and D. R. Posson, (1985), Chemical quality of goundwater in the northern part of the Albuquerque-Belen Basin, Bernalillo and Sandoval Counties, New Mexico: in New Mexico Geological Society Guidebook, 26th Field Conference, (ed. W. R. Seager, et al) Nov. 13-15, p. 219-235.

Jiracek, G. R., E. P. Gustafson, and M. D. Parker, (1982), Geophysical exploration for geothermal prospects west of Albuquerque, New Mexico: New Mexico Geol. Society Guidebook, 33rd Field Conf. Albuquerque County II, p. 333-342.

Joesting, H. R., J. E. Case, and L. E. Cordell, (1961), The Rio Grande trough near Albuquerque, New Mexico: New Mexico Geol. Society Guidebook, 12th Field Conf. Albuquerque County, p. 148-150.

Kelley, Vincent, C., (1977), Geology of the Albuquerque Basin, New Mexico: New Mexico Bureau of Mines and Mineral Resources, Memoir 33, 60 p.

Kelley, Vincent, C., (1982), Albuquerque, its mountains, valley, water and volcanoes: New Mexico Bureau of Mines and Mineral Resources, Scenic Trips to the Geologic Past, No.9, (3rd. ed.), 106 p.

Kelley, V. C., and A. M. Kudo, (1978), Volcanoes and related basalts of Albuquerque Basin, New Mexico: New Mexico Bureau of Mines & Mineral Resources, Circular 156, 30 p.

Kelley, V. C., and S. A. Northrop, (1975), Geology of the Sandia Mountains and vicinity, New Mexico: New Mexico Bureau of Mines and Mineral Resources, Memoir 29, 136 p.

Kelly, T. E., (1974), Reconnaissance investigation of ground-water resources of the Rio Grande drainage basin: U. S. Geol. Survey Hydrologic Atlas HA-510, 4 sheets.

Kelly, T. E., (1982), History of water use in the greater Albuquerque area: New Mexico Geol. Society Guidebook, 33rd Field Conf. Albuquerque County II, p. 351-355.

Kernodle, John M., and William B. Scott, (1986), Three-dimensional model simulation of steady-state ground-water flow in the Albuquerque-Belen Basin, New Mexico: U.S. Geol. Survey Water Resources Invest. Rept. 84-4353, 58 p.

Kernodle, J. M., R. S. Miller, and W. B. Scott,(1987), Three-dimensional model simulation of transient ground-water flow in the Albuquerque-Belen Basin, New Mexico: U.S. Geol. Survey Water Resources Invest. Report, 86-4194, 86 p.

Kues, G. E., (1987), Ground-water level data for the Albuquerque-Belen Basin, New Mexico, through water year 1985: U.S. Geol. Survey Open-File Report 87-116, 51p.

Lambert, Paul W., (1968), Quaternary Stratigraphy of the Albuquerque Area, New Mexico: Ph.D. thesis, Univ. of New Mexico, 329 p.

Lozinsky, Richard P., (1988), Stratigraphy, Sedimentology, and Sand Petrology of the Santa Fe Group and Pre-Santa Fe Tertiary Deposits in the Albuquerque Basin, Central New Mexico: Ph.D. thesis, New Mexioc Institute of Mining and Technology, Socorro, New Mexico, 298 p.

Morgan, P., W. R. Seager, and M. P. Golombek, (1986), Cenozoic thermal, mechanical and techtonic evolution of the Rio Grande rift: Journal of Geophysical Research, v. 91, p. 6263-6276.

NMEID, (1974), New Mexico Public Water Supplies Chemical Data 1974: New Mexico Environmental Improvement Division, 157p.

NMEID, (1980), Chemical Quality of New Mexico Community Water Supplies 1980: New Mexico Environmental Improvement Division.

National Oceanic and Atmospheric Administration, U. S. Dept. of Commerce, (1981), Local Climatological Data: Environmental Data Service, National Climatic Center, Federal Building, Ashville, N.C. 28891.

O'Brien, Ken and Assoc., (1971), City of Albuquerque, Sandia Foothills Drainage Study: Unpublished report for Albuquerque Dept. of Public Works.

Popp, C.J., D.K. Brandvold, R.W. Ohline and L.A. Brandvold, (1984), Nature of precipitation and atmospheric particulates in central and northern New Mexico: New Mexico Bureau of Mines and Mineral Resources, Hydrologic Report no. 7, pp. 1-13.

Reeder, H. O., Bjorklund, L. J., and G. A. Dinwiddie,(1967), Quantitative Analysis of Water Resources in the Albuquerque Area, New Mexico: State Engineer, Santa Fe, New Mexico, Technical Report 33, 27 p.

Rogers, R. J., (1989), Geochemical comparison of ground water in areas of New England, New York, and Pennsylvania:Ground Water, v. 27, no. 5, Sept.-Oct. pp. 690-712.

Rollins, Larry, (1987), PCWATEQ: Shadoware, 215 Cedar Lane, Woodland, CA. (mineral equilibrium software based on WATEQF).

Science Applications, Inc. (1985), Installation Restoration Program Phase II, Stage I for Kirtland Air Force Base, Albuquerque, New Mexico: Unpublished report for KAFB.

Stumm, W., and J. J. Morgan, (1981), Aquatic Chemistry, 2nd ed., Wiley-Interscience, New York, 780 p.

Summers, W. K., (1972), Factors affecting the validity of chemical analyses of natural water: Ground Water, v. 10, no. 2, March-April, reprint.

Thompson, Stephen A. (1986), Urbanization and the Middle Rio Grande Conservancy District: Geographical Review, v. 76, no. 1, pp. 35-50.

Theis, C. V., (1938), Groundwater in the Middle Rio Grande Valley, in [U.S.] National Resources Committee, Regional planning, Part VI - the Rio Grande Joint Investigation in the upper Rio Grande Basin in Colorado, New Mexico and Texas, 1936-37: Wash., U.S. Govt. Printing Office, v.1, pt. 2, p. 268-291.

Titus, Frank B. Jr., (1961), Ground-water geology of the Rio Grande trough in north-central New Mexico, with sections on the Jemez Caldera and the Lucero Uplift: New Mexico Geol. Society Guidebook, 12th Field Conf. Albuquerque County, p. 186-192.

Titus, Frank B., (1980), Ground water in the Sandia and northern Manzano Mountains, New Mexico: New Mexico Bureau of Mines and Mineral Resources, Hydrologic Rept. 5, 66 p.

Todd, David K. (1980), Groundwater Hydrology: John Wiley and Son, Inc., New York, (2nd ed.) 535p.

Truesdell, A. H., and B. F. Jones, (1974), WATEQ, a computer program for calculating chemical equilibria of natural waters: U.S. Geol. Survey Journal of Research, v.2, no.2, pp. 233-248.

U. S. Army Corps of Engineers, (1979), Albuquerque greater urban area, urban studies program, Water supply appendix III: U. S. Army Corps of Engineers, Albuquerque district, Albuquerque, New Mexico.

U. S. Department of Agriculture Soil Conservation Service, (1977), Soil Survey of Bernalillo County and Parts of Sandoval and Valencia County, New Mexico: U.S. Dept. of Agriculture, 98 p.

von Eschen, G. F., (1959), Climate of the States - New Mexico: U. S. Weather Bureau Climatography of the United States no. 60-29, 15 p.

Wagner, G. H., and K. F. Steele, (1985), Use of rain and dry depositions for interpreting ground-water chemistry: Ground Water, v. 23, no. 5, September-October, p. 611-616.

Wilkins, D. W., (1987), Characteristics and properties of the basin-fill aquifer determined from three test wells west of Albuquerque, Bernalillo County, New Mexico: U. S. Geological Survey Water-Resources Investigations Report 86-4187, 78 p.

Yapp, Crayton J.,(1985), D/H variations of meteoric waters in Albuquerque, New Mexico, U.S.A.: Journal of Hydrology, v. 76, p. 63-84.